DEVELOPMENT OF NANO CHARACTERISTICS OF CLAY RESOURCES
FOR ADOBE PRODUCTION


A THESIS SUBMITTED TO
THE GRADUATE SCHOOL OF NATURAL AND APPLIED SCIENCES
OF
MIDDLE EAST TECHNICAL UNIVERSITY


BY

MELTEM ERDİL BÖLÜKBAŞI


IN PARTIAL FULFILLMENT OF THE REQUIREMENTS
FOR
THE DEGREE OF DOCTOR OF PHILOSOPHY
IN
BUILDING SCIENCE IN ARCHITECTURE


JANUARY 2024

Approval of the thesis:

## DEVELOPMENT OF NANO CHARACTERISTICS OF CLAY RESOURCES FOR ADOBE PRODUCTION

submitted by **MELTEM ERDİL BÖLÜKBAŞI** in partial fulfillment of the requirements for the degree of **Doctor of Philosophy** i**n Building Science in Architecture, Middle East Technical University** by,

Prof. Dr. Halil Kalıpçılar
Dean, Graduate School of **Natural and Applied Sciences**

Assoc. Prof. Dr. Ayşem Berrin Zeytun Çakmaklı
Head of the Department, **Architecture**

Assoc. Prof. Dr. Ayşe Duman
Supervisor, **Architecture, METU**

Prof. Dr. Emine N. Caner Saltık
Co-Supervisor, **Architecture, METU**

**Examining Committee Members:**

Assist. Prof. Dr. Bekir Özer Ay
Architecture, METU

Assoc. Prof. Dr. Ayşe Duman
Architecture, METU

Prof. Dr. Sinan Turhan Erdoğan
Civi Engineering, METU

Prof. Dr. Gülser Çelebi
Interior Architecture, Çankaya University

Assist. Prof. Dr. Müge Bahçeci
Architecture, Başkent University

Date: 22.01.2024

**I hereby declare that all information in this document has been obtained and presented in accordance with academic rules and ethical conduct. I also declare that, as required by these rules and conduct, I have fully cited and referenced all material and results that are not original to this work.**


Name Last name : Meltem Erdil Bölükbaşı

Signature :

# ABSTRACT

## DEVELOPMENT OF NANO CHARACTERISTICS OF CLAY RESOURCES FOR ADOBE PRODUCTION

Erdil Bölükbaşı, Meltem
Doctor of Philosophy, Building Science in Architecture
Supervisor: Assoc. Prof. Dr. Ayşe Duman
Co-Supervisor: Prof. Dr. Emine N. Caner-Saltık

January 2024, 229 pages

Qualified adobe products need to be produced due to decreasing sources of proper raw materials and the need for affordable and sustainable construction. Within the scope of developing the qualified adobe products, the study covers two main aims: "Developing a practical Nano-clay enrichment method in the laboratory to increase the Nano-clay in the clay content of adobe soil" and "developing qualified adobe products having enriched Nano-clay content". The proper soil samples were selected according to their potential for Nano-clay enrichment and adobe production. The clay type is a crucial parameter for Nano-clay enrichment by ultrasonic treatment. The soils rich in montmorillonite were more suitable for Nano-clay enrichment than those rich in illite, kaolinite and chlorite. Nano-clay enriched qualified adobe was achieved by having improved compressive and flexural strengths which are higher than the requirements of the regulations/codes while keeping their inherent breathable and capillary water absorption features. Total Nano-clay contents and pozzolanic characteristics of the treated adobe products were the main factors affecting the compressive and flexural strengths, respectively. In addition, the use of Nano-sized calcium oxide additive was effective in treated adobe products including montmorillonite as the main clay. Effective use of soil resources not appropriate for adobe production was provided by Nano-clay enrichment by ultrasonic treatment. In

addition to its contribution to the fields of innovative adobe construction industry and archaeology, the Nano-clay enrichment treatment in adobe soil can be practically applied in rural areas by teaching the local people the soil resource selection and the treatment process.

Keywords: Adobe, Clay, Nano-clay Enrichment, Ultrasonic Treatment, Physical and Mechanical Properties

# ÖZ

## KERPİÇ ÜRETİMİ İÇİN KİL KAYNAKLARININ NANO ÖZELLİKLERİNİN GELİŞTİRİLMESİ

Erdil Bölükbaşı, Meltem
Doktora, Yapı Bilimleri, Mimarlık
Tez Yöneticisi: Doç. Dr. Ayşe Duman
Ortak Tez Yöneticisi: Prof. Dr. Emine N. Caner Saltık

Ocak 2024, 229 sayfa

Uygun hammadde kaynaklarının azalması, ekonomik ve sürdürülebilir yapım ihtiyacı nedeniyle nitelikli kerpiç ürünlerin üretilmesi gerekmektedir. Nitelikli kerpiç ürünlerinin geliştirilmesi kapsamında yapılan bu çalışma iki ana amacı kapsamaktadır: "Kerpiç toprağın kil içeriğindeki Nano kili arttırmak için laboratuvarda pratik bir Nano kil zenginleştirme yöntemi geliştirmek" ve "zenginleştirilmiş Nano kil içeriğine sahip nitelikli kerpiç malzemelerin geliştirilmesi". Uygun toprak örnekleri Nano kil bakımından zenginleşme ve kerpiç üretimi açısından uygunluk potansiyelleri göz önüne alınarak seçilmiştir. Kil türü, ultrasonik işlem ile Nano kil zenginleştirme için çok önemli bir parametredir. Montmorillonit kilince zengin topraklar, illit, kaolinit ve klorit bakımından zengin olanlara göre Nano kil üretimi için daha uygun bulunmuştur. Nano kil ile zenginleştirilmiş nitelikli kerpiç ürünleri, Nano kil üretimi öncesi var olan nefes alabilirliği ve kılcal su emme özelliklerini korurken, yönetmelik/kodların gerekliliklerinden daha yüksek basınç ve eğilme dayanımlarına sahip olmuşlardır. İşlem görmüş kerpiç ürünlerin toplam Nano kil içeriği ve puzolanik özellikleri, sırasıyla basınç ve eğilme dayanımlarını etkileyen başlıca unsurlardır. Ayrıca, Nano taneli kalsiyum oksit katkısının kullanılması montmorillonit kilce zengin işlem

görmüş kerpiç ürünlerinde etkili olduğu görülmüştür. Kerpiç üretimine uygun olmayan toprak kaynaklarının etkin kullanımı ultrasonik işlemle Nano kil zenginleştirmesi ile sağlanabilmiştir. Kerpiç toprağında Nano kil zenginleştirme işlemi, yenilikçi kerpiç yapım endüstrisi ve arkeoloji alanlarına sağlayabileceği katkının yanı sıra, toprak kaynağı seçimi ve Nano kil zenginleştirme işlemi sürecinin yerel halka öğretilmesi ile kırsal alanlarda pratik hayatta da uygulanabilir.


Anahtar Kelimeler: Kerpiç, Kil, Nano kilce Zenginleştirme, Ultrasonik İşlem, Fiziksel ve Mekanik Özellikler

To All Working Class

# ACKNOWLEDGMENTS

# TABLE OF CONTENTS

# LIST OF TABLES

**LIST OF FIGURES**

FIGURES

xxii

# CHAPTER 1

# INTRODUCTION

The construction of adobe structures dates back to Neolithic times, about 8000 BC (Houben et al., 1994; Minke, 2009). Those structures about 30% of buildings in the world are still in developing countries and also in developed countries due to their low carbon footprint, low cost, easy construction and their contribution to indoor climate conditions and indoor air quality through the low thermal conductivity properties (Calkins, 2008; Minke, 2009; Mishra & Usmani, 2013; Shukla et al., 2009). Despite a significant part of the population in underdeveloped and developing countries living in adobe buildings and the interest in adobe structures has also increased in developed countries, there is little interest in adobe materials and construction technology in our country. While research on adobe materials and construction enhances knowledge accumulation, it is observed that this knowledge gained through research cannot be transferred to the construction sector and applications. The most efficient tools to strengthen that knowledge transfer and enable the widespread use of adobe materials and construction practices are building and material regulations and standards. However, regulations, standards and specifications for adobe construction, construction and material technologies, defining and testing performance criteria, and maintenance/repair are limited. In short, there is insufficient availability of guiding resources for defining the performance characteristics of adobe materials and structures, and for the production and application of qualified adobe materials (Houben et al., 1994; Vyncke et al., 2018).

The study focuses on a scientific research topic for the production of qualified adobe construction materials by utilizing the opportunities provided by Nanotechnology. The objective of the study is to evaluate and compile the scientific knowledge

acquired within the scope of the research in a way that can be transferred to standards that will contribute to the widespread production of adobe construction materials.

Adobe structures, although providing breathable and energy-efficient building envelopes, have been abandoned over time and eventually disappeared due to their susceptibility to precipitation and earthquakes, lack of maintenance, and improper interventions. Continuous maintenance is one of the main criteria for the long-term durability of adobe structures, which can be a laborious task for building occupants. This factor reduces the widespread use of adobe materials, which have strong sustainability and environmentally friendly qualities, as a local construction material. Stabilization of adobe material is crucial to enhance the durability of adobe materials and structures, specifically improving their resistance to strength loss due to saturation, as well as their weak performance against wind and water erosion in harsh climate conditions. Numerous studies exist regarding the selection and preparation of raw materials, mixture preparation, stabilization, maintenance, and strengthening of adobe structures to increase the long-term durability of adobe (Blondet et al., 2008; Giuffrida et al., 2021; Işık, 2011; Widder, 2017). Some studies have revealed that since the transition of humans to settled life, people have considered the stabilization of adobe, utilized conscious and qualified local raw material sources, and prepared different mixtures of adobe products based on their functional roles in the construction (Uğuryol & Kulakoglu, 2013; Uzun, 2019). Most of the current research on adobe technology focuses on improving the performance and mechanical properties of adobe materials by incorporating binding agents or additives/stabilizers such as lime, gypsum, various plant fibres, waste tea residues, boron waste, and polymer fibres into the adobe mixture (Abanto et al., 2017; Bahobail, 2012; Binici et al., 2005, 2007, 2009; Calatan et al., 2016; Danso et al., 2015; Işık, 2011; Pekmezci et al., 2012; Pekrioglu Balkis, 2017; Sharma et al., 2016; Vilane, 2010). Among those researches focusing on strengthening adobe materials, Nano-sized additives were also made a current issue. For instance, there are studies on the application of Nano-sized lime ($Ca(OH)_2$) solution to strengthen adobe surfaces found in archaeological sites and examining the effect of Nano-sized lime solution on the existing

2

composition of adobe materials (Camerini et al., 2018; Elert et al., 2022; Michalopoulou et al., 2020). Those studies have shown the positive effects of applying Nano-sized lime solution on the pozzolanic and mechanical properties, water as well as the control of swelling and shrinkage behaviour of adobe. However, there is limited research in the literature regarding the use of Nano-sized additives to improve the performance properties of adobe materials. That study is designed to fill this gap in the literature; comprehensive scientific analyses were planned to investigate the influence of Nano-sized lime additives, especially Nano-clay content on the performance of adobe. The research aims to generate scientific data that will contribute to the development, application, and innovation fields of the construction sector and construction material production technologies.

After evaluating the literature data on adobe material technology and discussing its weaknesses in widespread use in the construction sector, the scope of the study was determined by raising the following research questions:

— Can Nano-clay be produced from adobe soil with a practical method?
— How does the increase in Nano-clay content in adobe soil affect the performance properties of the produced adobe material?
— Can the plasticity and swelling behaviour of adobe soil with increased Nano-clay content be controlled with Nano-CaO additives?
— As a result, can local clay/adobe soil resources be transformed into efficient qualified raw material sources for the production of qualified adobe by increasing the Nano-clay content and also adding Nano-CaO?

The research results are expected to contribute to the development of current adobe material and construction technologies, as well as the conservation of adobe cultural assets and archaeological sites.

## 1.1    Argument

Regarding the potential of adobe structures in terms of having low embodied energy, affordable and providing healthy and high-quality indoor comfort conditions, they have been seen as an alternative housing type to sustainable architecture, especially in rural areas in recent years (Papayianni & Pachta, 2017; Vyncke et al., 2018). Adobe building envelopes also can improve indoor air quality due to their performance of balancing the humidity inside and high breathability (Minke, 2009; Schroeder, 2015; Yüncü et al., 2014). The COVID-19 pandemic has demonstrated the cruciality of providing healthy indoor air conditions and highlighting the need to achieve these conditions through sustainable and energy-efficient building materials, construction technologies, and principles of building physics rather than solely mechanical ventilation methods (Monge-Barrio et al., 2022; Park et al., 2021). The limited existence of adobe technology, which can meet these requirements as a sustainable construction system, in the contemporary construction industry, despite its development since the Neolithic period worldwide and in Anatolia, is a subject that needs to be discussed.

In the context of adobe technology, non-expansive clays such as kaolin play a prominent role in producing qualified adobe material. However, the local clay/adobe soil resources in Anatolia contain multiple clay types together. For instance, illite, montmorillonite, chlorite, and/or the other clay types may co-exist with or without kaolinite. The use of Nano-clay additives in adobe products can be provided by either producing the Nano-sized clay particles or extracting them from natural clay sources. Both production approaches are laborious operations. In this regard, practical solutions need to be developed to increase the amount of Nano-clay in adobe soil, rather than producing or extracting Nano-sized clay, which is a labour-intensive process. Considering those requirements, the Nano-clay content enrichment that can be done by a practical method can be a promising attempt to achieve qualified adobe construction material. That provides the local clay/adobe soil resources to be used more efficiently and an affordable, local and qualified adobe

construction material can be produced from adobe/clay soil with enriched Nano-clay content, which contributes to the widespread construction and technological development of the adobe.

## 1.2    Aims and Objectives

The main aims of the study are:

— Developing a practical method to enrich the amount of Nano-clay in adobe soil resources, rather than adding a specifically produced Nano-clay as an additive;

— Developing qualified adobe materials having enriched Nano-clay content to improve local adobe construction material technology.

The objectives of the study directed towards those aims are as follows:

— Identification of local adobe soil/clay resources in terms of compositional and raw materials properties, and field soil tests;

— Determination of Nano-clay content in natural adobe soil/clay resources;

— Development of a practical method for Nano-clay enrichment in adobe soil,

— Consistency limits performance assessment of Nano-clay-riched adobe soil samples;

— Preparation of Nano-clay riched adobe products with/without Nano-CaO and slaked lime (Ca (OH)$_2$ additives;

— Performance assessment of Nano-clay riched adobe products in terms of basic physical and mechanical properties including vapour transmission and capillary water absorption features.

## 1.3    Disposition

The thesis comprises seven chapters, including an introduction, literature review, materials and methods, results, discussion, conclusion and appendices. In the

introduction chapter, brief information on adobe constructions, Nano-clay technology and deficiencies in the literature on those subjects was given. The argument part defines the assertion of the study, importance and contribution of the qualified adobe production by increasing the Nano-clay amount. The aims and objectives of the study were itemised. The flow and the content of the thesis were indicated in the disposition part.

In the second chapter, a literature review of the articles, thesis and book chapters was presented by the subjects on adobe, stabilization of adobe, clay, Nano-clay and Nano-clay production. In addition, literature data of studies on raw material characteristics, mechanical hydric and hygric performances of adobe soil and adobe samples were collected together with required performance levels by standards.

Materials and Methods starts with the description of the collected soil samples and the background data for the selection data for the soil resources. The analyses conducted on the samples: field soil tests, raw material characteristics tests (pH value, organic calcite and salt contents, pozzolanic activity, particle size distribution, simulation, stereo microscope analyses) mineralogical and elemental composition tests (XRD and XRF analyses), the process of Nano-clay production treatment by ultrasonic bath and laboratory mixer, preparation of the treated adobe samples, the basic physical, water vapour permeability, mechanical and capillary water absorption tests.

In the fourth chapter, the results of the study were given in consecutive stages, the proper soil samples were selected among the adobe soil/clay soils after each stage. Firstly, the raw materials and compositional properties of the collected soil/clay samples were determined then the amount of natural Nano-clay adobe/clay was assessed in terms of their sufficiency to be used as the adobe sample and Nano-clay production. Then the Nano-clay production process and the optimum times were determined and the enrichment in the amount of Nano-clay and morphological change on clay particles were proved. Later on, the treated soil samples having the increased Nano-clay contents were evaluated if they were proper for the adobe

material or not by the consistency limit tests. Lastly, the basic physical, water vapour permeability, mechanical and capillary water absorption characteristics of the adobe samples were determined.

In the discussion part, the performance of the collected soil/clay samples was assessed in terms of their sufficiency to be used as the adobe sample and for the Nano-clay production. The factors affecting Nano-clay production were uncovered. In the last part, the performance of the treated adobe samples and treated adobe samples including Nano-CaO or $CaOH_2$ were assessed compared to untreated ones in terms of their basic physical, water vapour permeability, mechanical and capillary water absorption properties regarding required levels by standards and related literature data.

In the conclusion part, the summary of the study, recommendations, and further studies were mentioned.

# CHAPTER 2

# LITERATURE REVIEW

This chapter includes a comprehensive literature review of the related subjects and studies, which constructs the background information for the thesis.

Firstly, adobe and clay materials were introduced. The history and use of the adobe in Anatolia and the production and construction methods of the adobe together with the stabilization of the adobe material were summarized. Since the clay content significantly affects the adobe material, the clay and its performances were mentioned. The mineralogical structures types of clay, and clay particle associations depending on the electrostatic interactions were presented together with cation exchange capacity performances of different types of clay and methylene blue tests identifying the cation exchange capacity of clays.

Nanotechnology has been a developing issue and is excessively used in construction materials; therefore, the literature started with a definition of the Nano-clay and then included aims of its use and studies on the use of the Nano-clay as soil stabilization. The data on the production methods of the Nano-clay were compiled to figure out the most efficient one for the development of a practical Nano-clay preparation. Particle size distribution including the sub-micron is the significant raw material characteristic affecting the e adobe soil performance. The different methods and scales of the particle size distribution analyses were summarized.

In the last part, the test methods for the evaluation of the adobe soil and adobe brick performance in terms of consistency limits, linear shrinkage ratio, water vapour permeability mechanical properties capillary water absorption together with performance data of previous studies, and some recommended levels defined by the regulations and standards were included.

## 2.1    Adobe

In Anatolia, the first adobe structure was constructed of wattle-and-daub method in Çayönü, South-Eastern region (ca. 7000 BC) (Bektaş, 2018). The other ancient adobe structures are as follows (Schroeder, 2015):

— 9000-year-old Çatalhöyük dwellings having adobe masonry exterior walls and timber posts positioned inside the dwellings to support the roof structure;

— the adobe dwellings in Hacılar-Burdur (5700-5600 BC),

— the adobe houses in the form of "Megaron" found in the archaeological sites of Beycesultan, Denizli (4000-3000BC), Troia and Kültepe (2450-2200 BC);

— "Beehive houses of Harran" in Şanlıurfa constructed as adobe masonry structures with a high conical adobe roof (ca. 2000 BC).

Adobe masonry houses were constructed extensively in the architecture of the Hittite period (2000-1000 BC) and the Urartu period (900-600 BC) (Bektaş, 2018). A growing interest was observed in adobe material and structures particularly in Western Europe and the USA for temporary housing after the Second World War. On the other hand, in that period, the studies on adobe in Turkey were restricted in number due to the common construction of reinforced concrete and brick masonry structures in Turkey (Kafescioglu, 2017). In the 1950s, negative perception of adobe structures was created by government policies, although Anatolia is the "home" of adobe, the number of them has decreased seriously (Kafescioglu, 2017).

Nowadays, the total number of traditional adobe masonry buildings and timber-framed with adobe infill structures in still use is about 615070 (State Institute of Statistics Prime Ministry Republic of Turkey, 2001). The distribution of percentages of adobe structures' presence in geographic regions in Turkey is given in Figure 2.1.
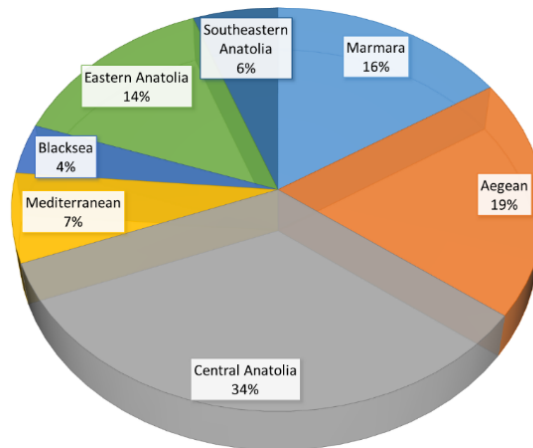
Figure 2.1 The data showing the percentages of adobe constructions in each geographic region (State Institute of Statistics Prime Ministry Republic of Turkey, 2001).

According to the data given by the State Institute of Statistics Prime Ministry Republic of Turkey (2001), a map showing the number of traditional adobe structures in each city and their distribution in Turkey was produced (State Institute of Statistics Prime Ministry Republic of Turkey, 2001). The common use of adobe constructions is observed to exist in the regions of especially Central Anatolia, Aegean and South Marmara, and in the cities of Ankara, Afyon, Eskişehir, Çorum, Denizli, İzmir, Konya Malatya, Manisa and Tokat. Among many clay types, the limited-expansive or non-expansive clay types, which are the illite and kaolinite clay deposits, are the clays preferred as binders for adobe material and adobe structures. According to "Mindat. Org", an open database of minerals, the illite and kaolinite clay resources are mostly found in İzmir, Eskişehir and Manisa (Ralph, 2023), where the number of traditional adobe houses is high in amount (State Institute of Statistics Prime Ministry Republic of Turkey, 2001).

The clay used as the raw material of adobe is supplied from clay-rich soil resources and alluvial or lacustrine deposits (lake deposits). Most adobe resources, either clay or adobe soil resources, are located on Neogene lacustrine sedimentary basins (Alkaç & Koral, 2022; de Ridder, 1965; Kadir & Karakas, 2002; Varol et al., 2002; Yeniyol, 2012), corresponding to the regions where traditional adobe houses have been

commonly constructed in Turkey (State Institute of Statistics Prime Ministry Republic of Turkey, 2001).

The adobe soil/clay resources belonging to prehistoric times are close to the archaeological settlements, such as Çatalhöyük (Konya), Ortaköy-Şapinuwa (Çorum), Boğazköy-Hattuşa (Çorum) and Sardes (Manisa) (Kıvrak, 2007; Koçu & Korkmaz, 2007; Özkan et al., 2010). In short, the settlements where traditional adobe constructions are concentrated have been positioned close to the adobe/clay resources of the region.
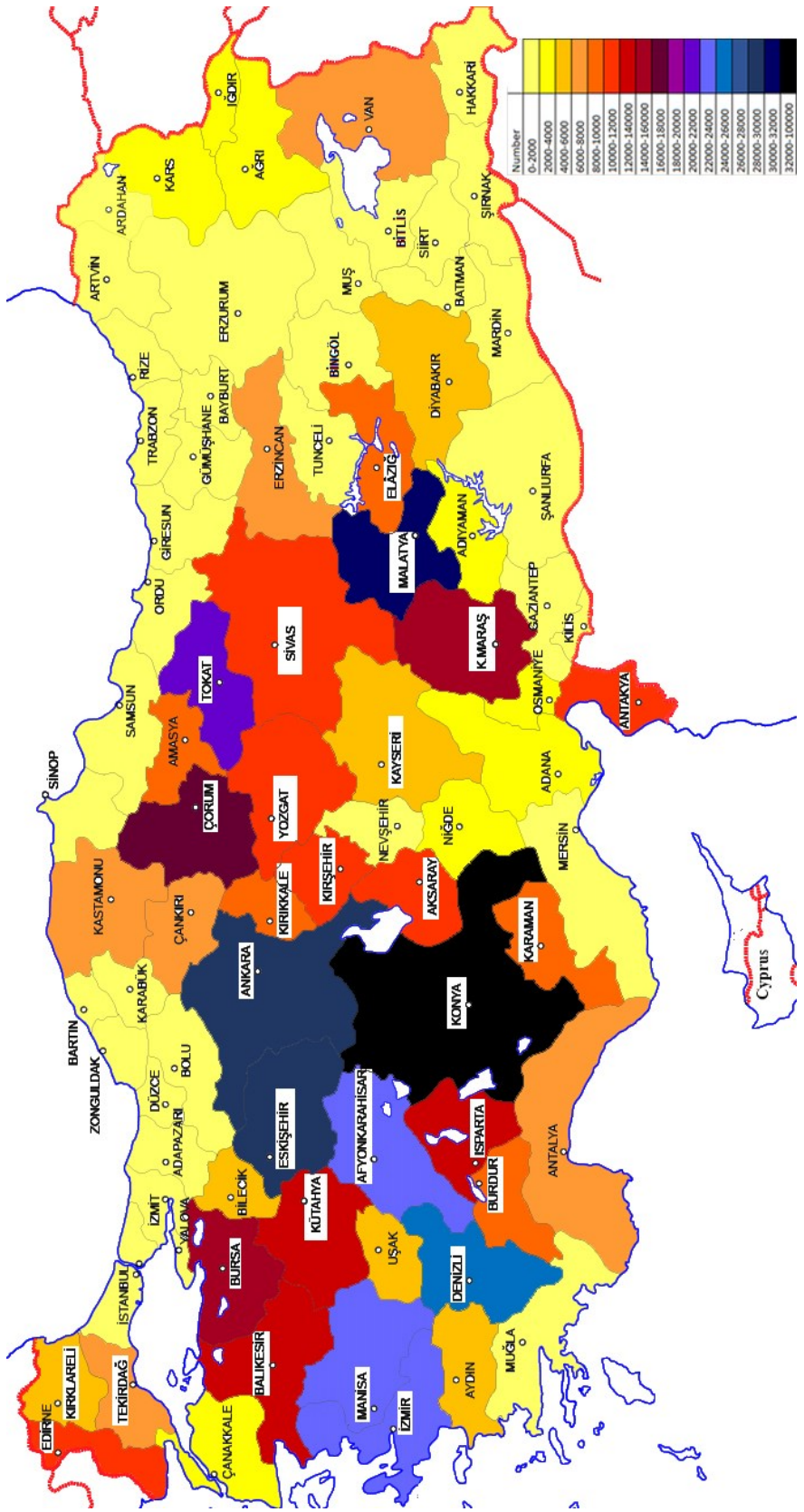
Figure 2.2 Turkey map coloured depending on the number of adobe constructions.

13

The traditional adobe used to be prepared with about 7-10 kg straw (1% by w.t) and 500 kg water per 1 m$^3$ of soil including 30-40 % clay by w.t, according to TS 2514:1977 inactive standard now (TS, 1977). The straw used in adobe should not be rotten and should be a maximum of 10-12 cm in length. Besides straw, animal hair, dung, gypsum, lime, wood ash and plant fibres were also used in traditional adobe mixture (Torraca, 1988). There was a need for a large area for curing the clay in the adobe mixture, adobe brick production, and its storage area that should be protected from the direct sun and rain. The preparation process for adobe can be divided into three stages (Aşanlı, 2021):

**Preparation of adobe mixture**: Soil, water, straw and some additives are put and mixed in a pit or a container and then let rest for about one day to improve the plasticity of clayey soil (Torraca, 1988) ( Figure 2.3).
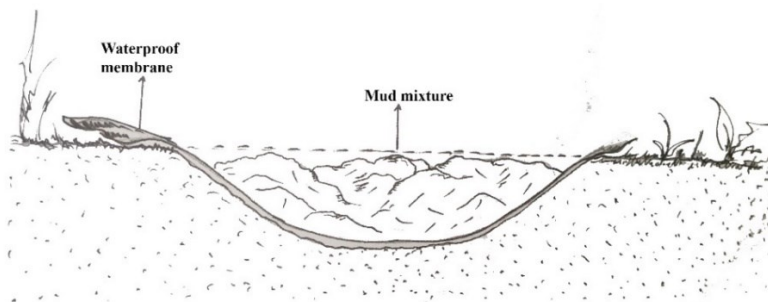


Figure 2.3 Preparation of adobe mixture (Aşanlı, 2021).

**Cutting of adobe**: Adobe mixture is thrown into moisturized wooden moulds and compressed on a plain surface covered by straw or sand (Figure 2.4). Dimensions of mould should be greater in the ratio of 3-5% that of the brick due to shrinkage while it's drying out. Adobe brick is cut generally in periods between May and September and also between April and October.
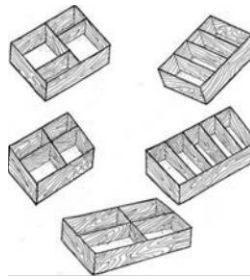
Figure 2.4 Wooden (plywood or MDF or chipboard) moulds (Acun & Gürdal, 2003).

**Drying of Adobe**: Adobe bricks taken out from moulds are dried out in the shadow by protecting from direct sun and wind. While drying, the traditional adobe brick must be turned upside-down in the field. Drying methods are shown in Figure 2.5. Drying slowly provides the formation of fewer cracks. The stability of adobe brick is gained after 15-21 days. Afterwards, they are stacked under tents, branches or weeds to protect them from rain.
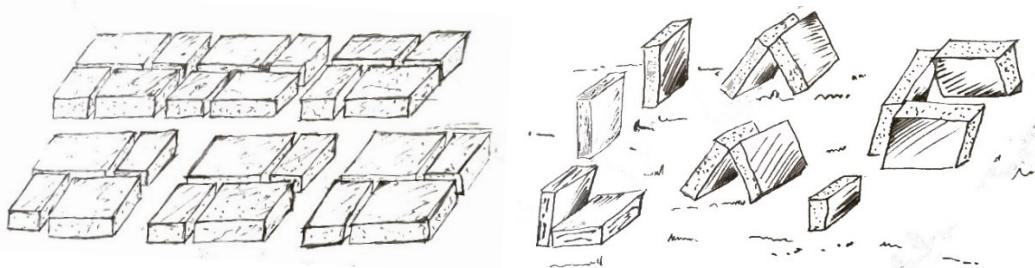


Figure 2.5 Drying of adobe bricks for 2 or 4 days (at left); drying of adobe bricks on the fourth or fifth day (at right) (Aşanlı, 2021).
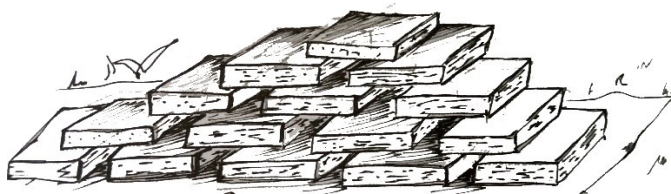


Figure 2.6 Stacking of dry adobe bricks (Aşanlı, 2021).

The common adobe dimensions that are general classifications of adobe brick as "ana" and "kuzu" are shown in Table 2.1.

Table 2.1 Ranges of dimensions of adobe used in Turkey (Acun & Gürdal, 2003).

| Adobe type | Kuzu –half brick, cm | Ana-whole brick, cm |
|---|---|---|
| Length | 30-38 | 30-38 |
| Width | 12-17 | 25-35 |
| Height | 10-12 | 10-12 |

The production process of adobe bricks requires time and intensive labour. On the other hand, mechanization of the manufacturing process allows obtaining adobe brick at a rate of 3000 bricks/day (Işik, 2010). The other adobe construction methods are cob, earth-filled bag (superadobe), rammed earth and 3D-printing adobe. Cob is one of the simplest forms of adobe construction as it is hand-formed into monolithic walls by stacking earth clumps/balls on top of one another, and lightly tamping them with the hands or feet, and no formwork, tamping or machinery (Figure 2.7) (Houben et al., 1994). Earth-filled bags, also called superadobe, are plastic and textile bags or long polypropylene tubes filled with sand, gravel or tamped solid (Figure 2.7) (Minke, 2009). Barbed wire can be placed between bags to hold them together.
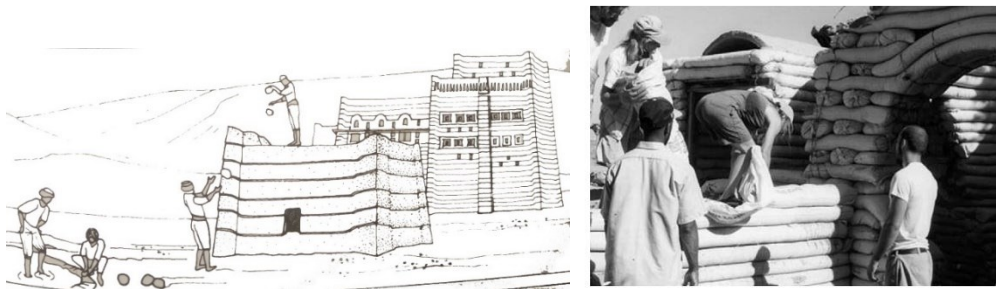


Figure 2.7 Cob (at left) (Houben et al., 1994) and earth-filled bag constructions (at right) (Calkins, 2008).

In the rammed earth technique, moist earth is poured into formwork and compacted with a wood or metal rammer composed of a long handle and flat head (Calkins, 2008) (Figure 2.8). The technique of pneumatically impacted stabilized earth (PISE)

where an earth mixture is sprayed onto one-sided formwork with high-pressure air was developed to reduce construction time and labour costs of rammed earth (Calkins, 2008) (Figure 2.8). That method is similar to dry mix shotcrete concrete.
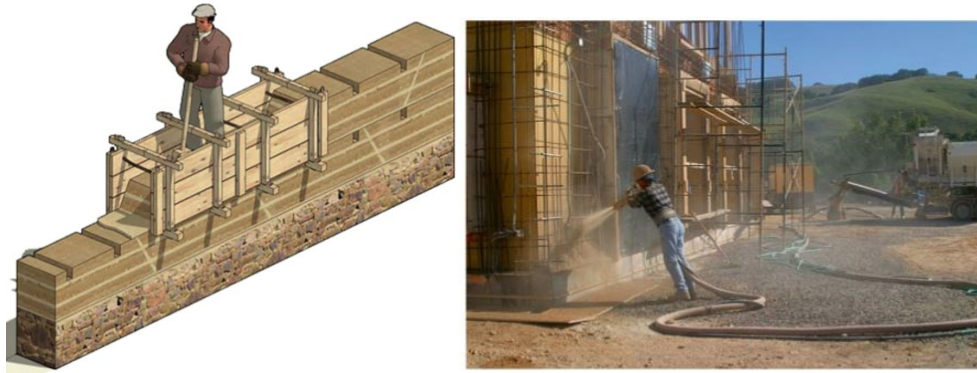


Figure 2.8 Rammed earth (at left)(*Betonarme: Bir Asrı Aşan Evliliğin Hikayesi*, 2023) and PISE technique including spraying the rammed earth onto one-sided formwork (at right) (Minke, 2009).

Robotic fabrication for architecture brings the opportunity for adobe construction in terms of increase in productivity and flexibility in the design. 3D-printed adobe construction by robots focused in some studies is a developing alternative method (Dubor et al., 2019; Khoshnevis, 2004) (Figure 2.9).
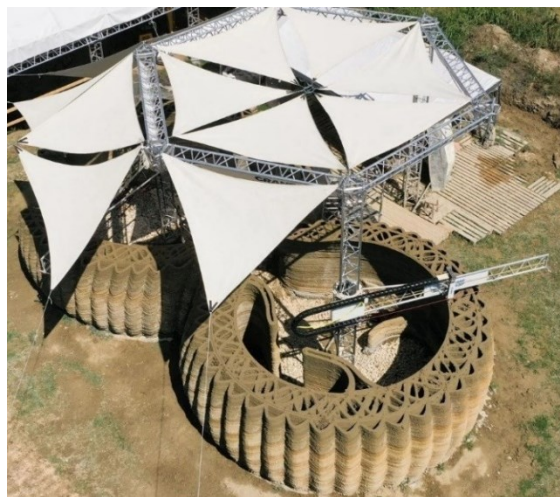


Figure 2.9 3D-printed adobe constructions by robots (*Arquitectura Viva*, 2023).

Adobe is a biodegradable and reusable material and generates no hazardous waste and also minimal waste, either during its production or at the end of its useful life span (Pacheco-Torgal & Jalali, 2011). In addition, its drying process is performed by excluding firing (Thiebat et al., 2023). The environmental benefits of adobe material can be defined by the Life Cycle Assessment (LCA) of its production (Christoforou et al., 2016). LCA is a technique to assess all the potential environmental impacts, inputs, and outputs of materials during the whole life cycle (ISO, 2006). In the LCA, system boundary conditions define which material/building life-cycle stages are included in a study (Miller & Ip, 2013; Morton, 2006). Some common system boundary conditions are cradle-to-gate and cradle-to-site. Cradle-to-gate contains the extraction of raw materials and manufacturing of construction materials that define the production process. Cradle-to-site includes the production and construction stages that comprise the transportation of materials to the site and the construction of a building. The embodied energy (MJ/kg) refers to the amount of energy consumed within the system boundaries of the study (Miller, 2013). Embodied carbon also called carbon footprint (kg $CO_{2eq}$/kg) is related to the amount of greenhouse gas emissions (GHGs) that are released within the system boundaries of the study (Miller & Ip, 2013).

Embodied energy and embodied carbon values of adobe brick and some other construction materials for comparison were given in Table 2.2. The embodied energy of the adobe brick production system through a cradle-to-site life cycle analysis was indicated as between 0.03 and 0.17 MJ/kg and its embodied carbon was between 0.0017 and 0.013 kg $CO_{2eq}$/kg. The values of adobe are in the range of 1% and 9% of embodied energy and carbon values of fired brick, hollow clay brick and lightweight concrete block. Those materials' values are too much higher than adobe's cradle-to-site analysis although their values belong to cradle-to-gate life cycle analysis that does not include the construction and transportation process of the material. In addition, the embodied energy and carbon values of the construction of the exposed adobe masonry house approximately 7% of the exposed reinforced concrete structure with brick infill wall (Güğercin et al., 2018).

18

Table 2.2 Embodied energy and embodied carbon values of adobe brick, fired clay brick, hollow clay brick and lightweight concrete block.

| Material | Embodied Energy, MJ/kg | System boundary | Embodied Carbon, kg $CO_{2eq}$/kg | Reference |
|---|---|---|---|---|
| Adobe brick | 0.03-0.08 | Cradle-to-site: on-site production | 0.0018-0.0054 | (Christoforou et al., 2016) |
| | 0.17 | off-site production | 0.013 | |
| Fired clay brick | 3-3.1 | Cradle-to-gate | 0.24 | (Christoforou et al., 2016; Morton, 2006) |
| Hollow clay brick | 1.76 | Cradle-to-gate | 0.20 | (Morton, 2006; Thiebat et al., 2023) |
| Lightweight concrete block | 1.8 | Cradle-to-gate | 0.2 | (Morton, 2006; Thiebat et al., 2023) |

## 2.2    Stabilization of Adobe

Additives/stabilizers improve the mechanical performance, water resistance and volume stability of the adobe material. While binding additives such as lime and gypsum generally enhance the durability and compressive strength of adobe, they decrease the thermal resistance performance of adobe (Bahobail, 2012; Ngowi, 1997; Vilane, 2010). Natural or polymer fibres such as straw, animal, human hair, coconuts, sisal, bamboo fibres, needles of trees and or synthetic fibres, depending on their dimensions, orientations, and quantities, reduce the shrinkage, bulk density, and thermal conductivity of adobe material while increasing its tensile strength and sound insulation performance (Berardi & Iannace, 2015; Calatan et al., 2016; Sharma et al., 2016; Yetgin et al., 2008). On the other hand, the excessive use of the fibre reduces the binding force between the soil and fibre decreasing the tensile and compressive strength of the adobe (Houben & Guillaud, 1994; Olivier & Mesbah, 1970; Yetgin et al., 2008).

Straw has been widely used since Neolithic times to control the volumetric stability of adobe and to hinder cracking upon drying of the adobe mixture by the distribution of tension arising during the shrinkage of the adobe mixture (Abanto et al., 2017; Calatan et al., 2016; Schroeder, 2015). The amount of straw used in adobe is observed to be in the range of 0.15%-3% by weight in some studies, while the optimum ratio is in the range of 1%-2% by weight (Binici et al., 2005; Meriç et al., 2017; Serrano et al., 2016; Turanli, 1985; Yüncü et al., 2014). The length of fibre varies in the range of 2 -5 cm (Berardi & Iannace, 2015; Güdücü, 2003; Yetgin et al., 2008).

Lime (CaO or Ca(OH)$_2$ is one of the oldest additives used in adobe mixtures in Anatolian territories, since ancient Greek and Roman times (for over 2000 years), to enhance mechanical strength such as compressive strength and shear strength and water impermeability of adobe materials (Al-Ajmi et al., 2016; Bell, 1996; Binici et al., 2007, 2009; Calkins, 2008; Love, 2012; Meriç et al., 2017; Norton, 1997; Pekmezci et al., 2012; Pekrioglu Balkis, 2017). In addition, calcium carbonate in clay content is detected in adobe samples belonging to Neolithic times (F. Erol et al., 2022; Love, 2012). By the ion exchange, the Ca$^{2+}$ ions of lime exchange with H$^+$ and Na$^+$ ions in the adobe mixture result in the flocculation of clay particles that lead to a reduction in the shrinkage ratio of and the plasticity of adobe soil (Kıvrak, 2007). The other additive generally used, gypsum, in adobe, causes the flocculation of clay particles by the ion exchange with the Ca$^{2+}$ ions of gypsum in the same manner and decreases the curing time of adobe which gains its rigidity in a short time and controls the shrinkage (Gürfidan, 2006; Işık & Tulbentci, 2008; Kafescioğlu et al., 1980; Kafescioğlu, 2016; Pekmezci et al., 2012).

Lime does not have a cement content, but it has a pozzolanic reaction with pozzolans or clay minerals in the presence of water or high humidity, and the stable and insoluble compounds possessing hydraulic cementitious properties are formed (Torraca, 1988). In addition, the carbonation of lime over time increases the compressive strength of adobe (Kıvrak, 2007). To sum up, the use of lime up to a certain limit in adobe provides to improves mechanical strength such as compressive

strength and shear strength, and water resistance and it decreases shrinkage (Al-Ajmi et al., 2016; Pekmezci et al., 2012). The lime has the pozzolanic reaction far more quickly with montmorillonite clays than with kaolinites (Bell, 1996). Some studies on adobe and soil stabilization with lime indicate that the optimum ratio for lime is 4% and 5% to provide an improvement in compressive strength performance. The other optimum ratios are 3% and 5% to control the swelling problem (Bell, 1996; Dash & Hussain, 2012; Kafescioğlu, 2016; Kafescioğlu et al., 1980; Pashabavandpouri & Jahangiri, 2015). Nano-sized lime (Nano-CaO) is also used for the stabilization of soil. Some studies indicate that the adequate amount for the Nano-CaO is determined as 1% for the improvement of compressive strength and plastic limit of soil samples (Choobbasti et al., 2019; Yazarloo et al., 2017).

According to the ASTM C125-20:2020 standard (ASTM, 2020), a pozzolan is identified as "a siliceous and aluminous material which, in itself, possesses little or no cementitious value but which will, in finely divided form in the presence of moisture, react chemically with calcium hydroxide at ordinary temperature to form compounds possessing cementitious properties". Pozzolanic activity means that the reaction ability of those materials with calcium hydroxide ($Ca(OH)_2$) leads to the form of a network of fibrous crystals or gelatinous amorphous materials of calcium–silicate-hydrate (C-S-H) that increases the mechanical strength and reduce the susceptibility of adobe against to water. (Norton, 1997). In addition, high pozzolanic soil samples indicate their high bonding capacity and high durability performances. The pozzolanic activity enhances the straw cohesion to the adobe matrix and enough adhesion of the fibres slows down the water penetration (Ouedraogo et al., 2019; Sharma et al., 2016). The reaction of lime with the clay minerals is slow. Therefore, the presence of natural pozzolan sources such as volcanic (pumice and tuffs) and diatomaceous soils (opal A) and naturally fired clays (metakaolin) in the soil sources is critical for the enhancing the pozzolanic activity of the soil sources (Lea, 1976).

**2.3    Clay**

Clay minerals consisting of a layered structure are formed by the chemical weathering of silicate minerals such as quartz, feldspar, and mica. The clay minerals, aluminosilicates, are generally termed phyllosilicates. The layered structure of clay minerals includes silicon-oxygen and aluminium-/magnesium-oxygen sheets (Tombácz, 2003). Those clay minerals are described based on their structures' configuration of tetrahedral and octahedral layers. Two sheets of silicate (tetrahedral sheet) and alumina/ magnesia (octahedral sheet) form a clay layer (Tombácz, 2003; Uddin, 2008) (Figure 2.10). The parallel clay layers are connected by the electrostatic force due to cations such as sodium (Na), calcium (Ca), potassium (K), magnesium (Mg) and iron (Fe), or Van der Waals force, or hydrogen bond (Houben & Guillaud, 1994; Keefe, 2005; Uddin, 2008) (Figure 2.10). Clay minerals are classified into four main groups: kaolinite, illite, smectite and chlorite (Houben & Guillaud, 1994; Uddin, 2008) (Figure 2.10 and Table 2.3):

— Kaolinite group: The clay mineral includes one tetrahedral silica sheet and one octahedral alumina or magnesia sheet in each layer that is named a 1:1 type. The clay layers are tightly bonded to each other by hydrogen bonding which constrains expansion (Barton & Karathanasis, 2002); therefore, that group is defined as non-expansive in contact with water.

— Smectite group: The clay mineral is composed of one octahedral alumina or magnesia sheet between two tetrahedral silicate sheets named a 2:1 type. Smectite layers contain exchangeable cations such as Ca, Na, Mg and K in the interlayer spaces (Velde & Meunier, 2008). Those inorganic cations can be exchanged by other inorganic and organic cations or water (Chen et al., 2008; Yu et al., 2014). The swelling potential of that clay group is affected when water and those cations penetrate through interlayer gaps. While the layers of smectites are held together by van der Waals and cations bondings in a limited strength in a dry state of clay, the clay swells dramatically when

22

water enters into the interlayer space between sheets and breaks those bonds (Barton & Karathanasis, 2002). Therefore, that group is named as expansive clay type.

— Illite-mica group: The structure of the clay mineral is similar to the stacking sequence of the smectite group in terms of one octahedral alumina or magnesia sheet in between two tetrahedral silicate sheets. The presence of dominantly low exchangeable potassium cations (K) content as an interlayer limits the swelling of the clays (Jawaid et al., 2016); therefore, that group is less expansive compared to the smectite group when in contact with water.

— Chlorite group: The clay mineral is formed of one octahedral alumina or magnesia sheet between two tetrahedral silicate sheets similar to the illite/mica group. On the other hand, the chlorite clay layers are separated by an additional hydroxyl (OH) interlayer (brucite layer) as an octahedral layer (Gazzè et al., 2014). The chlorite group is named the 2:1:1 type, an alteration of the 2:1 group (Gazzè et al., 2014). The presence of the hydroxyl layer controls the swelling of the clay. The expansion of the chlorites is near to the illite-mica group but less than the smectite group (Jawaid et al., 2016).
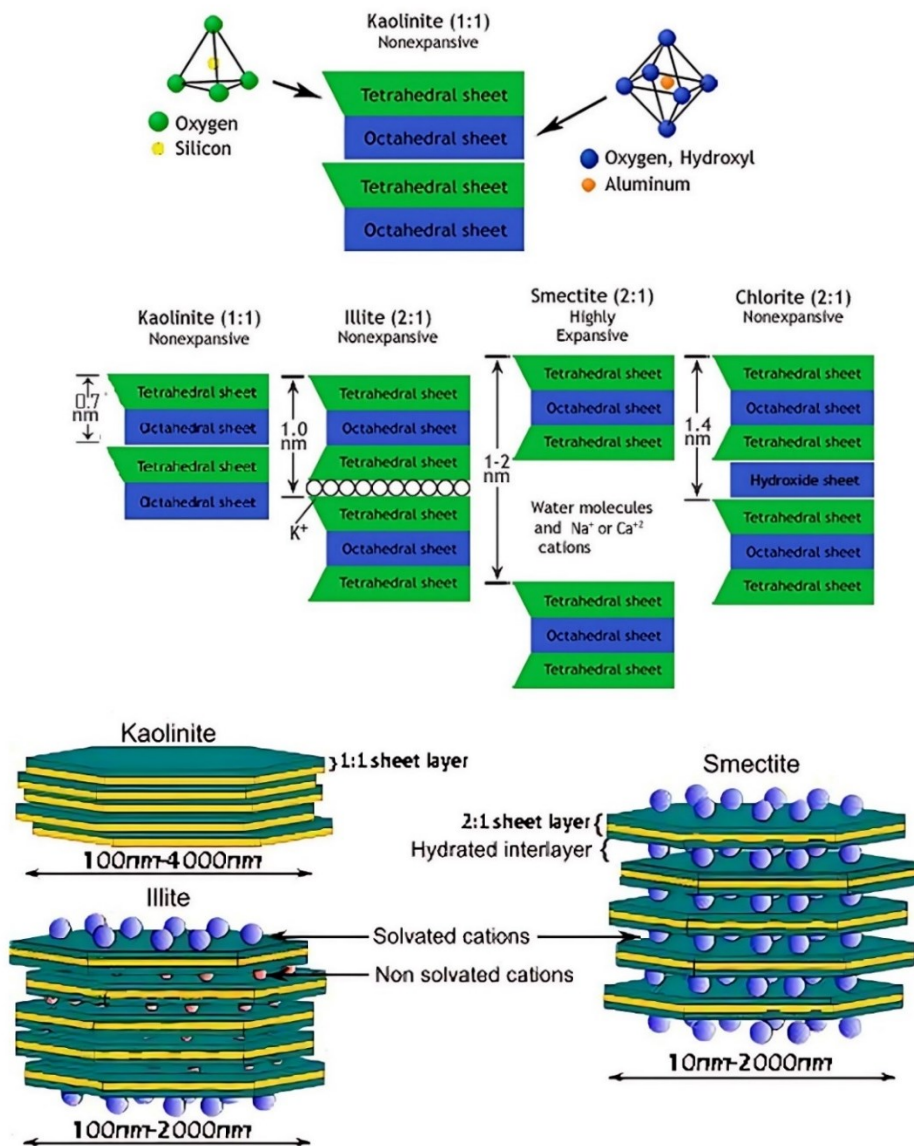
Figure 2.10 Structures of clay minerals (*Clay Minerals and Related Properties*, 2015; Tournassat et al., 2015).

24

Table 2.3 Classification of clay minerals and their major groups (Reeves et al., 2006).

| Group | Members | Property | Sheet type | Tetrahedral-octahedral sheet arrangement | General formula |
|---|---|---|---|---|---|
| Kaolinite-serpentine | Lizardite, berthierine, amesite, cronstedtite, nepouite, kellyite, fraipontite, brindleyite, kaolinite, dickite, nacrite, halloysite, odinite, serpentine | Non-expansive | 1:1 | T:O | $Al_2Si_2O_5(OH)_4$ |
| Illite-mica | Biotite, phlogopite, lepidolite, muscovite, illite, glauconite, celadonite, paragonite, clintonite, kinoshitalite, bityite, anandite, margarite | Non-expansive | 2:1 | T:O: T | $(K, H)Al_2(Si,Al)_4O_{10}(OH)_2XH_2O$<br><br>X represents varying level of water attached to the mineral |
| Smectite | Saponite, hetorite, sauconite, stevensite, swinefordite, montmorillonite, beidellite, nontronite, volkonskoite, bentonite, vermiculite, talc, pyrophyllite. | Expansive | 2:1 | T:O:T | $(Ca,Na,H)(Al,Mg,Fe,Zn)_2(Si, Al)_4O_{10}(OH)_2 \ XH_2O$<br><br>X represents the various levels of water attached to the mineral. |
| Chlorite | Amesite, chamosite, cookeite, nimite, daphnite, Clinochlore | Non-expansive | 2:1:1 | T:O: T | $(Ni, Mg, Fe, Al)_6(Al, Si)_4O_{10}(OH)_8$ |

### 2.3.1     Clay Particles Associations
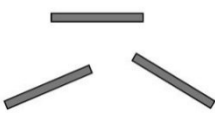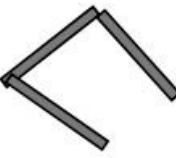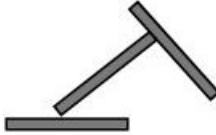
The clay particles are controlled by electrostatic interactions 'attractive or repulsive' between particles due to their cation exchange capacities and the attractive Van der Waals forces on the particles (Hillier, 1995). Clay particles associate in dispersed,

flocculated and aggregated configurations by those interactions. According to Van Olphen (1964), different modes of clay particle contact may occur in those associations: no face-to-face, face-to-face (FF), edge-to-face (EF), and edge-to-edge (EE) (Table 2.4).

- In the dispersed clay association, loose and easily disrupted clay particles move away from each other since the electrical forces between clay surfaces are repulsive (Du et al., 2009; Tuncan, 1992).

- The flocculated clay association includes particles connected edge-to-edge (EE) or/and edge-to-face (EF). That association causes the formation of lower-density clay particles three-dimensional voluminous such as "house-of-cards" (Du et al., 2009; Luckham & Rossi, 1999). Clay minerals have negatively charged surfaces whereas charges at the edge sites change depending on the broken bonds and pH properties of the medium (Hillier, 1995). The charges of the edges become mostly positive at the medium in low pH due to the adsorption of $H^+$ ions that cause more EF configurations. of the clay particles. The charges of the edges are more negative probability at the medium in high pH due to the adsorption of $OH^-$ ions (Hillier, 1995).

- Aggregated clay association is formed by collapsing parallel clay particles that are face-to-face (FF) connected and spaced 20 Å or less apart (Luckham & Rossi, 1999). The highest van der Waals interaction energy is present between the FF-connected clay particles (Hillier, 1995). Aggregated clay association results in thicker particles of higher density (Ravisangar et al., 2005).

In short, the aggregated clay association provides particles having denser structures and higher bonding strength to each other; on the other hand, flocculated clay association leads to obtaining the less dense, and more porous structured clay particles having a weak connection between them.

Table 2.4 Modes of clay particles associations according to the terminology of Van Olphen (Van Olphen, 1964).

| Dispersed | Flocculated | | Aggregated |
|---|---|---|---|
| no face-to-face | edge-to-edge contact (EE) | edge-to-face contact (EF) | face-to-face contact (FF) |
|  |  |  |  |

### 2.3.1    Cation Exchange Capacity (CEC)

Clay minerals have negatively charged surfaces. Those clay minerals pull cations such as $Ca^2$, $Mg^+$ and $H^+$ ions in the water. Cation Exchange Capacity (CEC) is the ability of the clay to adsorb those cations. CEC properties of clay minerals depend on the clay type, the specific surface area of the clays and interlayer spacings between their sheets (Figure 2.11 and Table 2.5). For instance, smectites have internal and external surface areas while kaolinites have no measurable internal surface area; therefore, smectites have a higher ratio of their surface area to volume than kaolinite minerals. That means smectites have higher CEC properties than kaolinite clays.
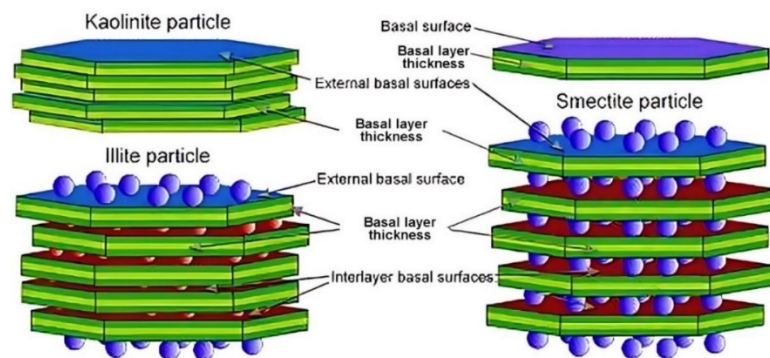


Figure 2.11 Schematic illustration of basal surfaces and basal layer thicknesses of kaolinite, illite, and smectite clays (Tournassat et al., 2015).

Table 2.5 Some physical properties determining the cation exchange capacity (CEC) of clays and their CEC values (Grim, 1968; Reeves et al., 2006).

| Property | Clay mineral | | | |
|---|---|---|---|---|
| | Kaolinite | Illite | Smectite | Chlorite |
| Basal Surface (Planar) diameter (nm) | 100-4000 | 100-2000 | 10-2000 | 100-2000 |
| Basal layer thickness (nm) | 0.7 | 1 | 1 | 1.4 |
| Specific surface ($m^2/g$) | 5-20 | 80-120 | 700-800 | 8 |
| Cation exchange capacity (meq/100g) | 3-15 | 15-40 10-40 | 80-100 80-150 | 20-40 10-40 |

The larger the specific surface area of clay, the higher the internal cohesive forces of clays which are relevant for the binding force and the compressive and tensile strength of adobe (Minke, 2009). On the other hand, smectite's higher specific surface areas and cation exchange capacity lead to high water absorption capacity. Therefore, the presence of illite and kaolinite clay types dominantly in adobe soil provides to control swelling and shrinkage problems (Torraca, 1988). In addition, the smectite clay particles have the highest dispersion characteristics due to their highest cation exchange capacity. The dispersion degree of illite- and chlorite-type clays is intermediate between smectite- and kaolinite-type clays (Rolfe et al., 1960).

### 2.3.1 Methylene Blue Test

The methylene blue (MB) test is used to identify the cation exchange capacity (CEC) and specific surface area of clay minerals (Arab et al., 2015; Hang & Brindley, 1970; Petkovšek et al., 2010).

The methylene blue ($C_{16}H_{18}ClN_3S$) is an organic dye formed of a positively charged ion ($MB^+$ cation) and a negatively charged ion ($Cl^-$ anion) (Verhoef et al., 1992). As methylene blue solution and diluted clay are mixed, the positive ion of MB replaces the cations on the external surface of the clay and then within interlayers of clay

silicate sheets. In other words, MB is adsorbed onto the negatively charged surfaces of clay silicates. Exchangeable cations replace methylene blue and clay as demonstrated below:

Ca-Na Clay + MB hydrochloride $\longrightarrow$ MB Clay + Ca-Na Chloride
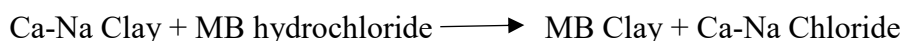
The process of cation replacement continues until all positive ions on and within clay silicates are replaced with MB cations.

## 2.4    Nano-Clay

The International Organization for Standardization (ISO) identifies the Nano-sized material as "material with any external dimension in the nanoscale or having an internal structure or surface structure in the nanoscale". The nanoscale is accepted as nearly in the range of 1 nm to 100 nm (ISO/TR, 2017). As shown in Figure 2.11 and Table 2.5, the clay minerals have a basal surface diameter of the sheets between 100nm and 4000nm, while the thickness of the sheets and their inter-layer spaces are between 0.7 and 2 nm within the nanoscale range. According to the ISO/TR 18401:2017 (ISO/TR, 2017), clay minerals are nanomaterial; therefore, the terms 'clay minerals' and 'Nano-clay' are interchangeable (Kertmen et al., 2020).

Nano-particles gain different qualities of the material's performances by size and shape-dependent properties such as their high specific surface area and a higher number of atoms at the surface (Gieseler et al., 2014; Hunyadi Murph et al., 2017). Nanotechnology is in the science fields of chemistry, biology, physics, material science and engineering that deals with Nano-sized particles to create materials with novel properties and functions (Gieseler et al., 2014; Sanchez & Sobolev, 2010). In this respect, nanotechnology has been excessively used in construction materials such as some cementitious composites, corrosion-resistant steel, heat and sound insulation and fire retardant materials, self-cleaning and colour-changing surface coatings/films/paints/adhesives, improved mechanical properties of building materials, thermal resistance performance, water impermeability and surface wear

resistance; Nanosensors and devices used for health monitoring and damage detection in concrete structures to improve performance properties such as resistance and reduction of $CO_2$ pollution (Khandve, 2014; Pacheco-Torgal & Jalali, 2011).

In this regard, "Nano-clay" is one of the remarkable inorganic raw materials that can be used as Nano additives/binders/fillers within polymer matrix/components to produce nanocomposite construction materials (Pacheco-Torgal & Jalali, 2011). RILEM, the International Union of Laboratories and Experts in Construction Materials, Systems and Structures, is interested in the use of nanotechnology for building materials as well as, the production of qualified earth-based construction materials. To support the research and development of standards, two technical committees in RILEM were established and the report "TC 197-NCM: Nanotechnology in Construction Materials" and the book "RILEM TC 274-TCE: Testing and Characterisation of Earth-based Building Materials and Elements" were published in 2004 and 2016, respectively. Although there is an emphasis on the use of Nano-clay in the construction materials area, the studies on the use of Nano-clay for stabilization of adobe are very limited in number (Niroumand et al., 2013).

The studies in a few numbers focused on two criteria, the type of clay and Nano-clay additive in the adobe mixture, and the amount of Nano-clay additive. In an experimental study, non-expansive clay, Nano-kaolinite was added to the adobe mixture as an additive, and five times higher compressive strength was provided by adding 5% Nano-sized kaolin to the reference adobe mixture (Niroumand et al., 2013). The use of non-expansive Nano-clay type as an additive in soil mixtures improves the dimensional stability and mechanical properties of the clay-rich soil, and a small amount of Nano-sized kaolinite significantly improves the geotechnical properties of kaolinite clay. For instance, after the addition of 3% Nano-sized kaolinite (by weight) to the kaolinite clay content and its compaction, higher dry density and lower hydraulic conductivity are achieved which signalling a reduction in air voids (Zainuddin et al., 2015). A similar study shows that the plasticity value, optimum moisture content and hydraulic conductivity value decrease and liquid

limit, plastic limit and maximum dry density slightly increase, after the addition of 3% Nano-sized kaolinite to the kaolinite clay content (Khalid et al., 2014). On the other hand, the plasticity and swelling behaviour of clay-rich soil increases with the addition of montmorillonite, expansive clay, which is not a preferable performance for adobe materials. Putting Nano-montmorillonite content exceeding 0.3% in residual soil including montmorillonite clay increases noticeably the total volume behaviour and; therefore, lowers the hydraulic conductivity of the soil (Azzam et al., 2013; Taha, 2018). In another study, drying cracks and self-healing properties of these soils were investigated by the addition of Nano-montmorillonite to kaolinite-rich soil and another soil containing clay in 60% (Tabassum & Bheemasetti, 2020). The threshold value for the montmorillonite additive was found as 5%. The self-healing properties increased with that amount of additive in both soils; however, it was stated that crack formations increased significantly in soils containing montmorillonite additives above that ratio.

## 2.5    Nano-Clay Production

Nano-clay production can be achieved by clay dispersion using mechanical and chemical treatments in the literature on the development of Nano-clay production methods. Those treatments are:

— Ultrasonic treatment: Ultrasonic bath or ultrasonic horn/sonicator instruments convert the electrical energy into high-frequency vibrations and clay particles are separated from each other by these vibrations (Niu et al., 2021; Poli et al., 2008).

— Grinding treatment: The clay minerals are broken up by a grinding instrument with high energy impact and friction effect to make it Nano-sized (Pérez-Maqueda et al., 2004).

— High shear mixer treatment: The device with high-speed rotors forms water turbulence at a level to create intense shear forces between clay phyllosilicates, thus ensuring the separation of clay layers (Janica et al., 2018; Li et al., 2015).

— Chemical dispersion treatment: Adding chemical dispersants such as Calgon (sodium hexametaphosphate), ethyl alcohol or glycerine to the distilled water in which the clay is present provides the separation of the clay layers (Tan et al., 2017).

Within the scope of Nano-clay production, there are two prominent issues in determining which of those treatments is the most appropriate method. The first one is to enable the production of more Nano-clay with less energy, which can be called the efficiency of the method. The second one is not to change the properties of the clay particles during the Nano-clay production process. The chemical dispersion method based on the use of chemical dispersants can change the properties of clay particles. For example, the cation exchange capacity and swelling properties of clays can increase with positively charged ions in chemical dispersants (Tan et al., 2017). Using the grinding instrument or the high-shear mixer requires much more energy consumption to break up and disperse the clay particles than the ultrasonic treatment (Figure 2.12). With the ultrasonic process, vibrations at high frequencies are transmitted to the water, creating small bubbles in the water, causing "sonic cavitation" as these bubbles burst, which separates the flocculated Nano-clay particles. The ultrasonic process does not cause an effect that changes the original properties of the clay. For instance, while the clay retains its plate-like morphological shape in ultrasonic treatment, the grinding process results in structural damage and changes in the clay particles (Pérez-Maqueda et al., 2004). The "ultrasonic treatment" is understood to be superior to the performances of the others as it is the most efficient method in terms of preserving the original properties of the clay during Nano-clay production and production in higher amounts of Nano-clay with low energy (Garrison, 2003; Hoke et al., 2014; Lam et al., 2005; Pérez-Rodríguez et al., 2006), as well as it provides to achieve Nano-clay with smaller particle size compared to the production of the other methods (Janica et al., 2018; Li et al., 2015; Pérez-Maqueda et al., 2004).
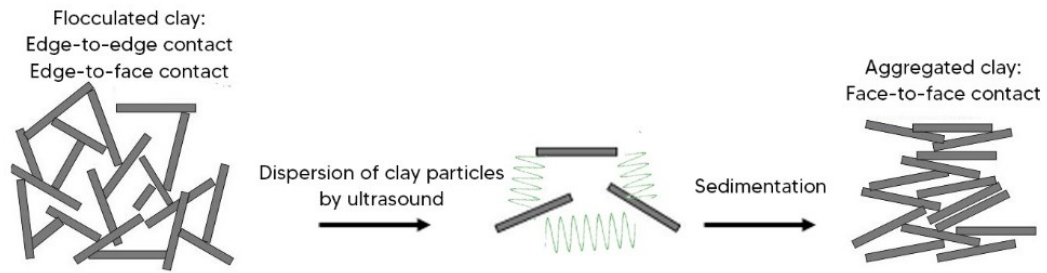
Figure 2.12 Flocculation and dispersion of clay particles by ultrasound (Adapted from Jamila & Zoukaghe, 2016).

## 2.6 Particle Size Distribution

Classification of the particle size distribution termed as clay, silt, sand, gravel and cobble are conducted regarding the standards and scales (Figure 2.13). Clay and silt content enhance compressive strength by improving the binding force between aggregates in adobe. The use of gravel size above 2mm in adobe contributes to its volume stability and, therefore, to the long-term durability of adobe material (Stefanidou & Papayianni, 2005). There is no universal consent for the scale or standard for the particle size due to the different acceptances by different scientific disciplines (Guggenheim et al., 1995). For instance, the clay is accepted below 4 μm in sedimentology and Udden and Wentworth scale (Tucker, 2001); in geology and soil science and TS EN ISO 14688-1:2018 Turkish standard (TS EN ISO, 2018), the size used is below 2 μm; and in colloid science, it is below 1 μm.

Figure 2.13 Soil classification by particle size (in millimetres) according to various standards and the scale.

Soil texture is defined according to the soil texture triangle organised by the United States Department of Agriculture (USDA) (Figure 2.14). Here, the percentages of clay, silt and sand can be followed on the three axes of the triangle. The adobe is a field-dependent material, but the RILEM Technical Committee 274-TCE (Fabbri et al., 2021) indicates a proper region for the adobe mixture shown with the dotted line in the soil texture triangle. There is no one standard or optimisation for the particle size distribution and preparation of adobe mixture. Therefore, there are various data accepted as recommended ranges for clay, silt and sand-gravel contents for adobe soil, as seen in Table 2.6.
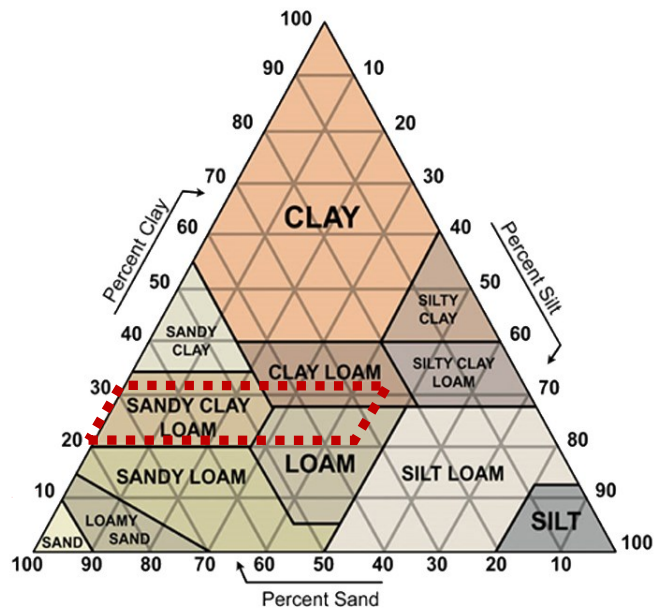
Figure 2.14 The soil texture triangle (United States Department of Agriculture - USDA) showing the soil classification system and the proper region for the adobe soil shown in red dotted line (Fabbri et al., 2021).

Table 2.6 Ranges of clay, silt and sand-gravel contents in soil mixture recommended to produce adobe masonry units.

| Reference | Clay Ratio, % | Silt Ratio, % | Sand-Gravel Ratio, % |
|---|---|---|---|
| Arizona University (Schwalen, 1935 in Kafescioğlu et al., 1980) | 13 | 25 | 62 |
| Australia Standards (Walker, 2001) | 10-40 | 10-30 | 30-75 |
| (Norton, 1997) | 15-30 | 10-30 | 40-75 |

Analyses on the particle size above 63 microns are conducted by the dry- and wet-sieving methods while for the particle size distribution of silt and clay aggregates below 63μm, sedimentation methods such as pipette, hydrometer and centrifuge are used. The theory of sedimentation methods is based on Stokes Law. This law deals with the settling down of suspended fine particles such as the clay and silt minerals in a liquid due to gravity. By considering all forces affecting the particles during the

move of particles downward in the liquid, the Equation 1 was generated as follows (Garrison, 2016):

$$v = g(\rho_s - \rho_i)X^2/18\eta \qquad\qquad 1$$

Where v is the settling velocity of the particle in mm/s; $\rho_S$ and $\rho_i$ are densities of the particle and liquid, respectively, in kg/m$^3$; X is the diameter of the particle in mm; $\eta$ is the viscosity of the liquid in kg/s/m; g is the gravity accepted as 9.8 m/s$^2$.

The sedimentation methods of pipette and hydrometer are generally used; on the other hand, those methods consume significant time, especially for clay sedimentation (Rockwell, 2000). In centrifugal sedimentation, the centrifuge instrument operates centrifugal force to separate the particles in liquid by rotating the centrifuge tubes in containers at high speed around an axis. During the rotation, the denser particles act outward in the radial direction, while the less dense particles are relocated and go toward the centre. The settlement time of the particles depends on their size, density, liquid viscosity, radius of rotation and rotation speed which is termed as revolutions per minute (rpm). Centrifugal sedimentation is preferable to pipette and hydrometer methods in terms of more rapid method (Fredericks, & Poppe, n.d.; Jackson, 1969).

In addition, the particle size distribution of soils including gypsum pre-treated with some chemicals such as barium chloride (BaCl$_2$) to dissolve gypsum in the soil as a standard method because gypsum prevents the dispersion of the clay, and clay minerals are flocculated. On the other hand, by those standard methods, the particle size distribution of that pre-treated soil sample without gypsum demonstrates only insoluble minerals, and this causes deflection of real results. In a study, a method was developed, that is sonication of the sample in an ethanol solution to include the gypsum particles in the particle size distribution analyses (Pearson et al., 2015).

## 2.7    Consistency Limits and Linear Shrinkage Ratio

The soil has various phases depending on its water content such as liquid, plastic, semisolid and solid. Consistency limits, namely the Atterberg limits are a measure of the critical water contents of soil to define the limits between those phases. The Atterberg limits involve liquid limit (LL), plastic limit (PL) and shrinkage limit (SL) (Figure 2.15).
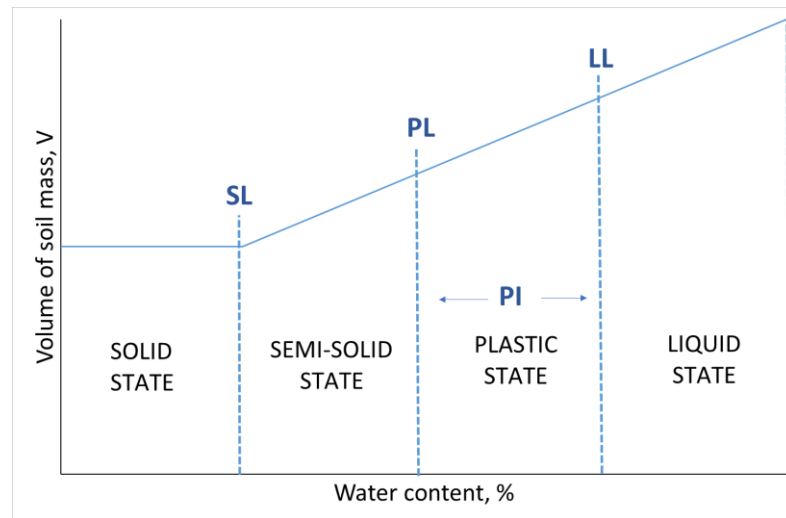


Figure 2.15 Atterberg limits at various phases of soil.

Those limits are expressed as percentage values. The water content of LL describes the transfer of the soil from plastic to a liquid consistency. The moisture content of PL defines its alteration from plastic to semisolid consistency. The difference between LL and PL is the plasticity index (PI=LL-PL). PI defines the level of plasticity of soil, and plasticity is the ability of materials to keep a deformation without rupture. PI is directly related to the workability of adobe soil (Delgado & Cañas, 2007; Schroeder, 2015). The moisture contents of SL identify the change of soil from a semisolid to a solid consistency. Similarly, the linear shrinkage (LS) ratio is the decrease in the length of a soil sample while it is drying out from a semisolid to a solid consistency. SL indicates the volume decrease during this transition while

LS expresses the decrease in one length of the soil sample. Those two limits provide to quantify the amount of shrinkage that is experienced by clayey soil. Some classifications based on linear shrinkage ratio values are given in Table 2.7. The linear shrinkage above 8%, is defined as the critical level at which possible of a cracking problem can be observed (Dawson et al., 1956).

Table 2.7 Some classifications based on linear shrinkage ratio values.

| LS ratio% | Comment | LS ratio% | Comment |
|-----------|---------|-----------|---------|
| <1.7 | Too sandy | <5 | Non-critical |
| 3.3-6.6 | Recommended | 5-8 | Marginal |
| >10 | Too clayey | >8 | Critical |
| (Harries & Sharma, 2020) | | (Dawson et al., 1956) | |

After achieving the LL and PI values, soil type can be classified in detail by the Casagrande plasticity chart (Figure 2.16). That chat was developed by Arthur Casagrande and then was adapted to a unified soil classification system (UCS) (ASTM, 2017a). Soil samples can be categorised by the position of the sample in reference to the A-line. Points plotted above the A-line in the chart are inorganic clays while points below the A-line indicate inorganic silt, organic silts or organic clays. That chart also shows the ranges of plasticity/compressibility and shrinkage potential of the soil samples.
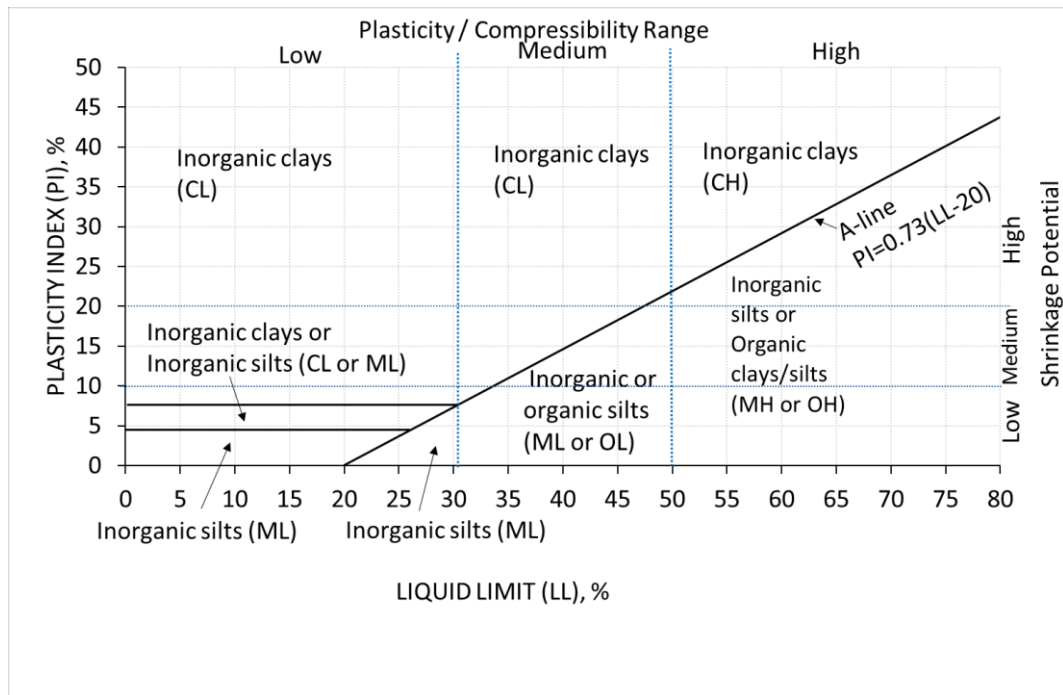
Figure 2.16 Casagrande plasticity chart showing unified soil classification together with their symbols (CL: Inorganic clay (lean clay); ML: Inorganic silt; OL: Organic clay (on or above A-line )-Organic silt (below A-line); CH: Inorganic clay (fat clay); MH: Inorganic silt (elastic silt); OH: Organic clay (on or above A-line) – Organic silt (below A-line) (ASTM, 2017a; Fabbri et al., 2021).

The acceptable range of LL values for the adobe brick is 31%–50% and its recommended range for the PI is 16%–33% (Delgado & Cañas, 2007; Houben & Guillaud, 1994). Soil having a low liquid limit or low plasticity signals its high water permeability characteristic and a high liquid limit or high plasticity means that it has little water permeability (Nwanosike et al., 2015). The PI values indicate the shrinkage potential of the soil sample.

## 2.8    Water Vapour Permeability

Water vapour permeability is the ability of the adobe material to allow water vapour to transfer through a route of interconnected pores. It is indicated if the pore sizes in the material are above 1 μm, water vapour can pass through their porous structure, but if they are below 1 μm, water vapour transmission has difficulty during the

moving through that structure (Lawrence, 1998). In addition, some studies remark that an increase in the clay content ratio in the adobe mixture decreases the vapour permeability (Dondi et al., 2003; Maillard & Aubert, 2014).

The water vapour permeability characteristics of the adobe are defined with the parameters of "water vapour resistance factor ($\mu$, unitless)" and "equivalent air thickness of water vapour permeability (SD, m)". Those parameters in high values mean more water vapour resistive material. According to the TS EN 1062-1:2006 standard, the SD values: if below 0.14 m shows high water vapour permeability of the material; above 1.4 m means low water vapour permeability; in the range between 0.14m and 1.4m is defined as the medium vapour permeable (TS EN, 2006). The $\mu$ and SD values of some adobe samples are given in Table 2.8. It is observed that adobe materials have a wide range of water vapour resistance factors. Those adobe samples have high and medium water vapour permeability properties and also have sufficient water vapour permanence.

Table 2.8 Literature data on water vapour permeability characteristics of adobe samples in terms of SD and $\mu$ values.

| Reference | Sample/Working area | $\mu$ value (unit less) | SD value (m) | Method |
|---|---|---|---|---|
| (Akkuzugil, 1997) | Traditional adobe sample/Ankara | 2.09 | 0.03 | Wet cup |
| (Ergin-Oruç, 2004) | Traditional adobe sample/Diyarbakır | 16-18 | 0.19-0.20 | Dry cup |
| (Güdücü, 2003) | Adobe sample/Archaeological site in Çorum (Ortaköy) | 0.99-0.57 | 0.02 | Wet cup |
| (Meric et al., 2013) | Traditional adobe sample/ Ankara | 1.4-1.6 | 0.04 | Wet cup |
| (Maillard & Aubert, 2014) | Adobe sample produced in a laboratory | 19-44 | 0.19-0.44 | Dry cup |
| (Yüncü, 2016) | Traditional adobe sample/Kırıkkale | 3.30 – 3.80 | 0.59 – 0.69 | Wet cup |

## 2.9 Mechanical Strength Properties

Some mechanical properties of the adobe material are flexural strength and compressive strength. The flexural strength ($\sigma_f$) specified by the three-point bending test is the ability of the material to resist bending load applied perpendicular to its longitudinal axis. The compressive strength ($\sigma_c$) is the maximum compressive load that the sample can withstand until it fractures. Some literature data and requirements/codes belonging to the mechanical strengths of adobe were summarized in Table 2.9 and Table 2.10. In addition, the compressive strengths of fired brick and concrete bricks as alternative materials for adobe bricks are in the ranges between 3.5 MPa and 35 MPa and 21 MPa and 50 MPa, respectively (Hendry et al., 1997; Subedi, 2020). The accepted minimum value of the flexural strength for masonry fired and concrete brick is accepted as 0.65 MPa (BS, 1981; Ramakrishnan et al., 2023).

Table 2.9 Literature data on the mechanical strengths of the adobe sample including some additives.

| Reference | Additives | | Results | |
|---|---|---|---|---|
| | Fibre | Binder | Compressive strength, MPa | Flexural strength, MPa |
| (Baliga & Nayak, 2018) | | 8% - 6% cement and 2% -4% lime (by w.t) | 1.7- 3 | |
| (Calatan et al., 2016) | 3%-15% straw; 10%-60% hemp fibre (by vol.) | | 0.7-2.6 | 1.7-3.1 |
| (Sharma et al., 2016) | 0.5%-2% natural vernacular fibres: Grewia Optivia (Beul) and Pinus Roxburghii (Chir Pine) (by w.t) | 2% cement (by w.t) | 0.95-3 | |
| (Vilane, 2010) | 5%-20% sawdust (by vol.) | 5%-20% molasses, cow-dung, sawdust (by vol.) | 2.8-8.1 | |
| | | 5%-20% Portland cement (OPC) (by vol.) | 11.1 | |
| (Ngowi, 1997) | - | 10%-20% cow-dung; 10%-20% bitumen; 5%-15% lime (by vol.) | 1.25-5 | |
| | | 5%-15% Portland cement (by vol.) | 4.55-10.64 | |
| (Pekrioglu Balkis, 2017) | 0.5% polymer fibre (by w.t) | 0.5%-2.0% waste marble dust; 10% gypsum;2% lime (by w.t) | 1.09-3.47 | 0.8-1.43 |
| (Pekmezci et al., 2012) | | 8%-10% gypsum; 2.5%-5% lime (by w.t) | 2.4-2.9 | |
| (Costi de Castrillo et al., 2021) | 30% -70% sawdust and straw (by vol.) | | 0.76-7.32 | 0.44-4.25 |
| (Limami et al., 2021) | 1%-20% Typha fibre (by vol.) | | 3.55-6.28 | |
| (Babé et al., 2020) | 1%- 4 % millet waste (by w.t) | | 3.67-6.5 | 0.9-4.5 |
| (Millogo et al., 2014) | 0.2%–0.8% Hibiscuscannabinus fibres (by w.t) | | 1.8-2.9 | 0.25-1.1 |
| (Binici et al., 2005) | 0.1% plastic fibre (by w.t) | 15% pumice + 10 % cement + 2% lime +3% gypsum (by w.t) | 5.1 | |
| (Pedergnana & Elias-Ozkan, 2021) | 0.2 %-4.9% chaw, straw, pine needle, flax, cow hair, long wool and short wool (by w.t) | | 0.79-4.31 | 0.58-1.60 |

Table 2.10 The requirements of compressive and flexural strengths of adobe in some codes.

| Normative document | | | Compressive strength, MPa | | Flexural strength, MPa |
|---|---|---|---|---|---|
| | | | Min. | Avg. | Min. |
| (DIN, 2018) (Germany) | Compressive strength class | 2 | 2 | 2.5 | |
| | | 3 | 3 | 3.8 | |
| | | 4 | 4 | 5 | |
| | | 5 | 5 | 6.3 | |
| | | 6 | 6 | 7.5 | |
| (IBC, 2018) (International Building Code) | | | 1.72 | 2.07 | 0.24 (average 0.35) |
| (NMAC, 2015) | | | 1.73 | 2.07 | 0.34 |
| (Federal Republic of Nigeria, 2006) | | | 1.60 | 1.70-2.75 | - |
| (NZS, 2020) (New Zeland) | | | 1.3 | - | 0.25 |
| (NTE, 2000) (Peru) | | | 1.18 | - | - |
| (IBC, 2021)(Pakistan) | | | 1.72 | 2.07 | |
| (Walker, 2001) (International Standards Australia) | | | 1.15 | | |

## 2.10   Capillary Water Absorption

Capillary water absorption (sorptivity) is the moving up of water through interconnected micropores (effective porosity) in adobe soil, as the surface tension (capillary force) of the soil particles is stronger than the gravity force (Hall & Hoff, 2002). The rise of water through micropores reduces the particles' surface tension and so the mechanical strength of adobe material (Fabbri et al., 2021). When the adobe is in contact with excess water, the clay completely disperses and it is eroded. Therefore, direct exposure to rain or the formation of running water in contact with the wall is the weathering agent for the adobe wall (Torraca, 1988).

Capillary water absorption is directly related to the porosity of the adobe samples (Zhao et al., 2019). Another significant factor for capillary absorption is the pozzolanic activity making the less porous structure of the adobe sample more impermeable (Villagrán-Zaccardi et al., 2021).

The capillary water absorption test simulates the movement of the capillary water from the foundation to the adobe walls. By this test, the capillary water absorption value, one of the achieved parameters, is the maximum quantity of water absorbed by adobe material immersed in the water at a defined time (Hall & Hoff, 2002). The other parameter, the capillary water absorption coefficient, depends on the quantity of water that can be absorbed over a defined period (Hall & Hoff, 2002). The capillary water absorption coefficient values of some adobe samples in the literature are given in Table 2.11.

Table 2.11 Literature data on capillary water absorption coefficient of adobe samples.

| Reference | Additive | Capillary water absorption coefficient | Units |
|---|---|---|---|
| (Lanzón & García-Ruiz, 2009) | Water repellents: stearates, oleates, silanes, silicone films | 0.1-1 | $kg/m^2.min^{0.5}$ |
| (Türkmen et al., 2017) | Reference sample | 1.8-2.3 | $kg/m^2.min^{0.5}$ |
| | Gypsum, slag | 1.6-2.1 | |
| (Baliga & Nayak, 2018) | Cement, lime, granite sludge | 0.39-1.20 | $kg/m^2.min$ |
| (Costi de Castrillo et al., 2021) | Reference sample | 0.06-0.1 | $kg/m^2.sec^{0.5}$ |
| | Additive: sawdust, straw | 0.007-0.1 | |
| (Olubisi & Humphrey, 2022) | Rice husk, lime | 0.06-0.29 | $kg/m^2.min$ |
| (Ribeiro et al., 2022) | Water repellents: siloxane, linseed oil, beeswax | 0.23-0.46 | $g/cm^2.sec.10^{-3}$ |

In addition, according to the DIN 18945-12:2018 norms, the adobe samples are visually observed at intervals of 30 min, 3 h and 24 h to detect cracks and permanent deformations due to swelling during the capillary water test (DIN, 2018; Muguda et al., 2020), and the classifications of the adobe are conducted according to that evaluation (Table 2.12).

Table 2.12 Classification of compressed adobe bricks according to DIN
18945:2018-12 norms (DIN, 2018).

| Class | Application | Capillary water absorption test (h) |
|-------|-------------|-------------------------------------|
| Ia | External wall exposed to natural weathering | ≥24h |
| Ib | Coated external wall | ≥3h |
| II | Internal Wall | ≥0.5h |
| III | Dry applications | No requirement |

In some studies on the addition of the Nano-clay into cement mortar mixtures, the water absorption coefficients and permeabilities of cement mortars were observed to be decreased by the blocking of the capillary pores with the Nano-clay particles expanded, which results in denser microstructure containing more stable bonding framework (Chang et al., 2007; Irshidat & Al-Saleh, 2018).

# CHAPTER 3

# MATERIAL AND METHODS

The overall research program is defined in Table 3.1. The research involves three main achievements. The first one is the enrichment of the Nano-sized clay content in the existing adobe soil and the development of a practical method for doing that. The second one is the performance assessment of Nano-clay enriched adobe soil, which has a particle size below 425 μm, and its comparison with the performance of natural adobe soil. The third one is the preparation of some adobe mixtures by using natural adobe soil and Nano-clay riched adobe soil with some additives of Nano-CaO, $Ca(OH)_2$ and straw. Their performance properties were tested to better understand the impact of Nano-clay as the binder and Nano-CaO, and $Ca(OH)_2$ as additives.

These three main studies were conducted in consecutive stages entitled below:

- Identification of local adobe soil/clay resources in terms of compositional and raw materials properties, and consistency limits including practical field soil tests;
- Determination of Nano-clay content in natural adobe soil resources;
- Enrichment of Nano-clay content in natural adobe soil resources and Nano-clay content assessment;
- Performance assessment of Nano-clay riched adobe soil samples (Treated adobe soil samples) by consistency limits;
- Preparation of Nano-clay riched adobe mixtures as adobe product samples (Treated adobe samples);
- Performance assessment of Nano-clay riched adobe product samples (Treated adobe samples) in terms of basic physical and mechanical properties including vapour transmission and capillary water absorption features.

The data obtained at each stage are the basic guiding steps of the next, which are used to plan the next stage of the research. The analyses/tests conducted in those stages are listed in Table 3.1.

Table 3.1 The analyses conducted in consecutive stages together with samples examined in each stage and the main achievements of the research and their outputs.

| The main expected achievements of the research | Consecutive Stages of the Research | | Tests conducted in the Research Stage | Samples examined in the Research stage | Outputs guiding the next research stage |
|---|---|---|---|---|---|
| Enrichment of the Nano-sized clay content in the existing adobe soil and the development of a practical method for doing that | 1 | Identification of local adobe soil/clay resources | Field soil test, pH value and organic, calcite and soluble salt contents tests, XRD analyses | Konya_Küçükköy Çorum_Karapınar Çorum_Kınık Çorum_Sarımbey Manisa_Kemer Eskişehir_Sorkun Eskişehir_Sazak | Selection of adobe soil samples according to Nano-clay enrichment performance properties |
| | 2 | Determination of Nano-clay content in natural adobe soil resources | Particle size distribution including submicron by sieving and centrifuge methods | Konya_Küçükköy Çorum_Karapınar Çorum_Kınık Çorum_Sarımbey Manisa_Kemer | |
| | 3 | Enrichment of Nano-clay content in natural adobe soil resources and Nano-Clay content assessment | Nano-clay production from soil samples by laboratory mixer and ultrasonic bath and methylene blue (MB) tests | Konya_Küçükköy Çorum_Karapınar Çorum_Kınık Çorum_Sarımbey | |
| Performance assessment of Nano-clay enriched adobe soil, and its comparison with the performance of natural adobe soil | 4 | Performance assessment of Nano-clay riched adobe soil samples (Treated adobe soil samples) | Laser diffraction particle size distribution, scanning electron microscope (SEM), transmission electron microscopy (TEM), stereo microscope, simulation (MAUD) and spectrophotometry analyses, mineralogical (by XRD) and elemental (by XRF) composition tests and consistency limits and linear shrinkage ratio tests. | Konya_Küçükköy Çorum_Karapınar Çorum_Kınık Çorum_Sarımbey | Selection of the Nano-clay enriched adobe soil samples to be used for the preparation of the adobe samples |
| Preparation and performance assessment of some adobe samples by using natural adobe soil and Nano-clay riched adobe soil with some additives of Nano-CaO, Ca(OH)$_2$ and straw. | 5 | Preparation of Nano-clay riched adobe mixtures as adobe product samples (Treated adobe samples) | Preparation of treated adobe samples | Konya_Küçükköy Çorum_Karapınar Çorum_Kınık | Discovering the impact of Nano-clay enrichment to achieve the qualified adobe sample |
| | 6 | Performance assessment of Nano-clay riched adobe product samples (Treated adobe samples) | Basic physical, water vapour permeability, mechanical and capillary water absorption tests. | Konya_Küçükköy Çorum_Karapınar Çorum_Kınık | |

Scientific analysis methods, materials and sample preparation to be used within the scope of the research, are explained in the following subheadings.

## 3.1    Materials – Soil Samples

Soil samples were collected as adobe soil/clay resources from the Eskişehir, Manisa, Konya and Çorum cities (Figure 3.1). The soil resources were in the Sorkun and Sazak villages in Mihalıççık/Eskişehir, Kemer village in Salihli/Manisa, and Küçükköy village in Çumra/Konya that is near Çatalhöyük about 2 km, and villages of Karapınar, Kınık and Sarımbey in Çorum. The soil samples were designated with the full names of the city and village, as shown in Table 3.2.



Figure 3.1 Cities and their villages/counties as soil resources and the coordinate data of places in Konya_Küçükköy (at left bottom), Manisa_Kemer (at middle bottom) and Eskişehir_Sazak (at right bottom).

Table 3.2 Designation and photos of the soil samples and where adobe soil/clay collected.

| Designation of soil sample | Photos | Where adobe soil/clay collected from |
|---|---|---|
| Konya_Küçükköy |  | The sample was taken from the area where villagers used it as an adobe soil resource. |
| Çorum_Karapınar |  | |
| Çorum_Kınık |  | The samples were taken from the brick factory (Vesfa factory in Çorum) where soil resources were used for adobe brick and fired brick. |
| Çorum_Sarımbey |  | |
| Manisa_Kemer |  | The sample was taken from the area where villagers used it as an adobe soil resource. |
| Eskişehir_Sorkun |  | The sample was from a pottery in Mihalıçcık, it is preferred because of its low shrinkage. |
| Eskişehir_Sazak |  | The sample was taken from the area where villagers used it as an adobe soil resource, especially as a top layer on roofs. |

The selection criteria for those sites are as follows:

— Those cities have adobe constructions in a higher number of locations than the other cities which signals the presence of adobe/clay resources (State Institute of Statistics Prime Ministry Republic of Turkey, 2001);

— Those adobe soil/clay resources exist in the cities of Konya, Çorum and Manisa, especially near archaeological sites (Kıvrak, 2007; Koçu & Korkmaz, 2007);

— Non-expansive or limited expansive clay types such as kaolinite and illite can be found in those areas (Ralph, 2023);

— Lacustrine (lake) sediments appropriate as clay or adobe soil resources are found in those areas (Alkaç & Koral, 2022; de Ridder, 1965; Kadir & Karakas, 2002; Varol et al., 2002; Yeniyol, 2012).

## 3.2    Field Soil Tests

Field tests were conducted on the soil samples of Konya_Küçükköy Çorum_Karapınar, Çorum_Kınık, Çorum_Sarımbey, Manisa_Kemer, Eskişehir_Sorkun and Eskişehir_Sazak by visual, smell, ribbon and feel tests (Food and Agriculture Organization, 2020; Houben & Guillaud, 1994) (Figure 3.2 and Table 3.3). By visual examination, the aggregate size of the soil was qualitatively and quickly observed. The presence of the organic content can be detected, in the case of smelling of soil musty in the smell test. Soil texture was detected with the ribbon and feel tests. Soil texture was mainly categorised as loam (soil containing clay silt, sand and gravel), clay loam and clay. In the ribbon test, the soil sample formed in a ball was pressed upward to form a ribbon up to breaking it by its weight. The length of the ribbon parts informed the soil texture If it does not form into a ball, then it is sand, and if it does not shape into a ribbon, the texture of the soil is sandy. After that examination, the feel test was conducted by rubbing the excessively wetted soil sample with a forefinger in the palm. The evaluation of the feeling on the finger while rubbing together with the ribbon test result concerning reference data given in Table 3.3 provided to determine the soil texture in detail. The procedures of ribbon and feel tests are given in Appendix A.



Figure 3.2 Ribbon test (at left) and feel test (at right) in the field.

Table 3.3 Categorisations of soil texture according to ribbon and feel tests.

| Ribbon Test | | Feel Test | |
|---|---|---|---|
| Ribbon length | Soil Texture | Feeling | Soil Texture |
| x≤ 2.5 cm | Loam | Gritty | Sandy loam |
| | | Smooth | Silty loam |
| | | Neither gritty nor Smooth | Loam |
| 2.5 cm <x<5 cm | Clay loam | Gritty | Sandy clay loam |
| | | Smooth | Silty clay loam |
| | | Neither gritty nor Smooth | Clay loam |
| x≥5 cm | Clay | Gritty | Sandy clay |
| | | Smooth | Silty clay |
| | | Neither gritty nor Smooth | Clay |

## 3.3 Raw Material Characteristics Tests

Raw materials characteristics tests were conducted to specify the pH value, organic and calcium carbonate content, soluble salts, pozzolanic properties and the particle size distribution of the collected soil samples.

### 3.3.1 pH Value and Organic, Calcite and Soluble Salt Contents

The tests of pH value and organic, calcite and soluble salt contents were executed on the samples of Konya_Küçükköy Çorum_Karapınar, Çorum_Kınık, Çorum_Sarımbey, Manisa_Kemer, Eskişehir_Sorkun and Eskişehir_Sazak.

The pH analyses were conducted on the soil samples with a pH strip method. The pH values were detected by the changing colour on the paper strip after the submerge of the pH paper strip into the water of the diluted soil samples' sediment (Figure 3.3).
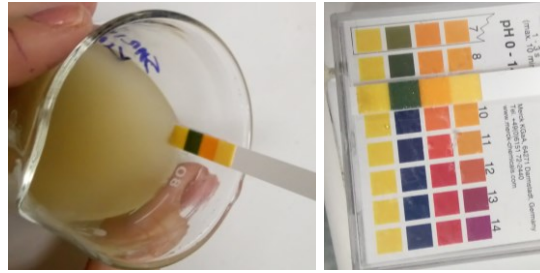
Figure 3.3 pH analyses with pH strip.

Organic and calcite (CaCO₃) contents of the soils were identified by loss on ignition (LOI) tests were conducted after soil samples in certain amounts (e.g. 20 g and 0.5 g) were dried out in an oven at 105°C for 24 hours to evaporate their all moisture content (Heiri et al., 2001). Then, those samples were heated in the oven at 550 ℃ and 950 ℃ about 2 hours to decompose the organic and calcite matters, respectively (Heiri et al., 2001) (Figure 3.4). The percentages of organic and CaCO₃ contents were found by the formulas (Equation 2 and 3) shown below:

$$\text{Organic content}, \% \ = [(W_{105} - W_{550}) \times 100]/W_{105} \qquad 2$$

Where $W_{105}$ is the weight of the sample after heating at 105 ºC; $W_{550}$ is the weight of the sample after heating at 550 ºC.

$$\text{CaCO}_3 \text{ content}, \% \ = [(W_{550} - W_{950}) \times 100]/W_{550} \qquad 3$$

Where $W_{950}$ is the weight of the sample after heating at 950 ºC.



Figure 3.4 The soil samples heated at 105 ℃, 550 ℃ and 950 ℃, respectively, in the oven and weighed after each heating.

The presence of soluble salts in adobe soil adversely affects the durability and mechanical performance of adobe (Clifton et al., 1979). Dissolved salts deposited in/on the adobe cause deterioration such as shrinkage cracks and crumbling on the adobe during wetting and drying cycles (United States National Park Service., 1997). Spot salt tests were conducted to detect the existence of phosphate ($PO_4^{-2}$), sulphate ($SO_4^-$), chloride ($Cl^-$), carbonate ($CO_3^{2-}$), nitrite ($NO_2^-$) and nitrate ($NO_3^-$) ions in soil samples (Teutonico et al., 1988)(Figure 3.5). The procedures of spot salt tests are represented in Appendix B.
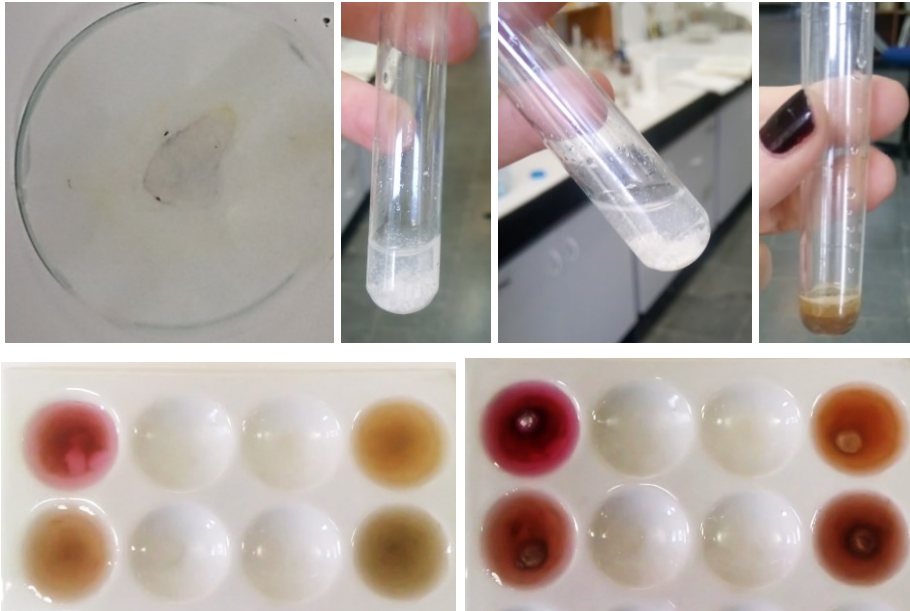


Figure 3.5 The spot tests of $PO_4^{-2}$ $SO_4$ $Cl^-$ $CO_3^{2-}$, $NO_2$ and $NO_3$, respectively.

### 3.3.2    Pozzolanic Activity

The pozzolanic properties of Konya_Küçükköy Çorum_Karapınar, Çorum_Kınık, Çorum_Sarımbey, Manisa_Kemer, Eskişehir_Sorkun and Eskişehir_Sazak samples were determined by testing the particle sizes below 125 μm with the EDTA titration method (chemical titration Method using Ethylenediaminetetraacetic acid) according to the TS EN 196-1:2016 standard (TS EN, 2016) (Figure 3.6). 0.2 g soil samples having an aggregate size below 125 μm were obtained by a standard sieve analysis.

Those samples were mixed with saturated $Ca(OH)_2$ solution (30ml) in containers and were sealed. All sample solutions and a solution without any soil sample as a blank sample were left in laboratory conditions for 14 days. Then, the titration mechanism with EDTA was set up to determine the rest of the free $Ca(OH)_2$ content in the solutions of samples after $Ca^{2+}$ ions were consumed during the reaction with pozzolan particles. 10 ml of sample solutions in the container were diluted to 100 ml solution. After 1 ml NaOH (10%) solution to provide its alkalinity and 3-4 drops of Calgon indicator were put into the diluted solutions, those solutions were titrated with EDTA (0.01M) up to their colour change from pink to blue (Black, 1965). The consumed volume of EDTA was recorded for each solution. Calculations were conducted considering the differences in the consumed volume of EDTA between the sample solutions and the blank solution.
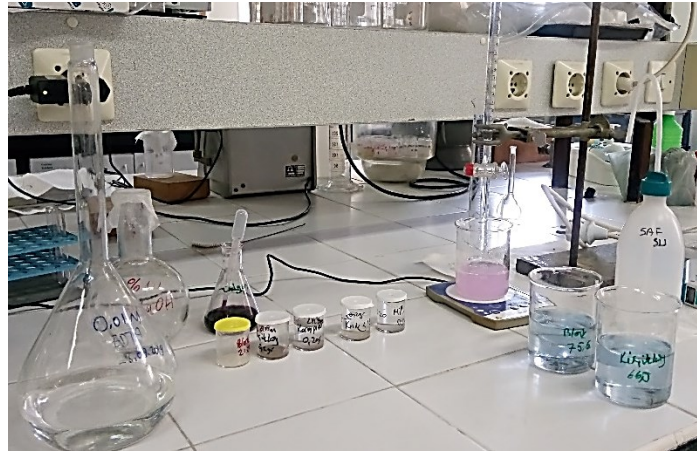


Figure 3.6 Pozzolanic activity test with the EDTA titration method.

### 3.3.3 Particle Size Distribution by Sieving and Centrifuge Methods

Particle size distribution including the submicron particle size distribution and clay percentage of Konya_Küçükköy Çorum_Karapınar, Çorum_Kınık, Çorum_Sarımbey and Manisa_Kemer samples were identified. Particle size

distribution analyses involve the dry-sieving, wet-sieving, sonication and centrifugal sedimentation methods (Figure 3.7).

The wet-sieving and the alternative method including wet-sieving and sonication methods were conducted to separate aggregates above 63 microns (μm) such as sands and gravels from aggregates below 63 μm such as silts and clays. After separating those parts, the particle size distribution of sands and gravels was carried out by dry-sieving, and centrifugal sedimentation was performed for silts and clays.
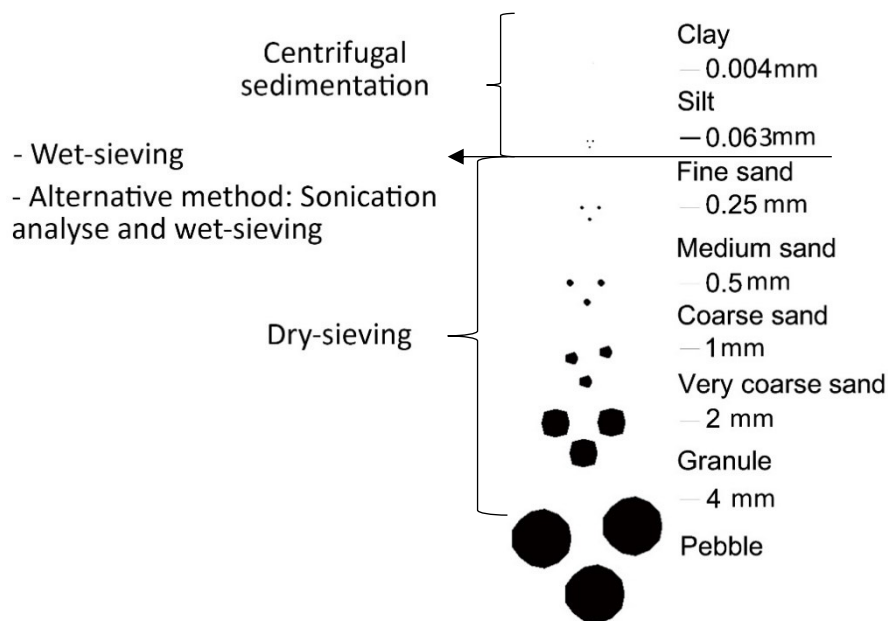


Figure 3.7 Particle size distribution analyses conducted on the samples.

Through the dry-sieving analyses conducted in two methods, the sieve sizes of 16mm, 8mm, 4mm, 2mm, 1mm, 0.500mm, 0.250mm, 0.125mm and 0.063 mm were used and their particle size distribution of aggregates was evaluated according to the Udden and Wentworth scale (Figure 2.13) (Tucker, 2001). The scales for the clays were determined according to geology and soil science (acceptance of clay content as the size below 1 μm) and according to TS EN ISO 14688-1:2018 Turkish standard, and colloid science (acceptance of clay content as the size below 2 μm) (TS EN ISO,

56

2018). Their soil textures were specified according to the USDA soil texture triangle (Figure 2.14).

### 3.3.3.1    Analyses of particle size above 63 microns

Two types of methods were conducted to separate gravel and sand particles (above 63 μm) from silt and clay (below 63 μm). The first method was applied with the wet-sieving method adapted from the TS 1900-1/T3:2017 Turkish standard (TS, 2017) (Appendix C) (Figure 3.8). That sieving method was conducted on Konya_Küçükköy, Çorum_Kınık, Çorum_Karapınar, Çorum_Sarımbey and Manisa_Kemer without considering gypsum content in soil samples. On the other hand, the gypsum content was found to be in some soil samples of Konya_Küçükköy, Çorum_Kınık, Çorum_Karapınar, Çorum_Sarımbey through the spot salt tests.

The second method referred to as an alternative method that includes the sonication method and wet-sieving was improved to analyse the particle size distribution of soils including gypsum (Pearson et al., 2015) (Appendix D) (Figure 3.9). The second method was applied to Konya_Küçükköy, Çorum_Kınık, Çorum_Karapınar samples Çorum_Sarımbey samples including gypsum. Some adaptations were made during the sonication method developed by Pearson et al. (2015). An ultrasonic bath at 37 kHz and 200W (Elmasonic S120) (Figure 3.9) was used, instead of a sonicator with a horn to supply ultrasound energy. Soil samples diluted with ethanol solutions were put into beakers to disperse them in the ultrasonic bath instruments. The ethanol solution was determined in the 70% ratio (7:3 ethanol: water) by considering the insolubility of gypsum in ethanol (Pearson et al., 2015). The sonication time that ultrasound energy was given was determined by observing the flocculation of particles in the soil sample. Ultrasound energy was given for one minute a few times until flocculation disappeared (Figure 3.10). The supernatant-suspended particles in distilled water above the sediment were discharged by wet-sieving with the sieve of 63 μm at each time to prevent the size of suspended particles in the water from making smaller.

Figure 3.8 Steps of the wet-sieving to separate the silt-clay content from the sand and gravel.

Figure 3.9 Steps of alternative method including sonication analyses (ultrasonic bath: Elmasonic S120 at 37 kHz, 200W) and wet-sieving to separate the silt-clay content from the sand and gravel.



Figure 3.10 Sonication and wet-sieving processes are repeated until not observing the flocculation of particles on the sediment by the naked eye.

After the separation of the silt clay content from the sand and gravel parts, dry-sieving analyses were conducted for the particle size distribution of sand and gravel (Figure 3.11).



Figure 3.11 Determination of the particle size above 63 microns by dry-sieving.

### 3.3.3.2    Analyses of particle sizes below 63 microns

Centrifugal sedimentation method was carried out to determine the distribution of particle sizes below 63 microns by using a Hettich-Rotofix 32A centrifuge instrument (Cat. No. 1624 rotor, Swing-out-4-place) with 100-ml centrifuge tubes (Figure 3.12).

Figure 3.12 Hettich-Rotofix 32A centrifuge instrument.

During the analyses, the data of revolutions per minute (rpm) (between 500-4000 rpm) and time are entered into the instrument. The revolution per minute and time data were identified by the formula given in Equation 4 (Jackson, 1969) which is generated from the Stokes Law formula (Equation 1). A schematic drawing of the centrifuge to show the parameters of a radius of sediment (R) and a radius of supernatant (S) used in the formula was given in Figure 3.13.

$$T_m = \frac{63 \times 10^8 \times \eta \times \log_{10}\left[\frac{R}{S}\right]}{N^2 \times D^2 \times \Delta s} \qquad\qquad 4$$

Where $T_m$ is time for sedimentation in a minute; $63x10^8$ is constant number; $\eta$ is the viscosity of distilled water in poise at the ambient temperature; $R$ is the radius in cm from the centre of rotation axis to the top of the sediment in the centrifuge tube; $S$ is the radius in cm from the centre of rotation axis to the surface of the supernatant (distilled water including suspended particles); $N$ is revolutions per minute (rpm); $D$ is the diameter of a particle in micron; $\Delta s$ is specific gravity (g/cm$^3$) difference between the particles of silt and clay and the distilled water used to dilute them.
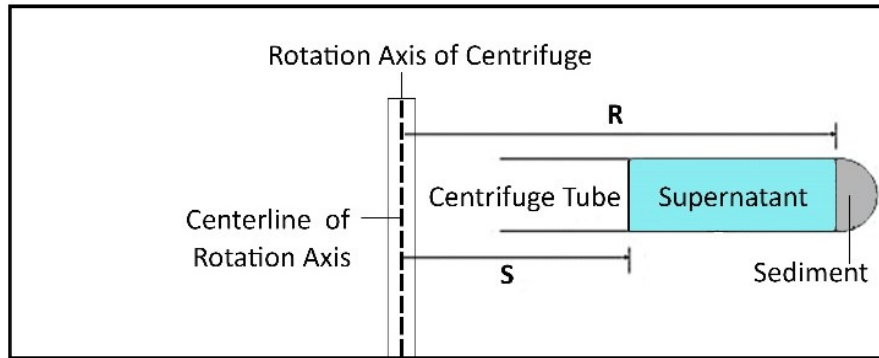
Figure 3.13 Schematic drawing of the centrifuge to show the parameters of Equation 4: R (radius of sediment) and S (radius of supernatant).

The silt and clay contents are not able to separate from each other at only one time; therefore, the procedure of centrifugation sedimentation to separate below 4 μm from the content of 63 μm and then to separate below 2μm from the content of 4μm (separation of the clay from the silt content) were repeated until the supernatant became clear. The samples were separated into particle sizes, and they were put into the beaker to dry in the oven at 60 ºC, and then they were weighed. The procedure of centrifugal sedimentation and data used in the formula shown in Equation 4 for the Çorum_Karapınar sample was given in Appendix E as an example.

Figure 3.14 Determination of the particle size below 63 µm s by centrifugal sedimentation.

Gypsum particles are generally present in the sand and silt sizes; therefore, the clay content without gypsum was assumed as the total clay content, and defined as only the clay percentage in total (Al-Barrak & Rowell, 2006; Aznar et al., 2013).

The percentage of clay content (below 2μ or 1μ) was found by the centrifuge method, and the ratios of gravel-sand content were uncovered by the alternative method and wet-sieving. The samples' silt (between 2 μ and 63μ or between 1μ and 63μ) ratios were estimated by subtracting the gravel-sand (above 63μ) and clay ratios from 100 %.

### 3.3.4 Laser Diffraction Particle Size Distribution, Scanning Electron Microscope and Transmission Electron Microscopy Analyses

The laser diffraction particle size distribution, scanning electron microscope (SEM) and transmission electron microscopy (TEM) analyses were conducted on the untreated and treated Konya_Küçükköy Çorum_Karapınar, Çorum_Kınık and Çorum_Sarımbey samples to validate the Nano-clay production by the ultrasonic treatment.

The laser diffraction particle size distribution was conducted by the Zetasizer method (Malvern Mastersizer 2000-Wet analysis in METU Central Lab) working with dynamic light scattering, to determine the particle size distribution of the samples including the nanosized particles. The particle size distribution of aggregates was evaluated according to the Udden and Wentworth scale (Figure 2.13) (Tucker, 1981). The scales for the clays were determined according to geology and soil science (acceptance of clay content as the size below 1 μm) and according to TS EN ISO 14688-1:2018 Turkish standard and colloid science (acceptance of clay content as the size below 2 μm) (TS EN ISO, 2018).

The soil samples below 4 μm before and after treatment and adobe samples prepared for the performance analyses were analysed by the scanning electron microscope (SEM, Quanta 400F Field Emission in METU Central Lab) to detect the effect of the ultrasonic treatment on the morphology of clay particles. In addition, the dispersion of clay by the ultrasonic method in the treated and untreated Konya_Küçükköy clay

sample was confirmed by transmission electron microscopy (TEM, FEI Tecnai G2 Spirit Biotwin in METU Central Lab).

### 3.3.1     Stereo Microscope, Simulation (MAUD) and Spectrophotometry Analyses

The untreated and treated Konya_Küçükköy Çorum_Karapınar, Çorum_Kınık and Çorum_Sarımbey soil samples below 63 μm were examined by the stereo microscope (Leica Z16 APO A) to detect the presence of clay and silt in different particle size ranges.

The simulation program MAUD is the general diffraction analysis program based on the Rietveld method. It provides the relative percentage value of the clay mineral to other minerals by fitting the defined minerals data to the diffraction data obtained by XRD analyses. The relative amounts of clay types of montmorillonite, kaolinite, illite and chlorite clay minerals in the untreated Konya_Küçükköy Çorum_Karapınar, Çorum_Kınık and Çorum_Sarımbey samples were approximately determined by MAUD software (version 2.99). The MAUD analyses were conducted on the untreated samples below 4 μm since the stereo microscope analyses showed the flocculated clay particles started to be observed at that particle size (Figure 4.32, Figure 4.33, Figure 4.34 and Figure 4.35).

All minerals defined by XRD tests on samples below 63 μm were searched in simulation analyses. During the calculations of clay ratios, mainly calcite minerals' percentages were taken into consideration.

Colours of Konya_Küçükköy Çorum_Karapınar, Çorum_Kınık and Çorum_Sarımbey samples were determined by using standard spectrophotometer handheld instrument (Konica Minolta CM-2600d ver.1.31). That instrument expresses colour as three values: L is for the lightness from black (0) to white (100), a is from green (− numbers) to red (+ numbers), and b is from blue (− numbers) to yellow (+numbers). The result data were evaluated in the SCI (Specular Component

Included) mode that excludes surface conditions of the sample to define the "true" colour of the soil sample.

## 3.4    Mineralogical and Elemental Composition Tests

The mineralogical composition of aggregates and clay was determined through X-ray diffraction (XRD) analyses on particles below 63 µm of the soil samples of Konya_Küçükköy    Çorum_Karapınar,    Çorum_Kınık,    Çorum_Sarımbey, Manisa_Kemer, Eskişehir_Sorkun and Eskişehir_Sazak. XRD experiments were conducted by directly putting the cover glass on the sample holder. The analyses were conducted by Bruker D8 Advance XRD Instrument. XRD traces recorded at $2\theta$ scale in the range of 5°-70° (0.002 increments, CuKα radiation) were evaluated by DIFFRACT.SUITE software.

Silt and clay minerals below 63 microns of the soil samples oriented with water were air-dried on a cover glass. Glycol and heating treatments were conducted on those oriented samples to detect some minerals in the soil samples during XRD analyses. After analyses of oriented samples, those samples were saturated with ethylene glycol vapour to expand the swelling clays, thus swelling smectite-type clays such as montmorillonite were discriminated from non-swelling clays such as kaolinite, illite-mica and chlorite.

The steps of the glycol treatment (Carroll, 1970; Mosser-Ruck et al., 2005; Poppe et al., 2001):

– Put the oriented sample on the cover glass on the shelf of the desiccator including ethylene glycol on its base.

– Put the desiccator in the oven at 60°C for overnight.

Heating treatments were gradually conducted on the glycol-treated samples in the oven at defined degrees for about 2 hours to specify the minerals (Table 3.4). Firstly, samples were heated at 600°C to identify kaolinite minerals (Carroll, 1970; Ilic et al., 2010). That heating treatment causes the transition of kaolinite minerals from

crystalline to amorphous phase; therefore, the peaks of kaolinite disappear in the XRD pattern. The following heating treatments were conducted at degrees of 700°C and 800°C to specify minerals of illite-mica, chlorite and calcite. The peaks of illite-mica and chlorite become less and disappear at 700°C, and 800°C respectively since the crystalline structure of those minerals cannot be stable anymore and collapses at those degrees (Carroll, 1970). The other clay mineral, sepiolite, keeps the mineral stable until about 850 ºC (Carroll, 1970). Calcite starts to decompose to calcium oxide about at 700°C (Lakshmi et al., 2013; Loy et al., 2016). After heat treatments, the peak intensities of those minerals decrease or disappear in the XRD pattern.

In the Çorum_Karapınar sample, due to the dominancy of lime and gypsum peaks other minerals were not detected in the XRD patterns of the sample (Figure 4.2); therefore, this sample firstly was treated with 2N Hydrochloric acid (HCL) to dissolve the calcite and gypsum minerals (Loveday, 1974). After being washed away with distilled water, it was prepared as the oriented sample for analysis by XRD.

In addition, asbestos clay minerals were suspected to be present in the Eskişehir_Sorkun sample. Asbestos clay minerals in the fibrous form are generally found in metamorphic and igneous rocks, including hydrated silicate minerals with varying portions of sodium, calcium, magnesium, and iron (Van Orden, 1964). Due to their crystalline minerals in fibre-like shape, significant health risks occur when their particles are inhaled (Mahltig & Pastore, 2018; Noonan & Pfau, 2011). Two main groups of asbestos are amphiboles and serpentine. The Amphibole group includes the minerals of crocidolite (blue asbestos), amosite, anthophyllite, tremolite, pargasite and actinolite, and the serpentine group covers only chrysotile mineral (white asbestos) (Van Orden, 1964). The thermal decomposition occurs at temperatures about 900°C, 950°C and 1000°C for the amphibole asbestos (Kusiorowski et al., 2012; Niida & Green, 1999) and temperatures about 700°C – 800°C for chrysotile (Kusiorowski et al., 2012). To validate the presence of asbestos minerals such as amphibole, pargasite and chrysotile, the scanning electron microscope (SEM-VEGA XMU) tests also be conducted on the Eskişehir_Sorkun sample.

The other minerals are gypsum ($CaSO_4 \cdot 2H_2O$), calcite ($CaCO_3$), quartz($SiO_2$), feldspar ($KAlSi_3O_8$–$NaAlSi_3O_8$–$CaAl_2Si_2O_8$), albite ($NaAlSi_3O_8$ in plagioclase feldspar group), diopside ($MgCaSi_2O_6$ in pyroxene group) and goethite ($FeO(OH)$). After heat treatments, the peak intensities of quartz, feldspar, albite, diopside and goethite remain stable or increase in the XRD pattern.

Table 3.4 Temperatures at which the crystalline structure of the mineral starts to decompose.

| Mineral | The temperature at which the decomposition occurs | | | | |
|---|---|---|---|---|---|
| | 600 °C | 700 °C | 800 °C | 900 °C | 950-1000 °C |
| Kaolinite | + | | | | |
| Illite-mica | | + | | | |
| Chlorite | | | + | | |
| Calcite | | + | | | |
| Sepiolite | | | + (850°C) | | |
| Chrysotile | | + | + | | |
| Amphibole | | | | + | + |
| Pargasite (Amphibole) | | | | | + |

In addition, the samples' particle sizes below 4 μm on the soil samples of Konya_Küçükköy Çorum_Karapınar, Çorum_Kınık and Çorum_Sarımbey were also analysed by XRD analyses to search for the presence of calcite and Nano-calcite in the clay and silt content. The effects of the Nano-calcite and calcite on the clayey soil are stated as the decrement in the liquid limit (LL) and plastic index (PI) while the increment in the plastic limit (PL) (Choobbasti et al., 2019; Yazarloo et al., 2017). The presence of Nano-calcite and calcite is expected to control the shrinkage and swelling problems of the adobe soil. In addition, a study showed that the activity of Nano-calcite is higher than the calcite particle through the higher specific surface of calcite in the Nano-scale (Yazarloo et al., 2017).

The elemental composition of the Konya_Küçükköy Çorum_Karapınar, Çorum_Kınık and Çorum_Sarımbey samples, including all particle sizes, was determined by the X-ray fluorescence (XRF) (by X-Ray Fluorescence Spectrometry,

Rigaku ZSX Primus II in METU Central Lab) technique to check and prove the samples' minerals defined by XRD analyses.

## 3.5     Nano-Clay Production from Soil Samples-Methylene Blue (MB) Tests

"Ultrasonic treatment" was selected as the most efficient method in terms of preserving the original properties of the clay during Nano-clay production and production in higher amounts of Nano-clay with low energy considering the evaluations mentioned about Nano-clay production methods in the literature review. In line with the aim of the study, a practical Nano-clay production method was developed to achieve adobe soil having enriched Nano-clay content in the laboratory.

The Konya_Küçükköy Çorum_Karapınar, Çorum_Kınık and Çorum_Sarımbey soil samples diluted with the distilled water were first mixed by a magnetic stirrer (IKA lab disc) to disperse coarser aggregates. The magnetic stirrer generates a rotating magnetic field that provides a magnetic bar submerged within the diluted sample to stir very fast. Through the stirring action, flocculation is dispersed in the water. Then they were treated by an ultrasonic bath (MEL at 22 kHz, 80 W) to provide Nano-clay by dispersion of clay minerals (Figure 3.15). During the ultrasonic treatment, stirrings by a spatula a few times were needed to disperse the flocculation of the soil particles.
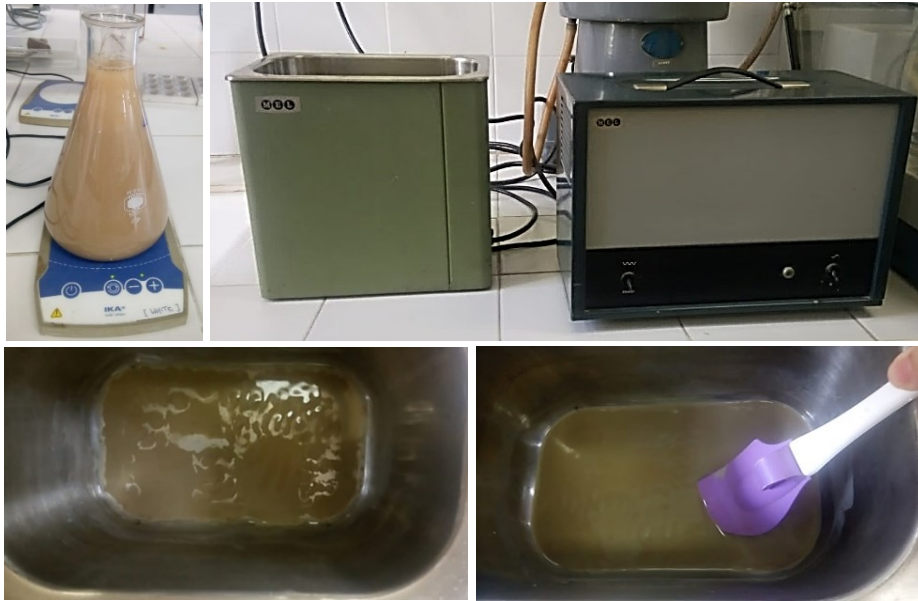
Figure 3.15 Nano-clay production method including firstly mixing by Magnetic stirrer (IKA lab disc) (at top left), then dispersion of clay particles by Ultrasonic treatment-ultrasonic bath *(MEL* at 22 kHz, 80 W).

The Methylene blue (MB) tests as a practical test method were conducted to control the Nano-clay production in adobe soil. The tests were proceeded step by step. At the first step of the Nano-clay production from the soil samples, the optimum times for magnetic stirring and ultrasonic treatment for the Nano-clay production were defined by Methylene blue (MB) tests, including a spot test and titration technique, regarding the cation exchange capacity (CEC) values (NF, 1998). The Methylene blue (MB) tests were conducted on the untreated samples having particle sizes below 4 μm to find out the required time to disperse the whole clay content in the sample by the ultrasonic treatment since the presence of the clay is observed in the beginning from this part of the soil samples in the stereo microscope analyses.

To identify the CEC properties of the samples by MB tests, the oven-dry samples of about 3.75 g were mixed with 25cc distilled water. The diluted samples were titrated with methylene blue (Methylene blue Gurr®) solution. The spot test was conducted on filter paper (Whatman 40) until a formation of a narrow light blue halo around the dark blue circle which means clay absorbs no more dye since the cation replacement

between clay and methylene blue stops (Figure 3.16). The sum of methylene blue solution adsorbed by a certain mass of the sample is used in the estimations of CEC. The detailed process of the test is given in Appendix F (NF, 1998).
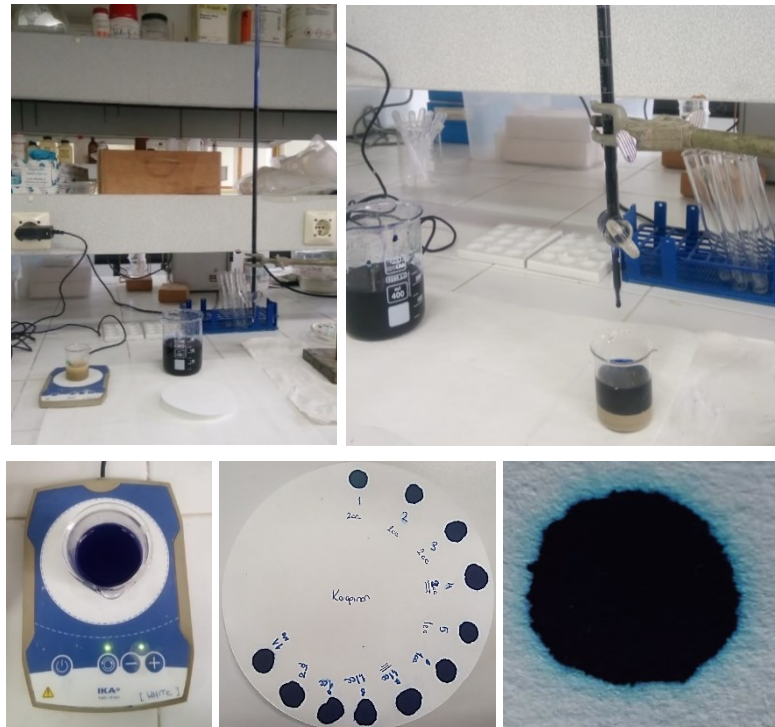


Figure 3.16 Process of the MB test.

To determine the optimum times for the soil samples' mixing with the magnetic stirrer and treatment by ultrasonic bath during the MB tests, the selected Konya_Küçükköy sample was firstly stirred by the magnetic stirrer for 1 day, 2, and 3 days, then it was treated by the ultrasonic bath from 1 hour to 6 hours (Caner, 2011). After the determination of the optimum times for the Konya_Küçükköy sample, the other samples were stirred by the magnetic stirrer, and then they were treated with the ultrasonic bath between 4 and 6 hours. After the determination of the optimum times, the MB tests were executed on the Konya_Küçükköy sample to uncover the effects of ultrasonic treatment on the CEC value of the sample having

increased weight by doubling the weight of the sample, and the sample including all particles sizes.

Some revisions were required to be conducted during the Nano-clay production process for the treatment process of the soils prepared as adobe samples. The first revision is about the amount of water used for mixing the soil sample. The MB tests were conducted by putting the soil sample into too much water (the soil-to-water ratio is 1:6 by w.t) to identify the effect of the ultrasonic treatment on the soil. On the other, there is a need for the water amount about the liquid limit of the soil (the soil-to-water ratio is about 1:1 by w.t for those samples) for the adobe preparation. It may require too much time to dry out of the diluted soil sample as the water amount used in MB tests until the water amount is of its liquid limit. Therefore, the MB tests were conducted to uncover the effect of decreasing the water amount in case the soil sample can be mixed by the magnetic stirrer and ultrasonic bath. The soil-to-water ratios of 1:4, 1:2 and 1:1 by w.t were tested on the Konya_Küçükköy sample, respectively, by MB tests. Then, the defined soil-to-water ratios for the Konya_Küçükköy sample were tested on Çorum_Karapınar, Çorum_Kınık and Çorum_Sarımbey samples.

The second revision concerns the mixing method of the soil sample in higher amounts. When the amount of soil increased, the magnetic stirrer remained incapable of mixing the sample. Instead of it, the laboratory mixer (Utest laboratory equipment) was preferred to use, although some differences were present between them. The mixer in the instrument has bidirectional rotation at the same time, one of them is a rotation of the mixer around its axis (62 rpm speed) and the other one planetary turn of the mixer (140 rpm speed). On the other hand, the magnetic stirrer (IKA lab disc) has only the rotation of the mixer around its axis (15 - 1500 rpm speed) (Figure 3.17).

In addition, the stirrer of the mixer laboratory is much larger than the magnetic stirrers. Therefore, the time was decreased compared to the time required for the magnetic stirrer. The Konya_Küçükköy sample in a higher amount laboratory mixer was mixed with the laboratory mixer for one hour and three hours. Then, it was

treated with the ultrasonic bath and the MB tests were conducted on the treated sample to decide which one was the optimum time.



Figure 3.17 Mixing the soil sample in a higher amount with the laboratory mixer (Utest laboratory equipment).


## 3.6 Consistency Limits and Linear Shrinkage Ratio Tests

Consistency limits and linear shrinkage ratio tests were conducted on the untreated and treated Konya_Küçükköy Çorum_Karapınar, Çorum_Kınık and Çorum_Sarımbey samples to find out to observe the effect of the Nano-clay production on the performance of the soil sample. Soil samples were selected according to the compatibility of their values with the Atterberg limit values for adobe soil. Consistency (Atterberg) limits such as plastic limit (PL), liquid limit (LL) plasticity index (PI) values, and linear shrinkage (LS) ratio of the soil samples were defined through TS 1900-1/T3:201 Turkish standard (TS, 2017) (Figure 3.18).

Their detailed procedures were given in Appendix G. Liquid limit tests were performed by the Casagrande apparatus, and moisture content corresponding to several blow numbers of the Casagrande apparatus was plotted in a flow chart. The

moisture content corresponding to 25 blow numbers in the flow chart indicates the liquid limit value of the soil sample. The plastic limit tests were executed by rolling a soil ball by hand on a glass surface. The moisture content at which the thread of soil crumbles, as it was rolled into a diameter of 3 mm indicates the plastic limit of the soil sample. The linear shrinkage tests were conducted on soil samples moulded in the shape having a length of 140 mm and a 12.5 mm radius. Those moulded soil samples were dried at various degrees defined by the standard. The linear shrinkage ratio was determined by the formula below:

$$\text{Linear shrinkage ratio, \%} = \left(1 - \frac{L_D}{L_O}\right) x 100 \qquad\qquad 5$$

where $L_o$ is the original length of the sample, and $L_D$ is the length of the oven-dry sample.
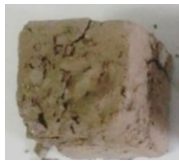


Figure 3.18 Liquid limit test performed by Casagrande apparatus (at top left) plastic limit test (at top right) linear shrinkage test (at the bottom).

## 3.7    Preparation of Adobe Samples

Adobe samples were prepared as the four sub-types from each Konya_Küçükköy, Çorum_Karapınar and Çorum_Kınık soil samples after Nano-clay production by ultrasonic treatments. Those sub-types are; untreated samples including straw as an additive, treated samples including straw as an additive, treated ones including additives of straw and of 1% by w.t Nano calcium oxide (Nano-CaO) (Aldrich particle size <160nm, BET 98%) and treated ones including additives of straw and 4% by w.t calcium hydroxide (CaOH$_2$) (Sigma Aldrich, Ph. Eur. ≥96%). According to previous studies as mentioned in the literature review, the optimum ratios were determined as 1% for Nano-CaO and 4% for Ca(OH)$_2$ (Bell, 1996; Dash & Hussain, 2012; Kafescioğlu, 2016; Kafescioğlu et al., 1980; Pashabavandpouri & Jahangiri, 2015). The use of Nano-calcite or calcite as an additive can positively affect the pozzolanic characteristics of the Çorum_Karapınar sample, and they can control the swelling potential of their dominant montmorillonite clay mineral content of the Konya_Küçükköy and Çorum_Kınık soil samples.

The straw type was selected as wheat in a length of between 0.5-3 cm. To decide the optimum straw ratio for those soil samples, the point load tests were conducted on the cubical samples, including straw 1% and 2 % by w.t, and crack formations were observed by eyes. The straw ratios of 1% and 2 % by w.t for the adobe samples were decided depending on prior knowledge. A study conducted in Çatalhöyük, very near Küçükköy village, indicates that the straw ratios in adobe used in the archaeological site are about 1% and 2 % by w.t (Tringham & Stevanović, 2012). Çorum_Karapınar and Çorum_Kınık soils are also used as soil sources by mixing them in a brick factory. The straw content is used as 1% in the mixture of those soils to produce the brick. The results of the point load tests indicate that the samples including 1% straw have higher strength in the range of 0.1 kN-0.5 kN than ones including 2% straw (Table 3.5). The difference observed in cracks on the sample is non-distinguishable As a result, the optimum ratio for all soil samples was determined as 1%.

Table 3.5 Point load test results and the photographs of soil samples including 1% and 2% straw.

| Straw content | Maximum Point Load Kilonewton (kN) | | |
|---|---|---|---|
| | Konya_Küçüköy | Çorum_Karapınar | Çorum_Kınık |
| 1 % wheat | 1.6 | 1 | 0.6 |
| |  |  |  |
| 2 % wheat | 1.49 | 0.5 | 0.38 |
| |  |  |  |

The untreated adobe sample was designed in the traditional method. The soil was mixed with water and straw and moulded after keeping it for a day.

The preparation of treated adobe samples started with the Nano clay production. The soil was diluted with water (1:2 the soil-to-water ratio) and mixed with a laboratory mixer and ultrasonic bath. Then the straw was added and mixed. While the diluted soil samples were waiting in the laboratory, treated samples including straw and untreated ones smelt bad, and it signalled the formation of microorganisms in them. For the samples including Nano-CaO and $CaOH_2$, those additives were added and mixed by the laboratory mixer after the Nano-clay production, as well as straw, because the calcite causes the agglomeration of the clay. The soil samples were put into the oven at 60 °C to dry out the excess water in the diluted sample until the consistency of the sample became within its liquid limit.

The basic steps for the preparation of the treated adobe samples are shown in Figure 3.19. The treated and untreated adobe soil samples' ingredients and preparation steps of the adobe mixtures are given in detail in Table 3.6. Three adobe samples were prepared for each four sub-types.
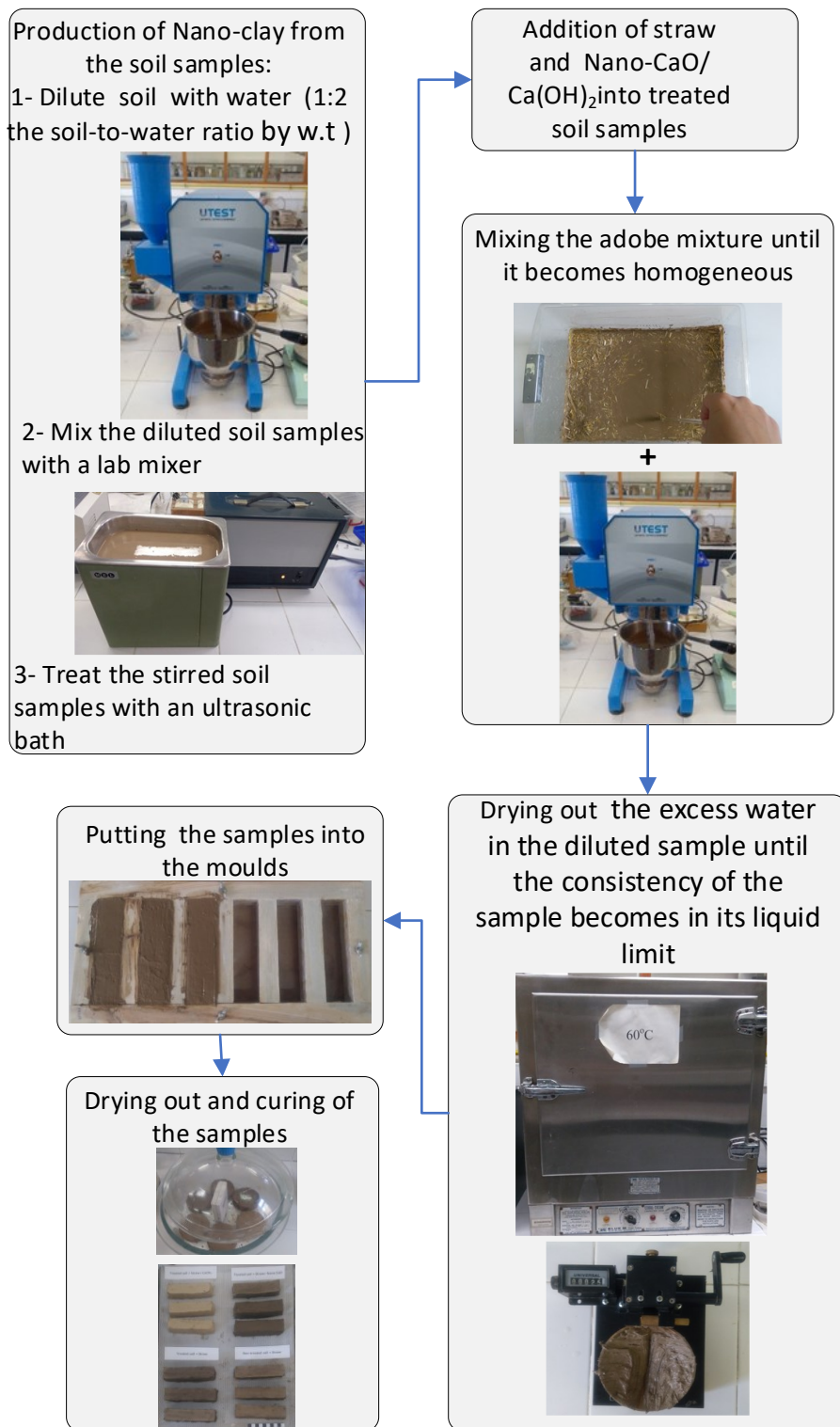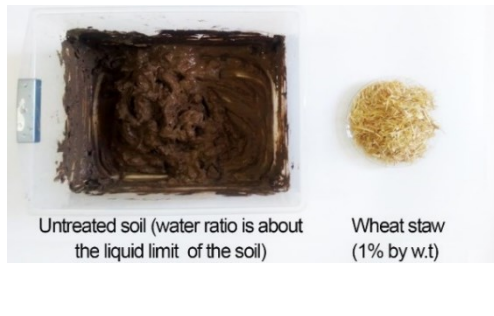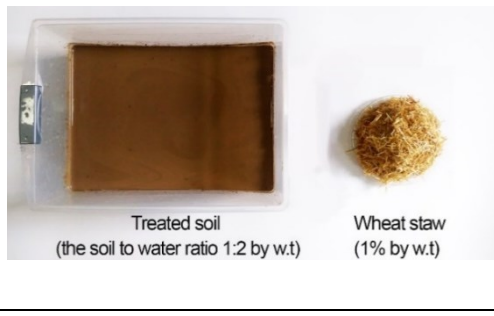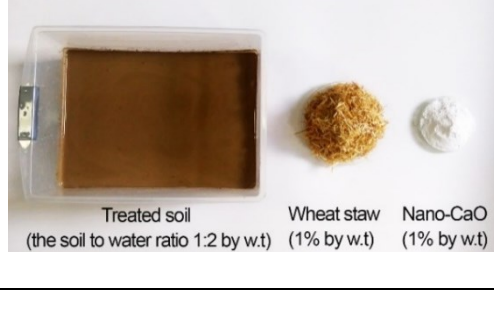
Figure 3.19 The basic steps for the preparation of the adobe samples.

Table 3.6 The adobe mixtures' types, ingredients and preparation steps for moulding.

| Type | Ingredient | Preparation steps of adobe mixtures | |
|---|---|---|---|
| Untreated sample +Straw |  Untreated soil (water ratio is about the liquid limit of the soil)   Wheat staw (1% by w.t) | 1-Mix the soil, the water in an amount at the liquid limit of the soil, and the straw by hand until it becomes homogenous.<br><br>2- Keep the mixture for a day in laboratory conditions. | |
| Treated sample + Straw |  Treated soil (the soil to water ratio 1:2 by w.t)   Wheat staw (1% by w.t) | 1- Dilute the soil with water (1:2 the soil-to-water ratio by w.t)<br><br>2-Mix the diluted soil with a laboratory mixer for about 3 hours.<br><br>3-Put the diluted sample into the ultrasonic bath for 4 or 5 hours.<br><br>4- Add straw into the mixture and mix by the glass rod until it becomes homogenous. | 5- Put the sample in the oven at 60 °C to dry out until its consistency becomes in its liquid limit. |
| Treated sample + Straw+ Nano-CaO |  Treated soil (the soil to water ratio 1:2 by w.t)   Wheat staw (1% by w.t)   Nano-CaO (1% by w.t) | | 5- Put the Nano-CaO /CaOH$_2$ into the mixture and mix in the laboratory mixer for about 1 hour.<br><br>6- Put the sample in the oven at 60 °C to dry out until its consistency becomes in its liquid limit. |
| Treated sample+ Straw+ Ca (OH)$_2$ |  Treated soil (the soil to water ratio 1:2 by w.t)   Wheat staw (1% by w.t)   Ca(OH)$_2$ (4% by w.t) | | |

Before the moulding of the adobe samples, the proper consistency for adobe soil was provided by achieving the water amount in the liquid limit of the soil. The

Casagrande apparatus was used to check the consistency of the samples if they were in the liquid limit or not (Figure 3.20). If the separated two parts of the soil come into contact when the number of bumps is about 25, the soil is accepted to have consistency in the liquid limit. Because, in the Atterberg limit tests, the water content of the soil corresponding to 25 bumps is referred to as the liquid limit.
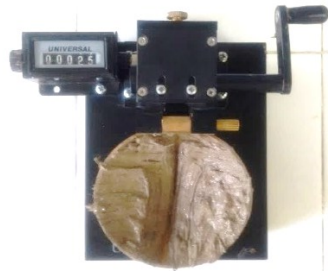


Figure 3.20 Casagrande apparatus to check the consistency of the samples.

The adobe samples were moulded in 4x4x16 cm for the compressive and tensile strength and capillary water absorption tests (Figure 3.21). The moulds 10 cm in diameter and 2.5 cm in height were used for the bulk density, porosity and water vapour permeability analyses (Figure 3.21). The samples demoulded were kept in the laboratory using a data logger for 28 days of curing time (Figure 3.22).



Figure 3.21 Moulded samples in 4x4x16 cm (at left) and in 10cm-diameter and 2.5 cm-height (at right).

The treated adobe samples containing Nano-CaO and Ca(OH)$_2$ were cured in a ventilated desiccator and chamber containing BaCl$_2$ solution providing 88% ± 6% humidity at 20°C ± 0.5°C for a while to occur the pozzolanic activity in those samples. The curing of the samples was provided to control the crack formations in those samples. The curing times were determined by checking the pH values of those samples with pH strips. When pH values of the samples became acidic below 7, the samples were left drying out together with the other samples in laboratory conditions at a humidity of 43 % ± 5% and at a temperature of 26 °C± 8°C.
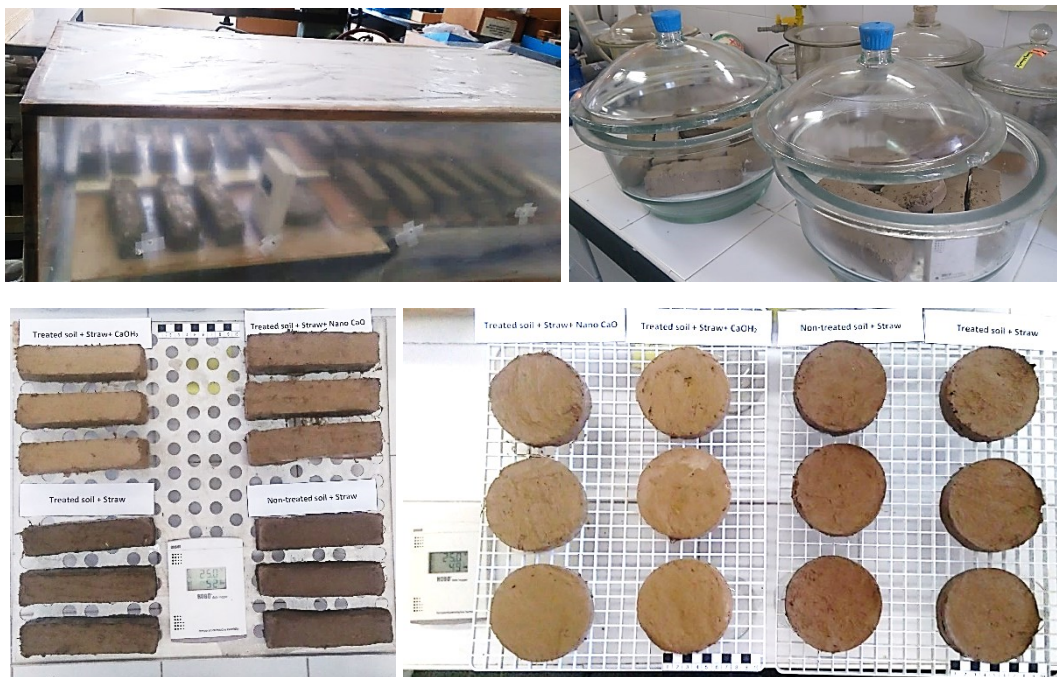


Figure 3.22 Curing and drying of the samples.

After 28 days involving the curing and drying times, before the tests, the surfaces of all samples were smoothened using sand papers to increase the accuracy of measurements. The adobe samples in prismatic and cylindric shapes were coded as shown in Table 3.7, Table 3.8 and Table 3.9.

Table 3.7 Codes and images belonging to 4 subtypes of Konya_Küçükköy samples in prismatic and cylindric shapes.
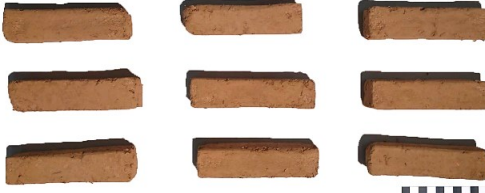
| KuU: Küçükköy- Untreated | KuT: Küçükköy- Treated |
|---|---|
|  |  |
|  |  |
| **KuTN**: **Kü**çükköy-Treated+NanoCaO | **KuTC**: **Kü**çükköy-Treated+$CaOH_2$ |
|  |  |
|  |  |

Table 3.8 Codes and images belonging to 4 subtypes of Çorum_Karapınar samples in prismatic and cylindric shapes.
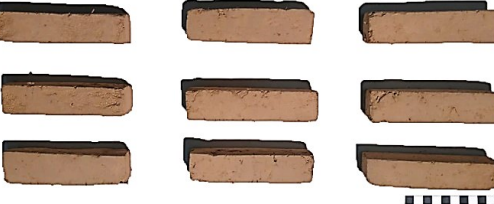
| KaU: Karapınar- Untreated | KaT: Karapınar- Treated |
|---|---|
|  |  |
|  |  |
| **KaTN: Karapınar-Treated+NanoCaO** | **KaTC: Karapınar-Treated+CaOH$_2$** |
|  |  |
|  |  |

Table 3.9 Codes and images belonging to 4 subtypes of Çorum_Kınık samples in prismatic and cylindric shapes.

| KıU: Kınık- Untreated | KıT: Kınık - Treated |
|---|---|
|  |  |
|  |  |
| **KıTN: Kınık-Treated+NanoCaO** | **KıTC: Kınık-Treated+CaOH$_2$** |
|  |  |
|  |  |
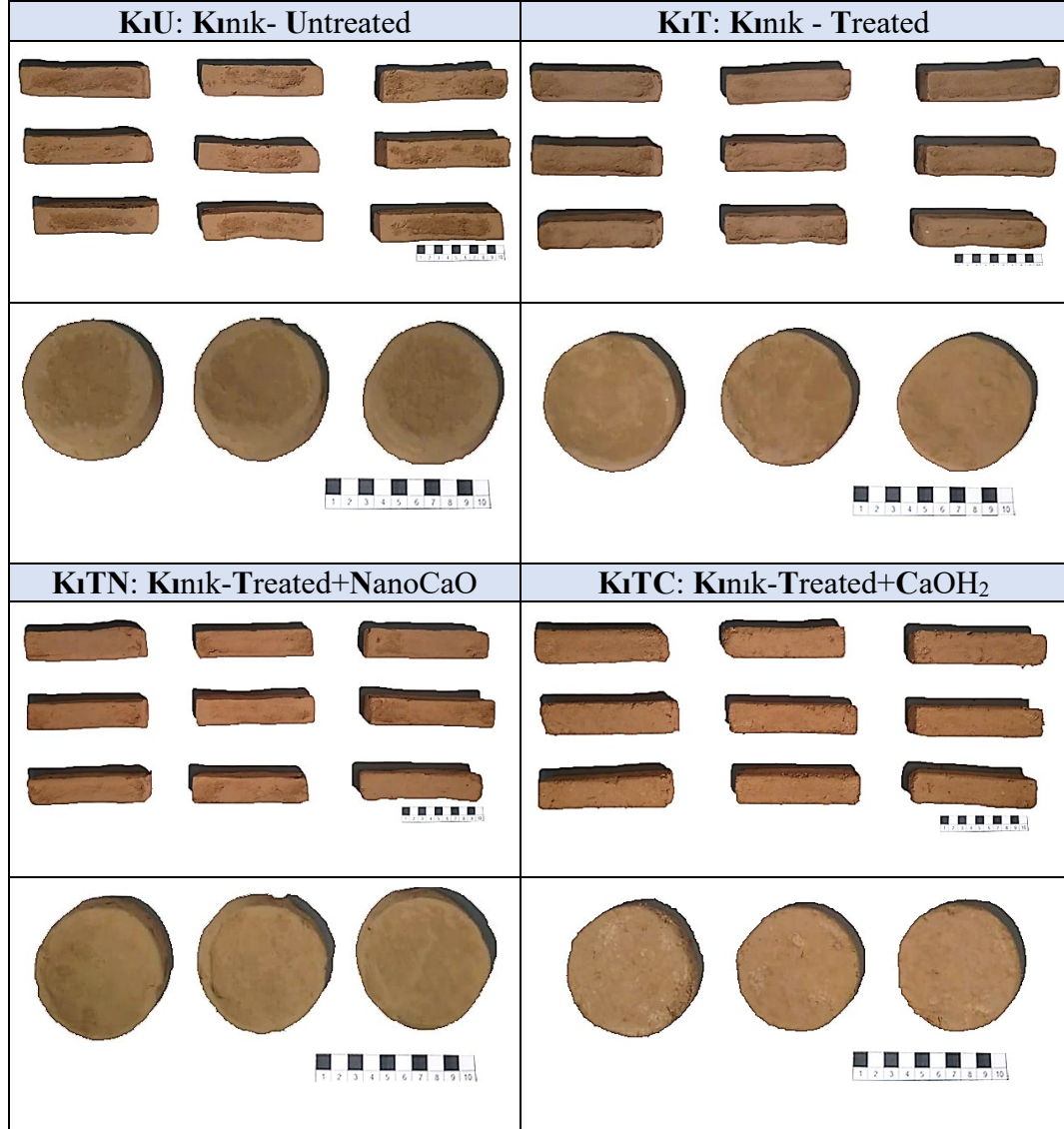
## 3.8    Basic Physical Tests

The particle density, bulk density (dry density) and porosity values of the adobe samples were specified in terms of the physical tests. Those tests were conducted on the Konya_Küçükköy, Çorum_Karapınar and Çorum_Kınık samples by using ASTM D 854 – 02 and ASTM D7263 − 21 standards and equation given in RILEM,

respectively (ASTM, 2017b, 2021; RILEM, 1980). The weight of adobe and soil samples oven-dried at a temperature of 60°C, and their bulk density values were calculated through their volumes measured by Archimedes weights (Figure 3.23). The particle density was found in the pycnometer method on the oven-dry samples (Figure 3.23). Their porosity values were calculated by the following formula (Equation 6):

$$P = \frac{D_{Particle} - D_{Bulk}}{D_{Particle}} \times 100 \qquad\qquad 6$$

Where P is porosity, %; $D_{Particle}$ is particle density, $g/cm_3$; $D_{Bulk\ is}$ Bulk density, $g/cm^3$.



Figure 3.23 Pycnometer method to detect particle density (at left) and oven-dried weight (at middle) and Archimedes weights of the samples (at right) to find out their bulk densities.

## 3.9 Water Vapour Permeability Test

The water vapour permeability tests were conducted by periodically weighing the adobe sample placed between ambiences with two different relative humidity until equilibrium was performed through the dry cup method according to the Turkish standard of TS EN ISO 12572:2016 (TS EN ISO, 2016). The dry cup method is designed to measure the vapour drive moving into the dry sample. In this method, the cup on which the sample is placed by sealing the sides contains a desiccant, with a humidity of 0–5%. The Konya_Küçükköy, Çorum_Karapınar and Çorum_Kınık

adobe samples together with the cups containing desiccants are put into a test chamber (Figure 3.24 and Figure 3.25). In the test assembly, the vapour in the test chamber maintained at a constant temperature of $23 \pm 1$°C and a relative humidity of $50 \pm 5\%$ is moving to desiccant under the samples.

Three samples were prepared for each sample type and thirty-six samples in total. Thicknesses and the upper and lower surfaces (exposed areas) of the samples were recorded. Before testing, those samples were kept at $23 \pm 5$ °C and $50 \pm 5$ % relative humidity until a constant weight was obtained. Silica gel with a minimum depth of 15 mm was put into the cup as desiccant leaving a small air gap ($15 \pm 5$ mm) between it and the sample. By using melted wax, all sides of the cylindrical samples were sealed and tightly attached to the open side of the cup. The first weight was taken of the sample together with the cup and the weighing proceeded until the change in the mass was constant within $\pm 5$ % of the mean value for the sample in five successive measurements.
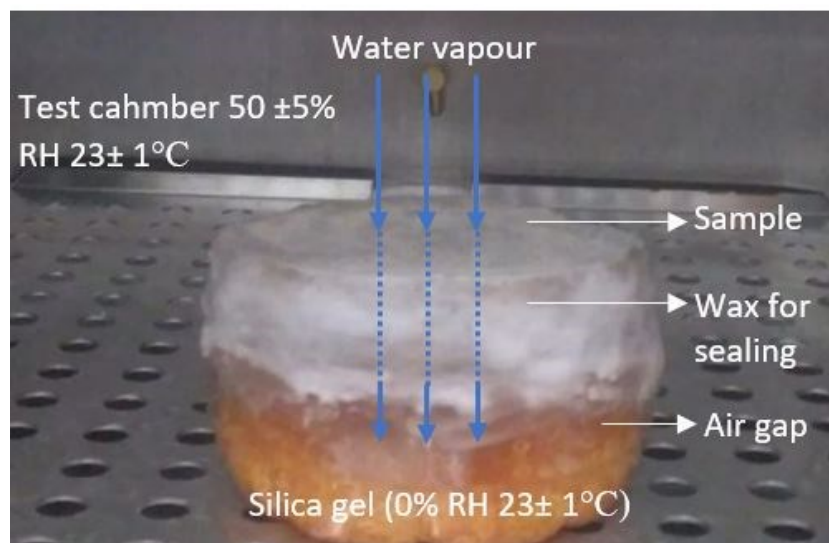


Figure 3.24 Schema of the dry cup method in the test assembly.

Figure 3.25 The samples kept in the test chamber in the dry cup method.

The parameters of "water vapour resistance factor ($\mu$, unitless)" and "equivalent air thickness of water vapour permeability (SD, m)" were found by calculation of the measurement data by the following equations (Equation 7, Equation 8 and Equation 9) (TS EN ISO, 2016).

$$SD = \mu \times d \qquad 7$$

$$\mu = d_{air}/(W/d) \qquad 8$$

$$W = Dm_{12}/(A_{mean}/Dp) \qquad 9$$

Where d is the thickness of the sample, m; W is water vapour permanence, $kg/m^2sPa$; $d_{air}$ is water vapour permeability of air (2.2 kg/msPa was accepted according to the standard); $Dm_{12}$ is change in mass per time for a single determination, kg/s; $A_{mean}$ is mean of the upper and lower surface areas, $m^2$; Dp is vapour pressure difference (1404 Pa was accepted according to the standard).

## 3.10 Mechanical Tests

The mechanical analyses were conducted on the Konya_Küçükköy, Çorum_Karapınar and Çorum_Kınık adobe samples to determine flexural strength (σf) and compressive strength (σc) values. The manual testing machine, LOS (Losenhausen, Maschinenbau AG Dusseldorf), equipped with 2 kg loading per second was used for those mechanical tests (Figure 3.26).



Figure 3.26 Flexural (at left) and compressive strength tests (at right) by the manual testing machine, LOS (Losenhausen, Maschinenbau AG Dusseldorf).

For the flexural strength test, the test mechanism is composed of two supporting rollers at a distance of 9 cm under the sample and the third roller a loading roller, which is located above the sample and midway between the supporting rollers. The flexural strength was tested on three samples in dimensions of 4x4x16 cm for each type of sample (TS EN, 2020). Dimensions of the samples were recorded concerning the width and height of the sample according to the placement configuration in the test machine. Flexural strength is calculated by the formula presented in Equation 10 and expressed in MPa.

$$\sigma f = 1.5 \times \frac{F \times L}{b \times d^2} \times 0.1 \text{Mpa} \qquad\qquad 10$$

Where σf is flexural strength, MPa; F is the maximum load applied to the sample, kg; L is the distance between the supports, 9 cm; b is the width of the sample, cm; d is the height of the sample, cm (Figure 3.27).
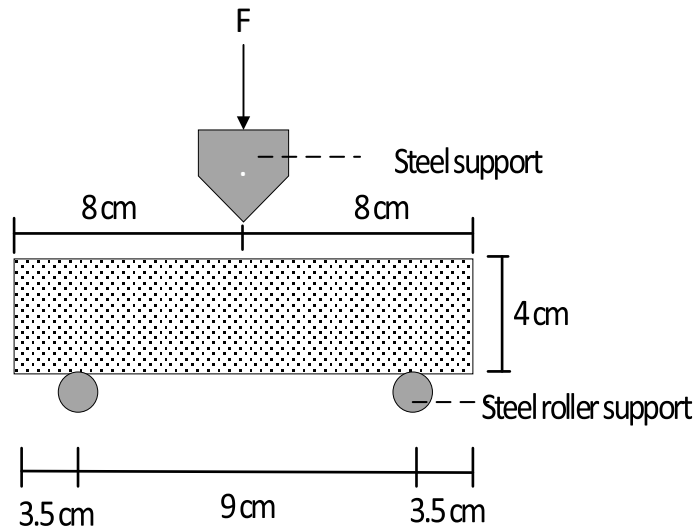


Figure 3.27 Schematic representation of the flexural strength test on adobe sample.

The compressive strength tests were conducted on the six broken half prisms obtained after the flexural strength of those samples was identified (TS EN, 2020). The adobe samples were placed between two square metal pads with dimensions of 3cm x 3cm for the compressive load at the testing machine, as the samples have cross-section dimensions smaller than 4cm due to the shrinkage. Compressive strength is calculated by the formula shown in Equation 11 and expressed in MPa.

$$\sigma c = \frac{F}{A} \times 0.1 \text{Mpa} \qquad\qquad 11$$

Where σc is the compressive strength, MPa; F achieved as an output of the test is the maximum load applied to the sample, kg; A is the area of bed-face, cm$^2$ (Figure 3.28).
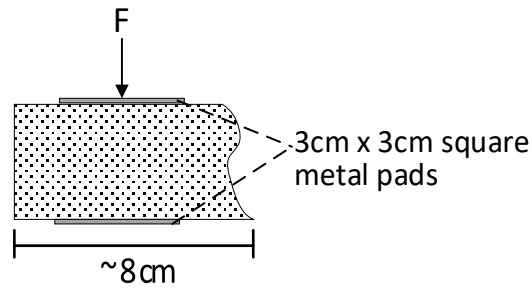
Figure 3.28 Schematic representation of the compressive strength test on broken half prisms of adobe sample.

## 3.11    Capillary Water Absorption Test

The capillary water absorption tests were conducted to find out capillary water absorption and capillary water absorption coefficient values of Konya_Küçükköy, Çorum_Karapınar and Çorum_Kınık adobe samples. The tests were performed by the partial immersion method according to the ASTM C1403-15:2015 standard (ASTM, 2015). Three prismatic adobe samples ($4x4x16$ cm$^3$) for each type were dried in the oven at 60°C then left in laboratory conditions (ca. 18°C and 40% RH). The adobe samples were placed on the plastic supports in plastic containers filled with water at a certain level. The methodology of the standard test was adapted by placing 3 mm thick water-saturated absorbent tissue as a bedding layer under the adobe samples to prevent direct contact with the water, which would lead to excessive material loss (Costi de Castrillo et al., 2021; Ribeiro et al., 2022). The configuration of the experiment is shown in Figure 3.29 and Figure 3.30. Keeping the constant water level in the container and continuously wet absorbent paper under the adobe samples was ensured during the test.
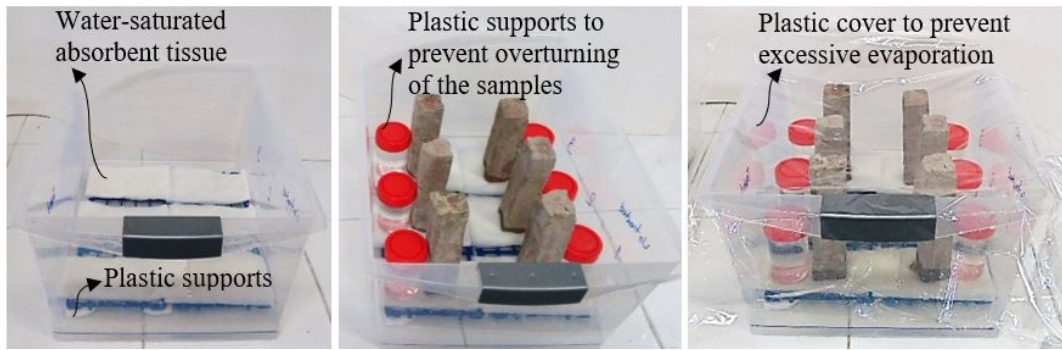
Figure 3.29 The configuration of the capillary water absorption experiment.
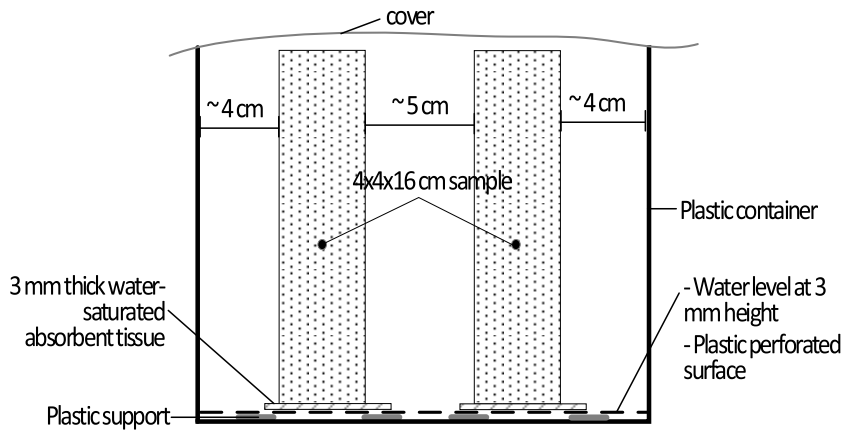


Figure 3.30 Schematic representation of the capillary water absorption test of adobe sample.

The capillary water absorption of the samples was measured by weighing the samples at regular time intervals at 15 minutes, 60 minutes and 240 minutes, respectively (Table 3.10). The test could be conducted for up to 240 minutes, as some adobe samples lost their integrities after that time. In that time interval, negligible material loss was observed in all samples. The capillary water absorption ($A_T$), cumulative water intake per unit of surface in kg/m$^2$, was calculated at each time by the formula in Equation 12 (ASTM, 2015).

$$A_T = \frac{w_T - w_O}{S} \qquad 12$$

Where $W_T$ is the wet weight of the sample at time T; $W_0$ is the dry weight at the initial time, in kg; S is the surface area of the specimen's cross-section, in $m^2$.

The capillary water absorption values were recorded as a function of the square root of each time ($\sqrt{t}$), and the capillary water absorption coefficient (A-value) was calculated by the following Equation 13 (Hall & Hoff, 2002).

$$A - value = \frac{W_T - W_O}{s\sqrt{t}} \qquad 13$$

Table 3.10 The adobe samples during the capillary water absorption test process.



| 15 min | | | | 60 min | | | | 240min | | | |
|---|---|---|---|---|---|---|---|---|---|---|---|
| KuU | KuT | KuTN | KuTC | KuU | KuT | KuTN | KuTC | KuU | KuT | KuTN | KuTC |
| KaU | KaT | KaTN | KaTC | KaU | KaT | KaTN | KaTC | KaU | KaT | KaTN | KaTC |
| K₁U | K₁T | K₁TN | K₁TC | K₁U | K₁T | K₁TN | K₁TC | K₁U | K₁T | K₁TN | K₁TC |
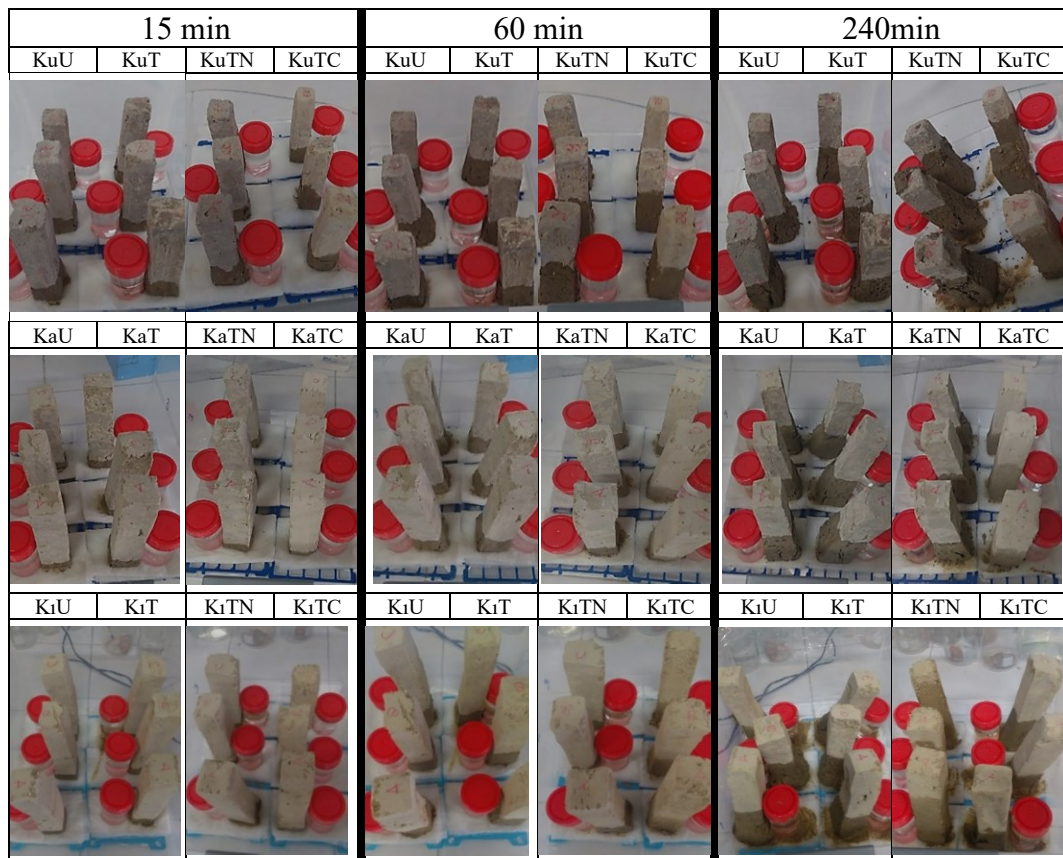
# CHAPTER 4

# RESULTS

In total, there are seven natural adobe samples to investigate, while the shortcomings related to the compositional and raw materials characteristics of these adobe resources identified during consecutive stages of the research allowed the elimination of the four ones for the comprehensive analyses. Table 4.1 summarizes the natural adobe soil types/samples which are more advantageous than the others for Nano-clay production in certain amounts and for adobe material production with the enriched Nano-clay content, considering their performance limitations. These limitations are listed below briefly:

- presence of asbestos minerals in the composition of adobe soil that makes it unhealthy,
- excessive swelling and shrinkage behaviour of the clay binder that makes it poor against the outside climate condition, in other words, no proper type of clay content is determined in the adobe soil,
- less amount of clay content which makes its amount of clay insufficient for Nano-clay production.

Table 4.1 Summarizing the elimination reasons of four natural adobe soil samples by considering the performances of the total seven adobe soil samples during the consecutive stages of their examination.

| Soil Sample | Konya_Küçükköy | Çorum_Karapınar | Çorum_Kınık | Çorum_Sarımbey | Manisa_Kemer | Eskişehir_Sorkun | Eskişehir_Sazak |
|---|---|---|---|---|---|---|---|
| Identification of Local Adobe/Clay Resources | ✔ | ✔ | ✔ | ✔ | ✔ | ✔ | ✔ |
| Determination of Nano-clay content in natural adobe soil resources | ✔ | ✔ | ✔ | ✔ | ✔ | Presence of asbestos minerals | Excessive swelling and shrinkage problems and no proper clay content |
| Enrichment of Nano-clay content in natural adobe soil resources and Nano-Clay content assessment | ✔ | ✔ | ✔ | ✔ | Too low clay content | | |
| Performance assessment of Nano-clay riched adobe soil samples (Treated adobe soil samples) | ✔ | ✔ | ✔ | ✔ | | | |
| Performance assessment of Nano-clay riched adobe product samples (Treated adobe samples) | ✔ | ✔ | ✔ | Not having proper consistency limits | | | |

## 4.1 Identification of Local Adobe/Clay Resources

The collected soil samples of Konya_Küçükköy Çorum_Karapınar, Çorum_Kınık, Çorum_Sarımbey, Manisa_Kemer, Eskişehir_Sorkun and Eskişehir_Sazak were firstly analysed by field tests then, their raw materials/composition characteristics

and their clay types were determined by laboratory analyses to find out whether they are proper as adobe soil or not. The results were given under the related subheadings.

## 4.1.1    Field Soil Test

The results of field soil tests including visual, smell ribbon and feel tests were indicated in Table 4.2. The samples of Konya_Küçükköy, Çorum_Karapınar and Çorum_Kınık were found to be silty clay loam; Çorum_Sarımbey was specified as silty loam; Manisa_Kemer and Eskişehir_Sorkun were detected as sandy loam; Eskişehir_Sazak was identified as clay loam.

Table 4.2 The results of field tests conducted on soil samples and soil types.

| Sample | Field Tests | | | | Soil Type |
|---|---|---|---|---|---|
| | Visual | Smell | Ribbon length, cm | Feel | |
| **Konya_Küçükköy** | Fine aggregates | No mould smell | 3.5-4 | Smooth | Silty clay loam |
| **Çorum_Karapınar** | Fine aggregates | No mould smell | 4 | Smooth | Silty clay loam |
| **Çorum_Kınık** | Fine aggregates | No mould smell | 3 | Smooth | Silty clay loam |
| **Çorum_Sarımbey** | Fine aggregates | No mould smell | 2 | Smooth | Silty loam |
| **Manisa_Kemer** | Coarse aggregates | No mould smell | 1-1.5 | Gritty | Sandy loam |
| **Eskişehir_Sorkun** | Fine aggregates | No mould smell | 1-1.5 | Gritty | Sandy loam |
| **Eskişehir_Sazak** | Flocculated coarse aggregates | No mould smell | 3.5-4.5 | Sticky | Clay loam |

**4.1.2    Raw Material Characteristics Tests**

The raw materials characteristics tests on the pH value, organic and calcium carbonate content, soluble salts and pozzolanic properties of the soil samples were given under related subheadings.

**4.1.2.1    pH values**

The results of the pH strip are shown in Table 4.3. The pH of Eskişehir_Sorkun samples was found to be neutral. The basic (alkaline) soil samples of Çorum_Kınık and Eskişehir_Sazak signal the presence of the minerals of calcium, magnesium and/or potassium, while in the acidic soil samples of Konya_Küçükköy, Çorum_Karapınar, Çorum_Sarımbey and Manisa_Kemer, sulphur and/or organic content may be found (Parnes, 2013).

Table 4.3 Acidity and alkalinity of soil samples by pH test results.

| Sample | pH Scale | |
|---|---|---|
| | 5.5-9 range | Result |
| Konya_Küçükköy | 6.5 | Asidic |
| Çorum_Karapınar | 5.5 | Asidic |
| Çorum_Kınık | 7.5 | Basic |
| Çorum_Sarımbey | 6.5 | Asidic |
| Manisa_Kemer | 5.5 | Asidic |
| Eskişehir_Sorkun | 7 | Nötr |
| Eskişehir_Sazak | 7.5 | Basic |

**4.1.2.2    Organic and Calcite Contents**

The organic and calcite ($CaCO_3$) contents achieved by loss on ignition analyses on all soil samples are indicated in Table 4.4. The organic and $CaCO_3$ contents of the samples are in the range of 0 %-4.3 % and 2 %-12 %, respectively.

Table 4.4 Organic and $CaCO_3$ content percentages of soil samples.

| Sample | Organic Content, % | CaCO$_3$ Content, % |
|---|---|---|
| **Konya_Küçükköy** | 4.3 | 9.2 |
| **Çorum_Karapınar** | 2.4 | 6.8 |
| **Çorum_Kınık** | 2.4 | 6.8 |
| **Çorum_Sarımbey** | 2.6 | 5.1 |
| **Manisa_Kemer** | 2 | 2 |
| **Eskişehir_Sorkun** | 0 | 10 |
| **Eskişehir_Sazak** | 2 | 12 |

### 4.1.2.3 Soluble Salts

Results of the spot salt tests of phosphate ($PO_4^{-2}$), sulphate ($SO_4^-$), chloride ($Cl^-$), nitrite ($NO_2^-$), nitrate ($NO_3^-$) and carbonate ($CO_3^{2-}$) ions in soil samples were indicated in Table 4.5.

Table 4.5 The results of spot salt tests conducted on samples.

| SPOT SALT TESTS | | | | | | |
|---|---|---|---|---|---|---|
| Sample | Sulphate ($SO_4^-$) | Carbonate ($CO_3^{2-}$) | Phosphate ($PO_4^{-2}$) | Nitrite ($NO_2^-$) | Nitrate ($NO_3^-$) | Chloride ($Cl^-$) |
| Konya_Küçükköy | + | + | + | + | + | + |
| Çorum_Karapınar | + | + | + | + | + | + |
| Çorum_Kınık | + | + | + | + | + | + |
| Çorum_Sarımbey | + | + | + | + | + | + |
| Manisa_Kemer | - | + | - | + | + | - |
| Eskişehir_Sorkun | + | + | - | - | - | + |
| Eskişehir_Sazak | + | + | + | + | + | + |

**Sulphate ($SO_4^-$)**: The $SO_4^-$ ion was detected in all samples except the Manisa_Kemer sample. This ion generally signals the existence of a hydrated form of calcium sulphate/gypsum ($CaSO_4.2H_2O$).

**Carbonate ($CO_3^{2-}$)**: The $CO_3^{2-}$ ion was detected in all soil samples that support the sample's XRD analysis results showing the presence of calcite/calcium carbonate ($CaCO_3$) mineral in all samples.

**Phosphate (PO$_4^{-2}$):** The ion of PO$_4^{-2}$ was found in all samples except the Manisa_Kemer and Eskişehir_Sorkun samples.

**Nitrite (NO$_2^-$)-Nitrate (NO$_3^-$):** The ions of NO$_2^-$ and NO$_3^-$ were detected in all samples except the Eskişehir_Sorkun sample. The initial form is NO$_2^-$, which turns into NO$_3^-$ form when it is oxidised.

**Chloride (Cl$^-$):** The ion of Cl$^-$ was found in all samples except the Manisa_Kemer sample. This ion is commonly found in halite (NaCl) and sylvite (KCl) minerals.

### 4.1.2.4    Pozzolanic Activity

The results of the pozzolanic activity test conducted by the method titration with EDTA on the soil samples are shown in Table 4.6. Pozzolanic activity values were found to be in the range of 227.9-16.1 mg Ca(OH)$_2$ /1g pozzolan.

Table 4.6 Pozzolanic activity values achieved by the method titration with EDTA.

| Samples | Weight (g) | EDTA (ml) | MOL EDTA | Ca (OH)$_2$ (g) | mg Ca (OH)$_2$/1 g Pozzolan |
|---|---|---|---|---|---|
| Konya_Küçükköy | 0.2 | 66.5 | 0.000665 | 0.008892 | 44.5 |
| Çorum_Karapınar | 0.2 | 50 | 0.0005 | 0.0455715 | 227.9 |
| Çorum_Kınık | 0.2 | 65 | 0.00065 | 0.0122265 | 61.1 |
| Çorum_Sarımbey | 0.2 | 52 | 0.00052 | 0.0411255 | 205.6 |
| Manisa_Kemer | 0.2 | 19.3 | 0.000193 | 0.0093366 | 45.2 |
| Eskişehir_Sorkun | 0.2 | 22 | 0.00022 | 0.0033345 | 16.1 |
| Eskişehir_Sazak | 0.2 | 17 | 0.00017 | 0.0144495 | 71.5 |

### 4.1.3    Composition (Mineralogical) Tests

The mineralogical composition of aggregates below 63 μm and clay types of Konya_Küçükköy,     Çorum_Karapınar,     Çorum_Kınık,     Çorum_Sarımbey,

Manisa_Kemer, Eskişehir_Sorkun and Eskişehir_Sazak soil samples were determined through X-ray diffraction (XRD) analyses and the results were given under the heading of each sample.

### 4.1.3.1    Konya_Küçükköy Sample

The minerals of montmorillonite, illite-mica, kaolinite, feldspar, calcite, goethite and quartz were found in the Konya_Küçükköy sample (Figure 4.1). After glycol treatment, expansions seemed at about 14 Å peak at the basal d spacing. That signalled the existence of montmorillonite. The peaks of kaolinite about 7 Å, and 3.5 Å were sighted to decrease in case of heating at 600°C significantly. Intensities of calcite and illite-mica peaks were observed to decrease or disappear after heating the sample at 700°C. Intensities of peaks belonging to quartz, goethite and feldspar thought to exist remained stable or increased.
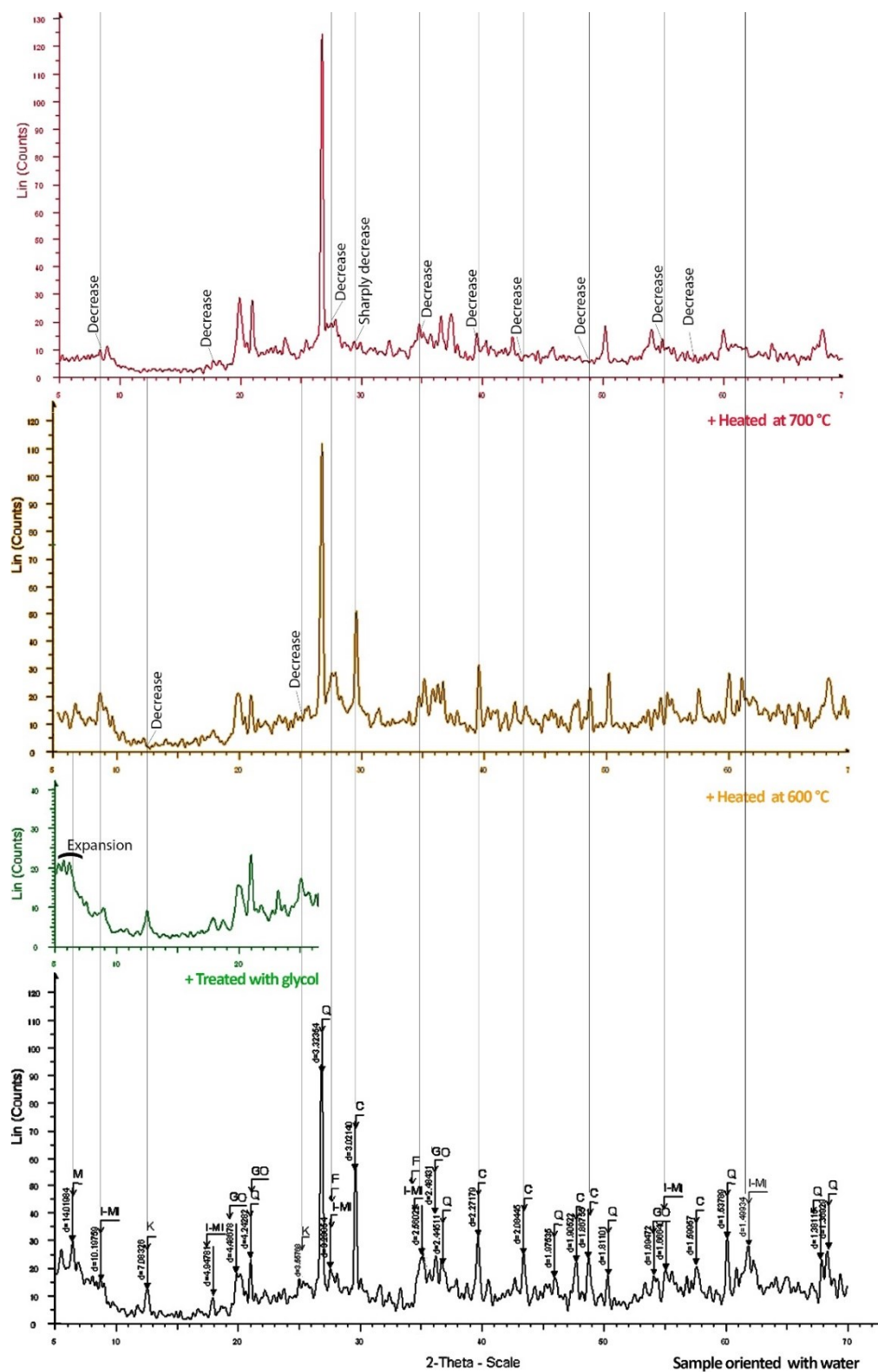
Figure 4.1 XRD patterns of Konya_Küçükköy sample (M: Montmorillonite; I-MI:
Illite-Mica; K: Kaolinite C: Calcite; F: Feldspar; G: Goethite; Q: Quartz).

### 4.1.3.2    Çorum_Karapınar Sample

In the first XRD analysis on the Çorum_Karapınar sample, only lime and gypsum minerals' peaks were observed (Figure 4.2); therefore, the HCL treatment was applied to remove the calcite and gypsum to be able to detect other minerals in the XRD pattern. After that treatment, the minerals of montmorillonite, chlorite, illite-mica, kaolinite, albite, diopside and quartz were found in the sample (Figure 4.3). After glycol treatment, the peak of 15.49 Å at the basal d spacing seemed to expand towards 17 Å. That signalled the existence of montmorillonite. The intensity of kaolinite peaks, 7 Å, 4.45 Å, 3.5 Å 3 Å and 2.38 Å at the basal d spacing, were observed to decrease in case of heating at 600°C significantly. The peaks of 7 Å at the basal d spacing were also thought to refer to chlorite mineral together with the peak of 14 Å. The illite-mica peaks at about 10 Å, 5 Å and 2.2 Å of in the sample heated at 800°C seemed to have lower intensity compared to the sample heated at 600°C, or they disappeared. Intensities of peaks belonging to quartz, feldspar, diopside and goethite thought to exist remained stable or increased.
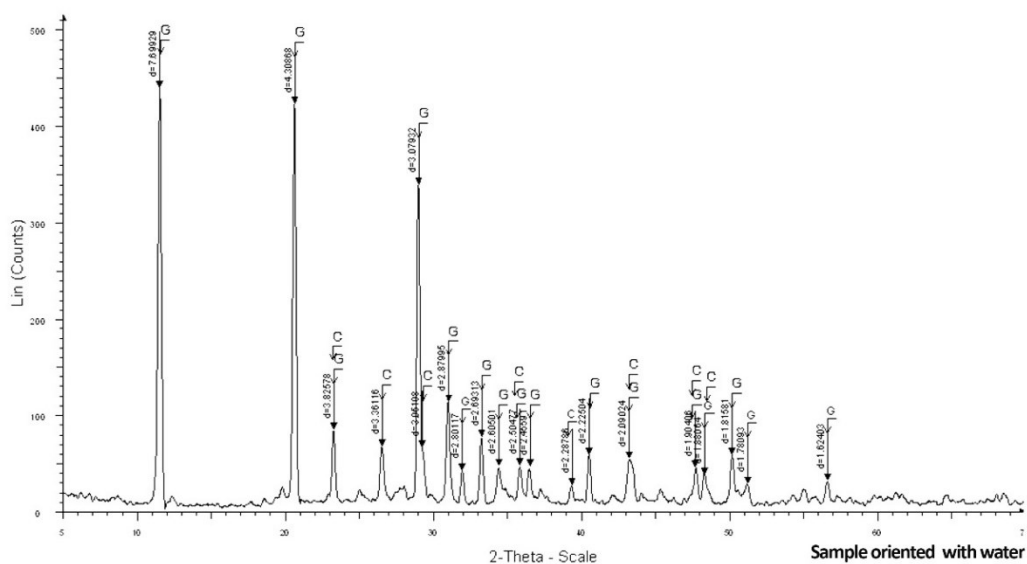


Figure 4.2 Before HCL treatment, XRD patterns of Çorum_Karapınar sample (G: Gypsum; C: Calcite).
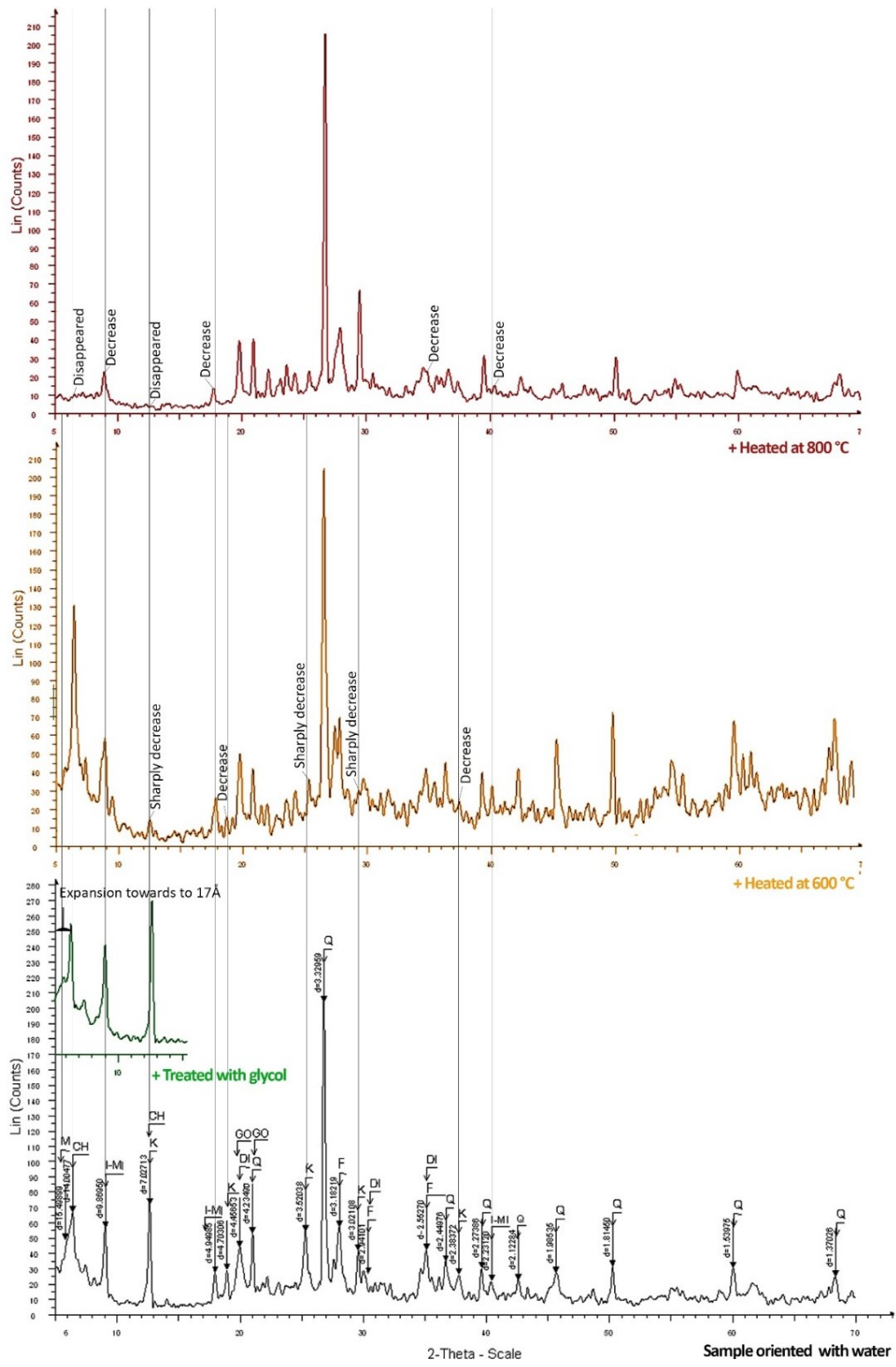
Figure 4.3 After HCL treatment, XRD patterns of Çorum_Karapınar sample (M: Montmorillonite; CH: Chlorite; I-MI: Illite-Mica; K: Kaolinite; F: Feldspar; D: Diopside; Q: Quartz; GO: Goethite).

### 4.1.3.3 Çorum_Kınık Sample

The minerals of montmorillonite, chloride, illite-mica, kaolinite, goethite, albite, calcite, diopside and quartz were found in the sample of Çorum_Kınık (Figure 4.4). After glycol treatment, expansion and a noticeable decrease of peaks of 11.89 Å and 14.33 Å were observed to be at the basal d spacing, respectively. That signalled the existence of montmorillonite. The peaks of 14.33 Å, 7 Å and 3.5 Å at the basal d spacing were anticipated to refer to chlorite mineral. Those peaks also belonging to montmorillonite and kaolinite did not disappear until heating at 800°C. The peaks of kaolinite about 7 Å, 3.5 Å, 3 Å, 1.9 Å and 1.8 Å were sighted to decrease in case of heating at 600°C. Peaks of calcite and illite-mica minerals heated at 800°C seemed to have lower intensity compared to ones heated at 600°C, or they disappeared. Intensities of peaks belonging to quartz, feldspar, diopside and goethite thought to exist remained stable or increased.
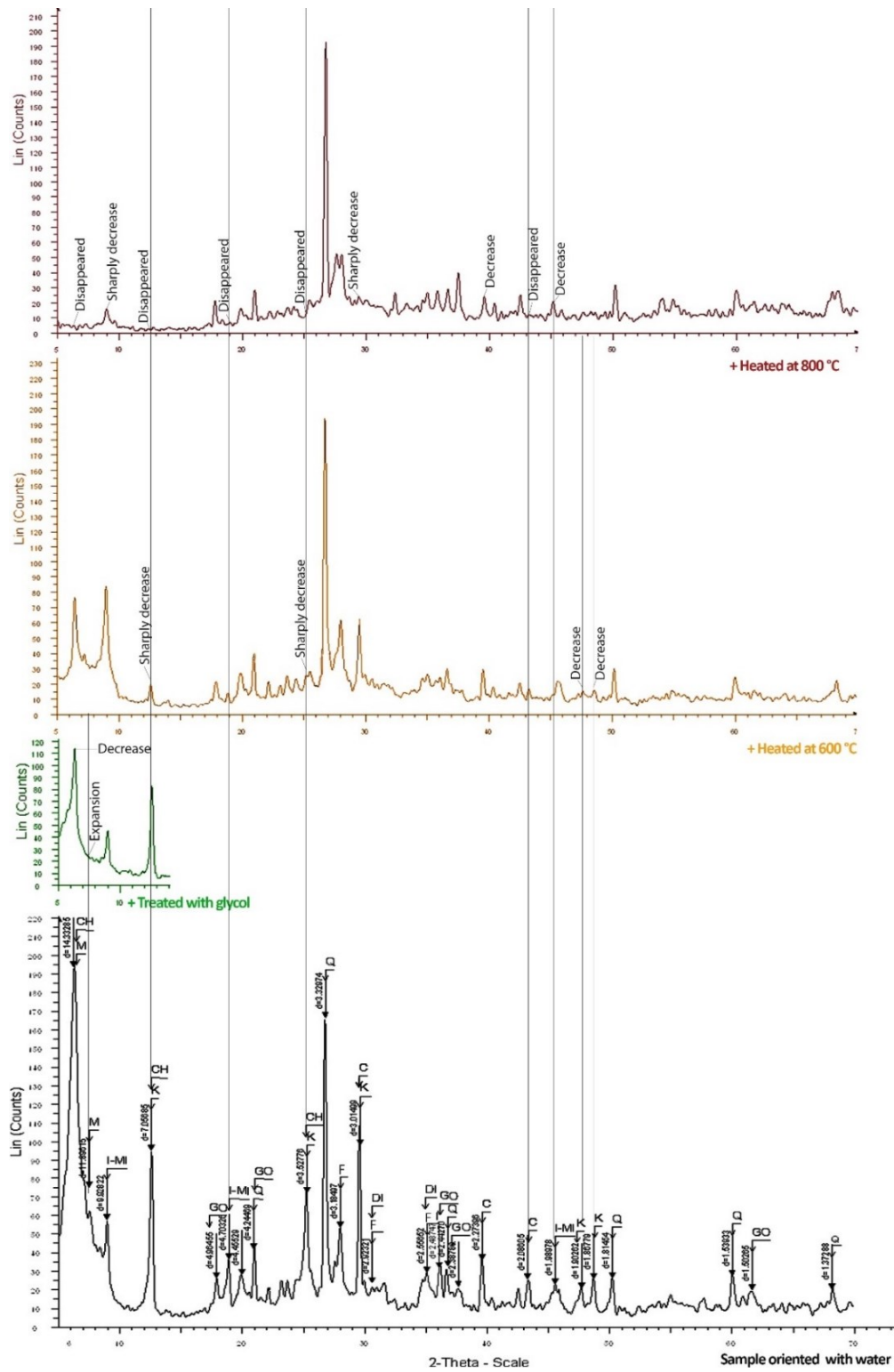
Figure 4.4. XRD patterns of Çorum_Kınık sample (M: Montmorillonite; CH: Chlorite; I-MI: Illite-Mica; K: Kaolinite; F: Feldspar; C: Calcite, D: Diopside; Q: Quartz; GO: Goethite).

### 4.1.3.4 Çorum_Sarımbey Sample

The minerals of montmorillonite, kaolinite, chlorite, goethite, calcite, albite, diopside and quartz were found in the sample of Çorum_Sarımbey (Figure 4.5). After glycol treatment, expansions seemed at 14.09 Å, 9.8 Å, 4.94 Å and 4.69 Å peaks at the basal d spacing. That signalled the existence of montmorillonite. The peaks of kaolinite at 7 Å and 3.52 Å were observed to decrease in case of heating at 600°C significantly. Peaks of illite-mica and calcite in the sample heated at 700°C seemed to have lower intensity compared to the sample heated at 600°C, or they disappeared. Intensities of peaks belonging to quartz, feldspar, diopside and goethite thought to exist remained stable or increased throughout heating treatments.
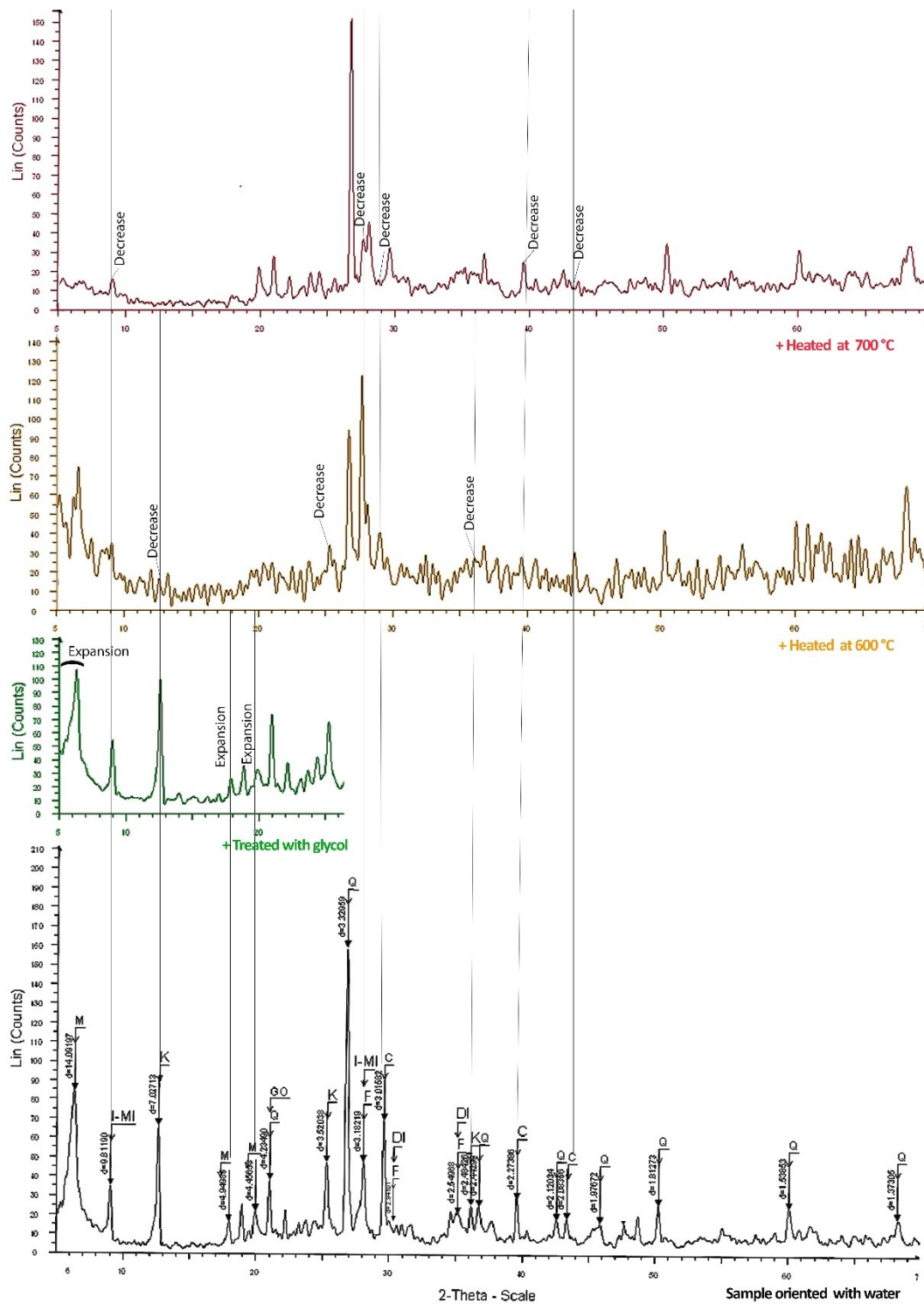
Figure 4.5 XRD patterns of Çorum_Sarımbey sample (M: Montmorillonite; K: Kaolinite; I-MI: Illite-Mica; C: Calcite; F: Feldspar; D: Diopside; Q: Quartz; GO: Goethite).

106

### 4.1.3.5    Manisa_Kemer Sample

The minerals of halloysite, montmorillonite, illite-mica, calcite and quartz were found in the Manisa_Kemer sample (Figure 4.6). After glycol treatment, the expansion and decrease were observed in the XRD pattern at about a peak of 15 Å at the basal d spacing. That signalled the existence of montmorillonite. The halloysite (in the kaolin group) mineral peaks of 10 Å, 7 Å, 3.5 Å and 3.1 Å at the basal d spacing disappeared or decreased at 600°C (Carroll, 1970). Intensities of peaks belonging to quartz and calcite thought to exist remained stable or increased throughout heating treatments.
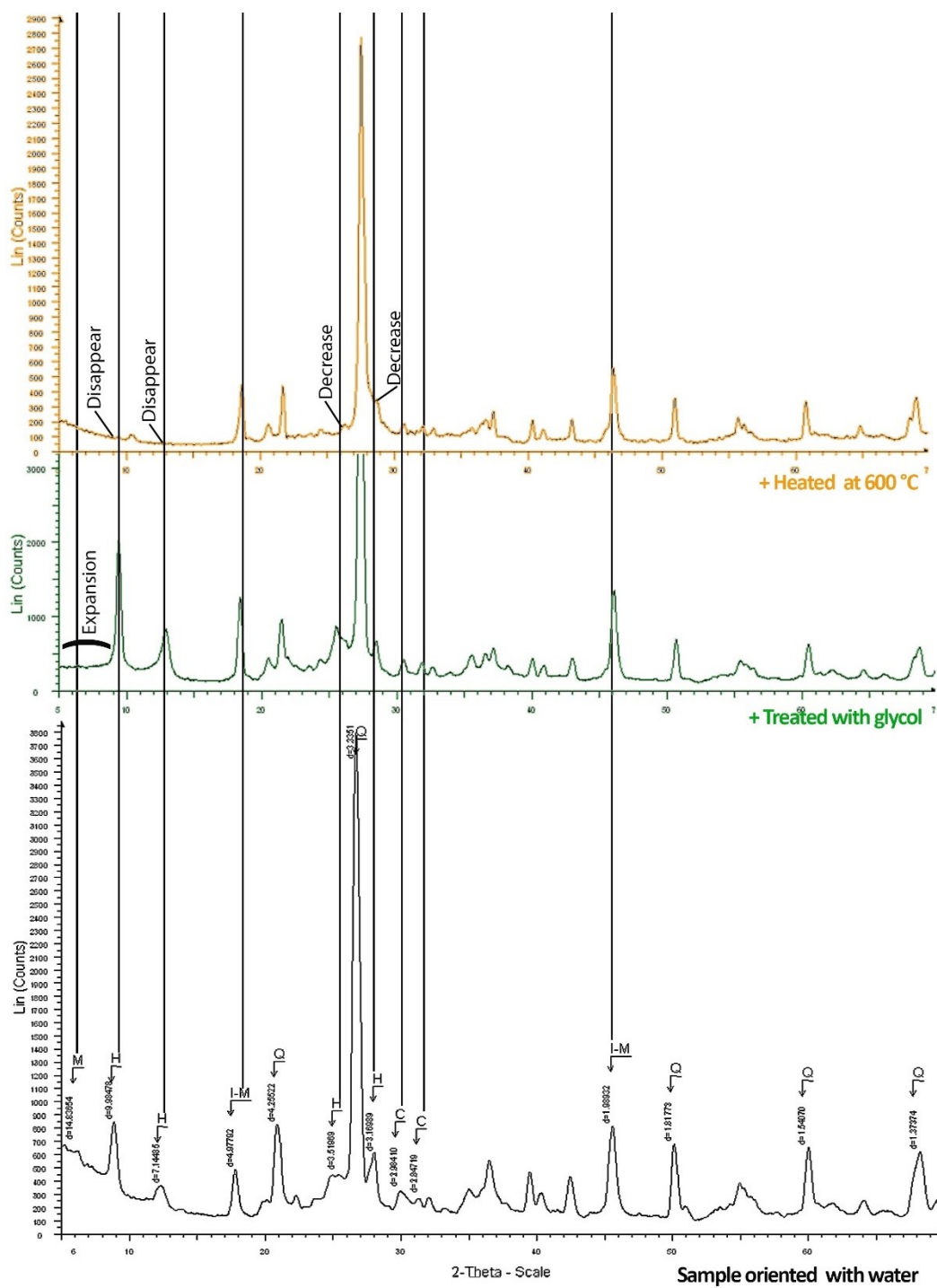
Figure 4.6 XRD patterns of Manisa_Kemer sample (M: Montmorillonite; H:
Halloysite; I-MI: Illite-Mica; C: Calcite; Q: Quartz).

### 4.1.3.6    Eskişehir_Sorkun Sample

The minerals of sepiolite, amphibole, chrysotile, pargasite, illite-mica, calcite and quartz were found in the Eskişehir_Sorkun sample (Figure 4.7). The significant decrease seemed at peaks of 13.8 Å and 3.3 Å belonging to sepiolite after treatment of glycation, and they did not disappear up to 950°C, since the decomposition temperature of sepiolite is about 850°C (Carroll, 1970). The existence of sepiolite in this region is also supported by a study (Kadir et al., 2002). The amphibole mineral was determined at the 9 Å peak that decreased only after heating at 950°C. The chrysotile mineral was identified at 8.1 Å and 6.9 Å peaks, which significantly decreased after heating at 700°C. The illite-mica mineral peaks of 4.6 Å and 3.5 Å at the basal d spacing in the sample heated at 700°C seemed to have significantly lower intensity compared to the sample heated at 600°C. The pargasite mineral was identified at the 8.1 Å and 3 Å peaks that decreased after heating at 950°C since that mineral starts to decompose at the temperatures of 950°C-1000°C (Niida & Green, 1999). The presence of pargasite in this region is also supported by a study (Uysal et al., 2009). Intensities of calcite peaks of 3 Å and 2.8 Å were observed to decrease after heating at 950°C. Intensities of peaks belonging to quartz minerals were observed to be more visible by increasing the temperature during the heating treatments.
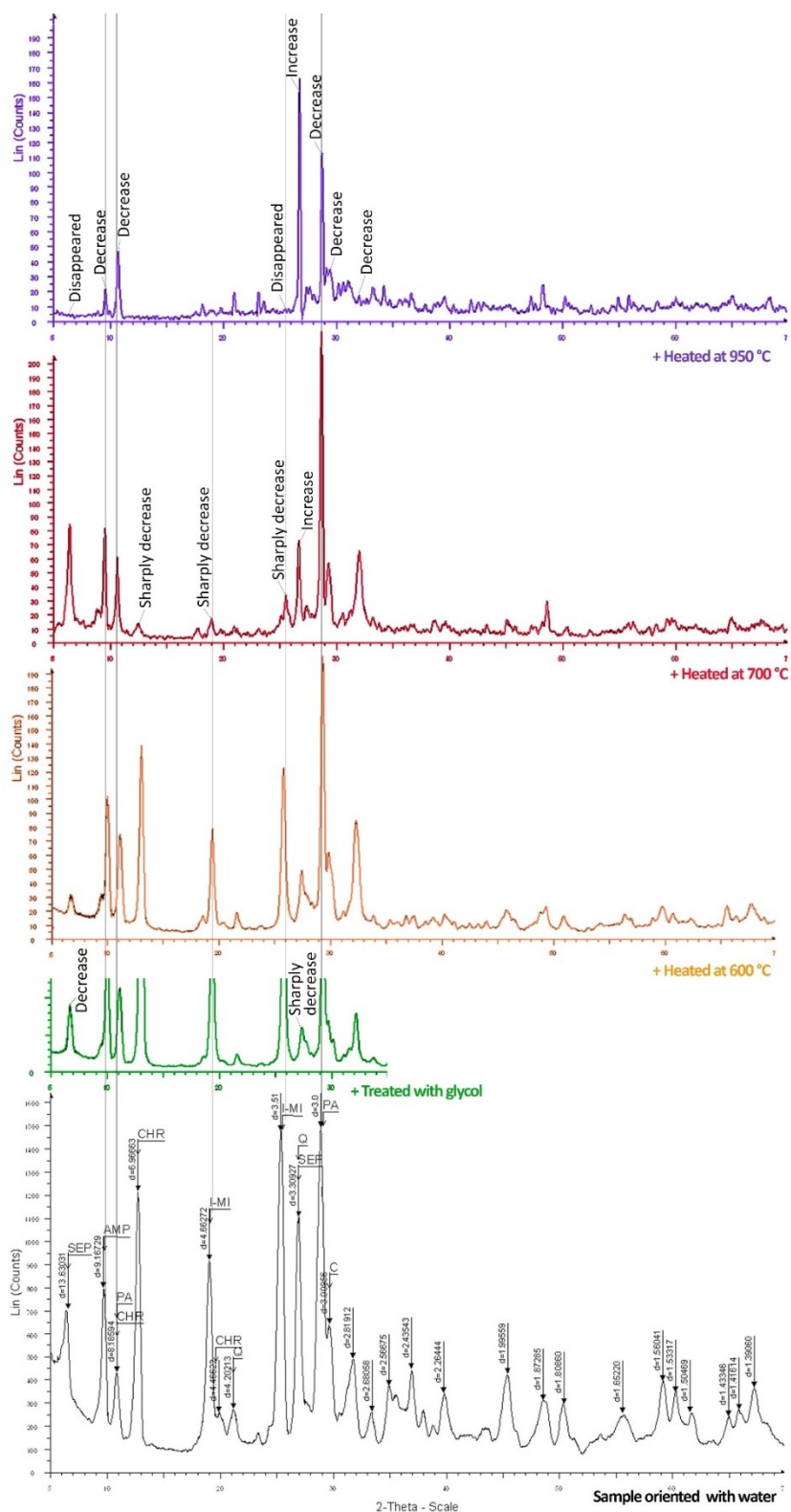
Figure 4.7 XRD patterns of Eskişehir_Sorkun (SEP: Sepiolite; AMP: Amphibole;
PA: Pargasite; CHR: Chrysotile; I-MI: Illite-Mica; C: Calcite; Q: Quartz).

The Eskişehir_Sorkun sample was also analysed by scanning electron microscope (VEGA XMU SEM) to prove the presence of the asbestos clay minerals such as amphibole, pargasite and chrysotile. Asbestos clay minerals in the fibrous form were observed in SEM images in the Eskişehir_Sorkun sample (Figure 4.8).
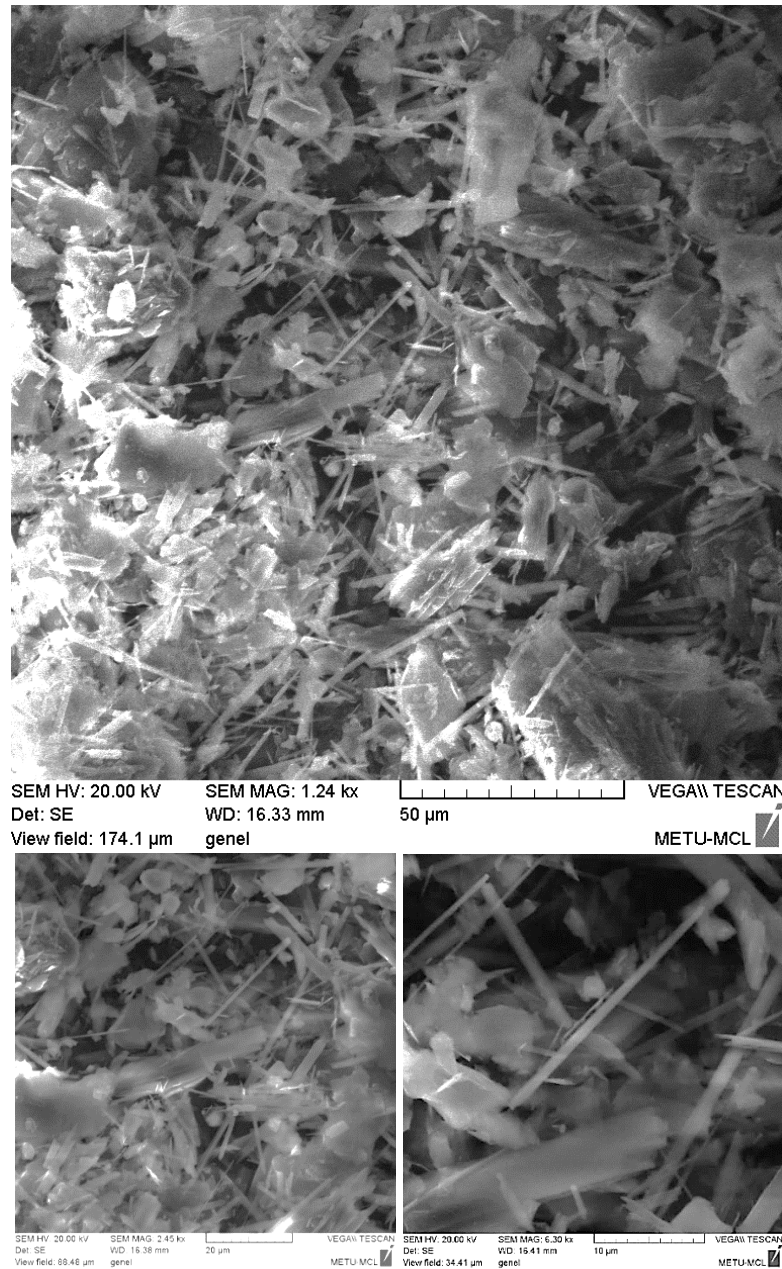


Figure 4.8 Fibrous asbestos clay minerals in the SEM images of Eskişehir_Sorkun sample.

### 4.1.3.7    Eskişehir_Sazak Sample

The minerals of sepiolite, montmorillonite, dolomite and quartz were found in the Eskişehir_Sazak sample supports a study on that area (Karakaş, 2006) (Figure 4.9). Sepiolite is frequently found to be together with dolomite (Carroll, 1970). The significant decrease and expansion seemed at peaks of 15 Å 10.7 Å, 4.5 Å and 3.2 Å, 2.5 Å, 2 Å and 1.5 Å belonging to sepiolite and montmorillonite after treatment of glycation. The intensities of peaks belonging to quartz and dolomite minerals remained the same after the glycol treatment.
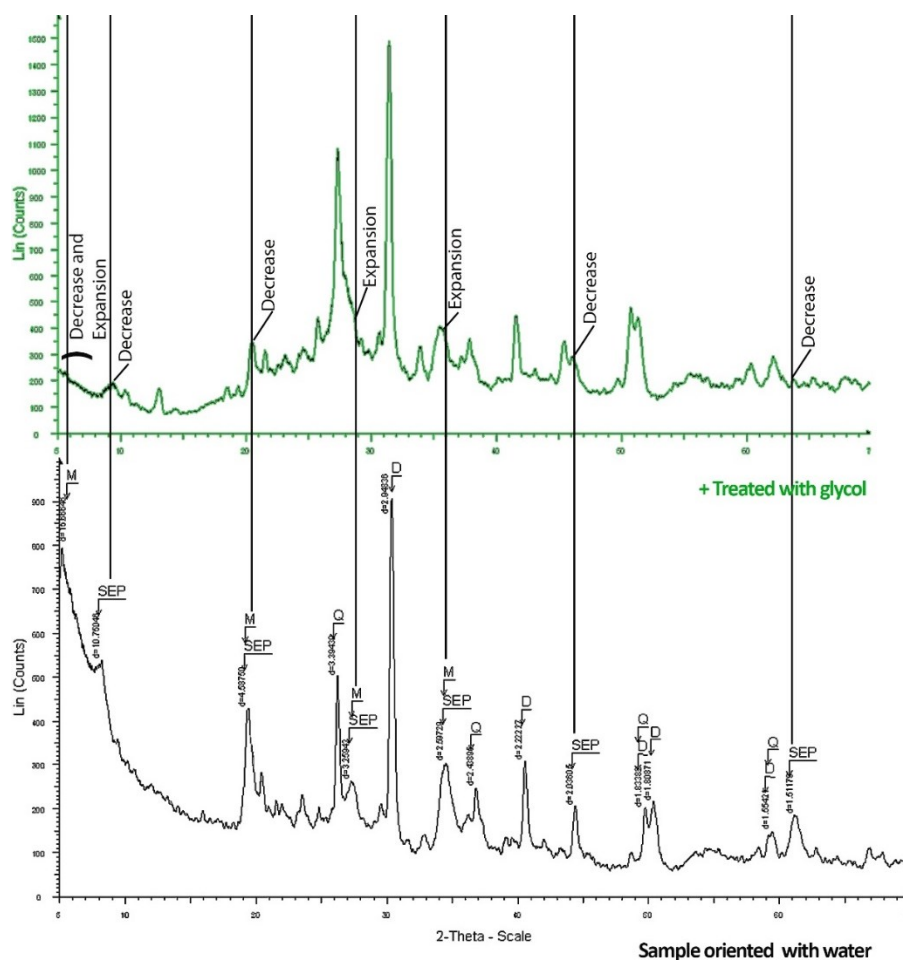


Figure 4.9 XRD patterns of Eskişehir_Sazak sample (M: Montmorillonite; SEP: Sepiolite; D: Dolomite; Q: Quartz).

Serious crack and excessive shrinkage problems resulted in serious difficulty during the preparation of the diluted Eskişehir_Sazak sample for the XRD analyses (Figure 4.10).



Figure 4.10 Excessive crack and shrinkage problems on the diluted sample of Eskişehir_Sazak.

In brief, due to the detection of asbestos materials causing lung cancer disease in Eskişehir_Sorkun (Atabey, 2015; Demir et al., 2018; Kadir & Erkoyun, 2015; Mahltig & Pastore, 2018; Noonan & Pfau, 2011; Uysal et al., 2009), and due to the presence of inappropriate clay contents sepiolite resulting in excessive shrinkage and cracks problem in Eskişehir_Sazak sample, those samples were eliminated at that stage. The Konya_Küçükköy, Çorum_Karapınar, Çorum_Kınık, Çorum_Sarımbey and Manisa_Kemer were found to be more appropriate for further analyses.

## 4.2 Determination of Nano-clay Content in Natural Adobe Soil Resources

The Konya_Küçükköy, Çorum_Karapınar, Çorum_Kınık, Çorum_Sarımbey and Manisa_Kemer soil samples were analysed in terms of particle size distribution including "submicron" particle sizes to determine whether they are proper for Nano-clay production and as adobe soil or not.

The aggregates above 63 microns (μm) such as sands and gravels were separated from the silts and clay contents by two sieving methods. The first one is the wet-

sieving and the other one is the alternative method including the wet-sieving and sonication methods. After separating those parts from each other, the particle size distribution of sands and gravels was carried out by dry-sieving. Centrifugal sedimentation was performed for silts and clays. The evaluations were made for the particles above 63 μm according to the scale of Udden and Wentworth (Tucker, 2001), and for particles below 63 μm according to the scales defined at TS EN ISO 14688-1:2018 and the colloid, geology and soil sciences (TS EN ISO, 2018). The results were given under the related subheadings.

## 4.2.1 Analyses of particle size above 63 microns

The alternative method was conducted on Konya_Küçükköy, Çorum_Karapınar, Çorum Kınık and Çorum Sarımbey samples to separate above and below 63 μm while the only method of wet-sieving was applied to Manisa_Kemer sample since it has no gypsum content, according to the spot salt tests. The dry-sieving was executed on all samples' particle sizes above 63 μm. According to particle size distribution results by the alternative method, the soil samples had higher gravel-sand ratios but lower silt-clay ratios compared to wet-sieving analyses (Figure 4.11). The higher silt-clay percentage obtained by wet and dry-sieving is due to the dissolution of gypsum during wet-sieving which causes the formation of fine particles in silt-clay sizes (Pearson et al., 2015; Sulieman & Sallam, 2016). Therefore, the results obtained from the alternative method were taken care of in the samples including gypsum content.
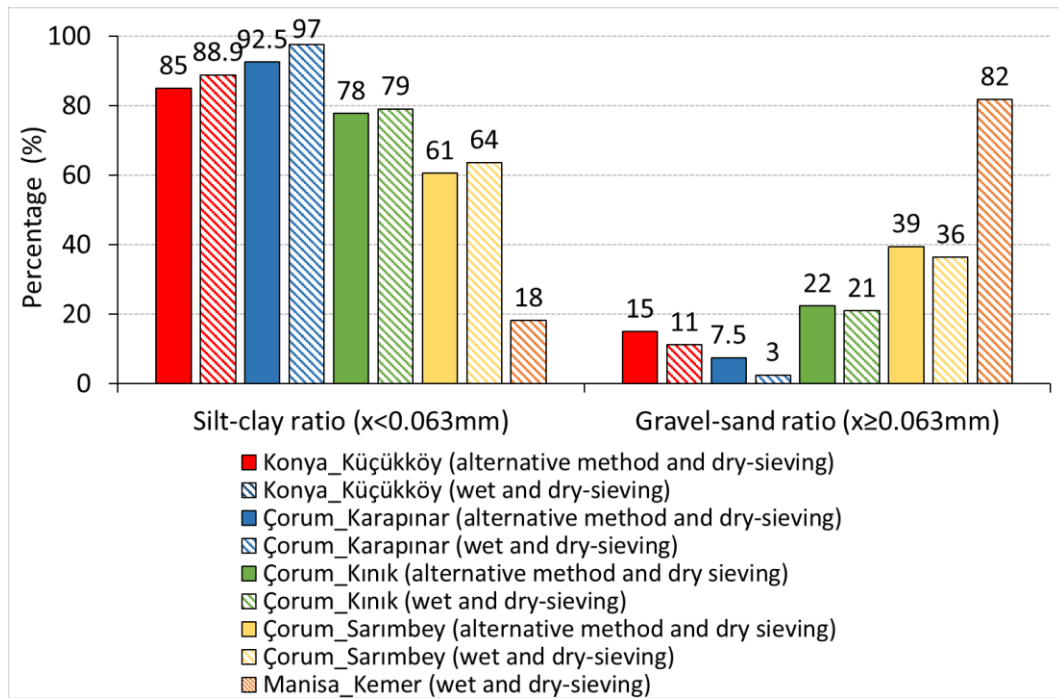
Figure 4.11 The soil samples' silt-clay and gravel-sand ratios achieved by the wet-sieving, alternative method and dry-sieving.

The gravel and sand ratios were found to be in the range of 15%,7.5%, 22%, 39% and 82% for the samples of Konya_Küçükköy, Çorum_Karapınar, Çorum Kınık, Çorum Sarımbey and Manisa_Kemer, respectively. Their silt and clay ratios are the other remaining parts in the 100%. Konya_Küçükköy, Çorum_Karapınar, Çorum Kınık, and Çorum Sarımbey samples have considerably high silt-clay content in the range of 61%-93% (Figure 4.12). Particles above 63 μm of those samples were substantially composed of fine and medium sands, while they have coarse and very coarse sands, granules and pebbles about or below 1% and 2%. Those contents are present in dominantly high amounts in the range of 6% and 13% in the Manisa_Kemer sample which has 63 % sand content and 17% gravel content (granules and pebbles).
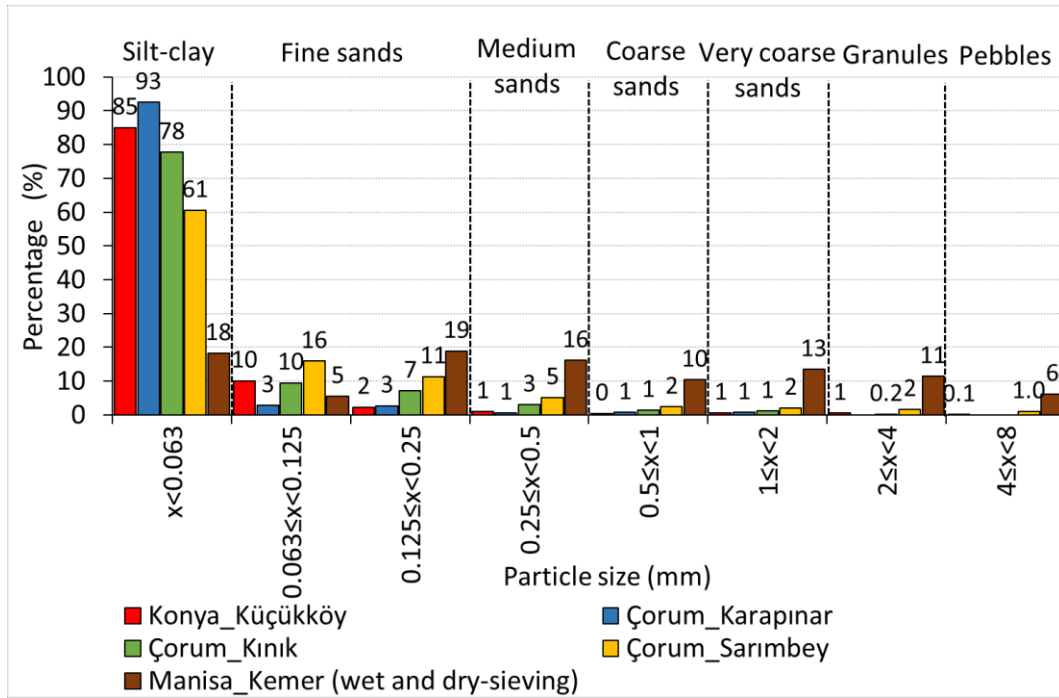
Figure 4.12 Particle size analyses of sands and gravels above 63 µm by the alternative method, wet-sieving and dry-sieving.

## 4.2.2 Analyses of particle size below 63 microns

The centrifuge sedimentation method was conducted on the separated particles below 63 µm for the particle size distribution analyses. The stereo microscope analyses indicated that the samples' particle size below 1 µm is totally clay, and their particles between 1 µm and 2 µm consist of main clay and fine silt content in a small amount (Figure 4.32, Figure 4.33, Figure 4.34 and Figure 4.35). Therefore, the amount of clay content in the sample was considered to be found in particle sizes below 1 µm as a lower limit and below 2 µm as an upper limit. That is consistent with accepted levels at TS EN ISO 14688-1:2018 Turkish standard and the colloid, geology and soil sciences (TS EN ISO, 2018).

The clay content below 1 µm and 2 µm were found to be in the range of 4.2%-13.5%, 4.9%-9.7%, 2.1%-5.5% and 0.3%-0.6 % for the samples of Konya_Küçükköy,

Çorum_Karapınar, Çorum Kınık, Çorum Sarımbey and Manisa_Kemer, respectively (Figure 4.13 and Figure 4.14). Their silt ratios are between 71.5%-81%, 83%-88%, 70.1%-75% and17.6%-18%, respectively. The highest clay content was present in all samples especially particle sizes between 1μm and 2 μm. The Konya_Küçükköy and Çorum_Karapınar samples had higher clay/Nano-clay content than the other samples as well and the highest silt content was found to be in the Çorum_Karapınar sample. On the other hand, the Manisa_Kemer sample had very limited clay content and it also had the lowest silt content.
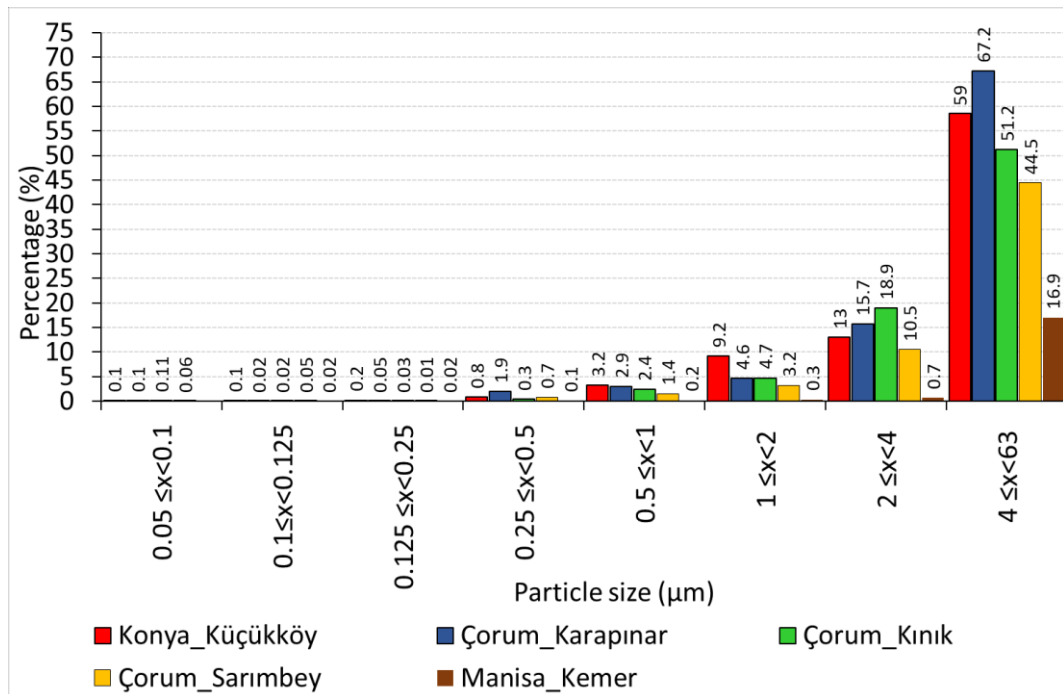


Figure 4.13 Analyses of particle size distribution below 63 μm by the centrifuge method.
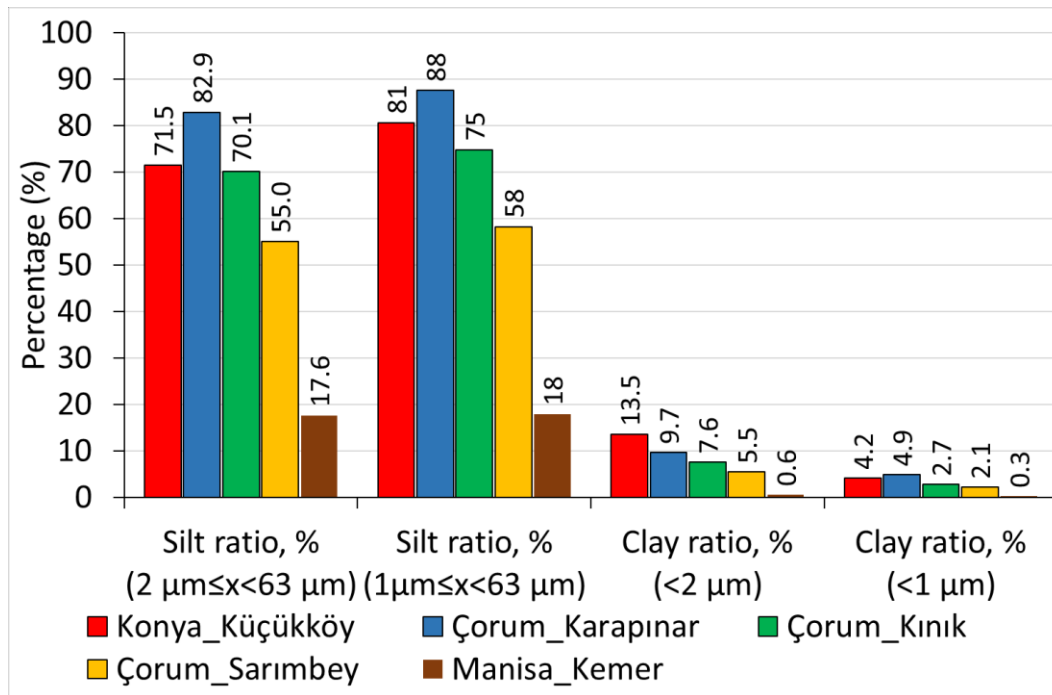
Figure 4.14 Silt ratios for both between 1 μm and 63 μm and between 2 μm and 63 μm; and clay ratios for both below 1 μm and 2 μm of the samples.

As a result, the Manisa_Kemer sample was not appropriate for Nano-clay production from the adobe soil due to its too-low clay content of about 0.3% and 0.6%; therefore, it was eliminated. Konya_Küçükköy, Çorum_Karapınar, Çorum_Kınık and Çorum_Sarımbey were selected for the Nano-clay production due to their clay content in the range of 2.1%-13.5%.

## 4.3 Enrichment of Nano-clay content in Natural Adobe Soil Resources and Nano-clay Content Assessment

The Methylene blue (MB) tests were conducted to determine effective times for the mixing and ultrasonic treatments for the Nano-clay production. The CEC results of the Konya_Küçükköy soil sample indicated that the increment of the days to mix by the magnetic stirrer did not provide a noticeable increase (Figure 4.15). On the other hand, ultrasonic analyses increased the CEC values up to 4 hours for the Konya_Küçükköy sample having particle sizes below 4 μm. After determination of

effective times for the Konya_Küçükköy sample, the Çorum_Karapınar Çorum_Kınık and Çorum_Sarımbey samples having particle sizes below 4 μm were stirred by the magnetic stirrer during 1 day. They were treated with sonication analyses between 4 and 6 hours. 4 hours for the Çorum_Kınık and Çorum_Sarımbey samples and 5 hours for the Çorum_Karapınar sample provided to gain maximum CEC values in the ultrasonic bath (Figure 4.16). The difference between samples may be due to the higher gypsum presence in the Çorum_Karapınar sample that causes the flocculation of clay particles. As a result, the efficient time for the magnetic stirrer was found 1-day for all samples, and 4 hours was determined as the optimum time for ultrasonic treatment of Konya_Küçükköy, Çorum_Kınık and Çorum_Sarımbey samples, while 5 hours for the Çorum_Karapınar sample.
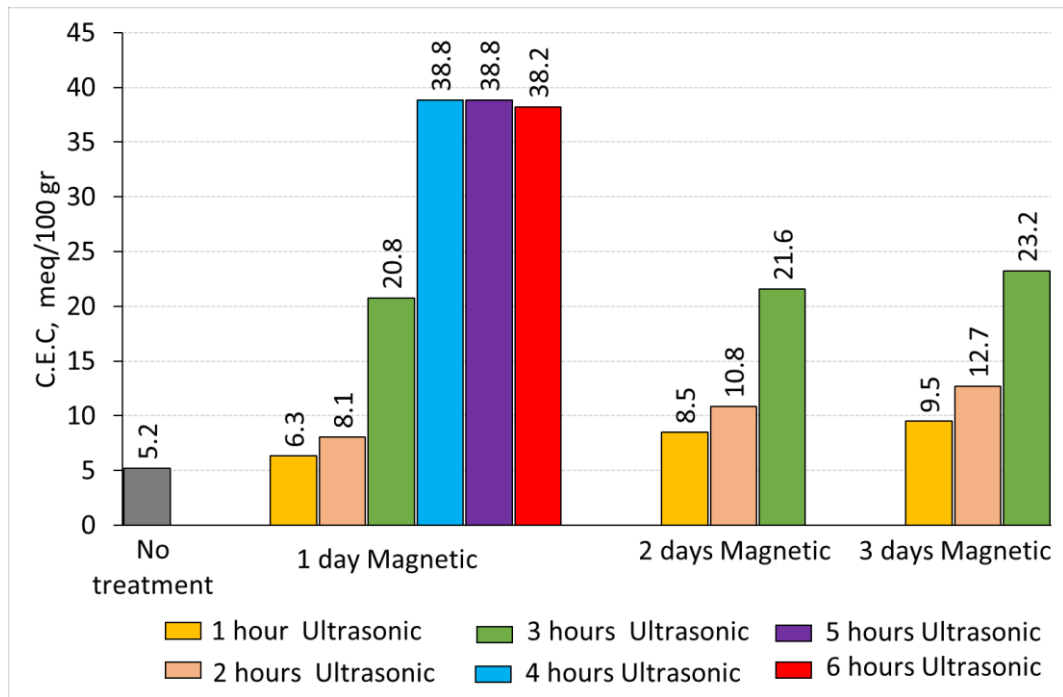


Figure 4.15 CEC values of Konya_Küçükköy sample having particle sizes below 4 μm.
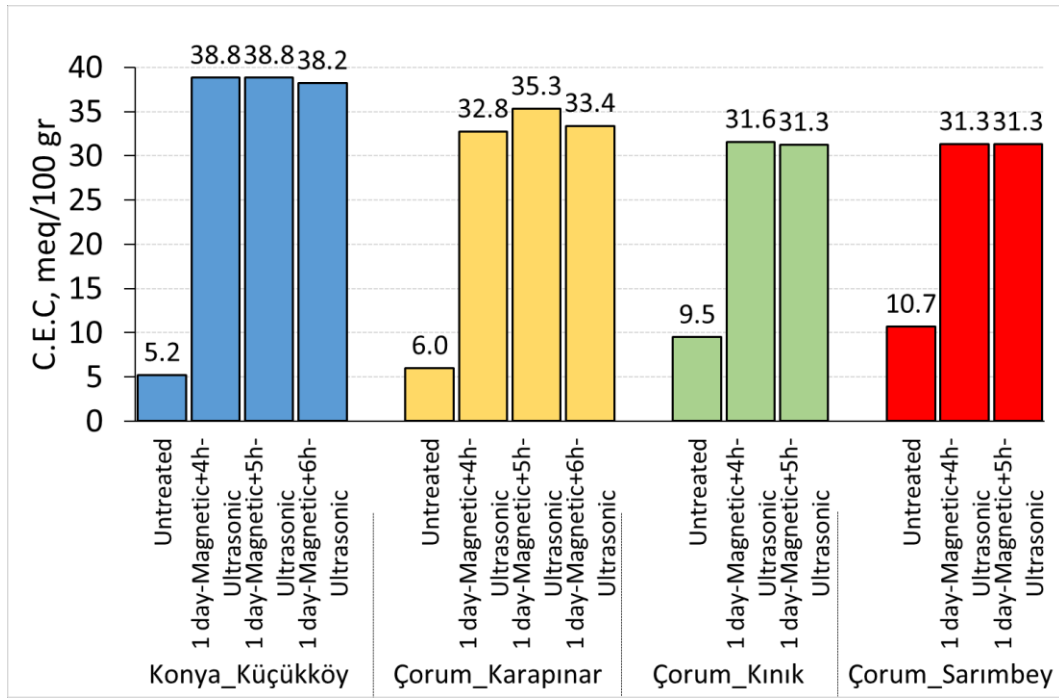
Figure 4.16 CEC values of Konya_Küçükköy, Çorum_Karapınar,
Çorum_Sarımbey and Çorum_Kınık samples having particle sizes below 4 μm.

The CEC values of 5.2, 6, 9.5 and 10.7 meq/100 g were found for the untreated
Konya_Küçükköy, Çorum_Karapınar, Çorum_Kınık and Çorum_Sarımbey
samples, respectively, but after the treatment, those CEC values increased up to 38.8,
35.3,31.6 and 31.3 meq/100 g, respectively (Figure 4.16). That treatment was
provided to increase the CEC values of the samples up to 7.4, 5.9, 3.3 and 2.9 times.
Among the untreated samples, the lower CEC values of Konya_Küçükköy having
the highest montmorillonite content than Çorum_Karapınar Çorum_Kınık and
Çorum_Sarımbey samples was due to the higher flocculation of clay particles in that
samples. Together with the ultrasonic treatment, the dispersion of clay was provided,
and the amount of clay in the samples was observed to be the most effective factor
for their CEC values. After the treatment, the highest CEC value belonged to the
Konya_Küçükköy sample having the highest clay amount in the range of between
24.2 % and 37.6 %. The Çorum_Karapınar, Çorum_Kınık and Çorum_Sarımbey
samples had lower CEC values having direct relation to their clay amount in ranges
of % 18.3 %-28.1 %, 7.9 %-21.2 % and 8.6 %-17.4 %, respectively.

The MB tests were executed on the Konya_Küçükköy sample to uncover the effects of ultrasonic treatment on the CEC value of the sample having increased weight and the sample including all particle sizes (Figure 4.17). Doubling the weight of the sample was observed to cause no change in CEC values for 4 hours. That result indicated that the change in the weight of the sample did not affect the optimum duration. The other MB tests were conducted to find out the effect of the use of samples including all particle sizes during the ultrasonic treatment. Those CEC values increased up to 7.5 times in the treated one in reference to the untreated one, as seen in between the treated and untreated samples having particle sizes below 4 µm (Figure 4.17). In addition, the finding of lower value in the case of the 5-hour-ultrasonic treatment showed that 4 hours was still valid as the optimum time.
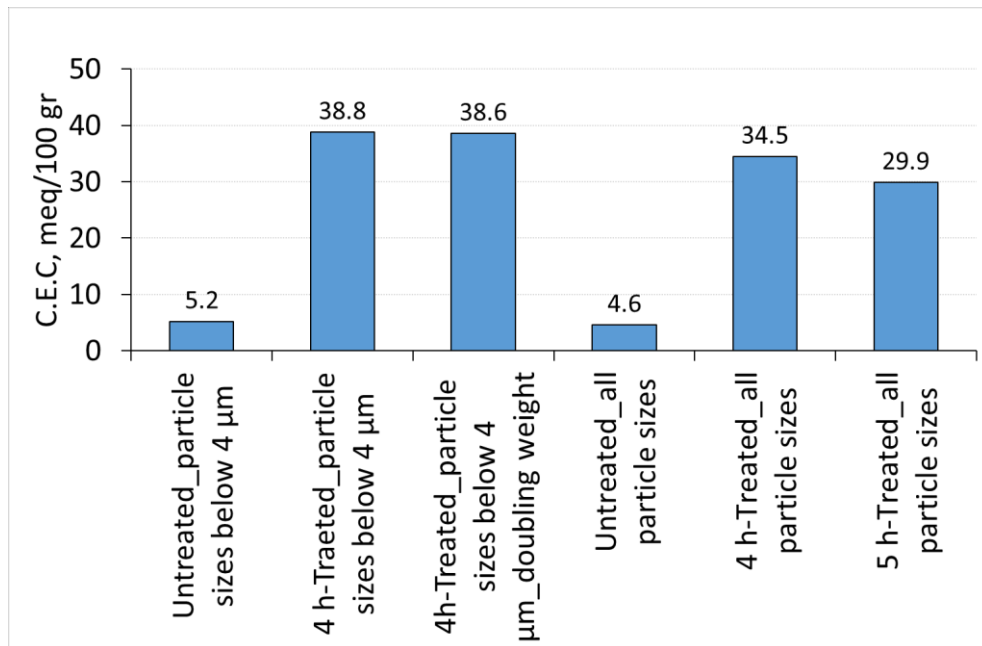


Figure 4.17 CEC values of Konya_Küçükköy sample having increased weight and the sample including all particle sizes.

The optimum times specified for the soil samples below 4 µm by the methylene blue (MB) tests were found to be valid during the mixing and the ultrasonic treatment of adobe samples having all particle sizes and in higher amounts. The revisions on the test method of the Nano-clay production process of the samples prepared as adobe

soil were checked by the MB tests. Firstly, the effect of decreasing the amount of water till the ability to mix the soil sample in water by the magnetic stirrer and ultrasonic bath was uncovered by MB tests. The soil-to-water ratios of 1:4, 1:2 and 1:1 by w.t were tested on the Konya_Küçükköy sample, respectively. In the case of the 1:1 ratio, the soil mixture could not be mixed due to its viscosity; therefore, it could not be tested. The CEC value of the soil sample having particles below 4 µm had a non-critical decrease from 38.8 meq/100g to 37.6 meq/100g in the case of the use of 1:2 for the soil-to-water ratio. Using the 1:4 ratio also results in a value of 38 meq/100g (Figure 4.18). A little difference was found between the outcomes of the tests in 1:2 and 1:4 ratios. Then, the soil-to-water ratio of 1:2 was tested on Çorum_Karapınar, Çorum_Kınık and Çorum_Sarımbey samples. The CEC values in the case of the use 1:2 ratio were found to be very similar to previously treated samples' CEC values (the soil-to-water ratio 1:6). As a result, the use of 1:2 is selected as the optimum ratio for the production of the Nano-clay in the samples.
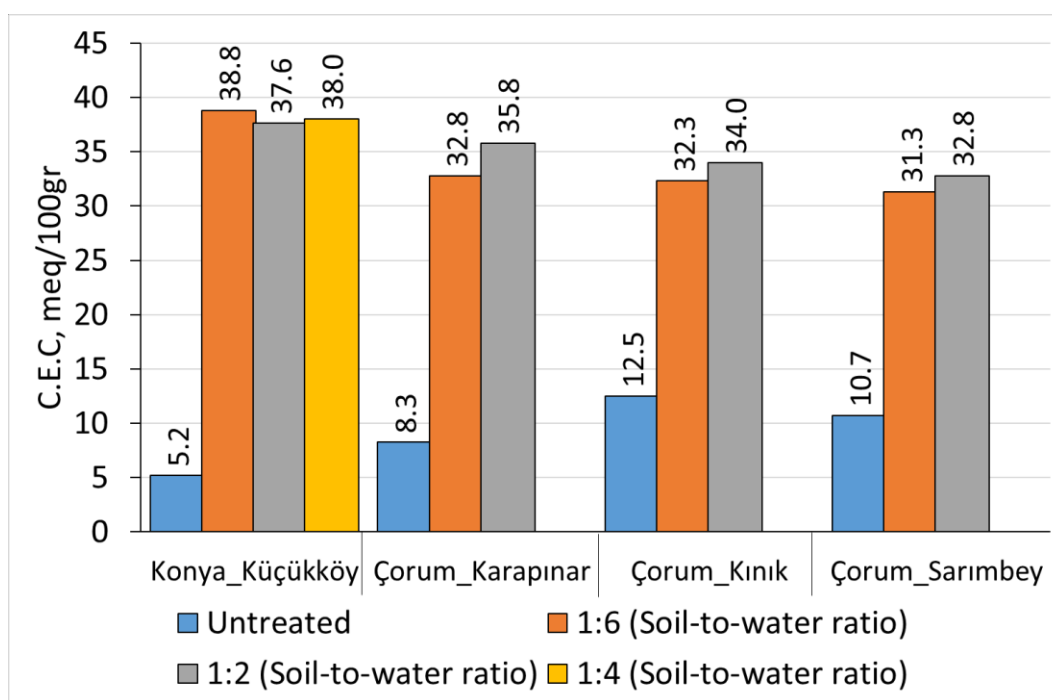


Figure 4.18 CEC values of the Konya_Küçükköy, Çorum_Karapınar, Çorum_Kınuk and Çorum_Sarımbeysamples (particle sizes <4 µm) in cases of the sample having decreased water amount.

In the other revision, the optimum time for the laboratory mixer was determined by mixing the Konya_Küçükköy sample for one hour and three hours. Mixing in one hour resulted in 30.9 meq/100g in the MB test; on the other hand, mixing for three hours provided to achieve 37.7 meq/100g, which is very near to the CEC value achieved by mixing with the magnetic stirrer the whole day (Figure 4.19). Therefore, three hours was selected as the optimum time for mixing the samples.
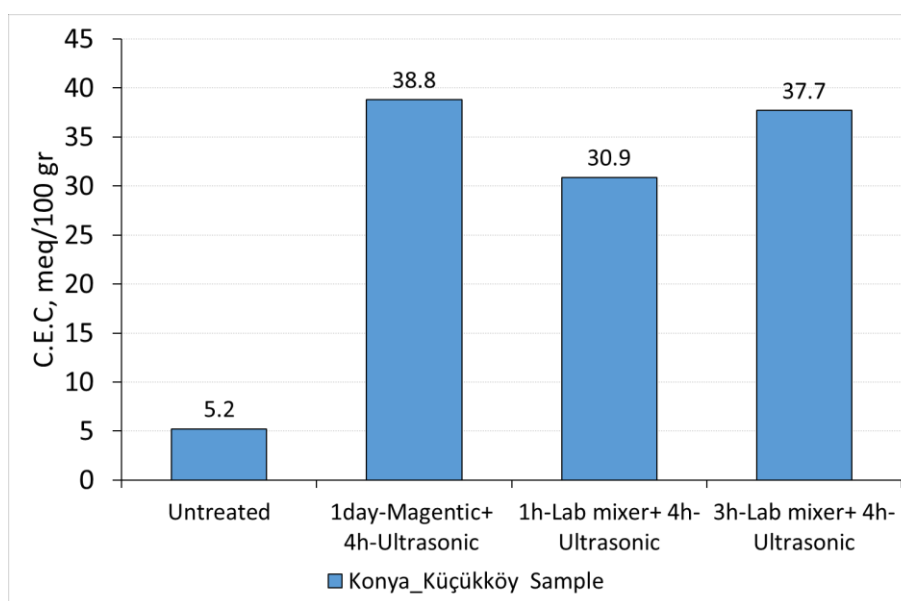


Figure 4.19 CEC values of the Konya_Küçükköy sample treated by laboratory mixer at different hours instead of the magnetic stirrer in cases of the sample including all particle sizes and particles below 4 µm.

## 4.4 Performance assessment of Nano-clay riched adobe soil samples (Treated adobe soil samples)

The evaluation of analyses on Nano-clay production by ultrasonic treatment in the Konya_Küçükköy, Çorum_Karapınar, Çorum_Kınık and Çorum_Sarımbey soil samples were given under the related sub-headings.

### 4.4.1      Laser Diffraction Particle Size Distribution Analyses

Particle size distribution (PSD) analyses of treated and untreated samples were conducted by laser diffraction method to quantitively observe the change in Nano-clay content in the soil samples. By the ultrasonic treatment, the increase in the number of particle sizes below 1 μm, namely clay content in all the samples, was proved by laser diffractometry analyses (Figure 4.20, Figure 4.21, Figure 4.22 and Figure 4.23). There were rises in clay and fine silts' particles between 1 and 15 μm in the samples of Konya_ Küçükköy, Çorum_Kınık and Çorum_Sarımbey, while the particles between 1 and 5 μm remain same number in the Çorum_Karapınar sample. After those levels, sharp decreases seem in the graphs, namely particle size of medium and coarse sands and gravels were no longer observable in the treated samples. These results indicated that flocculated/agglomerated clay particles, and fine silts stuck to each other by clay particles and clay particles stuck to coarser aggregates were dispersed by ultrasonic treatment.
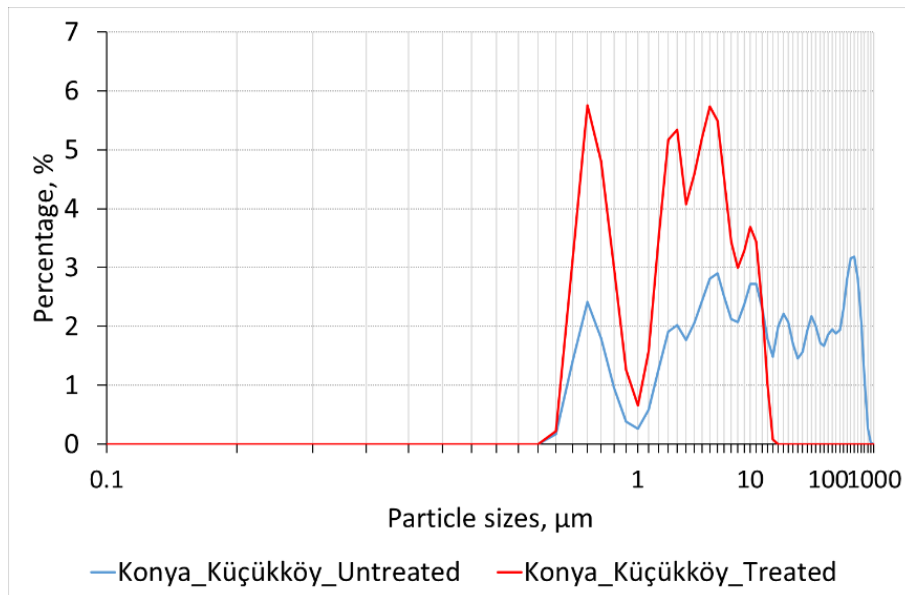


Figure 4.20 PSD by laser diffractometry analyses conducted on treated and untreated Konya_Küçükköy samples.
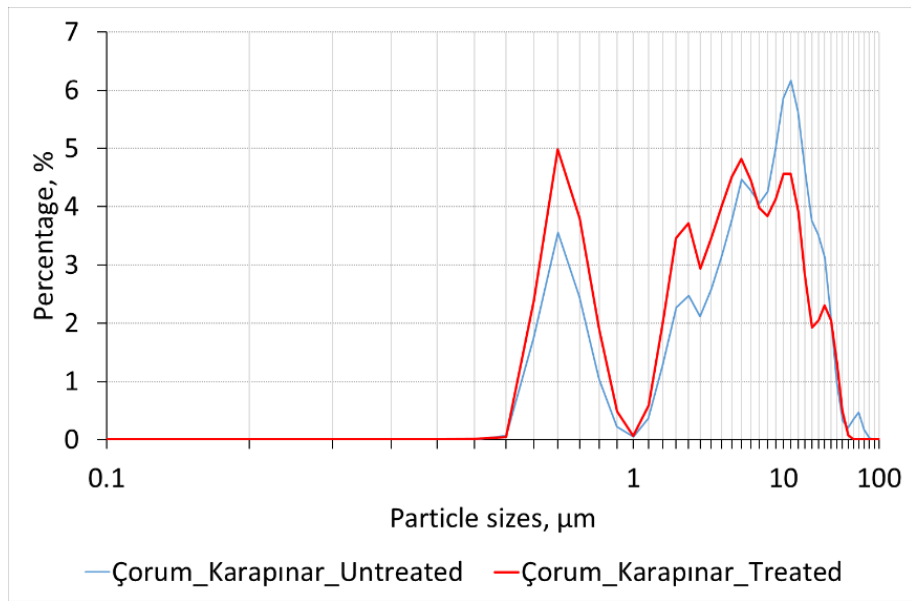
Figure 4.21 PSD by laser diffractometry analyses conducted on treated and untreated Çorum_Karapınar samples.
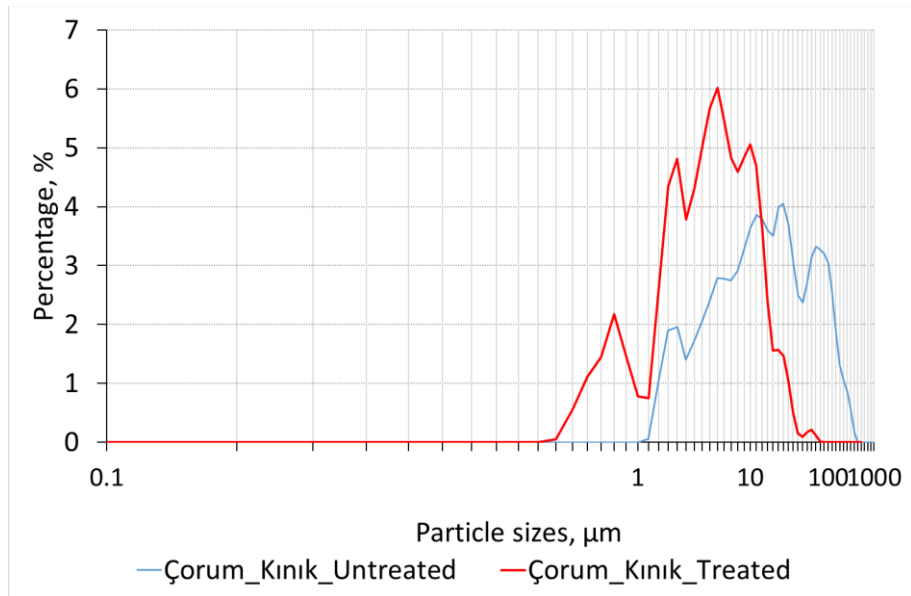


Figure 4.22 PSD by laser diffractometry analyses conducted on treated and untreated Çorum_Kınık samples.
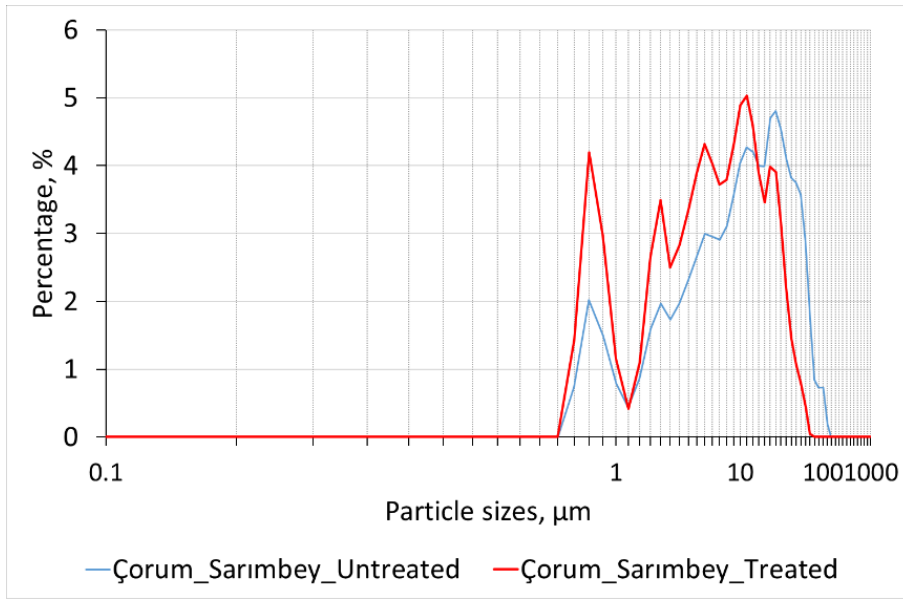
Figure 4.23 PSD by laser diffractometry analyses conducted on treated and untreated Çorum_Sarımbey samples.

The stereo microscope analyses demonstrated that the samples' particle size below 1 μm was totally clay, and their particles between 1 μm and 2 μm consisted of mainly clay and a little fine silt content. Therefore, the amount of clay content in the sample was considered to be found in particle sizes below 1 μm as a lower limit and below 2 μm as an upper limit. By considering those limits, before the ultrasonic treatment, the amounts of clay contents were found to be in the ranges of 9.5%-15.6 %, 12.5 %-19, 0 %-5 % and 4.3 %-9.9 % in the samples of Konya_Küçükköy, Çorum_Karapınar, Çorum_Kınık and Çorum_Sarımbey, respectively (Figure 4.24). After the ultrasonic treatment, their clay contents rose to the ranges of 24.2 %-37.6 %, 18.3 %-28.1 %, 7.9 %-21.2 % and 8.6 %-17.4 % (Figure 4.24). Those results showed that the soil samples had a clay content sufficient for, or very close to, the amount of clay required for adobe bricks, between 10% and 40% (Brown et al., 1979; Houben & Guillaud, 1994; Norton, 1997; Schwalen, 1935; Walker, 2001).
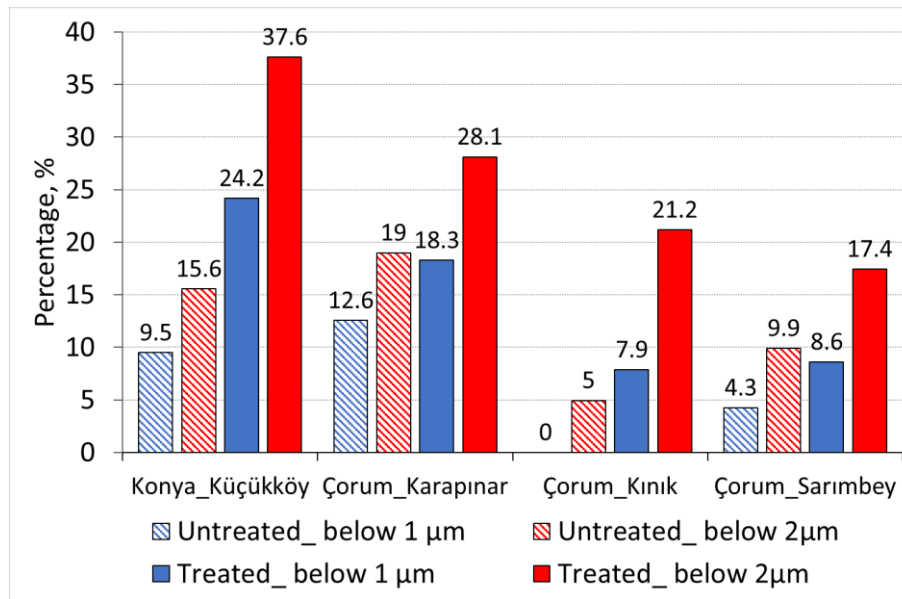
Figure 4.24 Clay ratios (particles below 1 µm and 2 µm) achieved by the laser diffractometry method.

### 4.4.1.1    Comparison of Particle Size Distribution Methods

The results of particle size distribution (PSD) analyses conducted on the untreated samples by three methods were compared. The first one was composed of the wet and dry-sieving and centrifuge method (W+D+C), the other one included the alternative method, the dry-sieving and centrifuge method (A+D+C), and the last one was the laser diffractometry method. The results of those methods were observed to have generally similar trends in the graphs in (Figure 4.25, Figure 4.26, Figure 4.27 and Figure 4.28). Laser diffractometry is the most reliable method, and the results signalled the other two methods could be useable to get an overall idea about PSD. The results of the A+D+C and W+D+C methods were observed to be very near to each other in samples except for Çorum_Karapınar. On the other hand, the results of the A+D+C were more similar results to the ones achieved by laser diffractometry by comparison to the W+D+C method. The average difference between the results of the A+D+C method and the laser diffractometry method was found to be between

5.1 ± 5.2 % and 1.6 ± 2.24% in all samples. On the other hand, the difference between W+D+C and laser diffractometry methods was in the average difference range of 6.3 ± 5.1 % and 3.4 ± 4.3 %, higher differences were seen between them.

The maximum variation was observed in the particle size range between 4 μm and 63 μm between 13 % and 22 % in all samples in comparisons of those three methods. The maximum difference of 22 % in that particle size range was observed in the Çorum_Karapınar sample between the laser diffractometry and the W+D+C method. On the other hand, this difference was about 0.2 % when the analysis was conducted on this sample the A+D+C method. That extreme difference was due to the presence of the 3.4 % gypsum in the Çorum_Karapınar sample. Those results support that the A+D+C is more reliable for the sample including gypsum content (Pearson et al., 2015).
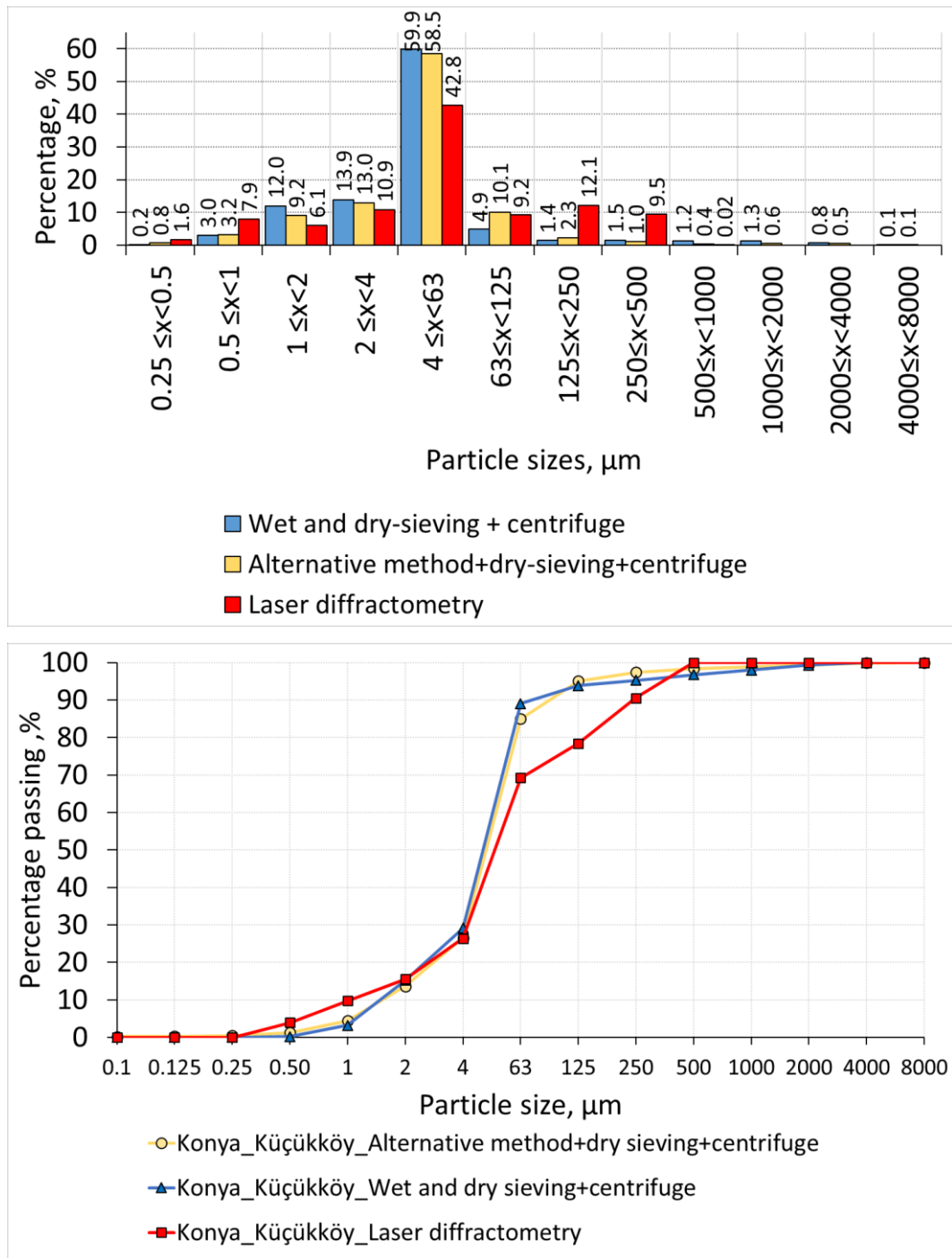
Figure 4.25 PSD analyses conducted by the alternative method + dry-sieving+centrifuge, the wet and dry-sieving+centrifuge and the laser diffractometry methods on the Konya_Küçükköy sample.
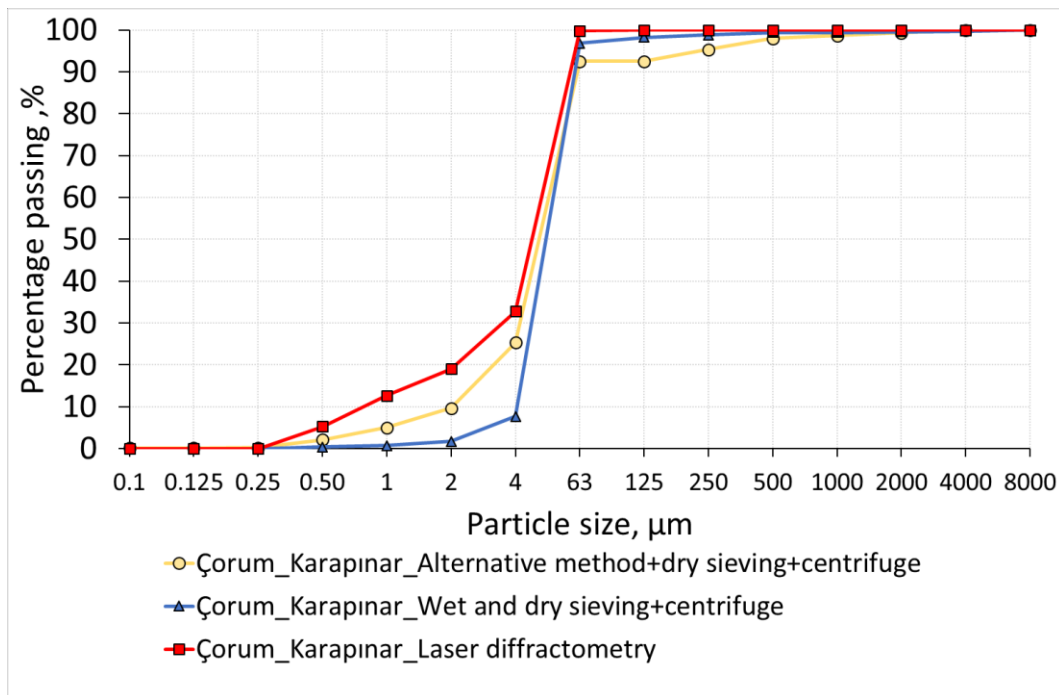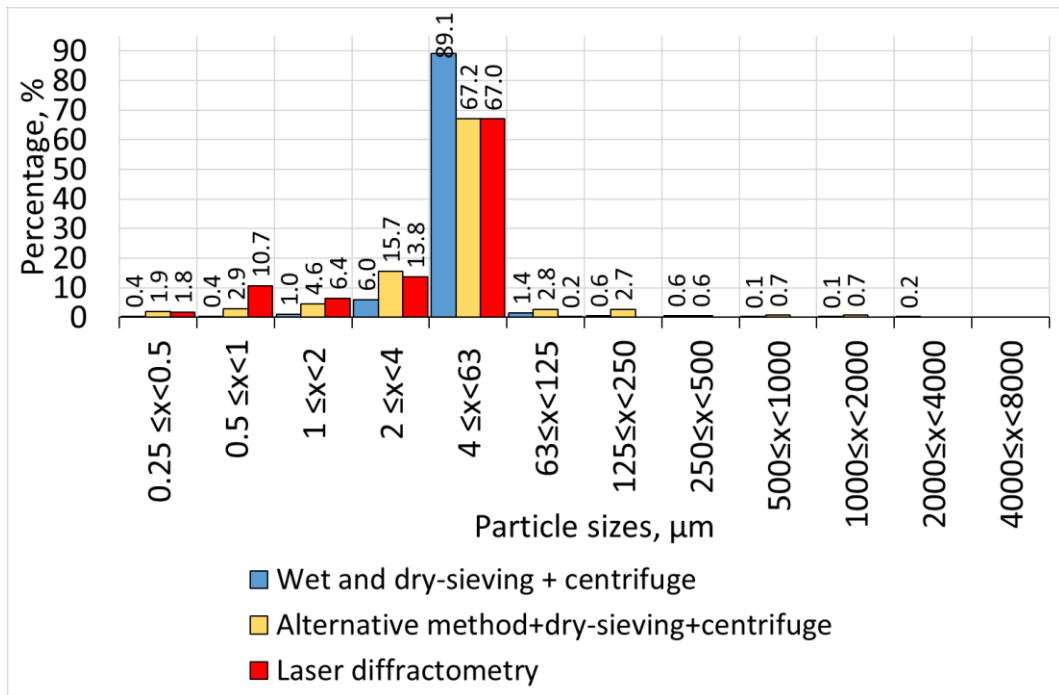
Figure 4.26 PSD analyses conducted by the alternative method + dry-sieving+centrifuge, wet and dry-sieving+centrifuge and laser diffractometry methods on the Çorum_Karapınar sample.
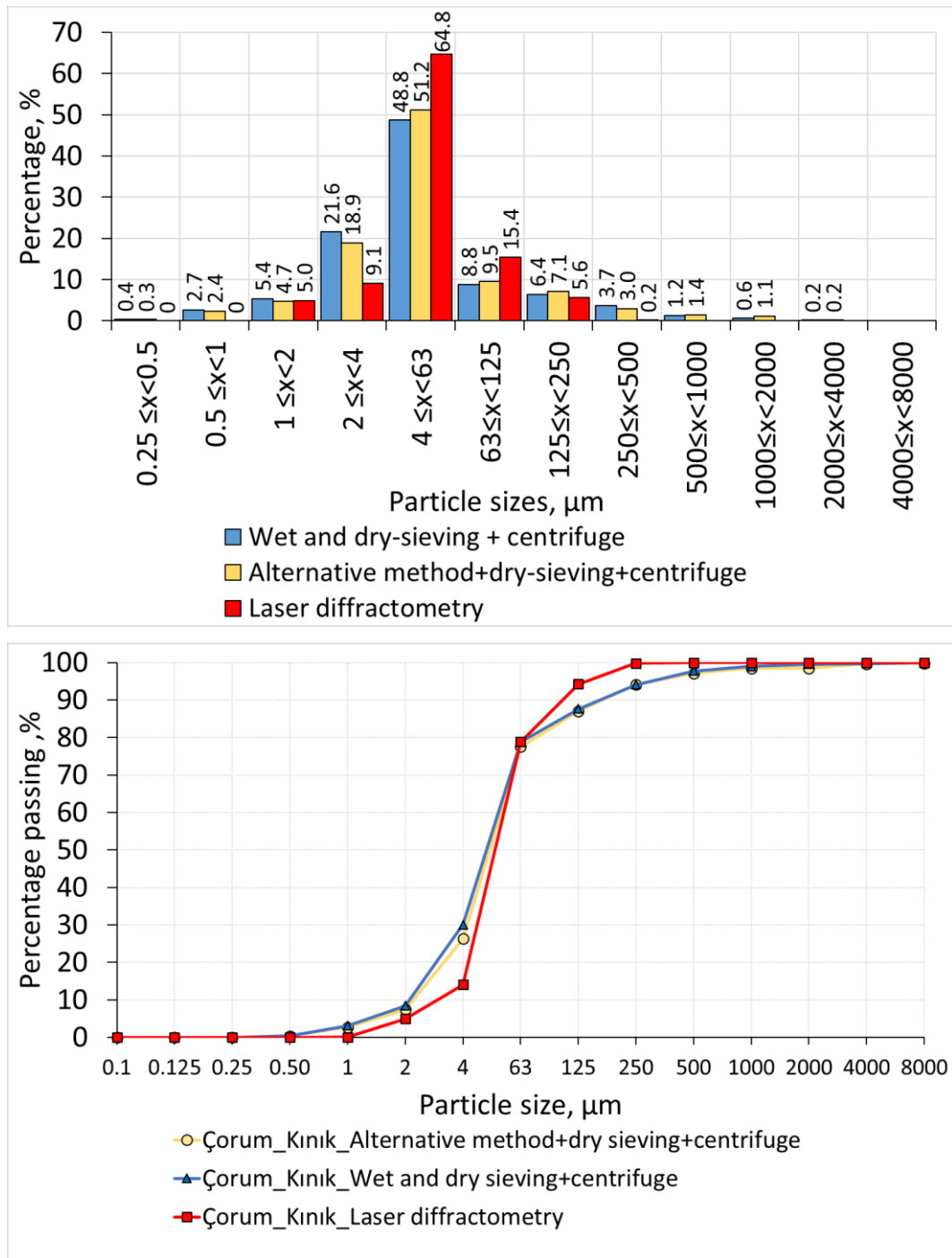
Figure 4.27 PSD analyses conducted by the alternative method + dry-sieving+centrifuge, the wet and dry-sieving+centrifuge and the laser diffractometry methods on the Çorum_Kınık sample.
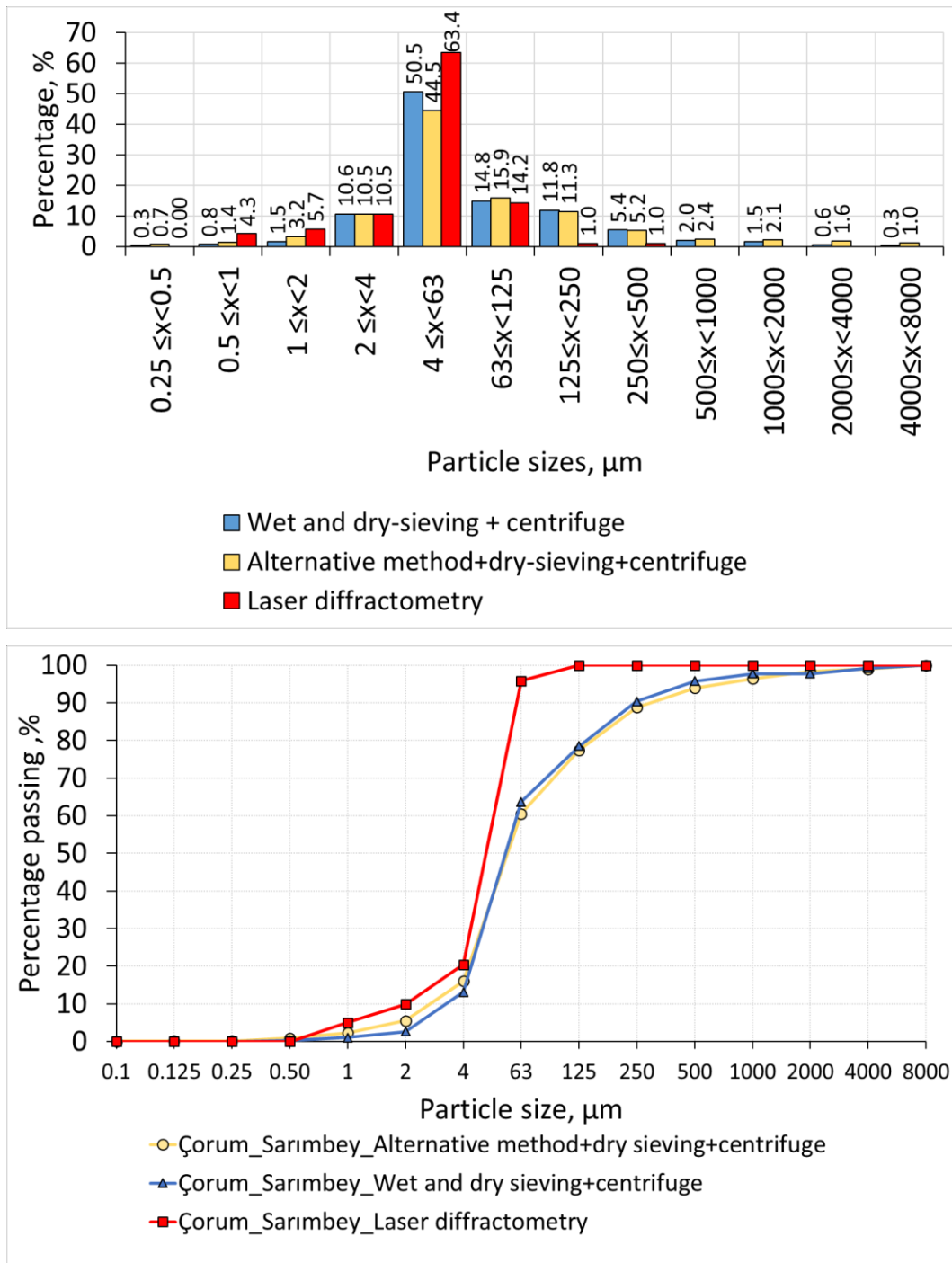
Figure 4.28 PSD analyses conducted by the alternative method + dry-sieving+centrifuge, wet and dry-sieving+centrifuge and laser diffractometry methods on the Çorum_Sarımbey sample.

## 4.4.2 Scanning Electron Microscope (SEM) and Transmission Electron Microscopy (TEM) Analyses

The treated and untreated Konya_Küçükköy, Çorum_Karapınar, Çorum_Kınık and Çorum_Sarımbey samples below 4 μm were analysed by the scanning electron microscope (SEM) to detect the effect of the ultrasonic treatment on the morphology of clay particles (Figure 4.29). Before the ultrasonic treatment, agglomerations of clay flakes forming larger particles were generally observed while after the treatment, as morphological change, a greater number of smaller aggregates of clay flakes seemed on their surface texture.
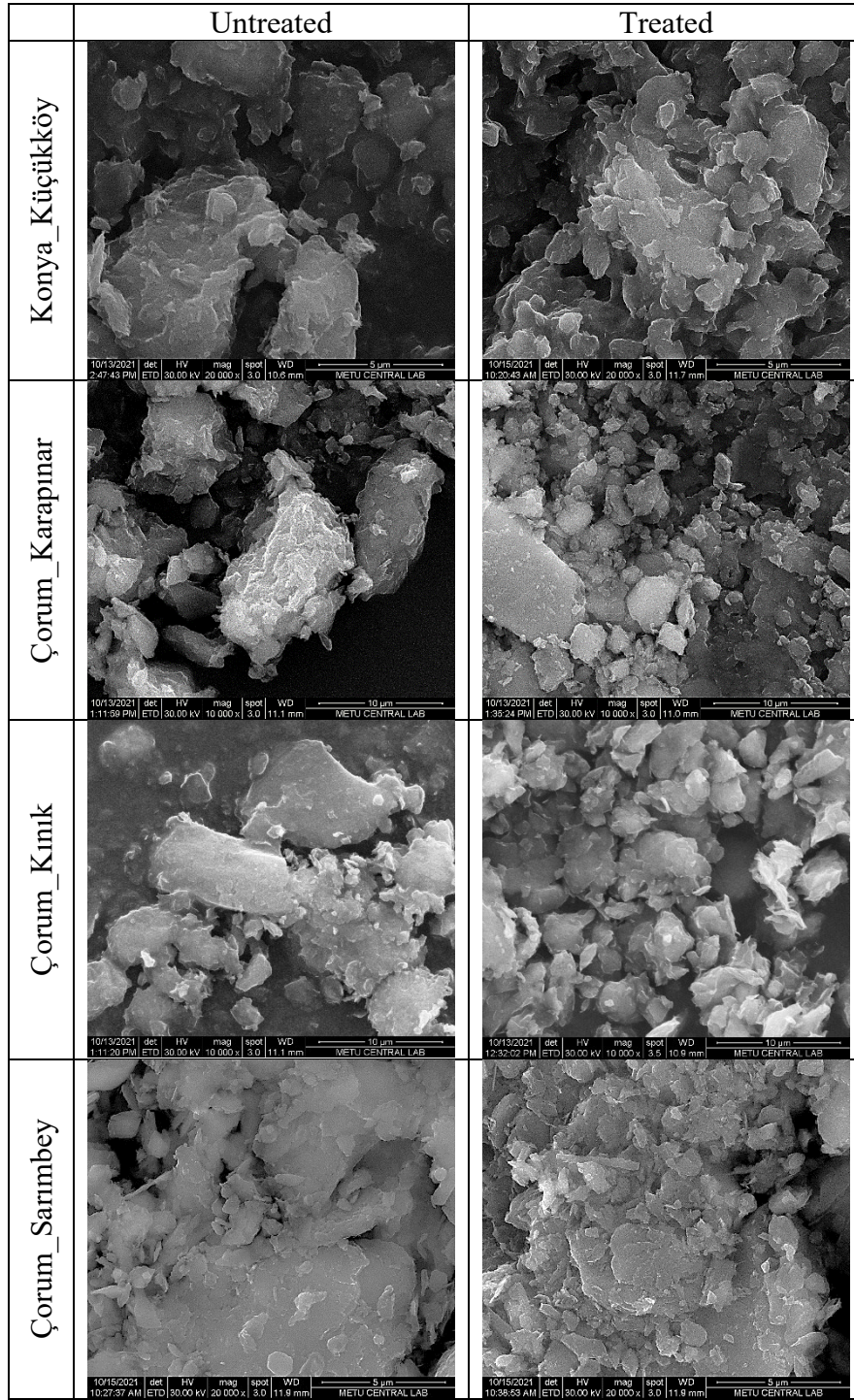
Figure 4.29 SEM images of the treated and untreated samples below 4 μm.

The treated and untreated clay particles in the Konya_Küçükköy sample were analysed by transmission electron microscopy (TEM) to confirm the dispersion of clay through the ultrasonic method. Before and after treatments, visible clay particles were marked with number codes (Figure 4.30 and Figure 4.31) on the TEM images, and approximate dimension measurements of the clay particles were conducted on those images. Coarser particles, clay-flocculants, were observed in the untreated sample, while the finer clay particles were in the treated one (Figure 4.30 and Figure 4.31). The dimensions of clay particles in circle-shaped decreased from Ø140nm to Ø35nm, and the particles in square or rectangle-shaped diminished from 152x293 nm to 28x70 nm on average. The results indicated that the surface area clay particle sizes became smaller between 1/16 and 1/20 of the untreated clay particles after the ultrasonic treatment.
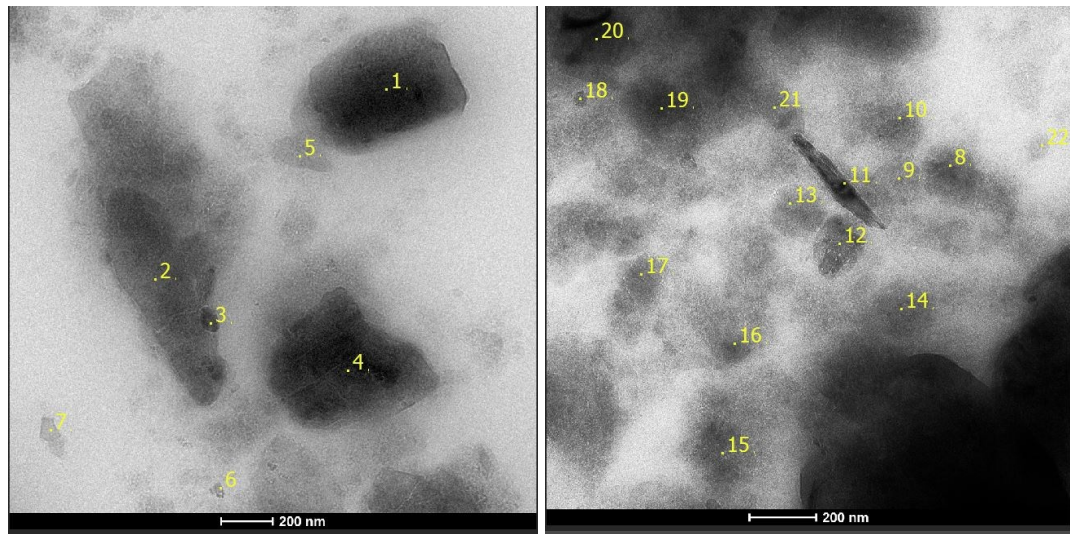


| Code | 1 | 2 | 3 | 4 | 5 | 6 | 7 | 8 | 9 | 10 | 11 |
|------|---|---|---|---|---|---|---|---|---|----|----|
| Dimensions nm | 375x 515 | 211x 877 | 67x 102 | 413x 441 | 107x 228 | 32x35 | 66x 162 | Ø160 | 127x 142 | Ø143 | 65x 381 |
| Code | 12 | 13 | 14 | 15 | 16 | 17 | 18 | 19 | 20 | 21 | 22 |
| Dimensions nm | 143x 153 | Ø154 | Ø163 | Ø182 | Ø80 | 103x 143 | Ø39 | Ø198 | Ø225 | 92x 194 | Ø56 |

Figure 4.30 TEM images (METU Central Lab) of the untreated Konya_Küçükköy clay particles marked with number codes and their dimension table given below.

135
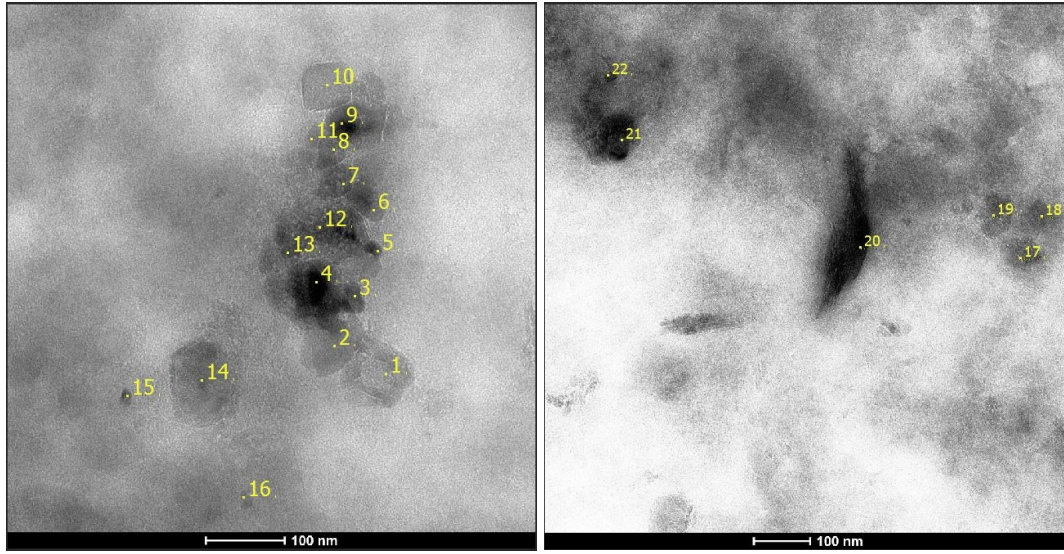
| Code | 1 | 2 | 3 | 4 | 5 | 6 | 7 | 8 | 9 | 10 | 11 |
|---|---|---|---|---|---|---|---|---|---|---|---|
| Dimensions, nm | Ø36 | 43x70 | 17x31 | 21x43 | Ø11 | Ø21 | Ø35 | Ø37 | Ø38 | 60x61 | Ø22 |
| Code | 12 | 13 | 14 | 15 | 16 | 17 | 18 | 19 | 20 | 21 | 22 |
| Dimensions, nm | Ø8 | 11x13 | Ø106 | Ø11 | 16x23 | Ø58 | Ø33 | Ø61 | 30x290 | 29x34 | Ø13 |

Figure 4.31 TEM images (METU Central Lab) of the treated Konya_Küçükköy clay particles marked with number codes and their dimension table given below.

### 4.4.3    Stereo Microscope Analyses

Before and after the Nano-clay production by the ultrasonic treatment, the soil samples below 63 μm were examined by the stereo microscope (Leica Z16 APO A) to detect the presence of clay and silt in different particle size ranges (Figure 4.32, Figure 4.33, Figure 4.34 and Figure 4.35). While the silt minerals have shapes like spherical granules clay minerals have flake shapes due to their sheet-shaped mineral structures. The dispersed silt granules seemed in particles between 63 μm and 4 μm on the other hand, flocculated clay in compacted form started to be observed in particles below 4 μm. It was observed that particle sizes of samples in the range between 63 μm and 4 μm consist of silt; in the ranges between 4 μm and 2 μm and between 2 μm and 1 μm comprise of fine silt and clay; in the range between 1 μm

and 0.5 μm compose of clay. The only clay content can be observed in the particle size below 1 μm.

After the treatment, the silt content was found to seriously increase in particles between 2 μm and 4 μm compared to the content before the ultrasonic treatment. As in the samples before treatment, the presence of mixed fine silt and clay in the particle sizes between 2 μm and 1 μm, and the clay-only contents present in the particle sizes below 1 μm were observed to be in those samples after the treatment. The results indicated the clay particles stuck on the fine silts that are between 1 μm and 4 μm were dispersed by ultrasonic energy. As a result, the clay content of the treated samples whose particle size distribution conducted by laser diffraction and centrifuge methods was accepted according to two scales; one including particles below 2 μm (in geology and soil science and Turkish standards) and the other one comprising the sizes below 1 μm (colloid science).

|  | Konya_Küçükköy | Çorum_Karapınar |
|---|---|---|
| 4 μm≤ x<63 μm (Silt) | | |
| 2 μm≤ x<4 μm (Clay + Silt) | | |
| 1 μm≤ x<2 μm (Clay + Silt) | | |
| 0.5 μm≤ x<1μm (Clay) | | |
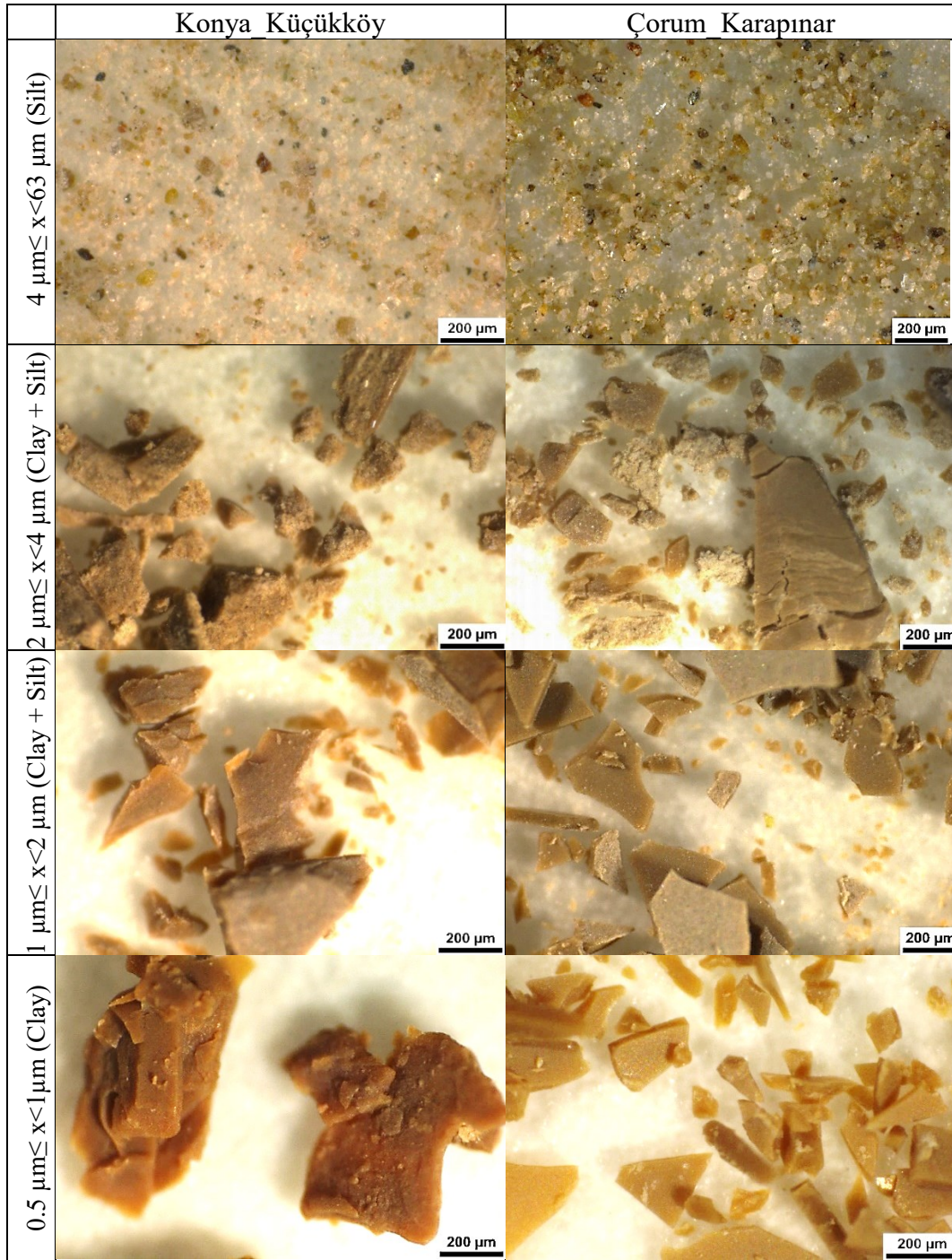
Figure 4.32 Photographs of the untreated Konya_Küçükköy and Çorum_Karapınar samples in the particle size range below 63 μm were taken by stereo microscope (Leica Z16 APO A).

|  | Çorum_Kınık | Çorum_Sarımbey |
|---|---|---|
| 4 μm≤ x<63 μm (Silt) |  |  |
| 2 μm≤ x<4 μm (Clay + Silt) |  |  |
| 1 μm≤ x<2 μm (Clay + Silt) |  |  |
| 0.5 μm≤ x<1μm (Clay) |  |  |
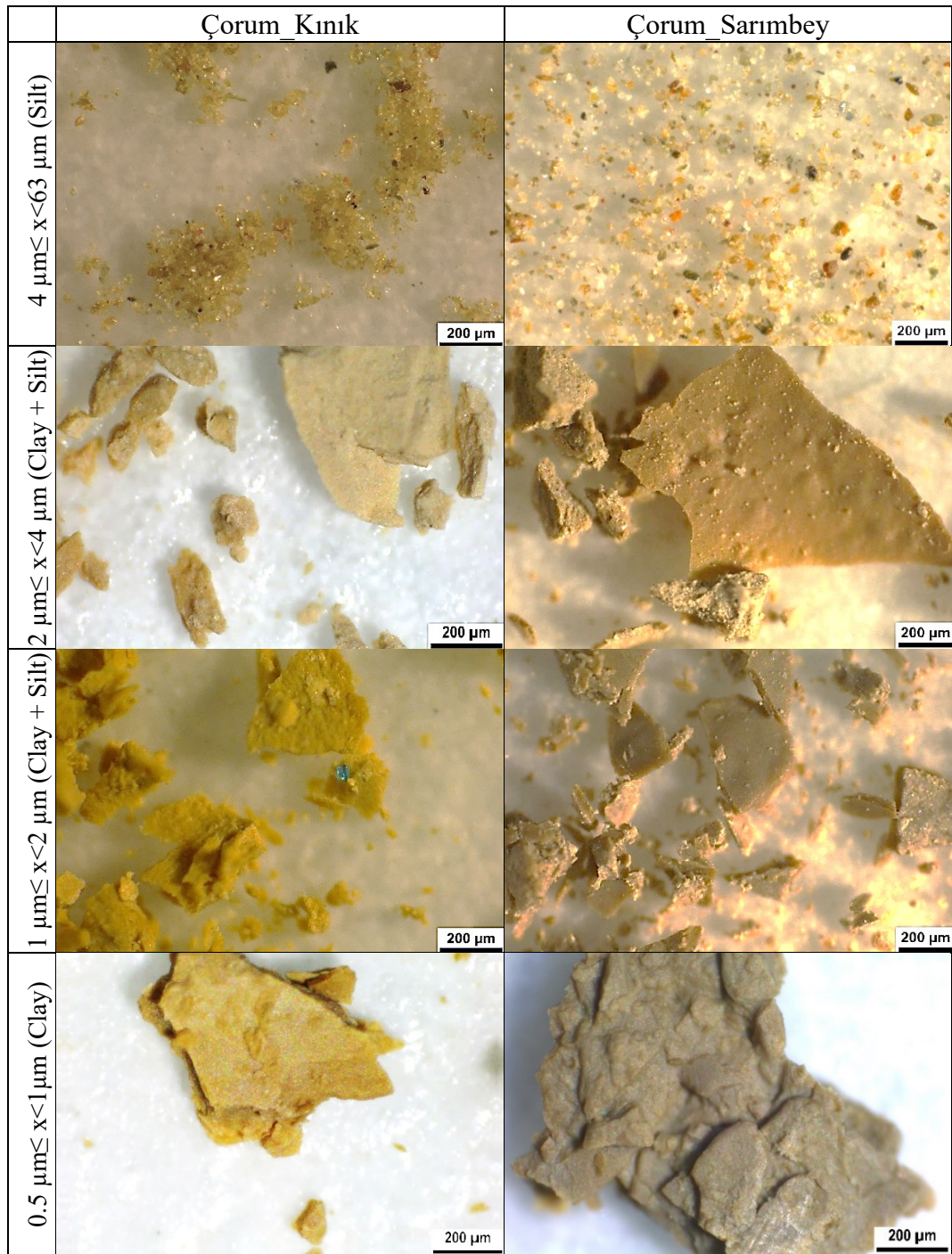
Figure 4.33 Photographs of the untreated Çorum_Kınık and Çorum_Sarımbey samples in the particle size range below 63 μm were taken by stereo microscope (Leica Z16 APO A).
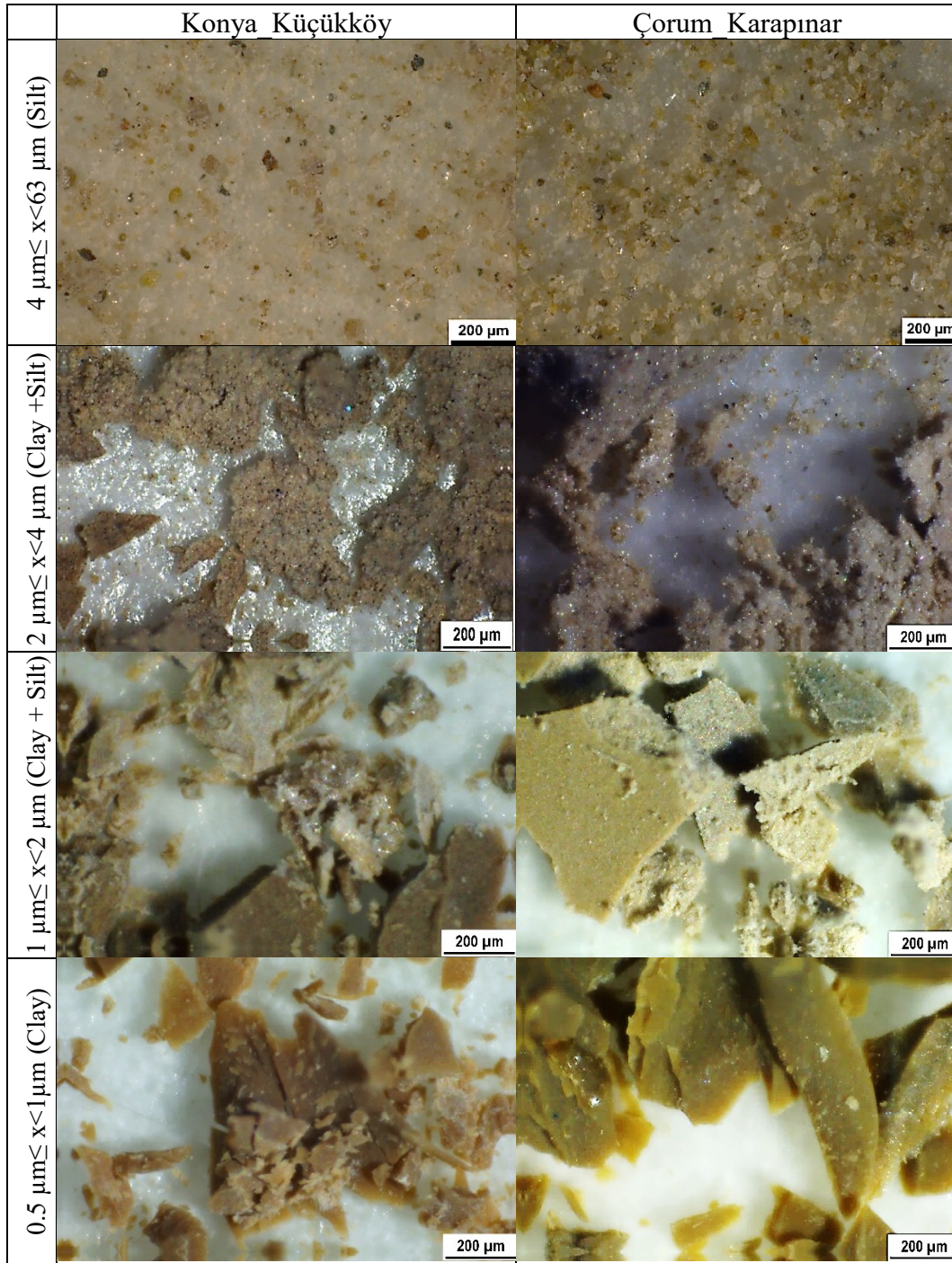
Figure 4.34 Photographs of the treated Konya_Küçükköy and Çorum_Karapınar samples in the particle size range below 63 μm were taken by stereo microscope (Leica Z16 APO A).

|  | Çorum_Kınık | Çorum_Sarımbey |
|---|---|---|
| 4 µm≤ x<63 µm (Silt) | | |
| 2 µm≤ x<4 µm (Clay + | | |
| 1 µm≤ x<2 µm (Clay + | | |
| 0.5 µm≤ x<1µm (Clay) | | |
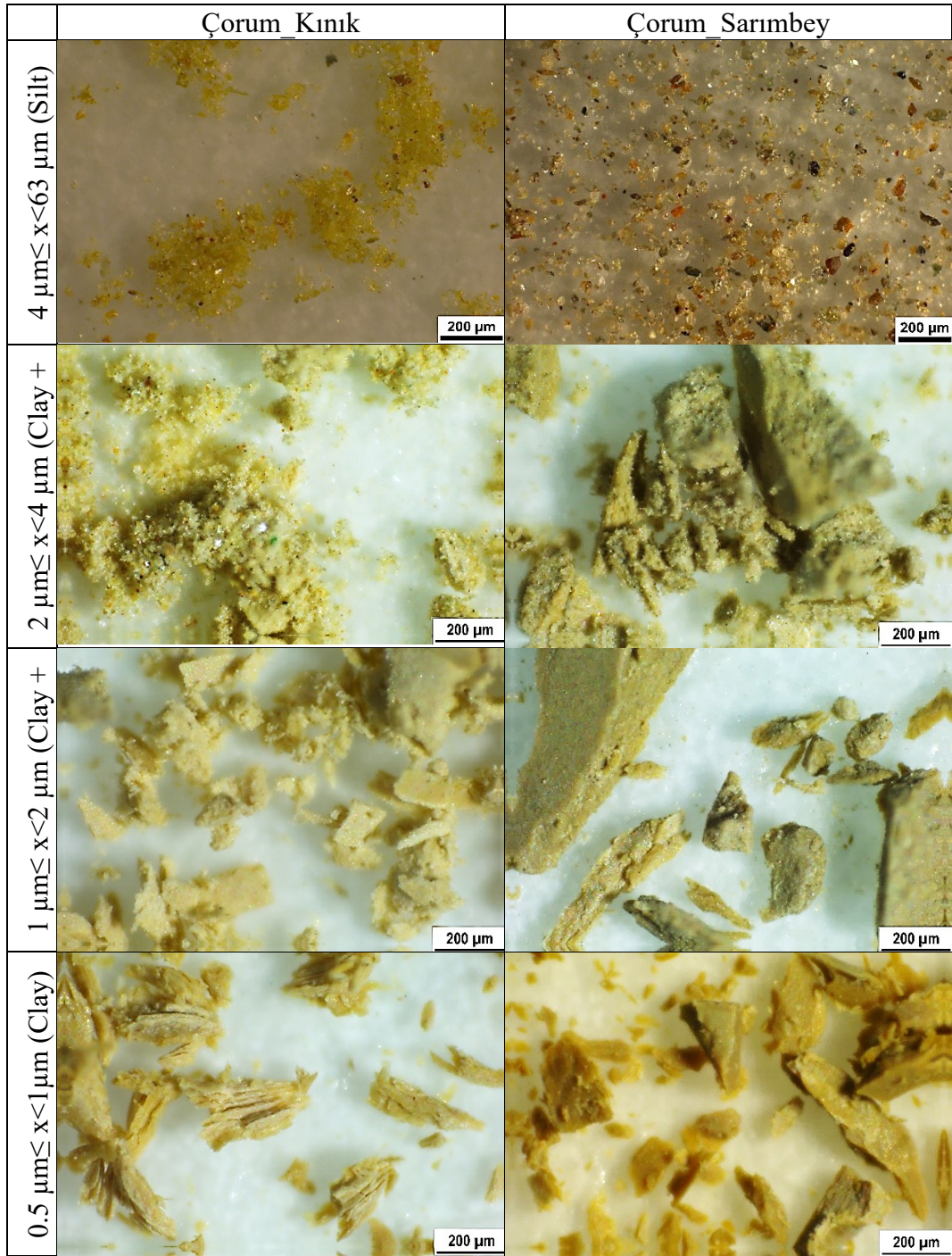
Figure 4.35 Photographs of the treated Çorum_Kınık and Çorum_Sarımbey samples in the particle size range below 4 µm were taken by stereo microscope (Leica Z16 APO A).

### 4.4.4 Simulation Analyses: MAUD

The relative ratios of montmorillonite, kaolinite, illite and chlorite clay minerals to each other and the other minerals in untreated soil samples below 4 μm were approximately determined by MAUD software (version 2.99) (Figure 4.36). All minerals found by XRD tests on the soil samples below 63μm were defined in MAUD simulation analyses. During the clay ratio calculation by the simulation analyses, some acceptations were conducted:

— The percentages of calcite ($CaCO_3$) of 6.2 %, 5.9 %, 6.9 % and 5% (Table 4.9) in the Konya_Küçükköy, Çorum_Karapınar, Çorum_Kınık and Çorum_Sarımbey soil samples, respectively, were studied to achieve during the calculations. Those percentages were defined by LOI tests conducted on the untreated soil samples below 4 μm.

— The main peak heights of clay minerals achieved in XRD analyses were taken into consideration to find a clue about which clay type has a higher amount than the others. That comparison was used to check the simulation analysis results.

The Konya_Küçükköy sample had mainly montmorillonite, swelling clay type, about 26.1%. On the other hand, in the Çorum_Karapınar sample, kaolinite and chlorite, non-swelling clays of about 24.3% and 20.8 % were predominantly found and its montmorillonite content was 0.7%, too little. The Çorum_Sarımbey sample also had a limited amount of montmorillonite, 2.6%, which was lower than the kaolinite, illite and chlorite clay which are each about 11%. Çorum_Kınık has higher montmorillonite and kaolinite clay contents, 7.9 % and 8.4%, respectively than the other types of clays.
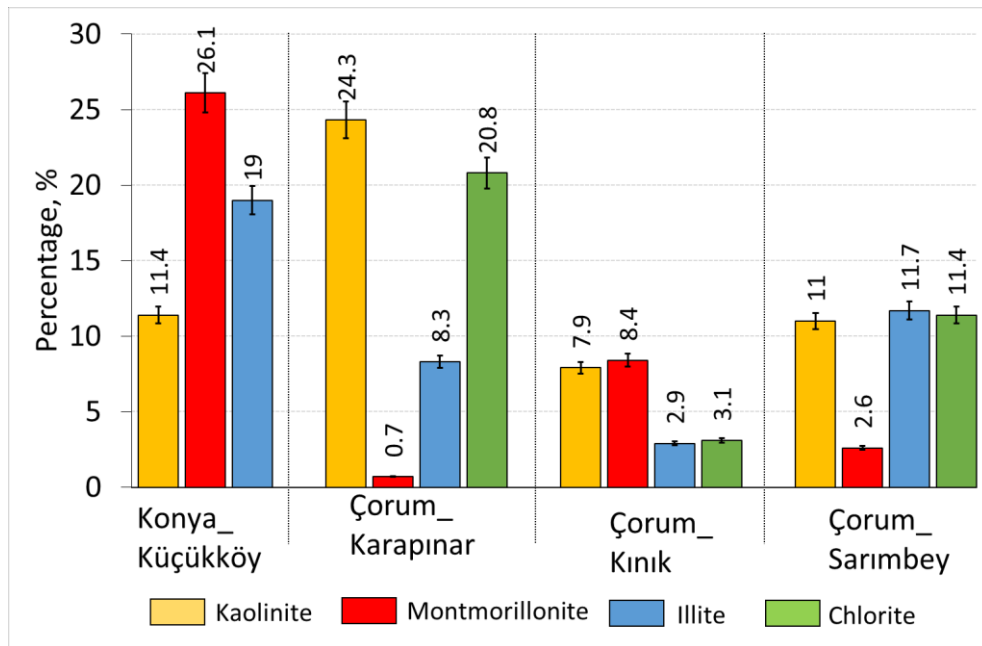
Figure 4.36 Clay ratios in the untreated soil samples having a particle size below 4 µm achieved by the simulation analyses.

### 4.4.5 Supportive Analyses on Composition of Soil Samples

The X-ray fluorescence (XRF), spectrophotometry test and X-ray diffraction (XRD) analyses were conducted to achieve detailed data about the composition of adobe soil to determine its effect on the Nano-clay production from the soil.

#### 4.4.5.1 X-ray fluorescence (XRF) Analyses

The elemental composition of the samples, including all particle sizes, was determined by X-ray fluorescence (XRF) to check the samples' minerals previously defined by XRD analyses. (Table 4.7).

Table 4.7 Elements found by XRFs instrument and minerals determined by XRD.

| Sample code | Element | % | Kaolinite Al₂Si₂O₅(OH)₄ | Illite (K,H)Al₂(Si,Al)₄O₁₀(OH)₂X H₂O | Chlorite (Mg, Fe, Al)₆(Al, Si)₄O₁₀(OH)₈ | Montmorillonite (Ca,Na,H)(Al,Mg, Fe,Zn)₂(Si,Al)₄O₁₀ (OH)₂ XH₂O | Goethite FeO(OH) | Feldspar (KAlSi₃O8, NaAlSi₃O₈, CaAl₂Si₂O₈) | Quartz SiO₂ | Diopside MgCaSi | Gypsum CaSO₄·2H₂O | Calcite CaCO₃ |
|---|---|---|---|---|---|---|---|---|---|---|---|---|
| Konya_Küçükköy | SiO₂ | 42.5 | | + | | + | | | + | | | |
| | Fe₂O₃ | 6.5 | | | | + | + | | | | | |
| | Al₂O₃ | 16.1 | | + | | + | | | | | | |
| | CaO | 10.7 | | | | | | + | | | + | + |
| | MgO | 2.82 | | | | + | | | | | | |
| | SO₃ | 0.19 | | | | | | | | | | |
| | K₂O | 2.2 | | | | | | + | | | | |
| | Na₂O | 0.43 | | | | + | | + | | | | |
| | P₂O₅ | 0.155 | | | | | | | | | | |
| | TiO₂ | 0.75 | | | | | | | | | | |
| | CO₂ | 17.2 | | | | | | | | | | |
| | Cl | 0.049 | | | | | | | | | | |
| Çorum_Karapınar | SiO₂ | 39.2 | + | + | + | + | | + | + | + | | |
| | Fe₂O₃ | 7.79 | | | + | + | + | | | | | |
| | Al₂O₃ | 15.1 | + | + | + | + | | + | | | | |
| | CaO | 10.1 | | | | + | | + | | + | + | + |
| | MgO | 4.67 | | | + | + | | + | | + | | |
| | SO₃ | 3.36 | | | | | | | | | + | |
| | K₂O | 2.56 | | | | | | + | | | | |
| | Na₂O | 1.12 | | | | | | + | | | | |
| | P₂O₅ | 0.19 | | | | | | | | | | |
| | TiO₂ | 1.07 | | | | | | | | | | |
| | CO₂ | 14.1 | | | | | | | | | | |
| | Cl | 0.43 | | | | | | | | | | |
| Çorum_Kınık | SiO₂ | 44.4 | + | + | + | + | | + | + | + | | |
| | Fe₂O₃ | 8.34 | | | + | + | + | | | | | |
| | Al₂O₃ | 15.2 | + | + | + | + | | + | | | | |
| | CaO | 8.31 | | | | + | | + | | | + | + |
| | MgO | 5.19 | | | + | + | | | | + | | |
| | SO₃ | 0.11 | | | | | | | | | | |
| | K₂O | 2.28 | | | | | | + | | | | |
| | Na₂O | 0.85 | | | | | | + | | | | |
| | P₂O₅ | 0.19 | | | | | | | | | | |
| | TiO₂ | 1.09 | | | | | | | | | | |
| | CO₂ | 13.7 | | | | | | | | | | |
| | Cl | 0.05 | | | | | | | | | | |
| Çorum_Sarımbey | SiO₂ | 45.9 | + | + | | + | | + | + | + | | |
| | Fe₂O₃ | 8.2 | | | | + | + | | | | | |
| | Al₂O₃ | 15.3 | + | + | | + | | + | | | | |
| | CaO | 7.91 | | | | + | | + | | | + | + |
| | MgO | 5.19 | | | | + | | | | + | | |
| | SO₃ | 0.29 | | | | | | | | | | |
| | K₂O | 2.27 | | | | | | + | | | | |
| | P₂O₅ | 0.29 | | | | | | | | | | |
| | Na₂O | 1.06 | | | | | | + | | | | |
| | TiO₂ | 1.13 | | | | | | | | | | |
| | CO₂ | 12.1 | | | | | | | | | | |
| | Cl | 0.049 | | | | | | | | | | |

The elements mainly found by XRF are silicon dioxide (SO₂), alumina oxide (Al₂O₃), magnesium oxide (MgO), calcium oxide (CaO), iron oxide (Fe₂O₃) and carbon dioxide (CO₂). The other minerals detected are sulphide (SO₃), potassium

oxide ($K_2O$), sodium oxide ($Na_2O$), phosphor pentoxide ($P_2O_5$), titanium oxide ($TiO_2$) and chloride (Cl). The elements determined by XRF supported the minerals found by XRD in the samples below 63 μm (Figure 4.1, Figure 4.3, Figure 4.4 and Figure 4.5). The presence of calcite in all samples was proved by XRD and XRF measurements. The samples have CaO content between 6% and 10%. The highest CaO content was found in the Konya_Küçükköy sample. Gypsum content in the Çorum_Karapınar sample detected by XRD was supported with the element $SO_3$ in 3.36 % found by XRF analyses. The $SO_3$ element in the other samples was found in a limited amount between 0.11% and 0.29 %. In addition, the presence of Cl and $P_2O_5$ found by XRF was also supported by the salt spot test detecting the phosphate chloride salts.

### 4.4.5.1     Spectrophotometry Test

The soil samples were found to be in dark brown and yellowish-dark brown colours by the spectrophotometer (Table 4.8). The presence and proportion of goethite in the samples can be determined by the yellowish hue in their colours (Scheinost & Schwertmann, 1999). The more yellowish hue was observed in the Çorum_Kınık and Çorum_Sarımbey samples in comparison to other samples that are supported by the XRF results including the highest ratio of iron/goethite minerals.

Table 4.8 Colour properties of the samples determined by the spectrophotometer.

| Konya_Küçükköy | Çorum_Karapınar | Çorum_Kınık | Çorum_Sarımbey |
|---|---|---|---|
| L:41  a:4  b:11 | L:42  a:2  b:10 | L:49  a:4  b:18 | L:46  a:3  b:16 |

#### 4.4.5.2    X-ray diffraction (XRD) Analyses

The samples' particle sizes below 4 µm were analysed by XRD analyses to search for the presence of calcite, Nano-calcite and pozzolanic amorphous minerals in the clay and silt content. The samples' particles below 63 µm had been analysed by XRD analyses to specify their clay minerals. The predetermined clay types were observed in the samples' different particle size ranges below 4 µm. The calcite and the Nano-calcite ($CaCO_3$) peaks were detected in all samples below 4 µm particle sizes (Figure 4.37, Figure 4.38, Figure 4.39 and Figure 4.40). The most dominant calcite peaks were in the Çorum_Kınık samples' particle size between 0.05 µm and 0.25 µm. That signalled the presence of the highest amount of Nano-calcite in the Çorum_Kınık sample among all samples. The Çorum_Karapınar and Çorum_Sarımbey samples also were observed to have very high calcite peaks at that particle size range. The amounts of calcite and Nano-calcite contents in the samples' particle sizes below 4µm were found to be between 5 % and -6.9 % by the loss on the ignition (LOI) test (Table 4.9). The highest Nano-calcite content in particle sizes below 4 µm was also determined to be in the Çorum_Kınık sample.

The results of XRD analyses showed that the pozzolanic amorphous mineral of Opal A was found in the Çorum_Karapınar and Çorum_Sarımbey samples. That is consistent with the pozzolanic activity test results (Table 4.6). The broad bands of Opal A in the XRD patterns of the samples were observed in particle sizes below 0.25 µm. The literature data also indicates that Opal A in the soil is present mainly at the sizes of particles below 0.5 µm (Drees et al., 2018).
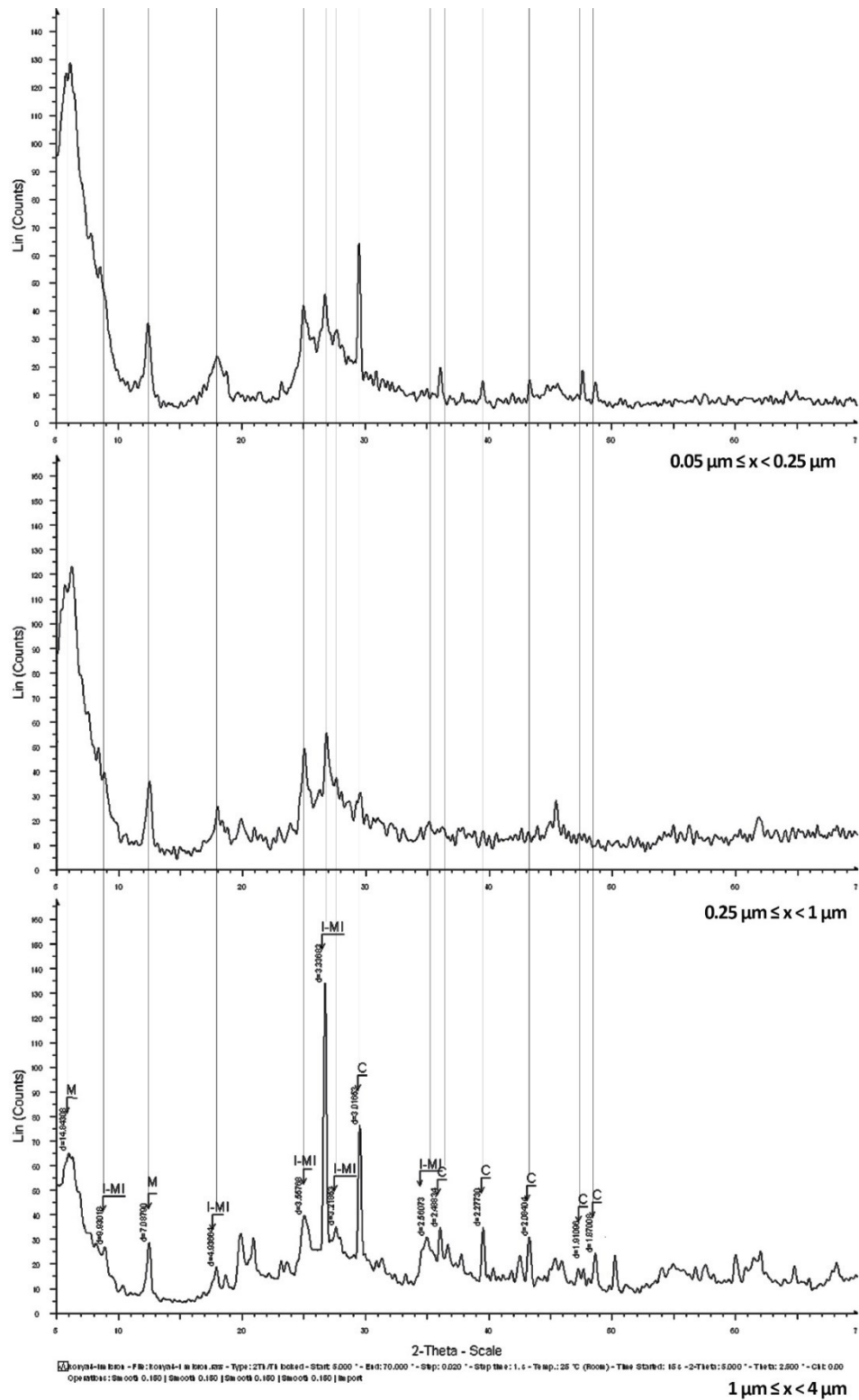
Figure 4.37 XRD patterns of Konya_Küçükköy sample below 4µm (M: Montmorillonite; I-MI: Illite-Mica; C: Calcite).
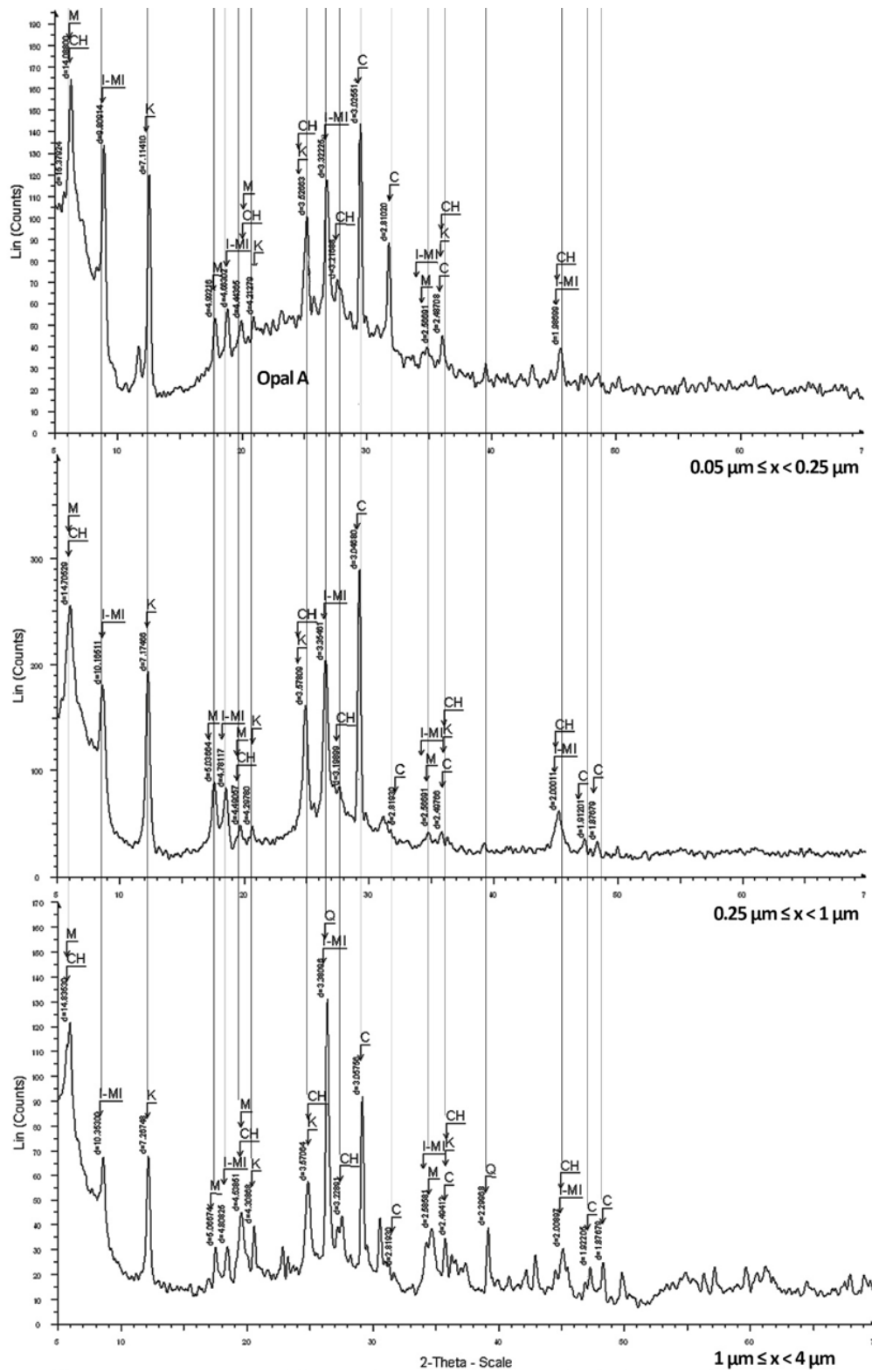
Figure 4.38 XRD patterns of Çorum_Karapınar sample below 4μm (M: Montmorillonite; CH: Chlorite; I-MI: Illite-Mica; K: Kaolinite; C: Calcite).
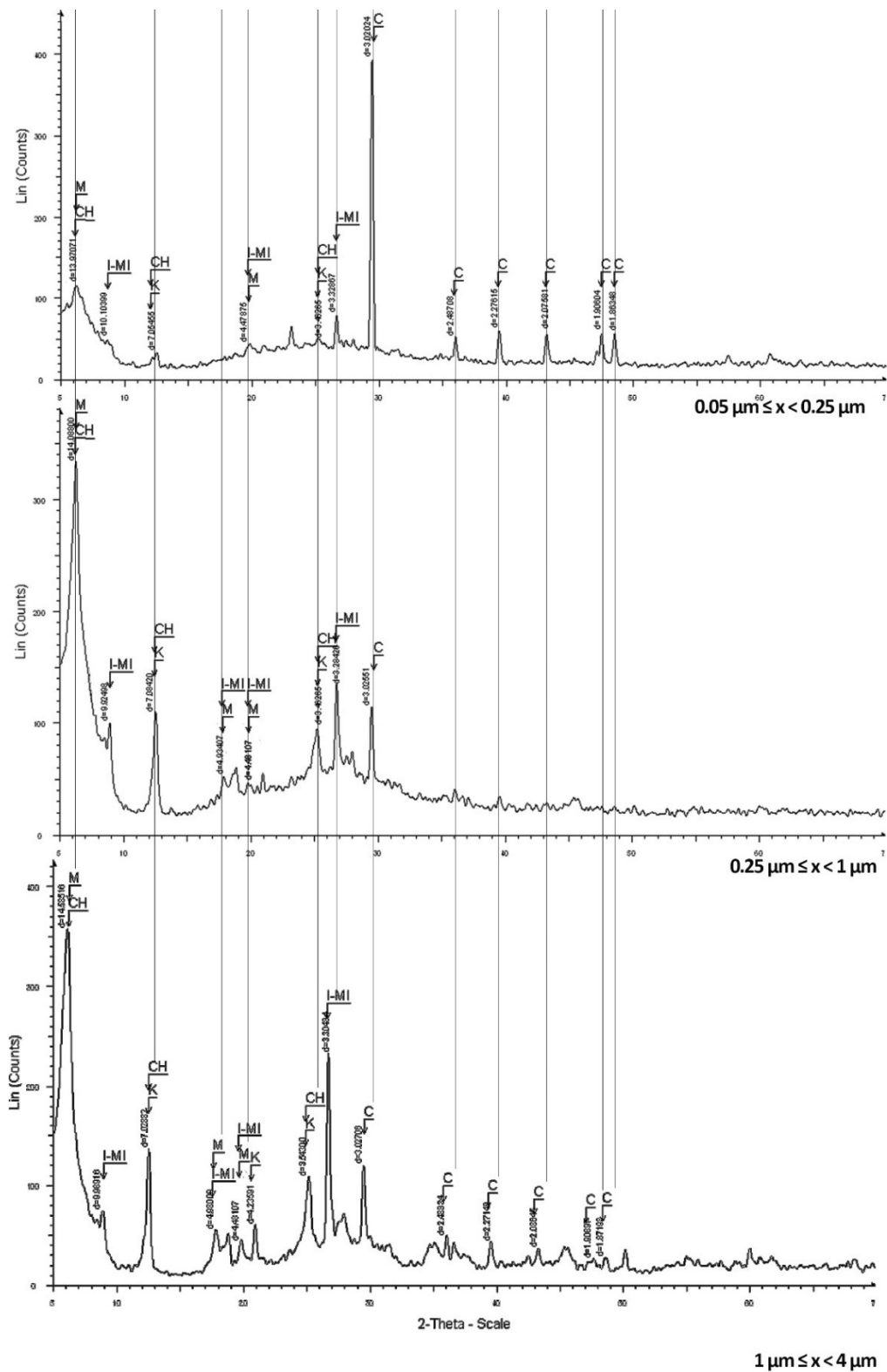
Figure 4.39 XRD patterns of Çorum_Kınık sample below 4µm (M: Montmorillonite; CH: Chlorite; I-MI: Illite-Mica; K: Kaolinite; C: Calcite).
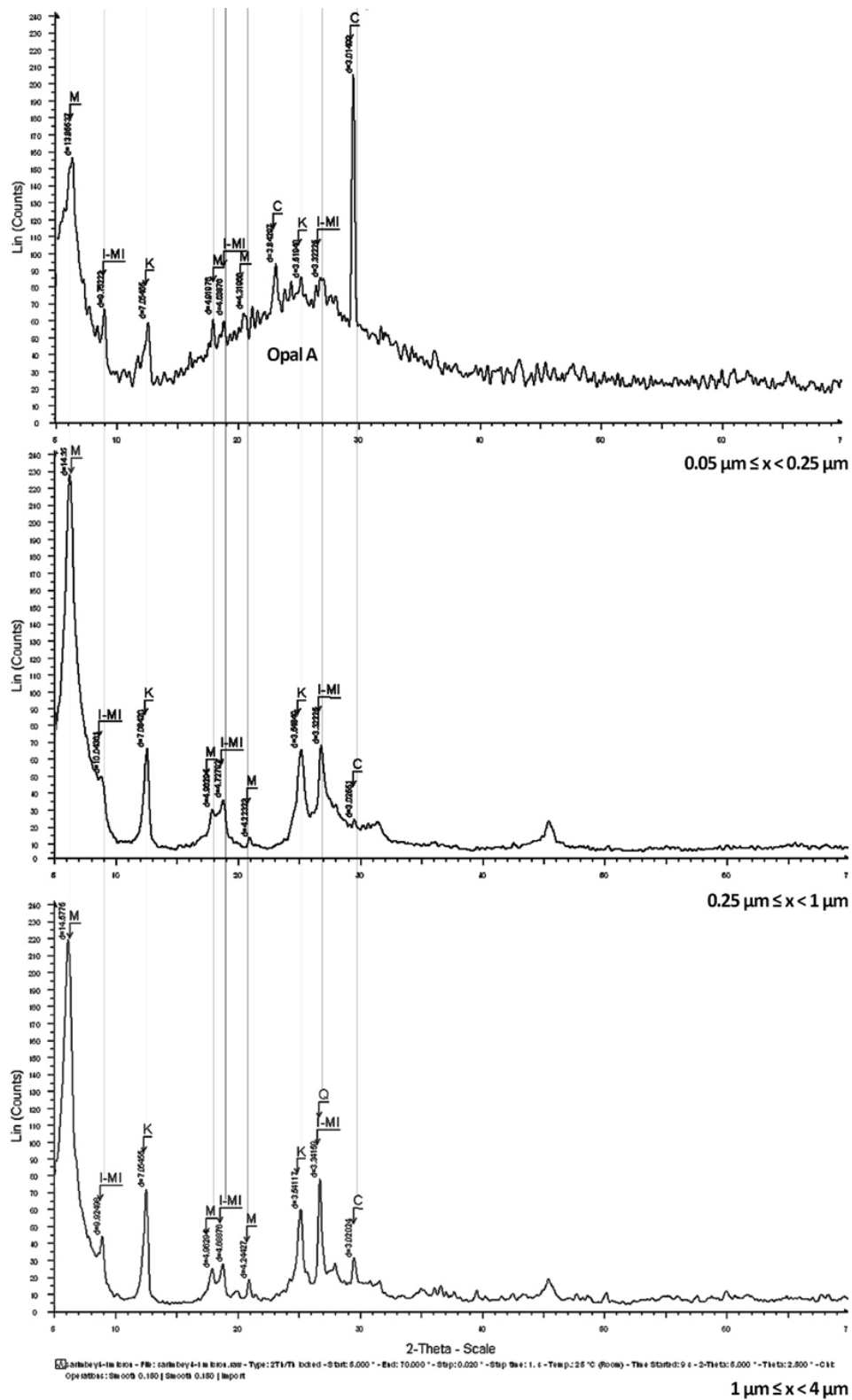
Figure 4.40 XRD patterns of Çorum_Sarımbey sample below 4µm (M: Montmorillonite; I-MI: Illite-Mica; K: Kaolinite; C: Calcite).

Table 4.9 The CaCO$_3$ content achieved by the loss on ignition (LOI) test in the samples below 4µm.

| Sample | CaCO$_3$, % |
|---|---|
| Konya_Küçükköy | 6.2 |
| Çorum_Karapınar | 5.9 |
| Çorum_Kınık | 6.9 |
| Çorum_Sarımbey | 5.0 |

### 4.4.6 Consistency Limits and Linear Shrinkage Ratio Analyses

Consistency (Atterberg) limits and linear shrinkage ratios of treated and untreated Konya_Küçükköy, Çorum_Kınık, Çorum_Karapınar and Çorum_Sarımbey samples were shown in Casagrande plasticity chart and the tables to observe the effect of the produced Nano-clay on the performance of the soil sample (Figure 4.41, Table 4.10, Table 4.11 and Table 4.12 ).
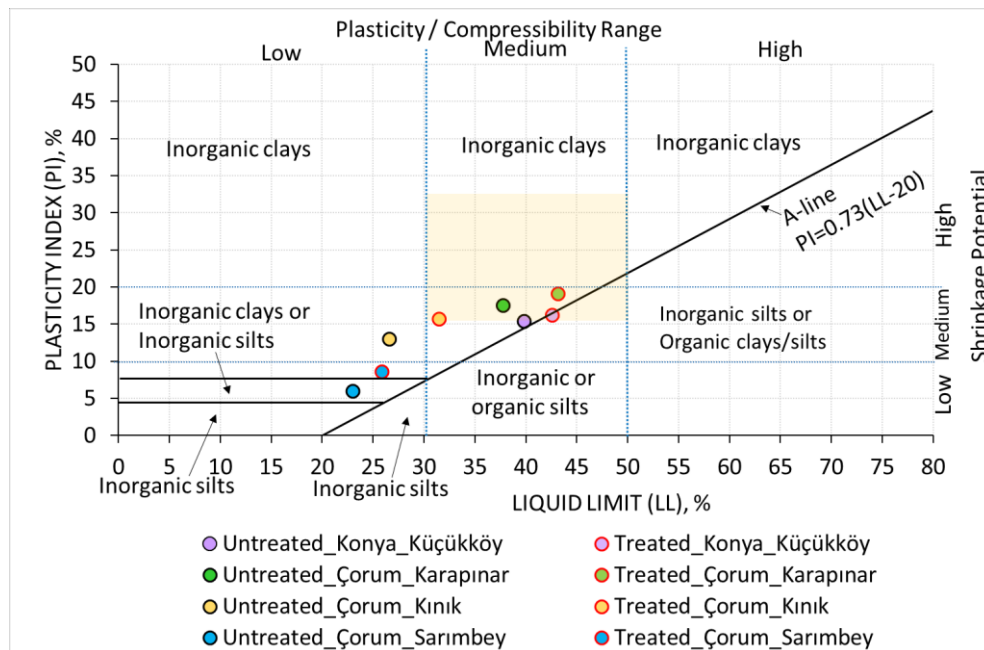


Figure 4.41 Atterberg limit values of untreated and treated Konya_Küçükköy, Çorum_Kınık, Çorum_Karapınar and Çorum_Sarımbey samples in Casagrande plasticity chart, and the proper range for the adobe soil shown in yellow colour.

Table 4.10 Atterberg limit values and types of untreated soil samples.

| Sample | LL, % | PL, % | PI, % | Type of soil |
|---|---|---|---|---|
| Konya_Küçükköy | 39.8 | 23.4 | 15.4 | Inorganic clays (CL) with medium plasticity |
| Çorum_Karapınar | 37.8 | 20.31 | 17.4 | Inorganic clays (CL) with medium plasticity |
| Çorum_Kınık | 26.6 | 13.6 | 13 | Inorganic clays (CL) with medium plasticity |
| Çorum_Sarımbey | 23 | 17.02 | 5.98 | Inorganic clays (CL) or Inorganic silts (ML) with low plasticity |

Table 4.11 Atterberg limit values of treated Konya_Küçükköy, Çorum_Karapınar Çorum_Kınık and Çorum_Sarımbey samples.

| Sample | LL, % | PL, % | PI, % | Type of soil |
|---|---|---|---|---|
| Konya_Küçükköy | 42.6 | 26.4 | 16.2 | Inorganic silt; (ML) or Organic clay/ Organic silt (OL) with medium plasticity |
| Çorum_Karapınar | 41.1 | 24.1 | 19.1 | Inorganic clays (CL) with medium plasticity |
| Çorum_Kınık | 31.5 | 15.9 | 15.6 | Inorganic clays (CL) with medium plasticity |
| Çorum_Sarımbey | 25.8 | 17.2 | 8.6 | Inorganic silts (CL) with low plasticity |

Table 4.12 Linear shrinkage ratios of the soil samples.

| Sample | Linear Shrinkage ratio, % | | |
|---|---|---|---|
| | Before Treatment | After Treatment | |
| Konya_Küçükköy | 17.1 | 21 |  |
| Çorum_Karapınar | 10.7 | 14.3 |  |
| Çorum_Kınık | 8.6 | 11.4 |  |
| Çorum_Sarımbey | 5 | 8.6 |  |

The results of the Atterberg limit and linear shrinkage (LS) ratios of the untreated samples were summarised below:

- The samples of Çorum_Karapınar and Konya_Küçükköy were positioned in the proper ranges for the adobe soil in the Casagrande chart, and they had the classification of the inorganic clays having medium plasticity, while the Çorum_Kınık and Çorum_Sarımbey samples were not found to be proper as adobe soil.
- The LL values of the samples ranged from 23 % to 39.8 %, which indicated low and medium plasticity. The LL values of Çorum_Karapınar and Konya_Küçükköy samples were found 37.8 % and 39.8%, respectively, which are in acceptable ranges of 31%–50% (Delgado & Cañas, 2007; Houben & Guillaud, 1994).
- The PI values of the samples ranged from 5.98 % to 17.4 %, which indicated low and medium shrinkage potential. The achieved PI values signalled that those soil samples could have volumetric shrinkage and swelling at low to medium levels when they get wet and dry.

- In the LS ratio test, the Konya_Küçükköy-only sample was observed to break.

- The LS ratios of the samples of Çorum_Karapınar and Konya_Küçükköy were found to be higher than the other ones, while the Çorum_Sarımbey sample has the lowest ratio. That shows the higher plasticity properties of Konya_Küçükköy and Çorum_Karapınar result in having higher linear shrinkage potential. Those data are compatible with the shrinkage potential of the samples in the Casagrande plasticity chart.

- The LS ratios of Konya_Küçükköy, Çorum_Karapınar and Çorum_Kınık samples were determined to be above the critical level of 8% (Dawson et al., 1956).

The results of the Atterberg limits and LS ratios of the treated samples were summarised below:

- The Atterberg limits and LS ratios of all samples increased since the specific surface area of the clay contents in all samples increased by the treatment for the Nano-clay production.

- The Atterberg limits and LS ratios of the samples from the highest to lowest are Konya_Küçükköy, Çorum_Karapınar, Çorum_Kınık and Çorum_Sarımbey, respectively, directly related to the amount of clay contents.

- The Atterberg limits of Konya_Küçükköy, Çorum_Karapınar and Çorum_Kınık samples fell into the proper region for the adobe in the plasticity chart, but the Çorum_Sarımbey sample was still found not to be proper as adobe soil.

- The LL values of Konya_Küçükköy, Çorum_Karapınar and Çorum_Kınık samples were found in the range of 31.5% and 42.6% which are in acceptable ranges of 31%–50% for the adobe and were determined to have medium plasticity (Delgado & Cañas, 2007; Houben & Guillaud, 1994). In addition,

154

the LL value of the Çorum_Sarımbey sample was determined as 25.8% indicating low plasticity property.

- The PI values of the Konya_Küçükköy, Çorum_Karapınar and Çorum_Kınık samples ranged from 11.7% to 19.1 %, which indicated medium shrinkage potential, while the PI values of the Çorum_Sarımbey sample was found to be as 8.6%. The achieved plastic index values signalled that the Çorum_Sarımbey sample had a higher potential to tolerate excessive swelling and shrinkage when they got wet and dry compared to Konya_Küçükköy, Çorum_Karapınar and Çorum_Kınık soil samples.

- The LS ratios of the samples were found to be in the range of 8.6%-21% which was above the critical level of 8% (Dawson et al., 1956); therefore, cracking problems may occur in adobe samples. The LS ratios of the samples from the highest to lowest were compatible with the shrinkage potential of the samples in the Casagrande plasticity chart.

In brief, after the Nano-clay production by the ultrasonic treatment, the proper soil samples of Konya_Küçükköy, Çorum_Karapınar and Çorum_Kınık were selected for advanced laboratory analyses since they had adequate Atterberg limit values for adobe soil despite of their higher linear shrinkage ratios than the acceptable values. On the other hand, the Çorum_Sarımbey sample still did not have proper characteristics in terms of its Atterberg limit even after the treatment; therefore, it was eliminated, despite its high pozzolanic properties.

## 4.5 Performance assessment of Nano-clay riched adobe product samples (Treated adobe samples)

The performance results of adobe samples produced from treated and untreated Konya_Küçükköy, Çorum_Karapınar and Çorum_Kınık soils were given under the related sub-headings.

### 4.5.1    Basic Physical Tests

The bulk density (dry density) values were found to be in the ranges of 1.51-2.06 g/cm$^3$, 1.45-2.25 g/cm$^3$ and 1.26-1.92 g/cm$^3$ for the Konya_Küçükköy, Çorum_Karapınar and Çorum_Kınık samples, respectively. The particle density values are in the ranges of 2.63-2.70 g/cm$^3$, 2.57-2.61 g/cm$^3$, 2.59-2.69 g/cm$^3$, and their porosity values are between 22.2-42.4 %, 12.4-43.4 % and 25.6-51.3%, respectively (Figure 4.42).
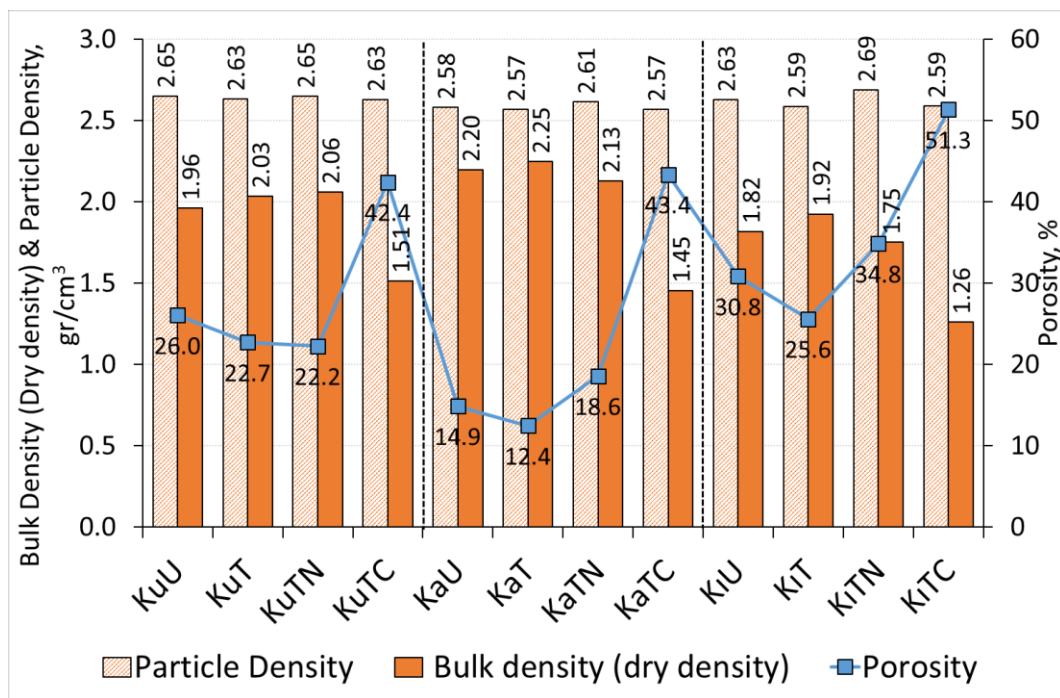


Figure 4.42 Particle density, bulk density (dry density) and porosity values of the adobe samples.

### 4.5.2    Water Vapour Permeability Tests

The water vapour resistance factor (μ, unitless) values of Konya_Küçükköy, Çorum_Karapınar and Çorum_Kınık samples were found to be in the ranges of 14.35-21.85, 11.48-33.80 and 7-17.48, respectively (Figure 4.43). Their equivalent

air thickness of water vapour permeability (SD, m) values are between 0.29-0.41m, 0.26-0.78m and 0.15-0.35m, respectively.
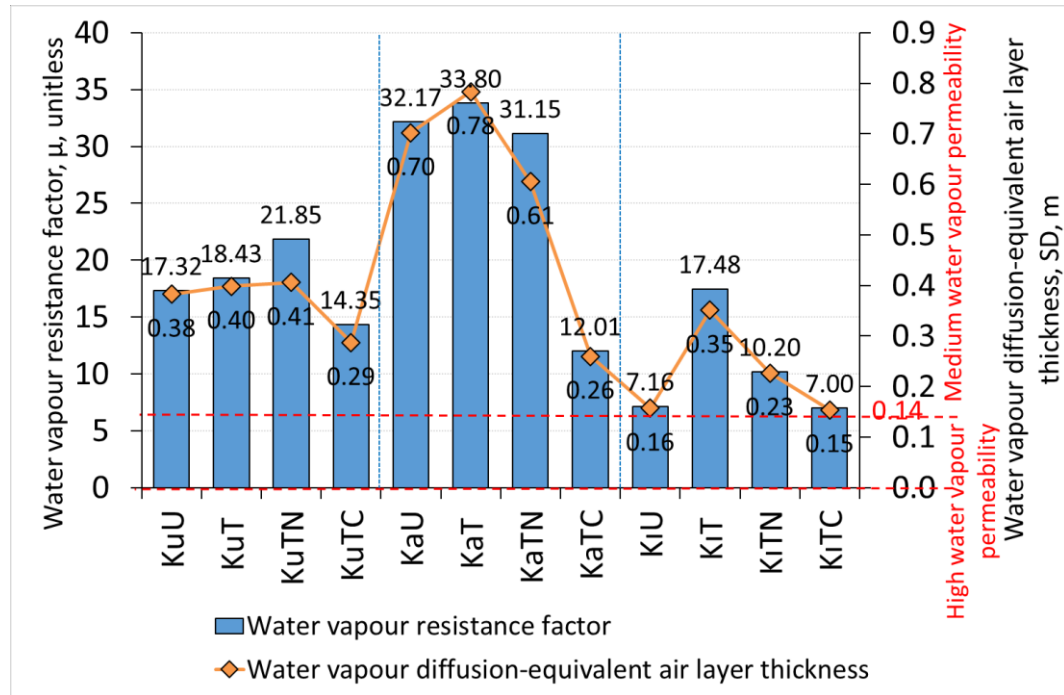


Figure 4.43 The water vapour resistance factor (µ, unitless) and water vapour diffusion equivalent air layer thickness (SD, m) values of the adobe samples.

### 4.5.3 Mechanical Tests

All data on the compressive and flexural strengths of the samples were given in Table 4.13 and their mean values were shown in Figure 4.44 and Figure 4.45. The mean values of compressive strengths found for untreated, treated, treated ones including Nano-CaO and treated ones including $CaOH_2$ were in the ranges of 2.81-6.94 MPa, 5.17-8.18 MPa, 2.92-8.72 MPa and 0.49-1.44 MPa, respectively, for the Konya_Küçükköy, Çorum_Karapınar and Çorum_Kınık samples. The mean values of flexural strengths for those samples were determined in the ranges of 0.14-0.31 MPa, 0.3-0.53 MPa, 0.16-0.43 MPa, and 0.03-0.08 MPa, respectively.

Table 4.13 All data on the compressive and flexural strengths of the samples.

| Sample | Compressive strength, MPa | | | | Flexural Strength, MPa | | | |
|---|---|---|---|---|---|---|---|---|
| | A | B | C | STD | A | B | C | STD |
| KuU | 6.65 | 6.94 | 6.88 | 0.15 | 0.27 | 0.23 | 0.26 | 0.02 |
| KuT | 7.33 | 9.52 | 7.68 | 1.18 | 0.30 | 0.30 | 0.16 | 0.08 |
| KuTN | 8.38 | 9.17 | 8.61 | 0.40 | 0.16 | 0.18 | 0.14 | 0.02 |
| KuTC | 1.44 | 1.56 | 1.46 | 0.07 | 0.12 | 0.06 | 0.05 | 0.04 |
| KaU | 6.18 | 7.93 | 6.69 | 0.90 | 0.33 | 0.30 | 0.28 | 0.02 |
| KaT | 8.31 | 7.06 | 7.61 | 0.63 | 0.57 | 0.53 | 0.48 | 0.05 |
| KaTN | 5.83 | 5.92 | 7.22 | 0.78 | 0.46 | 0.43 | 0.41 | 0.03 |
| KaTC | 1.03 | 1.11 | 1.19 | 0.08 | 0.06 | 0.07 | 0.06 | 0.01 |
| KıU | 2.63 | 2.72 | 3.09 | 0.24 | 0.14 | 0.17 | 0.13 | 0.02 |
| KıT | 5.03 | 6.34 | 4.14 | 1.11 | 0.36 | 0.39 | 0.33 | 0.03 |
| KıTN | 2.33 | 3.78 | 2.64 | 0.76 | 0.20 | 0.21 | 0.18 | 0.02 |
| KıTC | 0.47 | 0.53 | 0.47 | 0.03 | 0.03 | 0.03 | 0.02 | 0.01 |
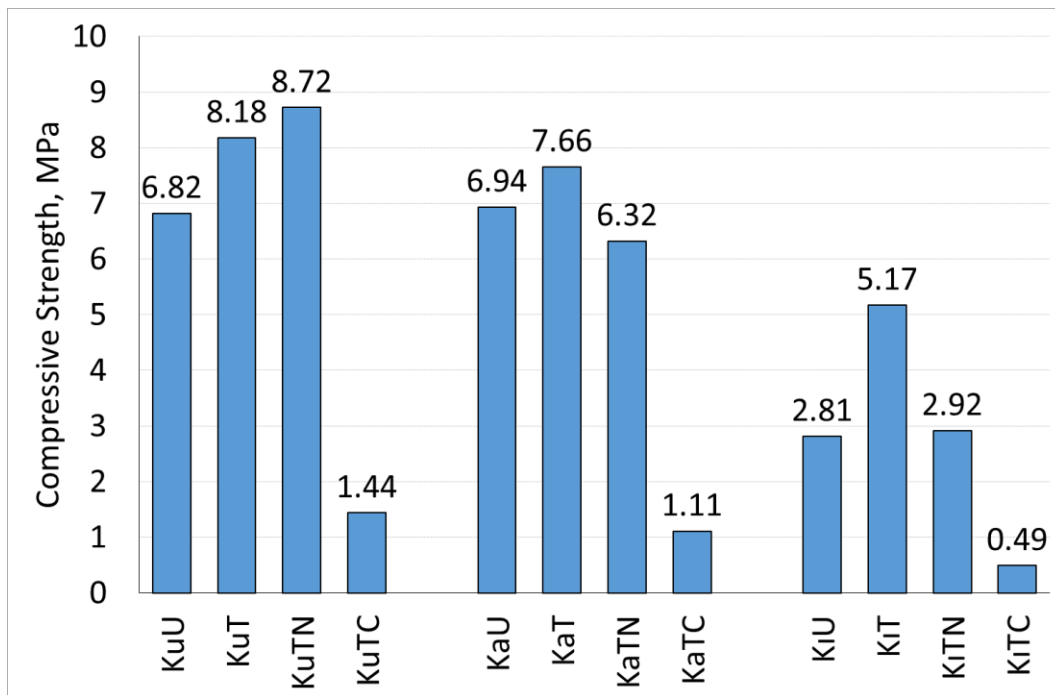


Figure 4.44 The mean values of compressive strength found for the samples.
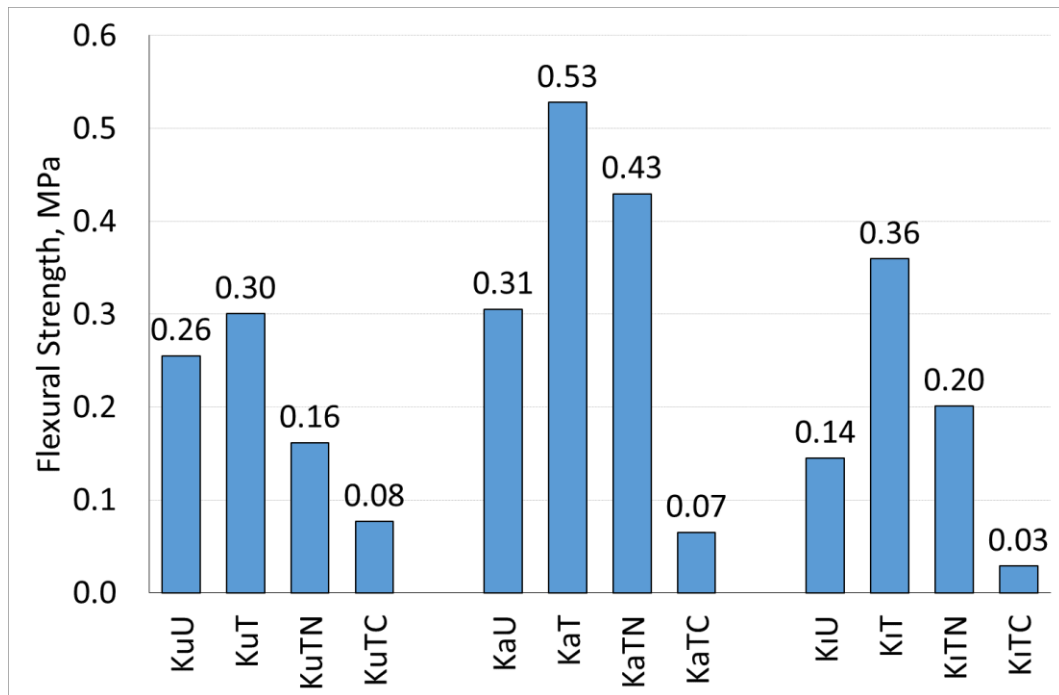
Figure 4.45 The mean values of flexural strength values found for the samples.

### 4.5.4　　Capillary Water Absorption Tests

The cumulative capillary water absorption values as a function of the square root of time were plotted in Figure 4.46 and the mean capillary water absorption coefficient values (A-value) are shown in Figure 4.47. The mean A-values in various units of the samples were also given in Table 4.14 to be able to evaluate the literature data on the capillary water absorption coefficient of adobe samples (Table 2.11).

The mean capillary water absorption values were found to be for Konya_Küçükköy samples' untreated, treated, treated one including Nano-CaO and treated one including $CaOH_2$ as $26.8\pm12$ kg/m$^2$, $28.5\pm15.7$ kg/m$^2$, $36.2\pm18.5$ kg/m$^2$ and $38.7\pm16.1$ kg/m$^2$, respectively. The values were determined as; $21.5\pm15.2$ kg/m$^2$, $22.4\pm16.3$ kg/m$^2$, $22.5\pm13.7$ kg/m$^2$ and $23.9\pm12.8$ kg/m$^2$, respectively, for Çorum_Karapınar sample, and $22\pm12.1$ kg/m$^2$, $21.5\pm10.2$ kg/m$^2$, $23.7\pm9.9$ kg/m$^2$ and $34.4\pm14.7$ kg/m$^2$, respectively, for the Çorum_Kınık sample. The A-values are

in the ranges of 0.39-0.59 kg/m$^2$.sec, 0.28-0.34 kg/m$^2$.sec, 0.28-0.52 kg/m$^2$.sec for the Konya_Küçükköy, Çorum_Karapınar and Çorum_Kınık samples, respectively.
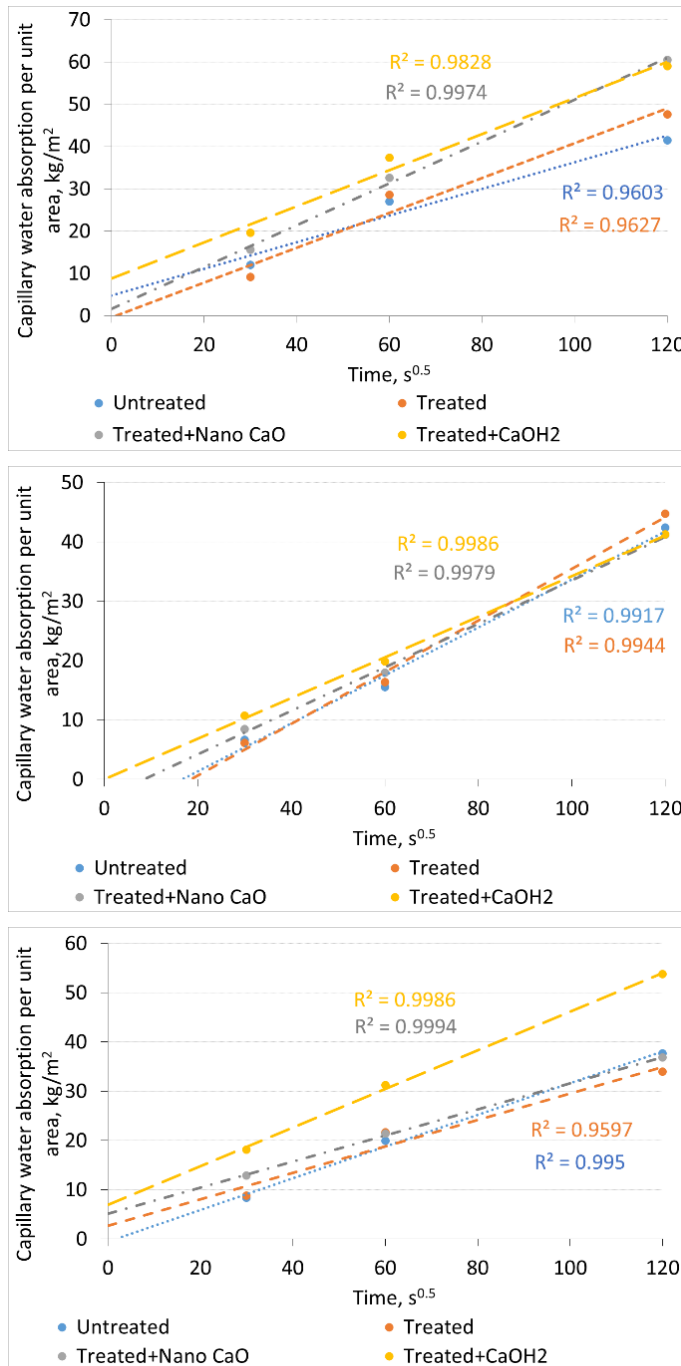


Figure 4.46 Capillary water absorption values of Konya_Küçükköy (at the top), Çorum_Karapınar (at the middle), and Çorum_Kınık samples (at the bottom).
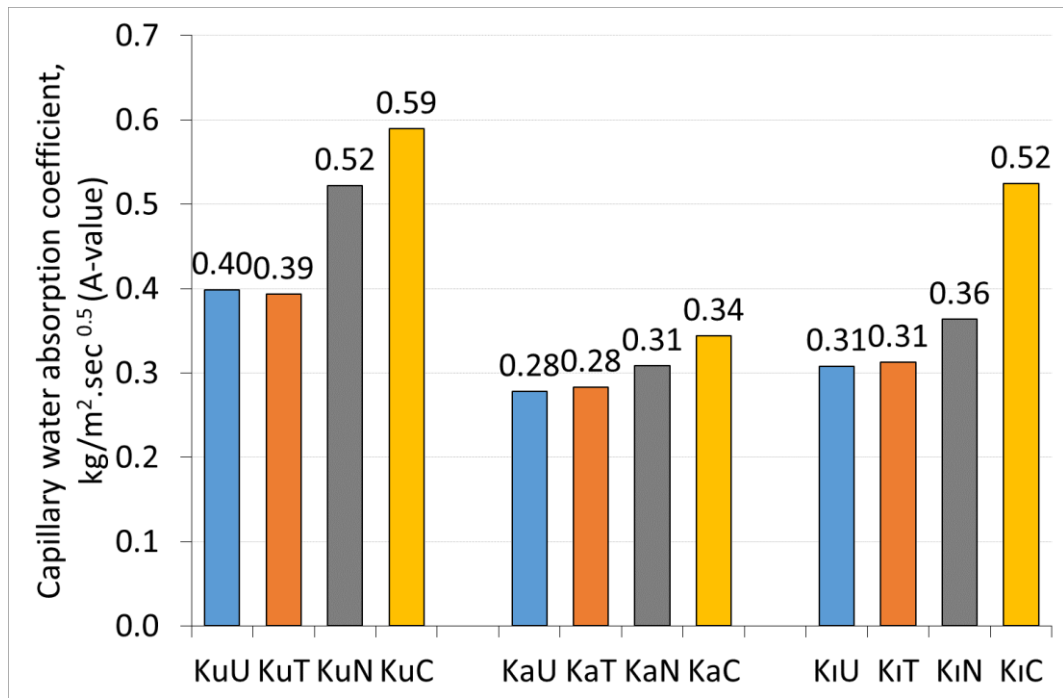
Figure 4.47 Mean capillary water absorption coefficient values (A-value) of the
Konya_Küçükköy, Çorum_Karapınar and Çorum_Kınık samples.


Table 4.14 The capillary water absorption coefficient values (A-values) in various
units of the samples.

| Sample | Capillary water absorption coefficient values (A-value) | | |
|---|---|---|---|
| | $kg/m^2.min^{0.5}$ | $g/cm^2.sec.100^{-3}$ | $kg/m^2.min$ |
| KuU | 3.09 | 0.79 | 0.47 |
| KuT | 3.05 | 0.72 | 0.43 |
| KuTN | 4.04 | 1.02 | 0.61 |
| KuTC | 4.56 | 1.21 | 0.73 |
| KaU | 2.15 | 0.49 | 0.29 |
| KaT | 2.19 | 0.48 | 0.29 |
| KaTN | 2.39 | 0.58 | 0.35 |
| KaTC | 2.66 | 0.67 | 0.40 |
| KıU | 2.39 | 1.18 | 0.71 |
| KıT | 2.42 | 1.19 | 0.72 |
| KıTN | 2.82 | 1.22 | 0.73 |
| KıTC | 4.06 | 1.78 | 1.07 |

### 4.5.5 Scanning Electron Microscope (SEM) Analyses

The SEM analyses were conducted on Konya_Küçükköy and Çorum_Karapınar adobe samples (Figure 4.48 and Figure 4.49 as a supportive test for their morphological and raw material characteristics. Larger pores were observed in the untreated Konya_Küçükköy adobe sample while the ones in smaller sizes were seen in the treated and treated one including the Nano-CaO adobe sample which was consistent with the result of the bulk density values of that adobe sample. The presence of the flocculated clay association having edge-to-edge and edge-to-face connections and aggregated clay particles having face-to-face connections could be observed together in untreated Konya_Küçükköy sample and treated Çorum_Karapınar adobe sample including Nano-CaO. The aggregated clay particles could be seen in Konya_Küçükköy adobe samples treated one and treated one including Nano-CaO as well as in the treated Çorum_Karapınar adobe sample. In addition, opal A, a natural pozzolan mineral, was detected in the untreated Çorum_Karapınar sample. That visually proved the results of XRD and pozzolanic activity tests.

| Konya_Küçükköy-Untreated | A: Clay Particles |
|---|---|
|  |  |
| Konya_Küçükköy-Treated | B: Clay Particles |
|  |  |
| Konya_Küçükköy-Treated+Nano CaO | C: Clay Particles |
|  |  |
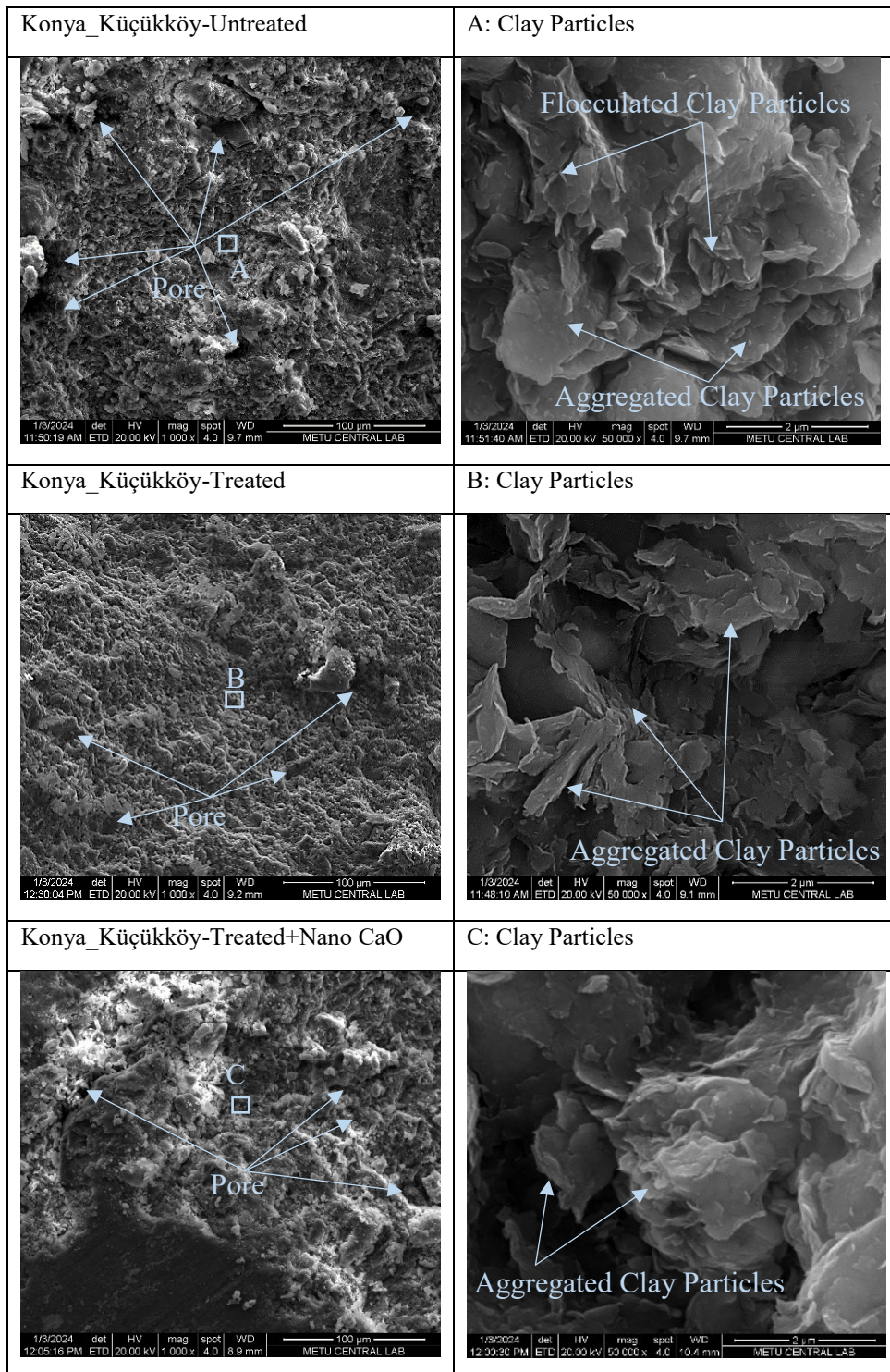
Figure 4.48 The SEM analyses conducted on Konya_Küçükköy adobe samples.

| Çorum_Karapınar-Untreated | A:Opal A |
|---|---|
|  |  |
| Çorum_Karapınar-Treated | B: Clay Particles |
|  |  |
| Çorum_Karapınar-Treated+Nano CaO | C: Clay Particles |
|  |  |
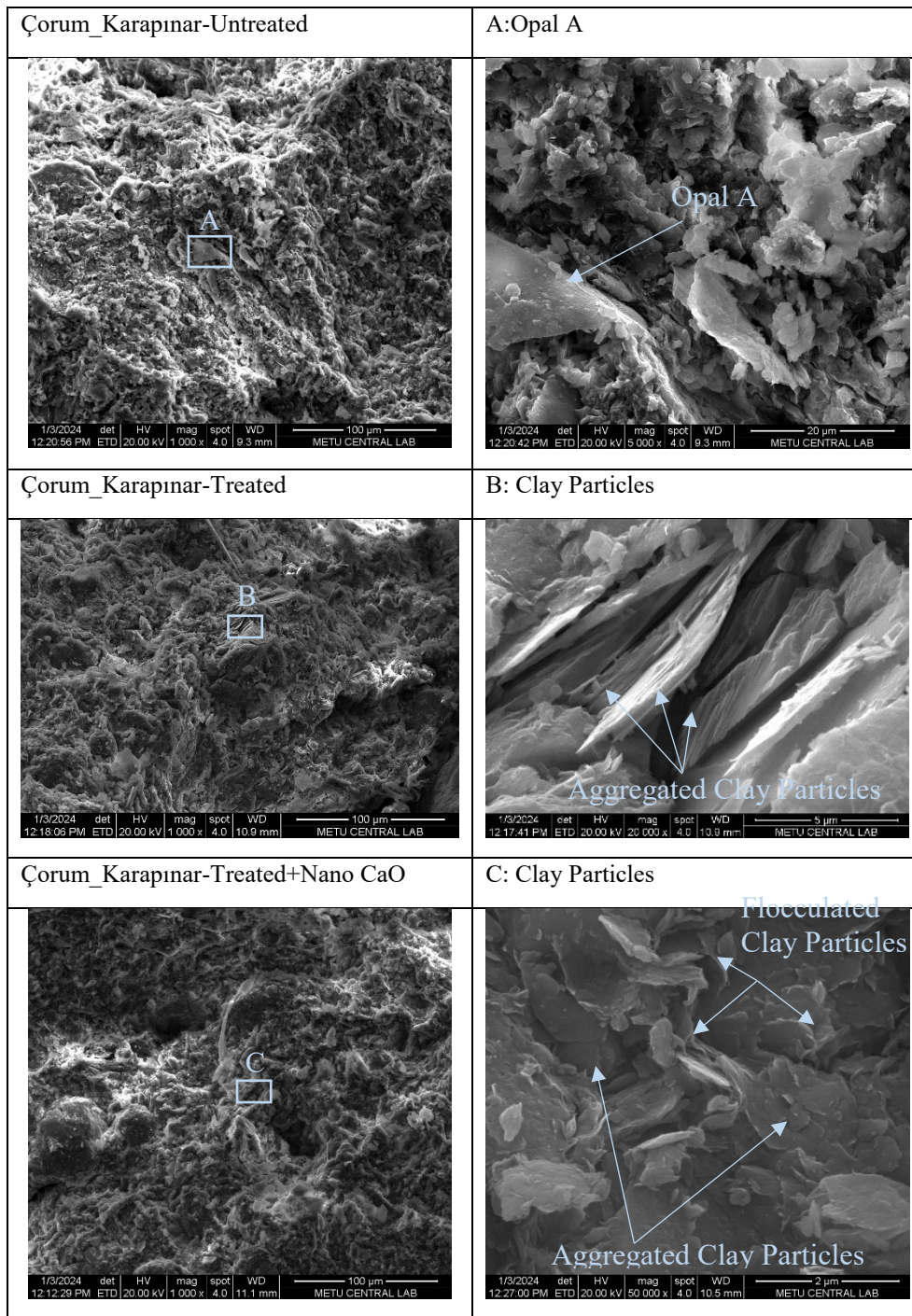
Figure 4.49 The SEM analyses conducted on Çorum_Karapınar adobe samples.

# CHAPTER 5

# DISCUSSION

In this section, the overall data of conducted analyses and literature knowledge are interpreted together in detail under respective subheadings. Firstly, the properties of soil/clay samples were evaluated in terms of their sufficiency to be used for the Nano-clay production and adobe sample. Then, during the Nano-clay production by ultrasonic treatment, the criteria affecting Nano-clay production were uncovered. Later on, the treated adobe soils having the enriched Nano-clay contents were evaluated if they were proper for the adobe material or not. In the last part, the performance results of prepared some adobe mixtures by using natural adobe soil and Nano-clay riched adobe soil with some additives of Nano-CaO and $Ca(OH)_2$ were discussed combined and comparatively according to recommended levels and related literature data.

## 5.1 Performance Assessment of Adobe Soil Resources

The adobe soil samples were collected from Çorum, Eskişehir, Konya and Manisa which represent the adobe soil/clay resources used in their regions for long periods in adobe building material production. According to field test results, the soil samples' compositions include high or low amounts of clay contents but they are not in the proper region for the adobe in the soil texture triangle which the RILEM defines. On the other hand, that is not taken as a criterion for the selection of soil samples for the stage of Nano-clay production from the soil since the adobe soil is a field-dependent material and there is no one standard or optimisation in the particle size distribution. Therefore, all collected soil samples continued to be analysed through laboratory analyses.

All soil resources are located where lake basins existed during the Neogene period (Alkaç & Koral, 2022; de Ridder, 1965; Kadir & Karakas, 2002; Varol et al., 2002; Yeniyol, 2012). The salts of carbonate (present in e.g. limestone), sulphate (present in e.g. gypsum) and chloride (present in e.g. sodium chloride or potassium chloride) generally found in lake deposits are observed in the collected samples. Those soluble salts decrease the durability and mechanical performance of adobe since they cause deterioration such as shrinkage cracks and crumbling of the adobe soil (Clifton et al., 1979). On the other hand, the presence of calcite and gypsum up to a certain limit in adobe improves the mechanical strength such as compressive strength and shear strength, water resistance and control the volume stability. The presence of carbonate in all samples supports the finding of calcium carbonate/calcite ($CaCO_3$) and dolomite ($CaMg(CO_3)_2$) by the LOI and XRD analyses. The highest calcite contents are found in Eskişehir_Sazak and Eskişehir_Sorkun samples. The following one, the Konya_Küçükköy sample, has about 9.2% calcite content which falls into the range of 9-27% detected in the adobe samples used in Çatalhöyük (Love, 2012). The phosphate, nitrate and nitrate salts pointing out the existence of decomposed organic materials (Dar et al., 2017) are found in all samples except the Eskişehir_Sorkun sample which is consistent with the LOI test results. The only Konya_Küçükköy sample was found to be higher than the 2% recommended level of organic content for the adobe material (Uğuryol & Kulakoglu, 2013). The Manisa_Kemer and the Eskişehir_Sorkun samples have the advantage in terms of the having least types of soluble salt and organic content.

Pozzolanic properties that contribute to the mechanical strengths and water impermeability of the adobe are considerably higher in the Çorum_Karapınar and Çorum_Sarınmbey samples than the others and the natural pozzolan such as Opal A is also detected in only those two samples. As well as the Eskişehir_Sorkun has the lowest pozzolanic activity value.

At the starting stage of the study, the presence of kaolinite and illite minerals was searched in the clay content of the soil samples for the adobe material by XRD analyses. Those clay types having non or limited-swelling and -shrinkage potentials

166

are in Konya_Küçükköy, Çorum_Karapınar, Çorum_Kınık, Çorum_Sarınmbey and Manisa_Kemer samples. On the other hand, the asbestos minerals causing lung cancer disease are detected in the Eskişehir_Sorkun sample. The Eskişehir_Sazak sample has sepiolite clay as a main content resulting in excessive swelling and shrinkage problems. That causes serious crack problems inappropriate for the adobe construction materials. The Eskişehir_Sorkun and Eskişehir_Sazak samples were eliminated due to their inappropriate clay types, although they have properties such as high calcite contents and soluble salts and organic content in the least amount.

According to the particle size distribution analyses conducted in the laboratory to get an overall idea about the collected samples, the Konya_Küçükköy, Çorum_Karapınar and Çorum Kınık samples have higher ratios in the range of 79% and 97% silt-clay content than the recommended ranges in between 25% and 70%. In addition, they have lower gravel-sand content in the range of 7.5% and 22% lower than recommended levels of between 30% and 75% (Table 2.6). On the other hand, Çorum_Sarımbey has clay-silt and gravel-sand ratios in the proper range. The Manisa_Kemer sample having inadequate clay-sit content includes too high a ratio of gravel-sand at 82 % than the recommended ranges. According to the soil texture triangle, Konya_Küçükköy, Çorum_Karapınar and Çorum_Kınık samples have the soil texture of silty-clay loam, while the Çorum_Sarımbey sample has the texture of silt loam, and the Manisa_Kemer sample has loamy sand that refers considerable high gravel-sand content (Figure 2.14). Those results are consistent with the field soil test results for the Konya_Küçükköy, Çorum_Karapınar and Çorum_Kınık, and Çorum_Sarımbey samples, as well as a similar result for Manisa_Kemer sample found as the sandy loam. In addition, some studies have consistent results belonging to the soil samples collected from Çumra and Çatalhöyük near sites of Küçükköy, indicating that they have silty-clay texture (A. Erol et al., 2015; Love, 2012).

The study focused on the clay type and amount of clay content to evaluate the potential of Nano-clay production to be able to reach the defined range between 10% and 40% for the clay content (Table 2.6). The Konya_Küçükköy, and Çorum_Karapınar, Çorum_Kınık and Çorum_Sarımbey samples with the ranges of

4.2%-13.5%, 4.9%-9.7%, 2.7%-7.6% and 2.4%-5.5%, respectively, include montmorillonite clay type having high dispersion characteristics together with the other types of, illite-mica, kaolinite and chlorite clays; therefore, they have reached or have potential to reach the recommended level for the clay content. On the other hand, the Manisa_Kemer sample has too low clay content of about 0.3%-0.6 % and has the halloysite (kaolinite) and illite clay types that have less dispersion potential. Therefore, The Manisa_Kemer sample was eliminated since it has insufficient clay content to be able to catch the recommended level for the clay content even after Nano-clay production.

The Eskişehir_Sorkun soil sample absolutely should not be used as adobe material or direct usage as a construction material. The Eskişehir_Sazak sample including mainly sepiolite clay can be used as an additive in cement-based construction materials to improve their binding and fire resistance characteristics and it can also be used as a layer at roof or foundation components to control water leakage by its high adsorption capacity and low permeability (Abbaslou et al., 2023; Gure, 2016). In addition, there is a need for clay additive to use the Manisa_Kemer sample for the adobe construction material.

The Konya_Küçükköy and Çorum_Karapınar, Çorum_Kınık and Çorum_Sarımbey samples were selected for the Nano-clay enrichment from the adobe soil. On the other hand, for the advanced laboratory analyses on adobe samples, the Konya_Küçükköy, Çorum_Karapınar and Çorum_Kınık soil samples were selected since they have adequate Atterberg limits of LL and PI values for adobe soil, after the Nano-clay enrichment by the ultrasonic treatment. The Konya_Küçükköy and Çorum_Karapınar samples have adequate LL and PI values before the treatment, while Çorum_Kınık is only found to have sufficient for those values after the treatment. The Çorum_Sarımbey sample did not achieve those values even after the treatment; therefore, it was eliminated, despite its high pozzolanic properties. The improvement achieved by the Nano-clay enrichment by the treatment in the Çorum_Kınık sample points to the way that some improper soil samples can be used as adobe soil after that treatment. That provides the local adobe soil resources to be

used more efficiently and increases the interest of the construction industry in qualified adobe production technology.

The last selected three samples have different combinations of clay contents. The effect of the enrichment in different Nano-clay types on adobe performance is observed in this way.

The Konya_Küçükköy sample has the main montmorillonite clay type together with the kaolinite and illite. That sample has the highest produced Nano-clay through its high amount of montmorillonite. The Çorum_Karapınar sample has the highest pozzolanic characteristics among the collected samples, and its main clay content is kaolinite beside chlorite, illite and very limited montmorillonite resulting in the least Nano-clay production among the three samples. The results of the enrichment in the Nano-clay of the non-swelling or limited swelling clay types of kaolinite, chlorite and illite provide volume stability and crack control. The Çorum_Kınık sample has mainly montmorillonite and kaolinite clay types, as well as illite and chlorite. The near amounts of montmorillonite and kaolinite can contribute to balancing the adobe sample performance. Although the Nano-clay amount seriously increases in the sample after the treatment, volume stability of the adobe can be also provided.

## 5.2    Potentials and Limitations of the Examined Adobe Soil Resources for Nano-clay Production

The data achieved on the representative samples of local adobe soil resources collected from Konya_Küçükköy and Çorum_Karapınar, Çorum_Kınık and Çorum_Sarımbey adobe soil resources is discussed here. The joint interpretation of the data focuses on uncovering whether the adobe soil samples are suitable for the Nano-clay content enrichment process, and how effective is the soil resource in this regard. For that purpose, the potentials and limitations of the adobe soil resources were assessed in terms of clay content and Nano $CaCO_3$ content in the composition of adobe soil resources, pozzolanic activity, consistency limit (plastic and liquid

169

limits and plastic index) and linear shrinkage ratio. The discussions based on these selection criteria are summarized under respective subheadings.

## 5.2.1 The Effects of Pozzolanic Activity and CaCO$_3$ Content on Nano-clay Production

The data of the pozzolanic activity, CaCO$_3$ content and clay contents (existing clay and produced Nano-clay) in the soil samples is shown in Figure 5.1. The pozzolanic activity values of the Çorum_Karapınar and Çorum_Sarımbey samples are significantly higher than the other samples. On the other hand, the calcite (CaCO$_3$) content below 4 μm of the Çorum_Kınık sample is slightly higher than the other samples. The pozzolanic characteristics and CaCO$_3$ content of the samples are observed not to be directly proportional to the Nano-clay production.
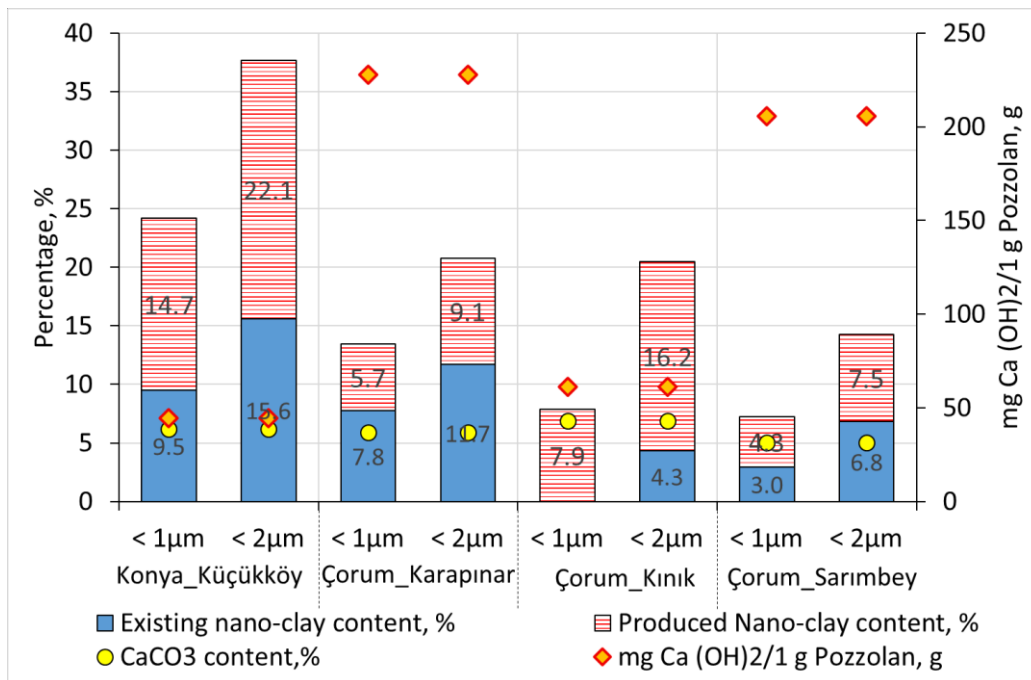


Figure 5.1 The graph showing the relation between the existing and produced Nano-clay/clay content below 1 μm and 2 μm and their pozzolanic activity values and CaCO$_3$ contents below 4 μm.

170

## 5.2.2    The Effects of Atterberg Limits on Nano-clay Production

The data of Atterberg limits-linear shrinkage ratio and the ratios of clay contents (existing clay and produced Nano-clay) in the soil samples are shown in Figure 5.2 and Figure 5.3. The relationship is not observed between the Nano-clay production and Atterberg limits of the untreated and treated samples. On the other hand, the total clay content composed of the existing clay content and produced Nano-clay (particle size below 2 μm) of the samples are observed to be generally directly proportional to LS (linear shrinkage ratio) and the PL (plastic limit) values of the untreated and treated samples.
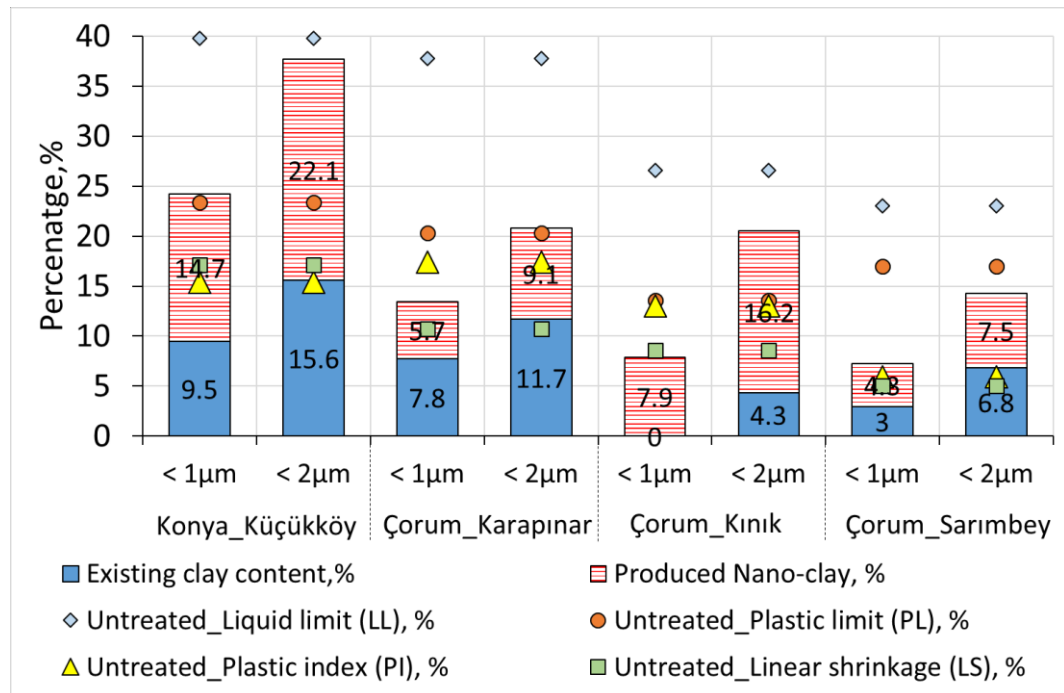


Figure 5.2 The percentages of the existing clay contents, the produced Nano-clay, and the Atterberg limits of the untreated samples.
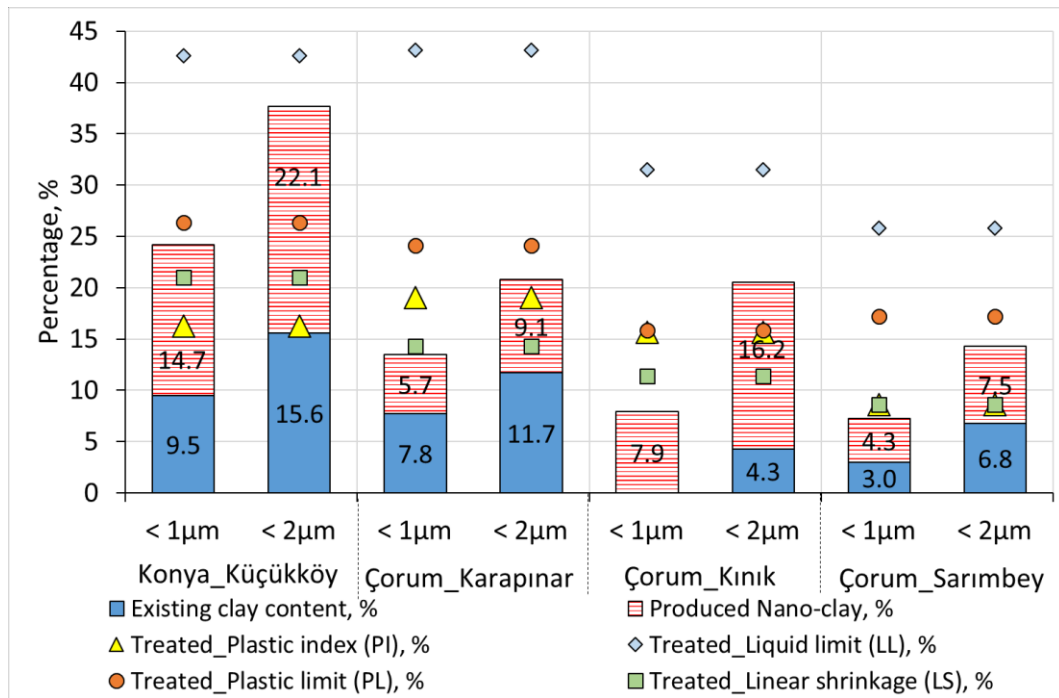
Figure 5.3 The percentages of the existing clay contents, the produced Nano-clay, and the Atterberg limits of the treated samples.

### 5.2.3 The Effects of Clay Content on Nano-clay Production

The data of the clay types and their amounts in the existing clay content and Nano-clay production is shown in Figure 5.4 and Figure 5.5. The percentages of each clay type defined by MAUD analyses (Figure 4.36) in the untreated sample were distributed in the clay proportions (below 1 µm and 2 µm) found by the laser diffraction particle size distribution analyses (Figure 4.20, Figure 4.21, Figure 4.22 and Figure 4.23). The correlations between the produced Nano-clay content to clay types, existing clay content and total clay content are indicated in Figure 5.6, Figure 5.7 and Figure 5.8. The highest correlation is observed between the produced Nano-clay content and the montmorillonite and then illite clay type (Figure 5.6). The Nano-clay production is mainly related to the amount of montmorillonite content having the highest dispersion characteristics among the other clay types in the soil samples. The maximum increase is observed, proportionally to their montmorillonite amount

172

together with the highest existing clay content in the Konya_Küçükköy sample, and the following rise seems in the Çorum_Kınık sample. Those two samples have montmorillonite clay type about half of the existing clay contents. The ratios of produced Nano-clay content to the existing clay content for the particle sizes below 2 μm of the Konya_Küçükköy, Çorum_Karapınar, Çorum_Kınık and Çorum_Sarımbey samples are 1.41, 0.78, 3.76 and 1.10, respectively. Those rates for the particle sizes below 1 μm are 1.55, 0.73, - and 1.45, respectively. After the treatment, while the highest total clay content is found in Konya_Küçükköy, the highest ratio of produced Nano-clay is present in the Çorum_Kınık sample despite its existing clay content in the least amount. In addition, although the Çorum_Karapınar sample is the second one having the highest existing clay amount and total clay amount after the treatment, it has the least increase rate. Here, the existing clay content and the total clay amount after the treatment are observed not to have a direct correlation for the potential of Nano-clay production (Figure 5.7 and Figure 5.8).
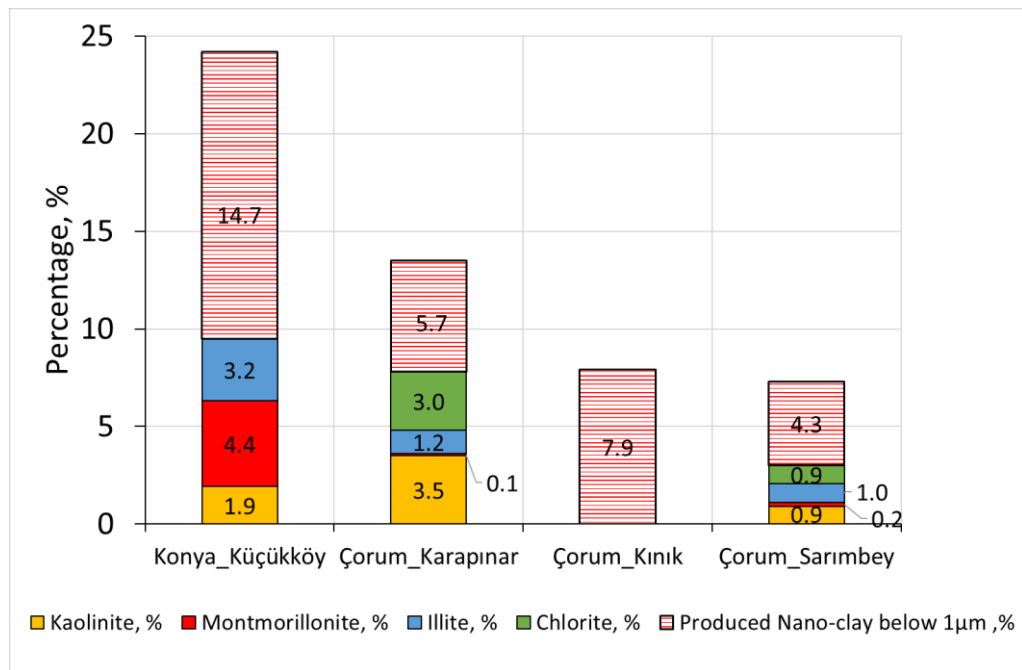


Figure 5.4 Percentages of clay types in the untreated samples, and produced Nano clay below 1 μm in the samples.
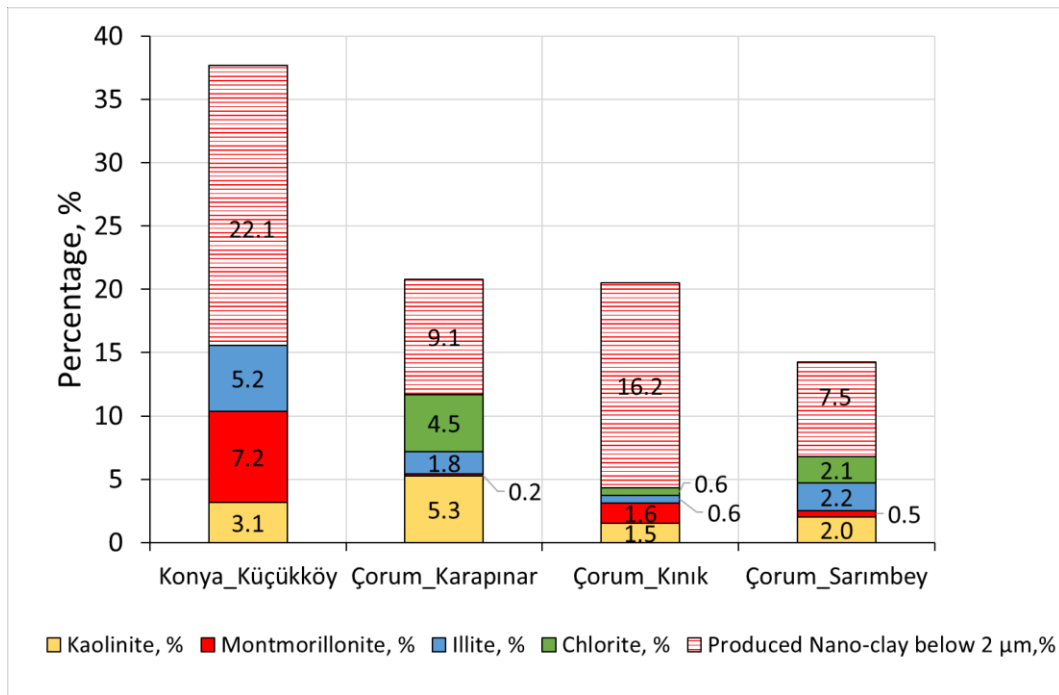
Figure 5.5 Percentages of clay types in the untreated samples, and produced Nano clay below 2 µm in the samples.
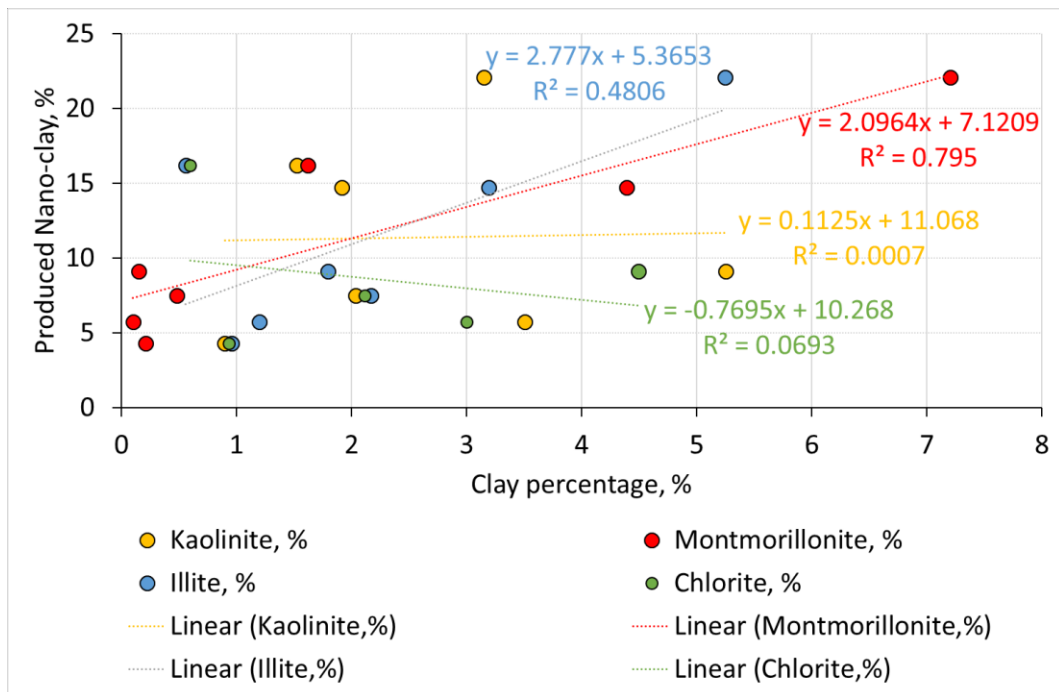


Figure 5.6 The correlation between produced Nano-clay content and the clay types.
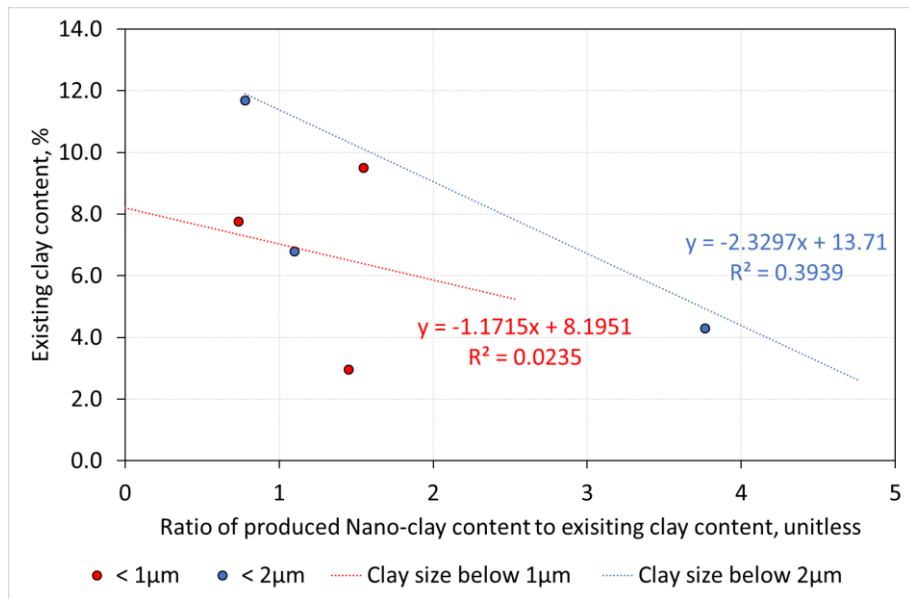
Figure 5.7 The correlation between the ratio of the produced Nano-clay content to existing clay content and the existing clay content.
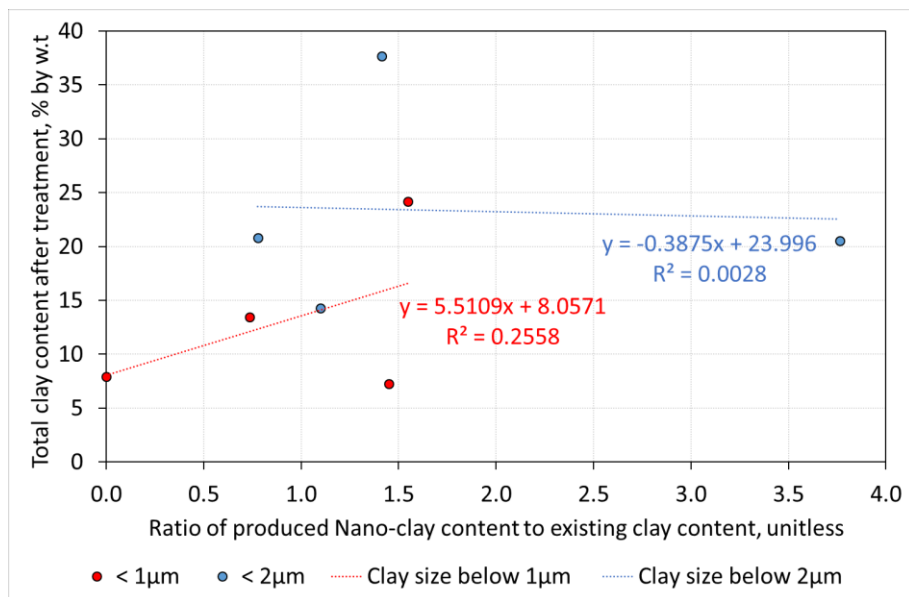


Figure 5.8 The correlation between the ratio of the produced Nano-clay content to existing clay content and the total clay content after treatment.

175

### 5.2.4 Soil Sample Selection Criteria for Production of Nano-clay enriched adobe sample

The study has shown that any adobe soil or clay resource can be assessed for its potential and whether it is efficient for the Nano-clay enrichment process. The adobe soil/clay resources used to produce qualified adobe building materials and the issues that need to be taken into consideration in terms of the composition and raw material properties of these resources are as follows:

— use of adobe soil/clay resources containing kaolin or mica-illite group clays (Torraca, 1988),

— the presence of calcium carbonate content in the clay size (F. Erol et al., 2022)

— the presence of coarse aggregates larger than 2 mm grain size in the adobe soil source or adobe mixture in a proportion more or less relevant to the performance of the adobe product (Stefanidou & Papayianni, 2005),

— the adobe/clay resource exhibits a plasticity index value in the range of 16%–33% corresponding to a liquid limit range of 31%-50% (Delgado & Cañas, 2007; Houben & Guillaud, 1994),

— the adobe mixture has high pozzolanic activity (Lea, 1976).

The above-mentioned parameters, which are important for the production of qualified adobe, showed differences when evaluated in terms of Nano-clay production. The assessment of the Nano-clay production can be done by taking into consideration the parameters explained below:

— The presence of MONTMORILLONITE CONTENT in the adobe soil/clay resource

— The inherent content of Nano-clay in the adobe soil/clay resource designates the inherent potential of the adobe soil/clay resource.

The remarks of the study are:

- CLAY TYPE is a crucial parameter for the ENRICHMENT of NANO-CLAY by the ULTRASONIC TREATMENT. Ultrasonic treatment is more effective in enhancing the Nano-clay content, particularly for montmorillonite and then illite clay types. The treatment is less effective/successful for the kaolinite and chlorite clay types compared to the montmorillonite and illite clay types.
- EFFECTIVE USE OF CLAY-RICH SOIL RESOURCES, which are not appropriate for adobe material production can be provided by Nano-clay enrichment in the soil resource.

In addition, the Nano-CaO additive in an optimum ratio can be used in adobe soil including montmorillonite as the main clay content and not including Nano-calcite content in the adobe soil.

## 5.3 Assessing the Impact of Nano-Clay as binder and Nano-CaO as additive on adobe sample

Here, the performance of the treated adobe samples is assessed in comparison to the untreated ones. The comparison is done based on the basic physical, water vapour permeability, mechanical and capillary water absorption properties of the treated adobe samples composed of-:

- the Nano-clay enriched binder and Nano-CaO and $Ca(OH)_2$ additive and
- the untreated ones keeping the natural soil compositions of Konya_Küçükköy, Çorum_Karapınar and Çorum_Kınık adobe soil resources.

In this regard, the impact of Nano-clay as a binder with or without Nano-CaO and $Ca(OH)_2$ additives on the performance properties of adobe building material samples was discussed under respective subheadings.

## 5.3.1 Basic Physical Properties

The bulk densities of the treated samples (KuT, KaT and KıT) are observed to increase compared to the untreated samples (KuT, KaT and KıT). They become lower porous material by integrating nanoparticles in the interparticle. Among those samples, the highest bulk density is found in the Çorum_Karapınar adobe sample, while the least dense one is the Çorum_Kınık sample. The reason for the highest density of the Çorum_Karapınar sample may be due to its highest pozzolanic activity together with the high clay content decreasing the porosity of the adobe material (Meddah & Tagnit-Hamou, 2009). The inverse correlation between bulk density and porosity values can be observed clearly in all results (Figure 4.42). The particle density of treated samples is slightly lower than untreated samples due to the increase in Nano-sized particles. The particle density of untreated samples from the highest to the least values are samples of the Konya_Küçükköy, Çorum_Kınık and Çorum_Karapınar respectively, which have a direct relation with their course aggregate contents.

The addition of the Nano-CaO into the treated samples results in a higher bulk density and less porous treated Konya_Küçükköy adobe sample (KuTN). On the other hand, the additive of the Nano-CaO makes an opposite effect that causes more porous and less dense Çorum_Karapınar (KaTN) and Çorum_Kınık (KıTN) samples. In comparison to the treated sample, the more aggregated clay association (face-to-face (FF) connection) which provides clay particles having dense structures and high bonding strength to each other is observed in the KuTN (Figure 4.48). On the other hand, the flocculated clay association (edge-to-edge (EE) or/and edge-to-face (EF) connection) which leads to obtaining the less dense, and more porous structured clay particles having a weak connection seems in the KaTN and KıTN samples than the treated ones (Figure 4.49). In addition, that additive causes to achieve the highest particle density values in all samples.

The addition of $CaOH_2$ into the treated samples (KuTC, KaTC and KıTC) results in the range of one and a half and three times more porous and less dense adobe

materials compared to the untreated and treated ones. In addition, the least particle density values are found in those samples. The presence of excessive calcium cations results in flocculated clay associations (edge-to-edge (EE) or/and edge-to-face (EF) connection).

## 5.3.2 Water Vapour Permeability Properties

The water vapour resistance factor ($\mu$, unitless) and equivalent air thickness of water vapour permeability (SD, m) values of the treated samples (KuT, KaT and KıT) are higher in ranges of 1-10.3 and 0.2-0.17m, respectively compared to the untreated samples (KuU, KaU and KıU) (Figure 4.43). Because they became lower porous material by integrating nanoparticles in the interparticle. The highest changes are present in the Çorum_Kınık sample since the highest difference in porosity about 5.2 % between treated and untreated samples is observed in that sample.

The addition of the Nano-CaO into the treated samples results in higher water resistance values in the Konya_Küçükköy adobe sample (KuTN) while lower water resistance values seem in the Çorum_Karapınar (KaTN) and Çorum_Kınık (KıTN) samples compared to the treated samples (KuT, KaT and KıT). The Nano-CaO decreases the pore size due to the aggregated clay association (face-to-face (FF) connection) in the KuTN sample by its interaction with clay minerals (Figure 4.48). On the other hand, the KaTN and KıTN samples become more permeable compared to treated samples due to the more flocculated clay association (edge-to-edge (EE) or/and edge-to-face (EF) connection) (Figure 4.49).

The addition of $CaOH_2$ into the treated samples (KuTC, KaTC and KıTC) is observed to make the samples the most water vapour permeable. The excessive flocculated clay association made the sample the most porous and permeable. The treated Çorum_Kınık sample including $CaOH_2$ (KıTC) has a higher porosity of about 10% and lower density than the Çorum_Karapınar sample (KaTC); on the other hand, the SD and $\mu$ values of KıTC is slightly lower than the $\mu$ value of KaTC. The $CaOH_2$ additive in the treated Çorum_Kınık sample may result in more unconnected

pores or/and pores lower than 1 μm in clay fabrics of those samples compared to the Konya_Küçükköy sample.

The water vapour permeability and the porosity values are consistently observed to be directly proportional in all samples (Figure 4.42 and Figure 4.43). Among the three samples, the densest, the lowest porous, and the highest pozzolanic one Çorum_Karapınar sample has the highest SD and μ values. In addition, the Çorum_Kınık sample having the lowest SD and μ values possesses the highest porosity values.

The samples' μ values between 7 and 33.8 achieved from the analyses are consistent with the range of the values between 19-44 in literature data on the adobe samples produced in the laboratory while those μ values are too higher than the values between 0.6- 3.8 of adobe samples belonging to traditional and archaeological sites (Table 2.8). According to the TS EN 1062-1:2006 standard, the SD values of all samples are in the range between 0.14m and 1.4m which is defined as the medium vapour permeable (TS EN, 2006).

### 5.3.3    Mechanical Strengths

The compressive and flexural strengths of treated samples are observed to increase compared to the untreated ones since their higher density values than untreated samples. The use of Nano-CaO and $CaOH_2$ additives in treated Çorum_Karapınar and Çorum_Kınık samples decreases the compressive strengths of the treated samples, while the use of Nano-CaO additive improves the performance of the treated Konya_Küçükköy sample. The addition of those additives in the treated samples causes the flexural strength performances of those samples to decline compared to treated samples.

Compressive strengths of the Konya_Küçükköy (KuT), Çorum_Karapınar (KaT) and Çorum_Kınık (KıT) samples increase from 6.82 MPa to 8. 18 MPa, from 6.94 MPa to 7.66 MPa and from 2.81 MPa to 5.17 MPa by the treatment, respectively.

Those increases in the treated adobe samples correspond to 19.9 %, 10.4 % and 84%, respectively, in comparison to their untreated samples. The ratios of increases in compressive strengths are observed to be similar to 22.1% and 9.1% ratios, which are the amount of the produced Nano-clay below 2 μm, in the KuU and KaU samples, respectively. On the other hand, that similarity is not observed in the KıU sample since Nano-clay production is within the range of 7.9%-16.2% in that sample. That signals the substantial relation between the Nano-clay amount and compressive strength, especially in adobe samples having a certain strength. On the other hand, the compressive strength is observed to have an inconsistent relationship with the density and porosity physical properties among the three samples, contrary to expectations (Figure 4.42 and Figure 4.44). For instance, while the treated Çorum_Karapınar sample has the highest density, the treated Konya_Küçükköy sample indicates the maximum compressive strength performance. Those results also show that the main effect on the compressive strength is the total amount of Nano-clay in the adobe material.

Flexural strengths of Konya_Küçükköy (KuT), Çorum_Karapınar (KaT) and Çorum_Kınık sample (KıT) samples increase from 0.26 MPa to 0.30 MPa, from 0.31 MPa to 0.53 MPa and from 0.14 MPa to 0.36 MPa by the treatment, respectively. Those increases in the treated adobe samples correspond to 15.4%, 54.8 % and 157.1%, respectively, in comparison to their untreated samples. The highest flexural strength performance belongs to the KaT whose soil has the highest density and pozzolanic activity values. The highest increase in the flexural strength is observed in the KıT sample whose soil has the second highest pozzolanic activity value. It seems the pozzolanic activity increased after the dispersion of the montmorillonite by the ultrasonic treatment in that sample. The bonding of straw fibres to soil particles is one of the weakest parts of the adobe sample but the increase of the Nano-clay amount and the pozzolanic activity in the adobe samples improve the adhesion of straw fibres to adobe soil, which contributes to the flexural strength (Table 4.6 and Figure 4.45). The pozzolanic activity decreasing the porosity enhances the straw cohesion to the adobe matrix (Ouedraogo et al., 2019; Sharma et al., 2016).

The addition of the Nano-CaO in the treated Konya_Küçükköy sample (KuTN) provides to achieve the maximum value of compressive strength of 8.72 MPa. On the other hand, the Nano-CaO additive makes Çorum_Karapınar (KaTN) and Çorum_Kınık (KıTN) samples more brittle. With the Nano-CaO additive, there is a reduction of about 1.34 MPa and 2.25 MPa, respectively in their compressive strengths, which are close to the values of improvement achieved by the treated samples compared to untreated samples. In addition, the flexural strengths of the samples decrease in the range of 0.10-0.16 MPa in the treated ones' performances. The excessive calcium cations adsorption caused the formation of more flocculated clay association in the KıTN and the KaTN samples than in the KuT sample (Figure 4.49). The reason for the flocculation in the Çorum_Karapınar sample may be due to the presence of kaolinite and chlorite dominantly (Figure 4.36). The results show that there is no need for the addition of Nano-CaO in the case of the existing Nano-calcite content in the soil, and/or the presence of clay types having too low cation exchange capacity (CEC) values such as kaolinite and chlorite. The Çorum_Kınık sample's clay content is composed of mainly kaolinite and montmorillonite (Figure 4.36).

On the other hand, the total clay content of the untreated sample is in the range of 0 -5% (Figure 4.24) which is lower than the other samples. In addition, it has a high $CaCO_3$ content (below 4 µm) of 6.9%, especially the presence of the Nano-calcite under 0.25 µm was detected by XRD analyses (Figure 4.39). The results also indicate that there is no need for Nano-CaO as an additive in the Çorum_Karapınar sample including kaolinite and chlorite. The addition of Nano-CaO leads to the formation of excessive calcium cations, as a result, an increase in the flocculation of clay causes a decrease in the compressive and flexural strengths of those samples. On the other hand, the untreated Konya_Küçükköy soil sample has the highest clay content in the range of 9.5-15.6% (Figure 4.24) including dominantly montmorillonite clay type (Figure 4.36). The calcium cations found in the soil itself and ones coming from Nano-CaO did not increase the formation of clay flocculation as seen in the other samples, instead the further aggregated clay association (face-to-face (FF)) formed (Figure 4.48).

The addition of CaOH$_2$ in all treated samples leads to a dramatic decrease in the compressive and flexural strength performances of the samples. The presence of excessive calcium cations results in excessive flocculated clay association (edge-to-edge (EE) or/and edge-to-face (EF) connection) that causes crumbling in the samples.

Some literature data on the stabilization of the adobe sample with various additives (Table 2.9) indicates the results of compressive strength are in the range of 0.7-8.1 MPa. As well as with the cement additives the performance of the adobe can be achieved up to 11.1MPa. The results for the flexural strength of those adobe samples are in the range of 0.25-4.5 MPa. The requirements of compressive and flexural strengths in some codes are in the ranges of 1.15-2.75MPa and 0.24-0.35 MPa (Table 2.10). In this study, the compressive and flexural strengths of the treated samples are in the ranges of 5.17-8.18 MPa and 0.30-0.36 MPa, respectively. Those required performance levels, especially for compressive strength values, seem to be too low compared to the achieved data in the study. On the other hand, the higher compressive strength values of the adobe sample are classified by DIN 18945-12:2018 norms (DIN, 2018) regarding the minimum and mean values of the measurement data (Table 2.10). That classification (from the two to six) is conducted on the adobe sample including no additives such as gypsum and lime; therefore, only treated and untreated samples were categorised (Figure 5.9). The performance of the Çorum_Kınık sample increases from the second class to the fourth class by the treatment. In addition, the untreated Konya_Küçükköy and the Çorum_Karapınar samples don't meet the sixth class highest one but their treated samples exceed that highest class.
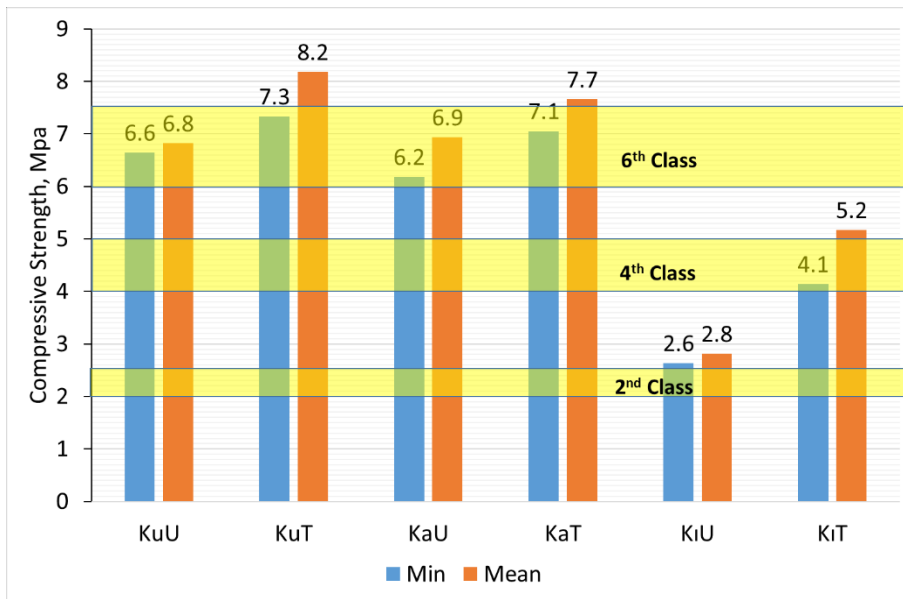
Figure 5.9 The classification according to DIN norms on the treated and untreated adobe samples (DIN, 2018).

In addition, the compressive strengths of the treated adobe samples despite having no binding additive exceed the performances of adobe samples including some that kind of additives such as gypsum lime, marble dust or cow dung. Both compressive and flexural strength performances of all treated samples are sufficient required levels in the codes. In addition, the performances of untreated Konya_Küçükköy and Çorum_Karapınar samples and treated Çorum_Karapınar samples including Nano-CaO achieve the both required levels. In comparison with fired brick as an alternative material to adobe brick, all types of the Konya_Küçükköy sample(KuU, KuT, KuTN and KuTC) and Çorum_Karapınar sample's untreated one (KaU), treated one (KaT) and treated one including Nano-CaO ((KaTN) and treated Çorum_Kınık sample (KıT) achieve the required level between 3.5 MPa and 35 MPa values expected from the fired brick's compressive strength performance (BS, 1981; Ramakrishnan et al., 2023).

### 5.3.4 Capillary Water Absorption Properties

The capillary water absorption values of untreated and treated samples are near in general while those values are predominantly lower than treated ones including Nano-CaO and treated ones including $CaOH_2$ (Figure 4.46). The alteration in the speed of the treated and untreated samples' water absorption is observed at the 60th minute. The treated Konya_Küçükköy sample has lower capillary water absorption values up to an initial 60 minutes than the untreated one. After that time, the capillary absorption performance of the treated samples becomes to be higher than in the untreated sample. A similar trend is also seen in the Çorum_Karapınar sample but the difference between treated and untreated ones is very slight. On the contrary, the treated sample of Çorum_Kınık is observed to have lower values of capillary absorption compared to its untreated one after 60 minutes.

The water absorption characteristics of treated Konya_Küçükköy and Çorum_Karapınar samples compared to their untreated ones in the first 60th minutes are observed to have a direct relation with their enriched Nano-clay contents (Figure 4.24 and Figure 4.46). The increase in Nano-clay content seems to slow down the speed of the capillary absorption up to a certain time. This reduction is due to the swelled Nano-clay particles by the water which stop the suction up to a certain time by closing the capillary pores. But after that time, the bonding between the clay particles may have broken, and thus the water absorption and swelling could have been increased due to high clay content. During the test, their treated samples were also observed to have more swelling compared to untreated ones after that time. Those results are consistent with the literature data (Irshidat & Al-Saleh, 2018). The difference between the treated Çorum_Kınık sample and other samples may be due to the high Nano-calcite in the soil itself. During the ultrasonic treatment, the Nano-calcite included in the soil is also dispersed, beside the Nano-clay. That dispersed Nano-calcite control the swelling of the clay with water, which prevents the blocking of the capillary pores. But after about 60 minutes, while the treated one keeps its

speed of water absorption, the water absorption of the untreated one is controlled by the adsorption of clays and its speed increases.

The capillary water absorption coefficient values (A-value) of treated samples are similar to the untreated ones (Figure 4.47). The reason why the change does not occur is that on the one hand, the porosity of the treated samples decreases by approximately 2.5-5% due to the Nano-sized clay particles produced filling the capillary pores; on the other hand, the Nano-clay content in the adobe samples increases by about 4.3%-22.1% that increase the water adsorption capacity.

A close relation between clay type, pozzolanic properties and capillary absorption coefficient values (A-value) is observed in the three samples. The lowest A-value is $0.28$ kg/m$^2$.sec$^{0.5}$ belonging to the untreated and treated Çorum_Karapınar sample, the reason is its main clay content non-expansive kaolinite and its highest pozzolanic characteristics (Ouedraogo et al., 2019; Sharma et al., 2016). On the other hand, the Konya_Küçükköy sample including mostly montmorillonite clay and the least pozzolans has the highest capillary absorption coefficient values in the range of $0.39$-$0.59$ kg/m$^2$.sec$^{0.5}$.

The addition of the $CaOH_2$ and Nano-CaO increases the A-values of all samples. The treated samples including $CaOH_2$ have the highest A-values due to their highest porosities. Those samples have the minimum volume change and no crack since the $Ca^{+2}$ ions control the clay minerals. On the other hand, those ions cause highly porous adobe samples having flocculated clay minerals in low bonding to each other in the manner of the edge-to-face (EF) or edge-to-edge connection (EF). By the Nano-calcite additive, the highest increase in the A-values seems to be in the Konya_Küçükköy sample among the three samples. The reason may be that the amount of the Nano-calcite fell short in the control of montmorillonite clay content in high amounts, as well as its low pozzolanic characteristics. On the other hand, the amount of the Nano-calcite is too much for the Çorum_Karapınar and the Çorum_Kınık samples since those samples become more porous than their treated samples due to the flocculation. The requirement of the smaller amount for those

samples is due to the presence of the mainly non-expansive clay types and high Nano-calcite in the soil itself, respectively.

The capillary water absorption coefficient (A-values) values of the untreated and treated Çoum_Karapınar (KaU and KaT) samples (2.15 kg/m$^2$.min$^{0.5}$ and 2.19 kg/m$^2$.min$^{0.5}$ in Table 4.14) fall into the range of values in literature data belonging to the adobe samples including additives of the gypsum and slag (1.6-2.1 kg/m$^2$.min$^{0.5}$), rice husk and lime (0.06-0.29 kg/m$^2$.min in Table 2.11). The A-values range of 0.28-0.59 kg/m$^2$.sec$^{0.5}$ (0.29-1.07 kg/m$^2$.min) of the adobe samples can be similar to the case of the values of adobe material having the addition of cement, lime and granite sludge (0.39-1.2 kg/m$^2$.min).

The swelling, cracks and detachments were visually observed in the samples of untreated (KuU, KaU and KıU), treated (KuT, KaT and KıT) and treated ones including Nano-CaO (KuTN, KaTN and KıTN) one hour after the start of the test. The minimum volume change and crack were observed in the treated samples including CaOH$_2$ (KuTC, KaTC and KıTC) (Table 3.10). According to the DIN 18945:2018-12 norms; therefore, those adobe samples were classified as internal walls (DIN, 2018) (Table 2.12).

## 5.4    Evaluation of the research outputs contributing to adobe technology in rural areas

The rural areas where adobe housing is common and archaeological settlements of adobe constructions are present are the regions reflecting the adobe technological culture of the past. Adobe craft in those lands signals the presence of clay and/or adobe soil resources of the region proper for construction. By the discovery of these resources and technological features of adobe in construction, the transfer of the knowledge achieved in the past to the new generations and technologies is possible. This means that adobe as a healthy and natural construction material is possible to survive in these regions.

Proper adobe soil resources have been used since the Neolithic times in Anatolia, where adobe emerged; therefore, many adobe archaeological sites have survived to the present day. However, many proper adobe soil resources have been forgotten or consumed/decreased in time. Therefore, it is observed that necessary attention is not paid to the choices of soil resources used in adobe production in rural areas and improper soil resources are used. Also, there is a lack of standards and regulations on the content and preparation of adobe materials and construction of adobe structures. Those reasons that weaken traditional adobe construction technology lead to less durable adobe constructions that increase their susceptibility to precipitation and earthquakes and their maintenance requirements. On the other hand, the Nano-clay enrichment process in adobe soil that increases the strength and durability of adobe structures will contribute to continuing to exist as an alternative construction method in the future through the development of adobe construction technology and its widespread use.

The existing and other environmental proper soil resources to be used for the Nano-clay enrichment process can be determined by critical analyses such as X-ray diffraction, particle size distribution and consistency limits analyses. Knowledge of proper soil resources and the production process of Nano-clay using industrial resources such as ultrasonic baths or other dispersion devices/methods available to the local community can be transferred to the community. Teaching/gaining the local people in terms of providing soil resource selection in the region and the enrichment of Nano-clay with the practical method by providing industrial resources has the potential for the continuation of traditional construction technology and the development of the rural area. In addition, the fortification of adobe constructions in archaeological settlements conducted by the Nano-clay enrichment provides interventions by keeping the authentic features of adobe materials.

# CHAPTER 6

## CONCLUSION

In the study, the practical method of Nano-clay enrichment in adobe soil was first developed using ultrasonic treatment in the laboratory and qualified adobe materials were produced from the adobe soils with increased Nano-clay content. Achievements of the study provided are:

- Enrichment of Nano-sized clay content in the existing adobe soil by the ultrasonic treatment;
- Verification of the improved performance of Nano-clay enriched adobe soil compared to the performance of natural adobe soils;
- Production of qualified adobe construction materials by using the adobe soils enriched in Nano-clay content by ultrasonic treatment.

The collected soil samples are evaluated and selected according to their potential for the Nano-clay enrichment and production of the adobe products. Adobe soil/clay resources rich in montmorillonite are more suitable for Nano-clay enrichment by ultrasonic treatment than those rich in illite, kaolinite and chlorite. Nano-clay enrichment by ultrasonic treatment is promising for the effective use of clay-rich soil resources which are not appropriate for adobe material production which can contribute to adobe production and the Nano-clay industry. Qualified adobe construction material produced by Nano-clay enriched adobe soil has an increase in compressive and flexural strength while still keeping its inherent breathable and capillary water absorption features. The treatment for the Nano-clay enrichment provides the obtaining of denser and lower porous adobe materials that lead to an increase in the compressive and flexural strengths which is higher than the requirements of the regulations/codes. The main factors are found to be total Nano-

clay content and pozzolanic characteristics of the treated adobe samples for the compressive and flexural strengths, respectively.

The $CaOH_2$ additive dramatically decreases mechanical performance and resistance to capillary water absorption performances of the Nano-clay enriched adobe samples. The impact of Nano-CaO additive on the performance properties of Nano-clay enriched adobe samples are summarized below:

- Increase in compressive strength of Nano-clay enriched adobe soil rich in montmorillonite
- Increase in capillary water absorption of adobe soil resources, while high pozzolanic activity characteristics of the adobe soil can control that adverse impact of Nano-CaO additive.

The study focused on the clay content of the selected soil samples for the Nano-clay enrichment process and the performance of produced adobe samples including additives in pre-defined amounts. In further studies, the effects of silt and coarser aggregate contents on the Nano-clay-enriched adobe sample and the optimum amount of the Nano-CaO additive in the Nano-clay-enriched adobe sample needs to be investigated for higher mechanical strength and less capillary absorption features. Performance analyses of Nano-clay enriched various soil resources should be continued to investigate the potential of the soil resources.

The Nano-clay enrichment in adobe soil can be applied in practical life by teaching/gaining the local people the soil resource selection in rural areas and the enrichment process of Nano-clay through industrial resources. The Nano-clay enrichment method also provides interventions by keeping the authentical features of adobe materials during the fortification of adobe constructions in archaeological settlements. In short, the effective use of soil resources and the production of Nano-clay-enriched adobe samples are expected to contribute to innovation fields of the adobe construction industry and the continuation of traditional adobe construction technology especially in rural areas and archaeological sites.

# REFERENCES

Abanto, G. A., Karkri, M., Lefebvre, G., Horn, M., Solis, J. L., & Gómez, M. M. (2017). Thermal properties of adobe employed in Peruvian rural areas: Experimental results and numerical simulation of a traditional bio-composite material. *Case Studies in Construction Materials*, *6*, 177–191. https://doi.org/10.1016/j.cscm.2017.02.001

Abbaslou, H., Martin Peinado, F. J., Ghanizadeh, A. R., & Shahrashoub, M. (2023). Properties of sepiolite clay soil as a natural material (Iran's sources clay). *Geomechanics and Geoengineering*, 1–12.

Acun, S., & Gürdal, E. (2003). Yenilenebilir Bir Malzeme: Kerpiç ve Alçili Kerpiç. *Türkiye Mühendislik Haberleri5*, *5*(427), 71–77.

Akkuzugil, E. (1997). *A Study of Historical Plasters* [Unpublished Master Thesis]. Middle East Technical University.

Al-Ajmi, F., Abdalla, H., Abdelghaffar, M., & Almatawah, J. (2016). Strength Behavior of Mud Brick in Building Construction. *Open Journal of Civil Engineering*, *06*, 482–494. https://doi.org/10.4236/ojce.2016.63041

Al-Barrak, K., & Rowell, D. L. (2006). The solubility of gypsum in calcareous soils. *Geoderma*, *136*(3), 830–837.

Alkaç, O., & Koral, H. (2022). Kınık (İzmir) ve Soma (Manisa) Arasındaki Bölgenin Neojen Stratigrafisi, Ortamsal Yorumlanması ve Paleocoğrafik Evrimi. *Süleyman Demirel Üniversitesi Fen Bilimleri Enstitüsü Dergis*, *26*(3), 523–536.

*Anton Paar -Viscosity of Water*. (2021). Anton Paar. https://wiki.anton-paar.com/en/water/

Arab, P. B., Araújo, T. P., & Pejon, O. J. (2015). Identification of clay minerals in mixtures subjected to differential thermal and thermogravimetry analyses and methylene blue adsorption tests. *Applied Clay Science*, *114*, 133–140. https://doi.org/10.1016/j.clay.2015.05.020

Aşanlı, M. (2021). *Geleneksel Yapı Teknikleri: Doğal ve Ekolojik Yapı Rehberi*. Yeni İnsan Yayınevi. https://books.google.com.tr/books?id=ptwmEAAAQBAJ

ASTM. (2015). *Standard Test Method for Rate of Water Absorption of Masonry Mortars* (ASTM C1403-15:2015). https://doi.org/10.1520/C1403-15

ASTM. (2017a). *Standard Practice for Classification of Soils for Engineering Purposes (Unified Soil Classification System)* (ASTM D2487-17e1:2017). https://doi.org/10.1520/D2487-17E01

ASTM. (2017b). *Standard Test Methods for Specific Gravity of Soil Solids by Water Pycnometer* (ASTM D 854 – 02:2017). https://doi.org/10.1520/D0854-02

ASTM. (2020). *Standard Terminology Relating to Concrete and Concrete Aggregates* (ASTM C125-20:2020). https://doi.org/10.1520/C0125-20

ASTM. (2021). *Standard Test Methods for Laboratory Determination of Density and Unit Weight of Soil Specimens* (ASTM D7263 − 21:2021). https://doi.org/10.1520/D7263-21

Atabey, E. (2015). Asbestos map of Turkey (Environmental exposure to asbestos-lung cancer-mesothelioma). *Tuberkuloz ve Toraks*, *63*, 199–219. https://doi.org/10.5578/tt.8966

Aznar, J. M., Poch, R. M., & Badía Villas, D. (2013). Soil catena along gypseous woodland in the middle Ebro Basin: Soil properties and micromorphology relationships. *Spanish Journal of Soil Science*, *3*(1), 28–44. Scopus. https://doi.org/10.3232/SJSS.2013.V3.N1.02

Azzam, E. M. S., Sayyah, S. M., & Taha, A. S. (2013). Fabrication and characterization of nanoclay composites using synthesized polymeric thiol surfactants assembled on gold nanoparticles. *Egyptian Journal of Petroleum*, *22*(4), 493–499. https://doi.org/10.1016/j.ejpe.2013.11.011

Babé, C., Kidmo, D. K., Tom, A., Mvondo, R. R. N., Boum, R. B. E., & Djongyang, N. (2020). Thermomechanical characterization and durability of adobes reinforced with millet waste fibers (sorghum bicolor). *Case Studies in Construction Materials*, *13*, e00422.

Bahobail, M. (2012). The Mud Additives and Their Effect on Thermal Conductivity of Adobe Bricks. *Journal of Engineering Sciences, Assiut University*, *40*, 21–34. https://doi.org/10.21608/jesaun.2012.112711

Baliga, R., & Nayak, B. C. (2018). *Examination of Compressive Strength and Water Absorption of Adobe Blocks Prepared using Black Cotton Soil and Granite Sludge.*

Barton, C., & Karathanasis, A. D. (2002). Clay minerals. In *Encyclopedia of soil science: Vol. In: Lal, R., Ed.* (pp. 187–192). Marcel Dekker.

Bektaş, C. (2018). *Türk evi*. Yapımevi Yayıncılık.

Bell, F. G. (1996). Lime stabilization of clay minerals and soils. *Engineering Geology*, *42*(4), 223–237. https://doi.org/10.1016/0013-7952(96)00028-2

Berardi, U., & Iannace, G. (2015). Acoustic characterization of natural fibers for sound absorption applications. *Building and Environment*, *94*, 840–852. https://doi.org/10.1016/j.buildenv.2015.05.029

*Betonarme: Bir Asrı Aşan Evliliğin Hikayesi*. (2023). Beton ve Çimento. https://www.betonvecimento.com/betonarme-yapilar/betonarme-bir-asri-asan-evliligin-hikayesi

Binici, H., Aksogan, O., Bakbak, D., Kaplan, H., & Isik, B. (2009). Sound insulation of fibre reinforced mud brick walls. *Construction and Building Materials*, *23*(2), 1035–1041. https://doi.org/10.1016/j.conbuildmat.2008.05.008

Binici, H., Aksogan, O., Bodur, M. N., Akca, E., & Kapur, S. (2007). Thermal isolation and mechanical properties of fibre reinforced mud bricks as wall materials. *Composites in Civil Engineering*, *21*(4), 901–906. https://doi.org/10.1016/j.conbuildmat.2005.11.004

Binici, H., Aksogan, O., & Shah, T. (2005). Investigation of fibre reinforced mud brick as a building material. *Construction and Building Materials*, *19*(4), 313–318. https://doi.org/10.1016/j.conbuildmat.2004.07.013

Black, C. A. (1965). *Methods of soil analysis*. American Society for Agronomy.

Blondet, M., Vargas-Neumann, J., & Tarque, N. (2008). *Available low-cost technologies to improve the seismic performance of earthen houses in developing countries.*

Brown, P. W., Robbins, C. R., & Clifton, J. R. (1979). Adobe. II: Factors Affecting the Durability of Adobe Structures. *Studies in Conservation*, *24*(1), 23–39. JSTOR. https://doi.org/10.2307/1505920

BS. (1981). *Precast concrete masonry units. Specification for precast concrete masonry units* (BS 6073-1:1981).

Calatan, G., Hegyi, A., Dico, C., & Mircea, C. (2016). Determining the Optimum Addition of Vegetable Materials in Adobe Bricks. *9th International Conference Interdisciplinarity in Engineering, INTER-ENG 2015, 8-9 October 2015, Tirgu Mures, Romania*, *22*, 259–265. https://doi.org/10.1016/j.protcy.2016.01.077

Calkins, M. (2008). *Materials for Sustainable Sites: A Complete Guide to the Evaluation, Selection, and Use of Sustainable Construction Materials*. John Wiley & Sons. https://books.google.com.tr/books?id=aOjZzwEACAAJ

Camerini, R., Chelazzi, D., Giorgi, R., & Baglioni, P. (2018). Hybrid nano-composites for the consolidation of earthen masonry. *Journal of Colloid and Interface Science*, *539*. https://doi.org/10.1016/j.jcis.2018.12.082

Caner, E. (2011). *Limestone decay in historic monuments and consolidation with nanodispersive calcium hydroxide solutions* [PhD Thesis, Middle East Technical University]. http://etd.lib.metu.edu.tr/upload/12613267/index.pdf

Carroll, D. (1970). *Clay Minerals: A Guide to Their X-ray Identification*. Geological Society of America. https://doi.org/10.1130/SPE126

Chang, T.-P., Shih, J.-Y., Yang, K.-M., & Hsiao, T.-C. (2007). Material properties of portland cement paste with nano-montmorillonite. *Journal of Materials Science*, *42*(17), 7478–7487. https://doi.org/10.1007/s10853-006-1462-0

Chen, D., Zhu, J. X., Yuan, P., Yang, S. J., Chen, T.-H., & He, H. P. (2008). Preparation and characterization of anion-cation surfactants modified montmorillonite. *Journal of Thermal Analysis and Calorimetry*, *94*(3), 841–848. https://doi.org/10.1007/s10973-007-8905-y

Choobbasti, A. J., Samakoosh, M. A., & Kutanaei, S. S. (2019). Mechanical properties soil stabilized with nano calcium carbonate and reinforced with

carpet waste fibers. *Construction and Building Materials*, *211*, 1094–1104. https://doi.org/10.1016/j.conbuildmat.2019.03.306

Christoforou, E., Kylili, A., Fokaides, P. A., & Ioannou, I. (2016). Cradle to site Life Cycle Assessment (LCA) of adobe bricks. *Journal of Cleaner Production*, *112*, 443–452. https://doi.org/10.1016/j.jclepro.2015.09.016

*Clay Minerals and Related Properties*. (2015, October 8). Soil Observation Institute. https://soilnews.feedsynews.com/clay-mineralogy/

Clifton, J. R., Davis, F. L., Service, U. S. N. P., & Standards, U. S. N. B. of. (1979). *Protecting Adobe Walls from Ground Water*. U.S. Department of Commerce, National Bureau of Standards.

Costi de Castrillo, M., Ioannou, I., & Philokyprou, M. (2021). Reproduction of traditional adobes using varying percentage contents of straw and sawdust. *Construction and Building Materials*, *294*, 123516.

Danso, H., Martinson, B., Ali, M., & Mant, C. (2015). Performance characteristics of enhanced soil blocks: A quantitative review. *Building Research & Information*, *43*(2), 253–262.

Dar, S., Khan, K., & Birch, W. D. (2017). Sedimentary: Phosphates. In *Reference Module in Earth Systems and Environmental Sciences*.

Dash, S., & Hussain, M. (2012). Lime Stabilization of Soils: Reappraisal. *Journal of Materials in Civil Engineering*, *24*, 707–714.

Dawson, R. F., Altmeyer, W. T., Barber, E. S., & Dubose, L. A. (1956). Discussion of Engineering Properties of Expansive Clays. *Transactions of the American Society of Civil Engineers*, *121*, 664–675.

de Ridder, N. A. (1965). Sediments of the Konya basin, central Anatolia, Turkey. *Palaeogeography, Palaeoclimatology, Palaeoecology*, *1*, 225–254. https://doi.org/10.1016/0031-0182(65)90017-9

Delgado, M., & Cañas, I. (2007). The selection of soils for unstabilised earth building: A normative review. *Construction and Building Materials*, *21*, 237–251. https://doi.org/10.1016/j.conbuildmat.2005.08.006

Demir, B., Ercan, S., Aktan, M., & Öztaşkın, H. (2018). Türkiye'nin Asbest Profili ve Asbest Güvenliği Sorunu. *Jeoloji Mühendisliği Dergisi*, 215–232. https://doi.org/10.24232/jmd.486031

DIN. (2018). *Earth blocks—Requirements, test and labelling* (DIN 18945:2018-12). German Institute for Standardization.

Dondi, M., Principi, P., Raimondo, M., & Zanarini, G. (2003). Water vapour permeability of clay bricks. *Construction and Building Materials*, *17*(4), 253–258. https://doi.org/10.1016/S0950-0618(02)00117-4

Drees, L. R., Wilding, L. P., Smeck, N. E., & Senkayi, A. L. (2018). Silica in Soils: Quartz and Disordered Silica Polymorphs. *SSSA Book Series*.

Du, J., Pushkarova, R. A., & Smart, R. St. C. (2009). A cryo-SEM study of aggregate and floc structure changes during clay settling and raking processes. *International Journal of Mineral Processing*, *93*(1), 66–72. https://doi.org/10.1016/j.minpro.2009.06.004

Dubor, A., Izard, J.-B., Cabay, E., Sollazzo, A., Markopoulou, A., & Rodriguez, M. (2019). *On-Site Robotics for Sustainable Construction: Foreword by Sigrid Brell-Çokcan and Johannes Braumann, Association for Robots in Architecture* (pp. 390–401). https://doi.org/10.1007/978-3-319-92294-2_30

Elert, K., Jroundi, F., Benavides-Reyes, C., Correa Gómez, E., Gulotta, D., & Rodriguez-Navarro, C. (2022). Consolidation of clay-rich earthen building materials: A comparative study at the Alhambra fortress (Spain). *Journal of Building Engineering*, *50*, 104081.

Ergin-Oruç, Ş. (2004). *Kerpiç duvarlara uygulanan kil bağlayıcılı dış sıva hasarlarının irdelenmesi* [Master Thesis, Dicle University]. https://www.ulusaltezmerkezi.net/kerpic-duvarlara-uygulanan-kil-baglayicili-dis-siva-hasarlarinin-irdelenmesi/

Erol, A., Shein, E., Milanovskiy, E., Mikayilov, F., Er, F., & Ersahin, S. (2015). Physical and microbiological properties of alluvial calcareous Çumra province soils (Central Anatolia, Turkey). *Eurasian Journal of Soil Science*, *4*, 107–110. https://doi.org/10.18393/ejss.13596

Erol, F., Tavukçuoğlu, A., & Caner-Saltık, E. N. (2022). Neolitik dönem kerpiç yapı malzemelerinin teknolojik özellikleri: Ulucak Höyük yerleşimi, İzmir. *Gazi Üniversitesi Mühendislik Mimarlık Fakültesi Dergisi*, *37*(3), 1595–1608. https://doi.org/10.17341/gazimmfd.947185

Fabbri, A., Morel, J. C., Aubert, J. E., Bui, Q. B., Gallipoli, D., & Reddy, B. V. V. (2021). *Testing and Characterisation of Earth-based Building Materials and Elements: State-of-the-Art Report of the RILEM TC 274-TCE*. Springer International Publishing.

Federal Republic of Nigeria. (2006). *National Building Code* (NBCN:2006; 1st ed.). Butterworths, Capetown: LexisNexis.

Food and Agriculture Organization. (2020). *Soil testing methods manual: Doctors Global Programme – A farmer-to-farmer training programme*. Food & Agriculture Org. https://books.google.com.tr/books?id=J5XpDwAAQBAJ

Fredericks, J. J., & Poppe, L. J. (n.d.). *USGS OFR01-041: Procedures—Separation of the silt and clay fractions by centrifugation* (U. S. Geological Survey USGS OFR01-041). Coastal and Marine Geology Program. Retrieved 12 January 2021, from https://pubs.usgs.gov/of/2001/of01-041/htmldocs/methods/centrifu.htm

Garrison, E. (2003). *Techniques in Archaeological Geology*. Springer-Verlag Berlin and Heidelberg GmbH & Co. https://doi.org/10.1007/978-3-662-05163-4

Garrison, E. (2016). *Techniques in Archaeological Geology*. Springer International Publishing. https://books.google.com.tr/books?id=nfg0DAAAQBAJ

Gazzè, S. A., Stack, A. G., Ragnarsdottir, K. V., & McMaster, T. J. (2014). Chlorite topography and dissolution of the interlayer studied with atomic force microscopy. *American Mineralogist*, *99*(1), 128–138.

Gieseler, J., Quidant, R., Dellago, C., & Novotny, L. (2014). Dynamic relaxation of a levitated nanoparticle from a non-equilibrium steady state. *Nature Nanotechnology*, *9*(5), 358–364. https://doi.org/10.1038/nnano.2014.40

Giuffrida, G., Caponetto, R., Nocera, F., & Cuomo, M. (2021). Prototyping of a Novel Rammed Earth Technology. *Sustainability*, 11948.

Grim, R. E. (1968). *Clay Mineralogy* (2nd edition). McGraw-Hill.

Güdücü, G. (2003). *Archaeometrical investigation of mud plasters on Hittite buildings in Şapınuwa-Çorum* [Master Thesis]. Middle East Technical University.

Güğercin, Ö., Baytorun, A. N., & Sezen, S. M. (2018). Kerpiç ve Betonarme Konutlarda Kullanılan Bazı Yapı Malzemelerinin Üretiminde Enerji Gereksinimleri. *Çukurova Tarım ve Gıda Bilimleri Dergisi*, *33*(1), 29–36. https://dergipark.org.tr/tr/pub/cutarim/issue/38663/349451

Guggenheim, S., Martin, R. T., Alietti, A., Drits, V. A., Formoso, M., Galán, E., Köster, H. M., Morgan, D. J., Paquet, H., Watanabe, T., Bain, D. C., Ferrell, R. E., Bish, D., Fanning, D. S., Kodama, H., & Wicks, F. J. (1995). Definition of clay and clay mineral: Joint report of the AIPEA nomenclature and CMS nomenclature committees. *Clays and Clay Minerals*, *43*, 255–256. https://doi.org/10.1346/CCMN.1995.0430213

Gure, A. (2016). *Properties and Applications of Sepiolite Clay Mineral from El-Bur and its potential role for Somalia's long-term Economic Development*.

Gürfidan, A. (2006). *Safranbolu Evlerinde Kullanılan Kerpiç Malzemenin Granüle Yüksek Fırın Cürufu İle İyileştirilmesi* [Master Thesis]. Sakarya University.

Hall, C., & Hoff, W. D. (2002). *Water Transport in Brick, Stone and Concrete*. Taylor & Francis. https://books.google.com.tr/books?id=Z0OkPhRvUHcC

Hang, P. T., & Brindley, G. W. (1970). Methylene Blue Absorption by Clay Minerals. Determination of Surface Areas and Cation Exchange Capacities (Clay-Organic Studies XVIII). *Clays and Clay Minerals*, *18*(4), 203–212. https://doi.org/10.1346/CCMN.1970.0180404

Harries, K. A., & Sharma, B. (Eds.). (2020). Nonconventional and Vernacular Construction Materials Characterisation, Properties and Applications. In *Nonconventional and Vernacular Construction Materials (Second Edition)* (p. iii). Woodhead Publishing. https://doi.org/10.1016/B978-0-08-102704-2.01001-5

Heiri, O., Lotter, A., & Lemcke, G. (2001). Loss on Ignition as a Method for Estimating Organic and Carbonate Content in Sediments: Reproducibility and Comparability of Results. *Journal of Paleolimnology*, *25*. https://doi.org/10.1023/A:1008119611481

Hendry, A. W., Sinha, B. P., & Davies, S. R. (1997). *Design of Masonry Structures* (1 ed.). CRC Press.

Hillier, S. (1995). *Erosion, Sedimentation and Sedimentary Origin of Clays* (pp. 162–219). https://doi.org/10.1007/978-3-662-12648-6_4

Hoke, G. D., Schmitz, M. D., & Bowring, S. A. (2014). An ultrasonic method for isolating nonclay components from clay-rich material. *Geochemistry, Geophysics, Geosystems*, *15*(2), 492–498.

Houben, H., & Guillaud, H. (1994). *Earth Construction: A Comprehensive Guide*. Intermediate Technology Publications.

Hunyadi Murph, S., Coopersmith, K., & Larsen, G. (2017). *Nanoscale Materials: Fundamentals and Emergent Properties* (pp. 7–28).

IBC. (2018). *Empirical Design of Adobe Masonry* (IBC 2018 Section 2109:2018).

IBC. (2021). *Building Code of Pakistan* (IBC 2021:2021). International Building Code, International Code Council, Washington DC.

Ilic, B., Mitrović, A., & Ljiljana, M. (2010). Thermal treatment of kaolin clay to obtain metakaolin. *Hemijska Industrija*, *64*, 351–356.

Irshidat, M. R., & Al-Saleh, M. H. (2018). Influence of Nanoclay on the Properties and Morphology of Cement Mortar. *KSCE Journal of Civil Engineering*, *22*(10), 4056–4063. https://doi.org/10.1007/s12205-018-1642-x

Işik, B. (2010). Use of prefabricated concrete installation walls for self-built earthen housing projects in the gap region of South-Eastern Turkey. *Journal of Environmental Protection and Ecology*, *11*, 977–985.

Işık, B. (2011). Conformity of Gypsum Stabilized Earth- Alker Construction with 'Disaster Code 97' in Turkey. *International Journal of Civil & Environmental Engineering*, *11*(2). https://doi.org/110502-3939

ISO. (2006). *Environmental management -Life cycle assessment-Principles and framework* (1ISO 4040:2006). International Organization for Standardization, Geneva, Switzerland:

ISO/TR. (2017). *Nanotechnologies—Plain language explanation of selected terms from the ISO/IEC 80004 series* (ISO/TR 18401:2017).

Jackson, M. L. R. (1969). *Soil Chemical Analysis: Advanced Course*. University of Wisconsin. College of Agriculture.

Jamila, J., & Zoukaghe, M. (2016). Evolution of Expansive Soils Structure with Different Solicitations and Effect of Some Parameters on Swelling Properties – Review Article. *Theoretical & Applied Science*, *37*, 68–77. https://doi.org/10.15863/TAS.2016.05.37.14

Janica, I., Del Buffa, S., Mikołajczak, A., Ededia, M., Pakulski, D., Ciesielski, A., & Samorì, P. (2018). Thermal insulation with 2D materials: Liquid phase exfoliated vermiculite functional nanosheets. *Nanoscale*, *10*. https://doi.org/10.1039/C8NR08364A

Jawaid, M., Qaiss, A., & Bouhfid, R. (2016). *Nanoclay reinforced polymer composites: Natural fibre/Nanoclay Hybrid Composites*. Springer.

Kadir, S., BAS, H., & Karakas, Z. (2002). Origin of sepiolite and loughlinite in a Neogene volcano-sedimentary lacustrine environment, Mihaliccik-Eskisehir, Turkey. *Canadian Mineralogist - CAN MINERALOG*, *40*, 1091–1102. https://doi.org/10.2113/gscanmin.40.4.1091

Kadir, S., & Erkoyun, H. (2015). Characterization and distribution of fibrous tremolite and chrysotile minerals in the Eskişehir region of western Turkey. *Clay Minerals*, *50*, 441–458. https://doi.org/10.1180/claymin.2015.050.4.03

Kadir, S., & Karakas, Z. (2002). Distribution and origin of clay minerals in Konya neogene sedimentary basin, central Anatolia, Turkey. *Turkish Journal of Earth Sciences*, *11*, 161–167.

Kafescioğlu, R. (2016). Alker ve Nitelikleri. *Unpublished Paper*. https://www.academia.edu/29981089/Alker_ve_Nitelikleri_2016?source=s wp_share

Kafescioglu, R. (2017). Neden Toprak Yapılar? In Y. Aksoy (Ed.), *Yaşamın Her Karesinde Toprak* (pp. 133–159). İstanbul Aydın University.

Kafescioğlu, R., Toydemir, N., Gürdal, E., & Özüer, B. (1980). *Gypsum stabilized adobe as construction material* (Research Project MAG505). TUBİTAK (Turkish Scientific And Technical Reseach Institute).

Karakaş, Ö. (2006). *Sivrihisar-Biçer Civari Neojen (Üst Miyosen-Pliyosen) Basenindeki Kil Parajenezlerinin Ortamsal Yorumu* [Master Thesis]. Ankara University.

Keefe, L. (2005). *Earth Building: Methods and Materials, Repair and Conservation* (1. ed.). Taylor & Francis.

Kertmen, N., Dalbaşi, E. S., Körlü, A., Özgüney, A., & Yapar, S. (2020). A study on coating with nanoclay on the production of flame retardant cotton fabrics. *Textile and Apparel*, *30*(4), Article 4.

Khalid, N., Arshad, M., Mukri, M., Mohamad, K., & Kamarudin, F. (2014). *The properties of Nano-kaolin mixed with kaolin*. *19*, 4247–4255.

Khandve, P. (2014). Nanotechnology for Building Material. *International Journal of Basic and Applied Research*, *Volume 4*, 146–151.

Khoshnevis, B. (2004). Automated construction by contour crafting—Related robotics and information technologies. *The Best of ISARC 2002*, *13*(1), 5–19. https://doi.org/10.1016/j.autcon.2003.08.012

Kıvrak, J. (2007). *Silis dumanı katkılı kerpiçlerin mekanik ve fiziksel özelliklerinin araştırılması* [Master Thesis, Gazi University]. https://www.ulusaltezmerkezi.net/silis-dumani-katkili-kerpiclerin-mekanik-ve-fiziksel-ozelliklerinin-arastirilmasi/2/

Koçu, N., & Korkmaz, S. Z. (2007). Kerpiç malzeme ile üretilen yapılarda deprem etkilerinin tespiti. *The Role of Building Material in Architecture, Design and Practice*, 52–62.

Kusiorowski, R., Zaremba, T., Piotrowski, J., & Adamek, J. (2012). Thermal decomposition of different types of asbestos. *Journal of Thermal Analysis and Calorimetry*. https://doi.org/10.1007/s10973-012-2222-9

Lakshmi, R., Velmurugan, V., & Swamiappan, S. (2013). Preparation and Phase Evolution of Wollastonite by Sol-Gel Combustion Method Using Sucrose as the Fuel. *Combustion Science and Technology*, *185*.

Lam, C., Lau, K., Cheung, H., & Ling, H. (2005). Effect of ultrasound sonication in nanoclay clusters of nanoclay/epoxy composites. *Materials Letters*, *59*(11), 1369–1372. https://doi.org/10.1016/j.matlet.2004.12.048

Lanzón, M., & García-Ruiz, P. A. (2009). Evaluation of capillary water absorption in rendering mortars made with powdered waterproofing additives. *Construction and Building Materials*, *23*(10), 3287–3291. https://doi.org/10.1016/j.conbuildmat.2009.05.002

Lawrence, C. D. (1998). 4—The Constitution and Specification of Portland Cements. In P. C. Hewlett (Ed.), *Lea's Chemistry of Cement and Concrete (Fourth Edition)* (pp. 131–193). Butterworth-Heinemann.

Lea, F. M. (1976). *The chemistry of cement and concrete* (3rd ed.). Arnold London.

Li, H., Zhao, Y., Song, S., & Nahmad, Y. (2015). Comparison of Ultrasound Treatment with Mechanical Shearing for Montmorillonite Exfoliation in Aqueous Solutions. *Journal of Minerals*, *2*, 1–12.

Limami, H., Manssouri, I., Cherkaoui, K., & Khaldoun, A. (2021). Mechanical and physicochemical performances of reinforced unfired clay bricks with recycled Typha-fibers waste as a construction material additive. *Cleaner Engineering and Technology*, *2*, 100037.

Love, S. (2012). The Geoarchaeology of Mudbricks in Architecture: A Methodological Study from Çatalhöyük, Turkey. *Geoarchaeology*, *27*. https://doi.org/10.1002/gea.21401

Loveday, J. (1974). *Methods for Analysis of Irrigated Soils*. Commonwealth Agricultural Bureaux. https://books.google.com.tr/books?id=cEx-zQEACAAJ

Loy, C. W., Amin Matori, K., Lim, W. F., Schmid, S., Zainuddin, N., Abdul Wahab, Z., Nadakkavil Alassan, Z., & Mohd Zaid, M. H. (2016). Effects of Calcination on the Crystallography and Nonbiogenic Aragonite Formation of

Ark Clam Shell under Ambient Condition. *Advances in Materials Science and Engineering*, *2016*, 2914368. https://doi.org/10.1155/2016/2914368

Luckham, P. F., & Rossi, S. (1999). The colloidal and rheological properties of bentonite suspensions. *Advances in Colloid and Interface Science*, *82*(1), 43–92. https://doi.org/10.1016/S0001-8686(99)00005-6

Mahltig, B., & Pastore, C. (2018). Chapter 8—Mineral and Ceramic Fibers. In B. Mahltig & Y. Kyosev (Eds.), *Inorganic and Composite Fibers* (pp. 165–193). Woodhead Publishing. https://doi.org/10.1016/B978-0-08-102228-3.00008-6

Maillard, P., & Aubert, J. E. (2014). Effects of the anisotropy of extruded earth bricks on their hygrothermal properties. *Construction and Building Materials*, *63*, 56–61. https://doi.org/10.1016/j.conbuildmat.2014.04.001

Meddah, S., & Tagnit-Hamou, A. (2009). Pore Structure of Concrete with Mineral Admixtures and its Effect on Self-desiccation Shrinkage. *ACI Materials Journal*, *V. 106*, 241–250.

Meriç, I., Erdil, M., Madani, N., Alam, B., Tavukcuoglu, A., & Caner-Saltık, E. N. (2017). Material Characterization of Mudbrick and Neighbouring Plasters in Traditional Timber Framed Structures. *Improvements in Conservation and Rehabilitation – Integrated Methodologies*, 259–272.

Meric, I., Erdil, M., Madani, N., Alam, B., Tavukcuoglu, A., & Saltik, E. (2013). *Technological Properties of Earthen Building Materials in Traditional Timber Frame Structures*. Kerpic'13 International Conference, İstanbul:Turkey.

Michalopoulou, A., Maravelaki-Kalaitzaki, P., Stefanis, N.-A., Theoulakis, P., Andreou, S., Kilikoglou, V., & Karatasios, I. (2020). Evaluation of nanolime dispersions for the protection of archaeological clay-based building materials. *Mediterranean Archaeology and Archaeometry*, *20*, 221–242. https://doi.org/10.5281/zenodo.3960201

Miller, A., & Ip, K. (2013). Sustainable Construction Materials. In R. Yao (Ed.), *Design and Management of Sustainable Built Environments* (pp. 341–358). Springer London. https://doi.org/10.1007/978-1-4471-4781-7_17

Millogo, Y., Morel, J.-C., Aubert, J.-E., & Ghavami, K. (2014). Experimental analysis of Pressed Adobe Blocks reinforced with Hibiscus cannabinus fibers. *Construction and Building Materials*, *52*, 71–78.

Minke, G. (2009). *Building with Earth: Design and Technology of a Sustainable Architecture* (2nd ed.). Birkhäuser Architecture.

Mishra, S., & Usmani, J. A. (2013). Comparison of Embodied Energy in Different Masonry Wall Materials. *International Journal of Advanced Engineering Technology*, *4*(4), 90–92.

Monge-Barrio, A., Bes-Rastrollo, M., Dorregaray-Oyaregui, S., González-Martínez, P., Martin-Calvo, N., López-Hernández, D., Arriazu-Ramos, A., & Sánchez-Ostiz, A. (2022). Encouraging natural ventilation to improve indoor environmental conditions at schools. Case studies in the north of Spain before and during COVID. *Energy and Buildings*, *254*, 111567.

Morton, T. (2006). Feat of clay. *Materials World*, *14*(1), 3–24.

Mosser-Ruck, R., Devineau, K., Charpentier, D., & Cathelineau, M. (2005). Effects of Ethylene Glycol Saturation Protocols on XRD Patterns: A Critical Review and Discussion. *Clays and Clay Minerals*, *53*(6), 631–638.

Muguda, S., Lucas, G., Hughes, P. N., Augarde, C. E., Perlot, C., Bruno, A. W., & Gallipoli, D. (2020). Durability and hygroscopic behaviour of biopolymer stabilised earthen construction materials. *Construction and Building Materials*, *259*, 119725. https://doi.org/10.1016/j.conbuildmat.2020.119725

NF. (1998). *Soils: Recognition and tests—Measure of the blue methylene adsorption capacity of a soil or rocky material—Determining the blue methylene value of a soil or rocky material with the stain test.* (NF P94-068:1998). French Association of Normalization (ANFOR). La Défense, Paris, France.

Ngowi, A. B. (1997). Improving the traditional earth construction: A case study of Botswana. *Construction and Building Materials*, *11*(1), 1–7. https://doi.org/10.1016/S0950-0618(97)00006-8

Niida, K., & Green, D. (1999). Stability and chemical composition of pargasitic amphibole in MORB pyrolite under upper mantle conditions. *Contributions to Mineralogy and Petrology*, *135*, 18–40.

Niroumand, H., Zain, M. F. M., & Alhosseini, S. N. (2013). The Influence of Nano-Clays on Compressive Strength of Earth Bricks as Sustainable Materials. *Procedia - Social and Behavioral Sciences*, *89*.

Niu, X.-J., Li, Q.-B., Hu, Y., Tan, Y.-S., & Liu, C.-F. (2021). Properties of cement-based materials incorporating nano-clay and calcined nano-clay: A review. *Construction and Building Materials*, *284*, 122820.

NMAC. (2015). *New Mexico earthen building materials code* (NMAC 14.7.4:2015). New Mexico State: Construction Industries Division of the Regulation and Licensing Department.

Noonan, C. W., & Pfau, J. C. (2011). Asbestos Exposure and Autoimmune Disease. In J. O. Nriagu (Ed.), *Encyclopedia of Environmental Health* (pp. 193–203). Elsevier. https://doi.org/10.1016/B978-0-444-52272-6.00350-0

Norton, J. (1997). *Building with Earth: A Handbook*. Intermediate Technology Publications. https://books.google.com.tr/books?id=jHROAAAAYAAJ

NTE. (2000). *Adobe: Reglamento nacional de construcciones: Norma técnica de edificación* (NTE E.080:2000). Ministerio de Transportes y Comunicaciones, Peru.

Nwanosike, A., Eze, C., Jimoh, M., Unuevho, C., & Fahad, A. (2015). Geotechnical Assessment of Clay Deposits in Minna, North-Central Nigeria for Use as liners in Sanitary Landfill Design and Construction. *American Journal of Environmental Protection*, *3*, 67–75.

NZS. (2020). *Materials and construction for earth buildings* (NZS 4298:2020). Standards New Zeland, Wellington.

Olivier, M., & Mesbah, A. (1970). Behaviour Of Ancient And New StructuresMade Out Of Raw Earth. *WIT Transactions on the Built Environment*, *4*. https://api.semanticscholar.org/CorpusID:112236202

Olubisi, I., & Humphrey, D. (2022). Experimental Characterization of Adobe Bricks Stabilized with Rice Husk and Lime for Sustainable Construction. *Journal of Materials in Civil Engineering*, *34*(2), 04021420.

Ouedraogo, M., Dao, K., Millogo, Y., Aubert, J.-E., Messan, A., Seynou, M., & Zerbo, L. (2019). Physical, thermal and mechanical properties of adobes stabilized with fonio (Digitaria exilis) straw. *Journal of Building Engineering*, *23*. https://doi.org/10.1016/j.jobe.2019.02.005

Özkan, İ., Çolak, M., & Oyman, R. (2010). Characterization of waste clay from the Sardes (Salihli) placer gold mine and its utilization in floor-tile manufacture. *Applied Clay Science*, *49*, 420–425.

Pacheco-Torgal, F., & Jalali, S. (2011). Nanotechnology: Advantages and drawbacks in the field of construction and building materials. *Composite Materials and Adhesive Bonding Technology*, *25*(2), 582–590.

Papayianni, I., & Pachta, V. (2017). Earth Block Houses of Historic Centers. A Sustainable Upgrading with Compatible Repair Materials. *Sustainable Synergies from Buildings to the Urban Scale*, *38*, 274–282.

Park, S., Choi, Y., Song, D., & Kim, E. (2021). Natural ventilation strategy and related issues to prevent coronavirus disease 2019 (COVID-19) airborne transmission in a school building. *Science of The Total Environment*, *789*, 147764. https://doi.org/10.1016/j.scitotenv.2021.147764

Parnes, R. (2013, March). *Soil Fertility-A Guide to Organic and Inorganic Soil Amendments*. Northeast Organic Framing Association.

Pashabavandpouri, M. A., & Jahangiri, S. (2015). Effect of nano silica on swelling, compaction and strength properties of clayey soil stabilized with lime. *Journal of Applied Environmental and Biological Sciences*, *7s*(5), 538–548.

Pearson, M. J., Monteith, S. E., Ferguson, R. R., Hallmark, C. T., Hudnall, W. H., Monger, H. C., Reinsch, T. G., & West, L. T. (2015). A method to determine

particle size distribution in soils with gypsum. *Geoderma*, *237–238*, 318–324. https://doi.org/10.1016/j.geoderma.2014.09.016

Pedergnana, M., & Elias-Ozkan, S. T. (2021). Impact of various sands and fibres on the physical and mechanical properties of earth mortars for plasters and renders. *Construction and Building Materials*, *308*, 125013. https://doi.org/10.1016/j.conbuildmat.2021.125013

Pekmezci, B., Kafescioglu, R., & Agahzadeh, E. (2012). Improved Performance Of Earth Structures By Lime And Gypsum Addition. *METU Journal of the Faculty of Architecture*, *29*. https://doi.org/10.4305/METU.JFA.2012.2.9

Pekrioglu Balkis, A. (2017). The effects of waste marble dust and polypropylene fiber contents on mechanical properties of gypsum stabilized earthen. *Construction and Building Materials*, *134*, 556–562.

Pérez-Maqueda, L. A., de Haro, M. C. J., Poyato, J., & Pérez-Rodríguez, J. L. (2004). Comparative study of ground and sonicated vermiculite. *Journal of Materials Science*, *39*(16), 5347–5351.

Pérez-Rodríguez, J. L., Pascual, J., Franco, F., Jiménez de Haro, M. C., Duran, A., Ramírez del Valle, V., & Pérez-Maqueda, L. A. (2006). The influence of ultrasound on the thermal behaviour of clay minerals. *Journal of the European Ceramic Society*, *26*(4), 747–753.

Petkovšek, A., Maček, M., Pavšič, P., & Bohar, F. (2010). Fines characterization through the methylene blue and sand equivalent test: Comparison with other experimental techniques and application of criteria to the aggregate quality assessment. *Bulletin of Engineering Geology and the Environment*, *69*(4), 561–574. https://doi.org/10.1007/s10064-010-0274-2

Poli, A. L., Batista, T., Schmitt, C. C., Gessner, F., & Neumann, M. G. (2008). Effect of sonication on the particle size of montmorillonite clays. *Journal of Colloid and Interface Science*, *325*(2), 386–390.

Poppe, L. J., Paskevich, V. F., Hathaway, J. C., & Blackwood, D. S. (2001). *A laboratory manual for X-ray powder diffraction* (Report 2001–41; Open-File Report). USGS Publications Warehouse. https://doi.org/10.3133/ofr0141

Ralph, J. (2023, June 25). *Mindat.org* [Project]. Mindat.Org. https://www.mindat.org/

Ramakrishnan, K., Chellappa, V., & Chandrasekarabarathi, S. (2023). Manufacturing of Low-Cost Bricks Using Waste Materials. *Materials Proceedings*, *13*(1). https://doi.org/10.3390/materproc2023013025

Ravisangar, V., Sturm, T. W., & Amirtharajah, A. (2005). Influence of Sediment Structure on Erosional Strength and Density of Kaolinite Sediment Beds. *Journal of Hydraulic Engineering*, *131*(5), 356–365.

Reeves, G. M., Sims, I., Cripps, J. C., & London, G. S. of. (2006). *Clay Materials Used in Construction*. Geological Society.

Ribeiro, T., Oliveira, D. V., & Bracci, S. (2022). The Use of Contact Sponge Method to Measure Water Absorption in Earthen Heritage Treated with Water Repellents. *International Journal of Architectural Heritage*, *16*(1), 85–96. https://doi.org/10.1080/15583058.2020.1751344

RILEM. (1980). Tentative Recommendations, Comission-25-PEM, Recommended test to measure the deterioration of stone and to access the effectiveness of treatment methods. *Material and Structures*, *13*(73), 173–253.

Rockwell, T. (2000). Use of soil geomorphology in fault studies. In *Quaternary geoochronology: Methods and applications.* (pp. 273–292). American Geophysical Union.

Rolfe, B. N., Miller, R. F., & McQueen, I. S. (1960). *Dispersion characteristics of montmorillonite, kaolinite, and illite clays in waters of varying quality, and their control with phosphate dispersants* (Report 334G; Professional Paper). USGS Publications Warehouse. https://doi.org/10.3133/pp334G

Sanchez, F., & Sobolev, K. (2010). Nanotechnology in concrete – A review. *Construction and Building Materials*, *24*(11), 2060–2071.

Scheinost, A., & Schwertmann, U. (1999). Color Identification of Iron Oxides and Hydroxysulfates: Use and Limitations. *Soil Science Society of America Journal*, *63*, 1463–1471. https://doi.org/10.2136/sssaj1999.6351463x

Schroeder, H. (2015). *Sustainable Building with Earth* (p. 560).

Schwalen, H. C. (1935). *Effect of Soil Texture Upon the Physical Characteristics of Adobe Bricks*. University of Arizona.

Serrano, S., Barreneche, C., & Cabeza, L. F. (2016). Use of by-products as additives in adobe bricks: Mechanical properties characterisation. *Construction and Building Materials*, *108*, 105–111.

Sharma, V., Marwaha, B. M., & Vinayak, H. K. (2016). Enhancing durability of adobe by natural reinforcement for propagating sustainable mud housing. *International Journal of Sustainable Built Environment*, *5*(1), 141–155. https://doi.org/10.1016/j.ijsbe.2016.03.004

Shukla, A., Tiwari, G. N., & Sodha, M. S. (2009). Embodied energy analysis of adobe house. *Renewable Energy*, *34*(3), 755–761.

State Institute of Statistics Prime Ministry Republic of Turkey. (2001). *Building Census 2000*.

Stefanidou, M., & Papayianni, I. (2005). The role of aggregates on the structure and properties of lime mortars. *Cement and Concrete Composites*, *27*(9), 914–919. https://doi.org/10.1016/j.cemconcomp.2005.05.001

Subedi, S. K. (2020). Study of Characteristics of Bricks Produced in Kathmandu, Nepal. *American Journal of Civil Engineering*, *8*, 64.

Sulieman, M., & Sallam, A. (2016). Improved method to determine particle size distribution for somegypsiferous soils. A case study from Al-Ahsa Governorate, Saudi Arabia. *Eurasian Journal of Soil Science (EJSS)*, *5*, 322–331. https://doi.org/10.18393/ejss

Tabassum, T., & Bheemasetti, T. (2020). Self-Healing and Desiccation Crack Behavior of Kaolinite-Rich Clay Soil. *Geo-Congress 2020: Foundations, Soil Improvement, and Erosion*, 582–591.

Taha, M. (2018). Recent Developments in Nanomaterials for Geotechnical and Geoenvironmental Engineering. *MATEC Web of Conferences*, *149*. https://doi.org/10.1051/matecconf/201814902004

Tan, X., Liu, F., Hu, L., Reed, A. H., Furukawa, Y., & Zhang, G. (2017). Evaluation of the particle sizes of four clay minerals. *Applied Clay Science*, *135*, 313–324. https://doi.org/10.1016/j.clay.2016.10.012

*TECLA House, Massa Lombarda*. (2023, October 17). Arquitectura Viva. https://arquitecturaviva.com/works/prototipo-de-vivienda-circular-tecla-impresa-en-3d-5

Teutonico, J. M., Preservation, I. C. for the S. of the, & Property, the R. of C. (1988). *A Laboratory Manual for Architectural Conservators*. ICCROM. https://books.google.com.tr/books?id=2oLyAAAACAAJ

Thiebat, F., Roncone, M., Grazieschi, G., Carbonaro, C., & Asdrubali, F. (2023). Sustainability of Building Materials: Embodied Energy and Embodied Carbon of Masonry. *Energies*, *16*. https://doi.org/10.3390/en16041846

Tombácz, E. (2003). Effect of Environmental Relevant Organic Complexants on the Surface Charge and the Interaction of Clay Mineral and Metal Oxide Particles. *Role of Interfaces in Environmental Protection*, 397–424. https://doi.org/10.1007/978-94-010-0183-0_24

Torraca, G. (1988). *Porous Materials Building: Materials Science for Architectural Conservation*. ICCROM.

Tournassat, C., Bourg, I. C., Steefel, C. I., & Bergaya, F. (2015). Surface Properties of Clay Minerals. In C. Tournassat, C. I. Steefel, I. C. Bourg, & F. Bergaya (Eds.), *Developments in Clay Science* (Vol. 6, pp. 5–31). Elsevier. https://doi.org/10.1016/B978-0-08-100027-4.00001-2

Tringham, R., & Stevanović, M. (Eds.). (2012). *Last House on the Hill*. Cotsen Institute of Archaeology Press at UCLA; JSTOR.

TS. (1977). *Adobe Blocks and Production Methods* (TS 2514:11977). Turkish Standards Institution, Ankara, Turkey.

TS. (2017). *Methods of testing soils for civil engineering purposes in the laboratory—Part 1: Determination of physical properties* (TS 1900-1/T3:2017). Turkish Standards Institution, Ankara, Turkey.

TS EN. (2006). *Paints and varnishes—Coating materials and coating systems for exterior masonry and concrete—Part 1: Classification* (TS EN 1062-1:2006). Turkish Standards Institution, Ankara, Turkey.

TS EN. (2016). *Methods of testing cement—Part 1: Determination of strength* (TS EN 196-1:2016). Turkish Standards Institution, Ankara, Turkey.

TS EN. (2020). *Methods of test for mortar for masonry—Part 11: Determination of flexural and compressive strength of hardened mortar* (TS EN 1015-11: 2020).

TS EN ISO. (2016). *Hygrothermal performance of building materials and products—Determination of water vapour transmission properties—Cup method* (TS EN ISO 12572:2016).

TS EN ISO. (2018). *Geotechnical investigation and testing—Identification and classification of soil—Part 1: Identification and description* (TS EN ISO 14688-1:2018). Turkish Standards Institution, Ankara, Turkey.

Tucker, M. E. (1981). *Sedimentary petrology: An introduction*. Blackwell Scientific Publications,Oxford, England.

Tucker, M. E. (2001). *Sedimentary Petrology: An Introduction to the Origin of Sedimentary Rocks*. Wiley.

Tuncan, A. (1992). *Mechanics of a Marine Clay Based on Physico-Chemical Interactions with Organic Contaminants* [PhD Thesis, Lehigh University]. https://hdl.handle.net/11421/5387

Turanli, L. (1985). *Evaluation of some physical and mechanical properties of plain and stabilized adobe blocks* [Master Thesis]. METU.

Türkmen, İ., Ekinci, E., Kantarcı, F., & Sarıcı, T. (2017). The mechanical and physical properties of unfired earth bricks stabilized with gypsum and Elazığ Ferrochrome slag. *International Journal of Sustainable Built Environment*, *6*(2), 565–573. https://doi.org/10.1016/j.ijsbe.2017.12.003

Uddin, F. (2008). Clays, Nanoclays, and Montmorillonite Minerals. *Metallurgical and Materials Transactions A*, *39*(12), 2804–2814.

Uğuryol, M., & Kulakoglu, F. (2013). A preliminary study for the characterization of Kültepe's adobe soils with the purpose of providing data for conservation and archaeology. *Journal of Cultural Heritage*, *14*, e117–e124. https://doi.org/10.1016/j.culher.2012.12.008

United States National Park Service. (1997). *Preservation Brief 5: Preservation of Historic Adobe Buildings*. Heritage Preservation Services. chrome-extension://efaidnbmnnnibpcajpcglclefindmkaj/https://www.nps.gov/orgs/1739/upload/preservation-brief-05-adobe.pdf

Uysal, İ., Zaccarini, F., Sadiklar, M. B., Tarkian, M., Thalhammer, O., & Garuti, G. (2009). The podiform chromitites in the Dağküplü and Kavak mines, Eskişehir ophiolite (NW-Turkey): Genetic implications of mineralogical and geochemical data. *Geologica Acta*, *7*, 351–362.

Uzun, M. (2019). *MÖ 9. Ve 8. Bin yıl Kerpiç Mimarisine Mikroarkeolojik Bir Yaklaşım: Aşıklı Höyük'te Kerpiç ve Harç Tarifleri* [PhD Thesis]. İstanbul University.

Van Olphen, H. (1964). Internal mutual flocculation in clay suspensions. *Journal of Colloid Science*, *19*(4), 313–322.

Van Orden, D. R. (1964). Asbestos. In R. D. Morrison & B. L. Murphy (Eds.), *Environmental Forensics* (pp. 19–33). Academic Press.

Varol, B., Araz, H., Karadenizli, L., Kazancı, N., Seyitoglu, G., & Sen, S. (2002). Sedimentology of the Miocene evaporitic succession in the North of Çankiri-Çorum basin, Central Anatolia, Turkey. *Carbonates and Evaporites*, *17*, 197–209. https://doi.org/10.1007/BF03176485

Velde, B., & Meunier, A. (2008). The Origin of Clay Minerals in Soils and Weathered Rocks. In *The Origin of Clay Minerals in Soils and Weathered Rocks, by B. Velde and A. Meunier. Berlin: Springer, 2008. ISBN: 978-3-540-75633-0* (Vol. 418). https://doi.org/10.1007/978-3-540-75634-7

Verhoef, P. N. W., TU Delft, F. der M. en Petroleumwinning., & Sectie Ingenieursgeologie. (1992). *The methylene blue adsorption test applied to geomaterials*. TU Delft; /z-wcorg/.

Vilane, B. R. T. (2010). Assessment of stabilisation of adobes by confined compression tests. *Biosystems Engineering*, *106*(4), 551–558. https://doi.org/10.1016/j.biosystemseng.2010.06.008

Villagrán-Zaccardi, Y., Alderete, N., Pico-Cortés, C., Zega, C., Risdanareni, P., & De Belie, N. (2021). Effect of wastes as supplementary cementitious materials on the transport properties of concrete. In J. de Brito, C. Thomas, C. Medina, & F. Agrela (Eds.), *Waste and Byproducts in Cement-Based Materials* (pp. 191–227). Woodhead Publishing.

Vyncke, J., Kupers, L., & Denies, N. (2018). Earth as Building Material – an overview of RILEM activities and recent Innovations in Geotechnics. *MATEC Web of Conferences*, *149*, 02001.

Walker, P. (2001). *The Australian Earth Building Handbook*. Standards Australia International. https://books.google.com.tr/books?id=-RD4AAAACAAJ

Widder, L. (2017). Earth eco-building: Textile-reinforced earth block construction. *CISBAT 2017 International ConferenceFuture Buildings & Districts – Energy Efficiency from Nano to Urban Scale*, *122*, 757–762. https://doi.org/10.1016/j.egypro.2017.07.392

Yazarloo, R., Katooli, F. A., Golestani, M., Asadi, M., & Ebrahimi, S. (2017). *Adding Calcite and Nanocalcite to Improving the Plastic Properties of the Lean Clay*.

Yeniyol, M. (2012). Geology and mineralogy of a sepiolite-palygorskite occurrence from SW Eskiehir (Turkey). *Clay Minerals*, *47*.

Yetgin, Ş., Çavdar, Ö., & Çavdar, A. (2008). The effects of the fiber contents on the mechanic properties of the adobes. *Construction and Building Materials*, *22*(3), 222–227. https://doi.org/10.1016/j.conbuildmat.2006.08.022

Yu, W. H., Ren, Q. Q., Tong, D. S., Zhou, C. H., & Wang, H. (2014). Clean production of CTAB-montmorillonite: Formation mechanism and swelling behavior in xylene. *Applied Clay Science*, *97–98*, 222–234.

Yüncü, B. (2016). *Assessment of carbon dioxide transmission through porous building materials in relation to indoor air quality.* [Unpublished Master Thesis]. Middle East Technical University.

Yüncü, B., Tavukçuoğlu, A., & Caner-Saltık, E. N. (2014, 25 Semptember). Breathing features assessment of porous wall units in relation to indoor air quality. *Ventilation and Airtightness in Transforming the Building Stock to High Performance.* 35th AIVC Conference, Poznań, Poland.

Zainuddin, A. N., Norullain, S., Mukri, B., Azizah, N., & Che Lat, D. (2015). *Nano Kaolinite as Additives in Kaolinite Clay to Develop New Clay Liner Design in Landfill.*

Zhao, H., Ding, J., Huang, Y., Tang, Y., Xu, W., & Huang, D. (2019). Experimental analysis on the relationship between pore structure and capillary water absorption characteristics of cement-based materials. *Structural Concrete*, *20*. https://doi.org/10.1002/suco.201900184

# APPENDICES

## A. The procedures of ribbon and feel tests

<u>Ribbon Test</u>

— Wet a piece of soil in the palm until turning it into a humid paste.

— Form the paste into the ball (If it does not form into a ball, then it is sand).

— Put the ball between the thumb and forefinger.

— Press it upward to form a ribbon (If it is not able to form a ribbon, then it is loamy sand).

— Let the ribbon rupture by its weight.

— Measure the ribbon's length, if it is: $\leq 2.5$ cm, it is loam; between 2.5 cm and 5 cm, it is clay loam; $\geq 5$ cm, it is clay.

<u>Feel Test</u>

— Put a piece of soil in the palm.

— Wet the soil excessively.

— Rub it with a forefinger in the palm.

— Feel if it is gritty (like sugar), smooth (like flour), or neither gritty nor smooth/sticky.

— Combine ribbon and feel test results and determine the soil texture according to reference data given in Table 3.3.

B. **The procedure of salt spot test**

Sulphates

- — Put a few drops of the soil sample solution in a test tube.
- — Add 1-2 drops of dilute hydrochloric acid (HCl 2N) into the sample solution.
- — Add 1-2 drops of barium chloride solution ($BaCl_2$ 10%) into the sample solution.
- — The formation of a white precipitate indicates the presence of sulphate ions in the sample.

  Chemical reaction: $SO_4^2 + BaCl_2 \rightarrow BaSO_4 + 2Cl$

Carbonates

- — Put a few drops of the soil sample solution in a test tube.
- — Add 1-2 drops of hydrochloric acid solution (4M HCl) into the sample solution.
- — The formation of gas ($CO_2$) bubbles indicates the presence of carbonate ions in the sample.

  Chemical reaction: $CO_3^2 + 2\ HCl \rightarrow CO_2 + Cl + H_2O$

Phosphates

- — Put a drop of the soil sample solution on filter paper
- — Add a drop of ammonium molybdate into the sample solution.
- — Put the filter paper on heated wire gauze to accelerate the reaction.
- — Add a drop of benzidine reagent into the sample solution.
- — Hold the filter paper over the ammonia.
- — The formation of a blue fleck or ring on the filter paper indicates the presence of phosphate ions in the sample.
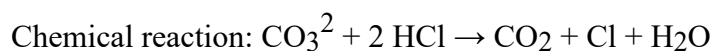
<u>Chlorides</u>

— Put a few drops of the soil sample solution in a test tube.

— Add 1-2 drops of dilute nitric acid ($HNO_3$) solution into the sample solution.

— Add 1-2 drops of silver nitrate solution ($AgNO_3$ 0.1 N) into the sample solution

— The formation of a white precipitate indicates the presence of chloride ions in the sample.

Chemical reaction: $Cl + AgNO_3 \rightarrow AgCl + N$
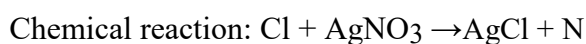
<u>Nitrites</u>

— Put a few drops of the soil sample solution on a spot plate.

— Add 1 drop of sulfanilic acid (4-aminobenzenesulfonic acid) solution into the sample solution.

— Add 1 drop of α-naphthylamine solution into the sample solution.

— Turning the solution into pink indicates the presence of nitrite ions in the sample.

<u>Nitrates</u>

— Put a few drops of the soil sample solution on a spot plate.

— Add 1 drop of acetic acid solution (2N) into the sample solution.

— Add 1 drop of sulfanilic acid (4-aminobenzenesulfonic acid) solution into the sample solution.

— Add 1 drop of α-naphthylamine solution into the sample solution.

— Add a few mg of zinc dust into the sample solution.

— Turning the solution into pink indicates the presence of nitrate ions in the sample.

C. **The procedure of the wet and dry-sieving analyses on particles above 63 microns sized (without taking care of gypsum content)**

- Add about 50 g soil sample.
- Place the sample in a drying oven at 105℃ for 24 hours.
- Note the weight of the oven-dry sample.
- Separate the silt clay content by dry-sieving with a 63μm sieve and note the weight of the silt and clay content (Because the soil samples generally have high silt and clay content, the dry sieve was conducted before the wet sieve).
- Conduct wet-sieving on the sample having particles above 63 μm:
    - Put the sieve of 63 μm in a large container.
    - Put the separated sample on the sieve.
    - Pour the distilled water into the sample.
    - Rub the sample on the sieve by hand to separate clay adherent on gravel and sand particles by caring not to crumble the aggregates while adding the distilled water.
    - Collect the silt and clay content passing through the sieve with water in a large container.
    - Repeat the process until the water passing through the sieve becomes clean.
    - Put the particles on the sieve and collect them in the container in different beakers.
    - Place those beakers in the drying oven at 105℃ for about a few days to provide oven-dryness of the samples.
- Weigh the oven-dried particles.
- Sump up the whole silt and clay achieved by dry and wet sieve analyses.
- Conduct particle size distribution analysis on aggregates above 63 μm by dry-sieving.

D. **The procedure of the alternative method composed of the sonication analyses and wet-sieving and dry-sieving analyses on particles above 63 microns sized (with taking care of gypsum content)**

 –   Take about 10 g soil sample.

 –   Place the sample in a drying oven at 35˚C (That temperature was preferred to prevent the dehydration of gypsum).

 –   Note the weight of the oven-dry sample.

 –   Put the sample into the 50 ml of 7:3 ethanol: water solution in a 50-mm diameter beaker.

 –   Put the sample in the beaker into the ultrasonic bath, including water for one minute.

 –   Sieve the suspended particles in the solution with the sieve of 63 μm.

 –   Add 50 ml of 7:3 ethanol: water solution on the particles in the beaker

 –   Repeat the sonication and wet-sieving processes until the flocculation of particles on the sediment is not observed by the naked eye anymore.

 –   Place particles above 63 μm in beakers in the drying oven at 35℃ about a few days up to provide oven-dry samples.

 –   Weigh the oven-dried particles.

 –   Conduct particle size distribution analysis on aggregates above 63 μm by dry-sieving.

E. **The procedure of centrifugal sedimentation**

- Add the distilled water to dilute the separated silt and clay content in a large container and keep waiting for the dissolution of the gypsum particles below 63 μm, especially in silts.
- Check the presence of gypsum by using hydrochloric acid (HCl 2N) barium chloride solution (BaCl$_2$ 10%) as explained in spot salt tests.

- Discharge and add the distilled water to dissolve the gypsum and repeat it until to are sure about the absence of gypsum in the water solution.

- Put the diluted sample in a beaker with a magnetic stirrer to disperse the flocculated clay particles formed during waiting. The stirring duration continued until flocculation disappeared.

- Put the diluted silt and clay content into 100 ml of centrifuge tubes.

- Determine the ambient temperature.

- Determine the specific gravity (*s)* and viscosity (η) values of distilled water according to ambient temperature (*Anton Paar -Viscosity of Water*, 2021).

- Determine the specific gravity (*s)* of clay and silt particles to estimate the specific gravity difference between the particles and the suspension liquid *Δs. (s* value of clay and silt particles was determined as 2.65 g/cm$^3$ (Meric et al., 2013).

- Measure the maximum height for the supernatant and the sediment (if it presents) in the centrifuge tube to determine R and S values.

- Calculate the required time (T$_m$) for sedimentation according to the formula given in Equation 4.

- Put the tubes in the centrifuge and assign the required time and revolutions per minute (N) to run the instrument.

- Decant the supernatant in a beaker for the next centrifuge sedimentation.

- Put the sediment in another beaker.

- Repeat the process till the achieving of particles is defined.

- Put the beakers including clay and silt particles separated into defined sizes in the oven at 105ºC.

- Weigh the oven-dried particles.

Table A.1 Data used in the formula shown in Equation 4 for the centrifugal sedimentation of Çorum_Karapınar sample.

| TºC | constant | η, poise | R, cm | S, cm | logR/S | N², rpm | D², micron | Δs, g/cm3 | Tm, minute |
|-----|----------|----------|-------|-------|--------|---------|------------|-----------|------------|
| 27 | 6300000000 | 0.008509 | 13.1 | 6.8 | 0.2847624 | 640000 | 16 | 1.6535 | 0.9 |
| 27 | 6300000000 | 0.008509 | 13.5 | 6.7 | 0.304259 | 640000 | 16 | 1.6535 | 1.0 |
| 27 | 6300000000 | 0.008509 | 13.5 | 6.5 | 0.3174204 | 640000 | 16 | 1.6535 | 1.0 |
| 27 | 6300000000 | 0.008509 | 13.6 | 6.2 | 0.3411472 | 360000 | 16 | 1.6535 | 1.9 |
| 27 | 6300000000 | 0.008509 | 13.5 | 5.5 | 0.3899711 | 810000 | 16 | 1.6535 | 1.0 |
| 27 | 6300000000 | 0.008509 | 13.2 | 6.2 | 0.3281822 | 640000 | 16 | 1.6535 | 1.0 |
| 27 | 6300000000 | 0.008509 | 13.5 | 6 | 0.3521825 | 810000 | 16 | 1.6535 | 0.9 |
| 27 | 6300000000 | 0.008509 | 14.5 | 6.4 | 0.355188 | 490000 | 4 | 1.6535 | 5.9 |
| 27 | 6300000000 | 0.008509 | 14.5 | 6.3 | 0.3620275 | 490000 | 4 | 1.6535 | 6.0 |
| 27 | 6300000000 | 0.008509 | 14.5 | 7.3 | 0.2980451 | 810000 | 4 | 1.6535 | 3.0 |
| 27 | 6300000000 | 0.008509 | 14.5 | 6.3 | 0.3620275 | 1960000 | 1 | 1.6535 | 6.0 |
| 27 | 6300000000 | 0.008509 | 14.5 | 6 | 0.3832168 | 4000000 | 1 | 1.6535 | 3.1 |
| 27 | 6300000000 | 0.008509 | 14.5 | 7.8 | 0.2692734 | 2890000 | 1 | 1.6535 | 3.0 |
| 27 | 6300000000 | 0.008509 | 14.5 | 6.3 | 0.3620275 | 3610000 | 0.25 | 1.6535 | 13.0 |
| 27 | 6300000000 | 0.008509 | 14.5 | 6.5 | 0.3484546 | 3240000 | 0.25 | 1.6535 | 13.9 |
| 27 | 6300000000 | 0.008509 | 14.5 | 7.4 | 0.2921363 | 2560000 | 0.25 | 1.6535 | 14.8 |
| 27 | 6300000000 | 0.008509 | 14.5 | 7.4 | 0.2921363 | 8410000 | 0.0625 | 1.6535 | 18.0 |
| 27 | 6300000000 | 0.008509 | 14.5 | 7.7 | 0.2748773 | 8410000 | 0.0625 | 1.6535 | 17.0 |
| 27 | 6300000000 | 0.008509 | 14.5 | 7.3 | 0.2980451 | 14440000 | 0.015625 | 1.6535 | 42.8 |
| 27 | 6300000000 | 0.008509 | 14.5 | 7.2 | 0.3040355 | 13690000 | 0.015625 | 1.6535 | 46.1 |
| 27 | 6300000000 | 0.008509 | 14.5 | 9.3 | 0.1928851 | 16000000 | 0.01 | 1.6535 | 39.1 |
| 27 | 6300000000 | 0.008509 | 14.5 | 9.4 | 0.1882401 | 16000000 | 0.0025 | 1.6535 | 152.6 |
| 27 | 6300000000 | 0.008509 | 14.5 | 9.9 | 0.1657328 | 14440000 | 0.0025 | 1.6535 | 148.8 |

F. **The procedure of methylene blue test (NF, 1998)**

— Determine the normality of methylene blue ($N_{MB}$) dye by the following formula (Equation 14):

$$N_{MB} = \frac{weight\ of\ MB}{320} + \frac{100-X}{100} \qquad 14$$

Where X is the moisture content of methylene blue dye; MB is methylene blue dye in g.

— Put the 10 g methylene blue whose normality is known in 1 litre distilled water and mix them with a magnetic stirrer very well

— Put the 3.75 g (30 g in the standard) oven-dry clay sample in 25 cc (200 cc in the standard) distilled water and mix it with the magnetic stirrer

— Put the methylene blue solution into the burette

— Start titration by putting 1 cc or 2 cc methylene blue solution from the burette into the diluted clay

— Stir the mixture for about 1 minute

— Drop the mixture on the filter paper with a glass rod.

— A circle dark blue spot is formed in apparent shape and is surrounded by a clear water hoop.

— Repeat the process until it is observed that the dark blue spot has a fuzzy edge or/and it is surrounded by a narrow light blue halo

— Do another test after 1 minute, if it disappears, more ethylene blue is added, but if it does not disappear, the spot test is repeated 4 more times without the addition of methylene blue solution. It is the end-point.

— Record the total volume of methylene blue dye added.

— Calculate the cation exchange capacity (CEC) by the following formula:

$$CEC = \frac{100}{f'} x\ V_{CC}\ x\ N_{MB} \qquad 15$$

Where f' dry weight of the sample in g; $V_{CC}$ is the volume of methylene blue solution added in the clay solution.

## G.  **Procedures of Liquid Limit, Plastic Limit and Linear Shrinkage Limit**

<u>Liquid limit test</u>

— Weigh about 150 g soil sample which passes the 425 μm test sieve by dry sieving.

— Place the soil sample on a glass plate.

— Add distilled water to the sample and mix thoroughly with a spatula until the bulk becomes a homogeneous paste.

— Put the paste in a desiccator and stand for about 24 hours to enable the water to permeate through the soil paste.

— Calibrate the Casagrande apparatus for liquid limit test

— Put the soil paste in a cup of the apparatus without entrapping air.

— Use the grooving tool to divide the soil paste into two equal parts.

— Lift and drop the cup, count the number of bumps.

— Continue until the two parts of the soil come into contact at the bottom of the groove along with a distance of 13 mm. Record the number of bumps at which this occurs.

— Take about 10 g of soil with a spatula.

— Put in an airtight container and determine the moisture content.

— Do it a minimum of five times for each sample.

— To determine the moisture contents of samples, put samples in the oven at 105℃ or 60℃ (If the soil contains gypsum) for about 24 hours.

—  Plot the values of moisture content of the sample and the corresponding number of bumps on a chart.

— Draw the flow curve fitting the plotted values.

— Record the moisture content at the flow curve corresponding to 25 blows that are referred to as liquid limit

Plastic limit test

— Take about 20 g of sample from the soil paste prepared for the liquid limit test.
— Shape the soil sample as a ball between the hands until slight cracks appear on its surface.
— Split the sample into about two subsamples of 10 g.
— Roll the subsamples as a thread between the fingers on the glass plate, respectively, until the thread's diameter is about 3 mm.
— Pick up the disaggregated pieces in a sample container.
— To determine the moisture contents of samples, put samples in the oven at 105 ℃ or 60 ℃ (If the soil contains gypsum) for about 24 hours.

Linear shrinkage ratio test

— Prepare the soil paste as prepared in the liquid limit test
— Carry out the liquid limit test to achieve the required soil consistency that is essential for about 25 bumps of the Casagrande apparatus.
— Put the soil paste in the mould defined in TS 1900-1/T3:2017 in three phases to prevent entrapped air and smooth the surface of the soil.
— Keep the moulded soil sample in the laboratory having conditions at 25°C at which the soil can air dry slowly until the soil sample shrinks away from the sides of the mould.
— Put the moulded sample in the oven at 60°C until shrinkage substantially remains stable.
— Put the moulded sample in the oven at 105°C to 110°C to achieve the oven-dry soil sample.
— Measure the length of the oven-dry soil sample.
— Calculate the shrinkage ratio in comparison with the initial length of the moulded soil sample.

— If the moulded sample becomes curved after heating treatments, the upper side and lower side of the sample lengths are measured, and the average value is taken.

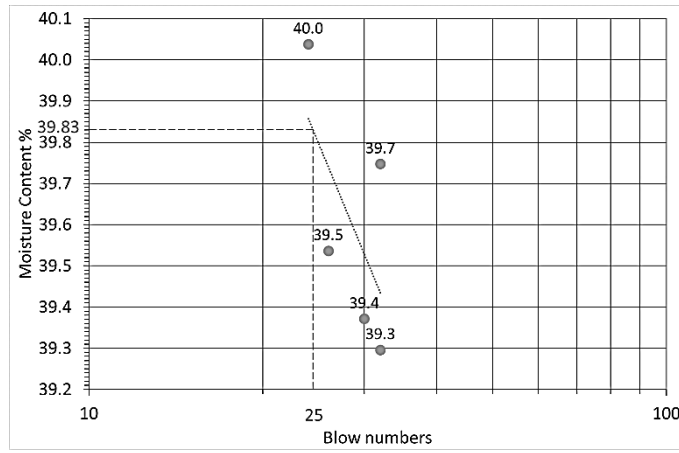Liquid limit values achieved by the Casagrande test method



Figure A.1 Casagrande test results of the Konya_Küçükköy sample.
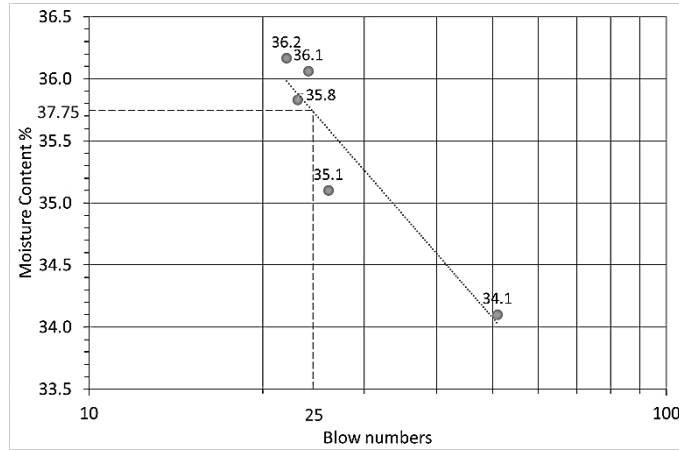


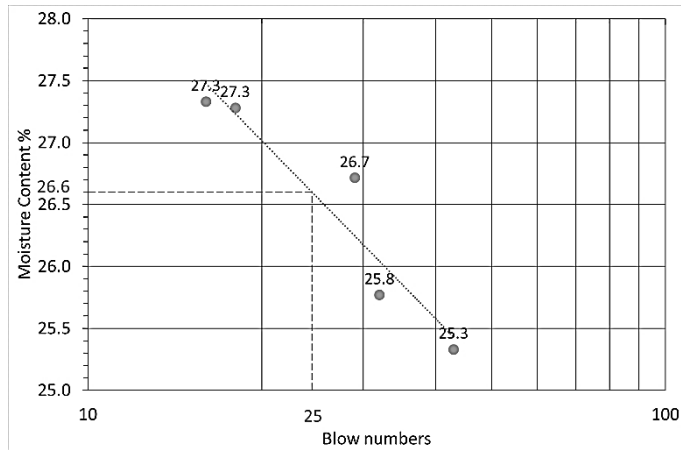Figure A.2 Casagrande test results of the Çorum_Karapınar sample.

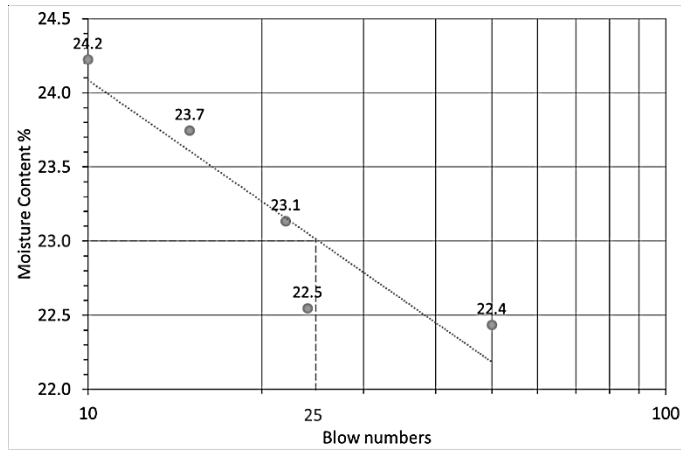Figure A.3 Casagrande test results of the Çorum_Kınık sample.



Figure A.4 Casagrande test results of the Çorum_Sarımbey sample.
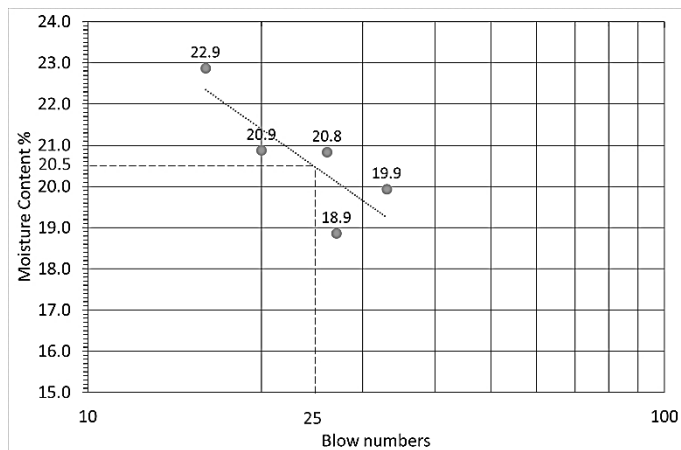


Figure A.5 Casagrande test results of the Manisa_Kemer sample.

# CURRICULUM VITAE

**EDUCATION**

| Degree | Institution | Year of Graduation |
|--------|-------------|--------------------|
| PhD | METU Building Science | 2024 |
| MS | METU Building Science | 2015 |
| BS | ITU Architecture | 2009 |
| High School | Nermin Mehmet Çekiç Anatolian High School, Ankara | 2004 |

**FOREIGN LANGUAGES**

Advanced English

**WORK EXPERIENCE**

02/2014-02/2022: Reseach Assistant, METU Architecture Department
03/2011-07/2011: Architect- Eyvan mimarlık eğitim sanat/Ankara
10/2009-04/2010: Archietct- İris proje/Ankara

**ARTICLES**

1) Erdil M.,Tavukçuoğlu A.,Çalışkan. (2023). *Sound Isolation Performance Assessment of Traditional and Retrofitted Timber-Framed Dwellings*, M. Journal of Architectural Engineering, vol.29, no.2.

**REFEREED CONGRESS / SYMPOSIUM PUBLICATIONS in PROCEEDINGS**

1) Erdil M., Tavukçuoğlu A., Çalışkan M. (2018). Geleneksel Ahşap Çatkı Duvarların Ses İletim Özellikleri ve Mevcut Durumu İyileştirmeye Yönelik Öneriler. *4. Ulusal Yapı Kongresi-Yapı sektöründe yenilikçi yaklaşımlar*, Antalya, Turkey, 6 - 08 December 2018, pp.513-529

2) Meriç I., Erdil M., Madani N., Alam B., Tavukçuoğlu A., Caner Saltık E. (2014). Material Characterization of Mudbrick and Neighbouring Plasters in Traditional Timber Framed Structures. *MONUBASIN 9- 9th International Symposium on the Conservation of Monuments in the Mediterranean Basin - Improvements in Conservation and Rehabilitation – Integrated Methodologies*, Ankara, Turkey, 3 - 05 June 2014, pp.259-272.

3) Atikoğlu C., Erdil M., Tavukçuoğlu A. (2017). Compatibility assessment with a focus on breathing capability in timber framed dwellings in Ankara and Mersin (Turkey*). Interdisciplinary Perspectives for Future Building Envelopes - ICBEST 2017 International Conference on Building Envelope Systems and Technologies*, İstanbul, Turkey, 15 - 18 May 2017, pp.608-620.

4) , Karahan Dağ F., Mısır Ç. T., Çömez S., Erdil M., Tavukçuoğlu A., Caner Saltık E. (2016). Assessment of Dolomite Conservation by Treatment with Nano Dispersive Calcium Hydroxide Solution. *Science and Art: A Future for Stone - 13th Int. Congress on the Deterioration and Conservation of Stone*, Paisley, United Kingdom, 6 - 10 September 2016, vol.2, pp.839-846.

5) Erdil M., Tavukçuoğlu A., Çalışkan M. (2016). Sound transmission analyses of impacts of wall renovation for traditional timber-framed dwellings. *Internoise-2016*, Hamburg, Germany, 21 - 24 August 2016, pp.3631-3639.

6) Erdil M., Tavukçuoğlu A., Çalışkan M. (2015). Assessment of sound transmission characteristics of traditional timber framed dwellings in Ankara Turkey. *Euronoise 2015*, Maastricht, Netherlands, 31 May - 03 June 2015, pp.967-972.

7) Meriç I., Erdil M., Madani N., Alam B., Tavukçuoğlu A., Caner Saltık E., (2013). Technological Properties of Earthen Building Materials in Traditional Timber Frame Structures. *Kerpic'13 - 3rd International Conference – New Generation Earthern Architecture: Learning from Heritage*, İstanbul, Turkey, 11 - 14 September 2013, vol.1, pp.465-473.

**PROJECTS INVOLVED**

1) TUBITAK-CNR–Bilateral Project-1001 Program: Stone consolidation with innovative nanodispersive products for the conservation of cultural heritage in the Mediterranean Basin, Scholar, METU, June 2014-June 2016.

2) TUBITAK -1002 Program: Development of a practical Nano-clay preparation technique and use of Nano-clay for production of qualified adobe, Scholar, METU June 2023-March 2024.

3) METU Scientific Research Project: (Continues), Günümüz Harm Günümüz Harman Tuğlasının Performans Özelliklerinin İyileştirilmesi Amacıyla Malzeme Analizleri, Tavukçuoğlu A (Executive), Atikoğlu M. C., Erol F.,Çetin Ö.,Güney B. A., Erdil M., 2017.

4) METU Scientific Research Project: Miselyum Tabanlı Biyolojik Bir Yapı Malzemesinin Laboratuvar Testleri Aracılığı İle Malzeme Özelliklerinin Belirlenmesi, Tanyer A. M.(Executive), Kızılkaya N.,Çetin Ö., Erol F.,Güney B. A.,Tavukçuoğlu A., et al. 2016 – 2020.

5) METU Scientific Research Project: Kireç esaslı sıvaların ses yutma özellikleri ile gözenek yapıları arasındaki ilişkinin incelenmesi, Tavukçuoğlu A. (Executive), Meriç Nursal I., Aleessa Alam B., Güney B. A.,Erdil M., Çalışkan M., 2015 – 2017.

6) METU Scientific Research Project: Yapılarda/sahada yapılan kızıl ötesi ısıl görüntüleme (ırt) çalışmaları için nicel analiz yöntemlerinin geliştirilmesi, Tavukçuoğlu A. (Executive),Sayın M., Mısır Ç. T., Güney B. A., Erdil M., 2016 – 2016.